AD NUMBER
AD914456
LIMITATION CHANGES
TO: **Approved for public release; distribution is unlimited.**
FROM: **Distribution authorized to U.S. Gov't. agencies only; Test and Evaluation; NOV 1973. Other requests shall be referred to Air Force Armament Laboratory, Attn: DLJA, Eglin AFB, FL 32542.**
AUTHORITY
AFAL ltr, 16 Dec 1975

AEDC-TR-73-186
AFATL-TR-73-211

EFFECT OF VARIOUS EXTERNAL STORES ON THE STATIC LONGITUDINAL STABILITY, LONGITUDINAL CONTROL, AND DRAG CHARACTERISTICS OF THE MODEL F-4C AIRPLANE

J. M. Whoric

ARO, Inc.

November 1973

This ... public release ... Per TAB 76-7 26 March, 1976

PROPULSION WIND TUNNEL FACILITY
ARNOLD ENGINEERING DEVELOPMENT CENTER
AIR FORCE SYSTEMS COMMAND
ARNOLD AIR FORCE STATION, TENNESSEE

NOTICES

When U. S. Government drawings specifications, or other data are used for any purpose other than a definitely related Government procurement operation, the Government thereby incurs no responsibility nor any obligation whatsoever, and the fact that the Government may have formulated, furnished, or in any way supplied the said drawings, specifications, or other data, is not to be regarded by implication or otherwise, or in any manner licensing the holder or any other person or corporation, or conveying any rights or permission to manufacture, use, or sell any patented invention that may in any way be related thereto.

Qualified users may obtain copies of this report from the Defense Documentation Center.

References to named commercial products in this report are not to be considered in any sense as an endorsement of the product by the United States Air Force or the Government.

EFFECT OF VARIOUS EXTERNAL STORES ON THE STATIC LONGITUDINAL STABILITY, LONGITUDINAL CONTROL, AND DRAG CHARACTERISTICS OF THE MODEL F-4C AIRPLANE

J. M. Whoric
ARO, Inc.

FOREWORD

The work reported herein was conducted by the Arnold Engineering Development Center (AEDC) under sponsorship of the Air Force Armament Laboratory (AFATL/DLGC), Air Force Systems Command (AFSC), under Program Element 62602F, Project 2567.

The test results presented were obtained by ARO, Inc. (a subsidiary of Sverdrup & Parcel and Associates, Inc.), contract operator of AEDC, AFSC, Arnold Air Force Station, Tennessee. The test was conducted from March 14 through 24, 1972, under ARO Project No. PC0242, and from October 3, 1972, through January 18, 1973, under ARO Project No. PA025. The manuscript was submitted for publication on September 17, 1973.

This technical report has been reviewed and is approved.

L. R. KISSLING
Lt Colonel, USAF
Chief Air Force Test Director, PWT
Directorate of Test

FRANK J. PASSARELLO
Colonel, USAF
Director of Test

ABSTRACT

The results from analysis of data obtained from wind tunnel tests, which were conducted to determine the effect of various external stores on the aerodynamic characteristics of the model F-4C airplane, are presented and discussed. The analysis includes evaluation of the static longitudinal stability, drag, and longitudinal control characteristics of the F-4C when loaded with the Pavestorm missile series, Modular Weapons series, Mark 84 EOGB, M-118 LGB, SUU-51B/B, SUU-30H/B, and Rockeye stores. Moreover, analysis of the probable cause as well as the wind tunnel verification of a pilot-reported "tuck-under" problem with the F-4C when carrying the Pavestorm series of stores is presented and discussed. Incremental drag rise and neutral-point shift associated with store loading are compared with results obtained from existing prediction methods and techniques. Data are presented for aircraft weights representative of each store loading at altitudes of sea level, 10-, 20-, and 30-thousand feet for aircraft center-of-gravity locations of 25, 33, and 36 percent of the mean aerodynamic chord over the Mach number range from 0.4 to 1.3.

CONTENTS

APPENDIXES

Figure Page

Figure | Page

Figure | Page

NOMENCLATURE

A_F	Total wing-mounted store or store-plus-suspension-equipment frontal area, ft^2
BL	Buttock line from plane of symmetry, in.
C_D	Drag coefficient, drag/$q_\infty S$
ΔC_D	Incremental change in drag coefficient caused by external stores
$C_{D\,trim}$	Drag coefficient at trim conditions
C_L	Lift coefficient, lift/$q_\infty S$
C_{L_α}	Slope of lift coefficient versus angle-of-attack curve at trim conditions, per degree
$C_{L_{\delta_s}}$	Slope of lift coefficient versus stabilator angle curve at trim conditions, per degree
$C_{m\,(0.33C)}$	Pitching-moment coefficient referenced to 33 percent of the mean aerodynamic chord and 1.55 WL, pitching moment/$q_\infty SC$
C_{m_o}	Pitching-moment coefficient at a lift coefficient of zero referenced to 33 percent of the MAC and 1.55 WL
ΔC_{m_o}	Incremental change in pitching-moment coefficient at zero lift caused by external stores
C_{m_α}	Slope of pitching-moment coefficient versus angle-of-attack curve at trim conditions, per degree
$C_{m_{\delta_s}}$	Slope of pitching-moment coefficient versus stabilator angle curve at trim conditions, per degree
C, MAC	Theoretical mean aerodynamic chord (see Fig. 3), 9.625 in.

cg	Center-of-gravity location, percent MAC
DN	Store or suspension equipment drag number, defined as the increment in drag coefficient at $M_\infty = 0.5$ attributable to the total number of stores times the reference area (S) times ten divided by the total number of stores or suspended store equipment, ft^2 per store
$d\epsilon/d\alpha$	Slope of downwash angle versus angle-of-attack curve
FS	Fuselage station, in.
GW	Aircraft-plus-stores gross weight, lb
H	Altitude, ft
M_∞	Free-stream Mach number
NP	Neutral-point location, percent MAC
ΔNP	Incremental change in neutral-point location at $C_L = 0.2$ caused by external stores (neutral-point location of the configuration X at $C_L = 0.2$ minus the neutral point of the clean configuration at $C_L = 0.2$), percent MAC
ΔNP_{TR}	Incremental change in neutral-point location caused by external stores at trim conditions (neutral-point location of configuration X at trim conditions minus the neutral-point location of the clean configuration at trim conditions), percent MAC
ΔNP_X	Incremental change in neutral-point location at $C_L = 0.2$ caused by the addition of external stores (neutral-point location of configuration X minus the neutral-point location of configuration Y), percent MAC
q_∞	Free-stream dynamic pressure, psf
S	Wing reference area, 1.3250 ft^2
WL	Waterline from reference horizontal plane, in.
α, α_W	Wing chord angle of attack, deg
$\alpha_{W\,trim}$	Wing chord angle of attack at trim conditions, deg
$\Delta\alpha_o$	Incremental change in the angle of zero lift caused by external stores (angle of zero lift of aircraft with stores minus the angle of zero lift of the clean aircraft), deg

δ_s	Stabilator angle measured with respect to wing chord plane, positive when trailing edge deflected down, deg
$\delta_{s_{trim}}$	Stabilator angle at trim conditions, deg
ϵ_o	Intercept value of downwash angle versus angle-of-attack curve, deg

SUBSCRIPTS

HT	Horizontal tail contribution
wB	Wing-body contribution

SECTION I
INTRODUCTION

One of the first and most severe effects of compressibility encountered in flight was the tendency of many airplanes to "tuck under." This tuck-under tendency occurred in the transonic Mach number range in high-speed dives during which severe nose-down pitching moments were experienced that required an abrupt and reverse sense change in the elevator angle to keep the aircraft trimmed. Coupled with these nose-down moments was an increase in longitudinal stability which resisted the efforts of the pilot to trim the aircraft at the desired lift coefficient to recover from the dive. The resulting elevator motions required to recover from the dive or even to prevent the dive from becoming steeper corresponded to excessive control forces, thus leading to the impression that the stick was frozen.

The data and analysis reported herein were obtained as a result of a wind tunnel test program which came about primarily to investigate this adverse handling quality (tuck-under) problem with the F-4C aircraft. The problem was reported by some pilots to occur when the F-4C was carrying the Pavestorm series of stores along with external 370-gal outboard fuel tanks. Also of interest at that time were the drag rise and neutral-point shift associated with several other external store configurations of the F-4C aircraft. A wind tunnel test program was evolved with the following objectives:

1. Determine if the reported tuck-under characteristics could be determined from wind tunnel tests on a 0.05-scale model of the F-4C.

2. Ascertain whether changes in wing downwash characteristics associated with the external stores configurations or changes in the aerodynamic center of the wing-body combination are responsible for the tuck-under.

3. Determine the shift in neutral-point location and the drag rise associated with a number of external store configurations of current interest.

4. Compare the neutral-point shift and the drag rise obtained from the wind tunnel tests with results obtained from existing prediction techniques.

The tests were conducted in the Aerodynamic Wind Tunnel (4T) of the AEDC Propulsion Wind Tunnel Facility (PWT) utilizing 0.05-scale models of the F-4C and stores of interest. Data were obtained with these models at Mach numbers from 0.4 to 1.3 and angles of attack ranging from -4 to 24 deg. In general, the stabilator angle was varied from -20.6 to 2.6 deg during these tests.

SECTION II
APPARATUS

2.1 TEST FACILITY

Tunnel 4T is a closed-loop, continuous flow, variable density tunnel in which the Mach number can be varied from 0.1 to 1.3. At all Mach numbers, the stagnation pressure

can be varied from 300 to 3700 psfa. The test section is 4 ft square and 12.5 ft long with perforated, variable porosity (0.5- to 10-percent open) walls. It is completely enclosed in a plenum chamber from which the air can be evacuated, allowing part of the tunnel airflow to be removed through the perforated walls of the test section. A more thorough description of the wind tunnel is given in Ref. 1.

2.2 TEST ARTICLES

The test articles were 0.05-scale models of the F-4C aircraft, the 370-gal fuel tanks, and Pavestorm 0, I, and II, M-118 LGB, MK 84 EOGB, Modular Weapons series, SUU-51B/B, SUU-30HB, and Rockeye stores. Figure 1 (Appendix I) is a photograph of the F-4C model configured with the Pavestorm II stores on the inboard MAU-12 pylons installed in the wind tunnel. A sketch showing the basic dimensions and armament stations of the F-4C model is shown in Fig. 2. The stabilator angle (δ_s) of the model F-4C is set manually and is measured with respect to the wing chord plane. Details and pertinent dimensions of the wing panel of the F-4C model are given in Fig. 3. For these tests, the store mounting surfaces of the centerline multiple ejection rack (MER) adapter and the inboard wing armament pylon shown in Fig. 4 were inclined at 2.5-deg and 1.0-deg nose-down angles, respectively, with respect to an aircraft waterline. The triple ejection rack (TER) and the MER shown in Figs. 5 and 6 were mounted on the inboard pylon and centerline MER adapter, respectively, for the required configurations. When the MER was used, it was installed on the fuselage centerline in the forward-shifted position.

Details and dimensions of the 0.05-scale models of the various external stores mentioned above are shown in Figs. 7 through 15. Note that the 370-gal fuel tank pylon (Fig. 7) is not the same as the outboard armament pylon shown in Fig. 4. The schematic diagram (Fig. 16) shows the profiles of the various stores and the load configurations in which they were tested. In this figure the store profiles are shown to scale with respect to each other, and the configurations are identified numerically for reference in the remainder of this report. The fin orientations of the stores as carried on the aircraft are also indicated in this figure.

2.3 INSTRUMENTATION

A six-component internal strain-gage balance was used to measure the forces and moments on the F-4C model. Three base pressure measurements were made using transducers and orifice tubes which extended just inside the base of the model.

SECTION III
TEST DESCRIPTION

3.1 TEST PROCEDURES AND CONDITIONS

Force and moment data were obtained in the conventional manner by varying the model angle of attack at a constant Mach number, Reynolds number, and stabilator angle

setting. The unit Reynolds number was held constant at a nominal value of 5.0 x 10^6 per foot for Mach numbers from 0.6 to 1.3, whereas at Mach number 0.4, the nominal Reynolds number was 4.0 x 10^6 per foot. The angle of attack was varied from -4 to 24 deg.

3.2 DATA REDUCTION AND CORRECTIONS

Wind tunnel force and moment data were reduced to coefficient form in the wind axis system. Base drag was calculated using an average of the three base pressure measurements along with the base area and was used to calculate forebody coefficients. However, the base drag measured in this manner was considered negligible, and therefore all coefficients presented are measured coefficients. Corrections for the components of model weight in the axial- and normal-force directions, normally termed static tares, were also applied to the data.

The angle of attack was corrected for sting and balance deflections caused by the aerodynamic loads. The model was tested both upright and inverted to provide the data to correct for tunnel-flow angularity and model-balance misalignment. Based on these data, the angle of attack was corrected for 0.4-deg upwash at Mach number 0.4 and for 0.3 deg upwash at Mach numbers 0.6, 0.8, and 0.85. No other flow angle corrections were made.

3.3 PRECISION OF MEASUREMENTS

The precision of the data presented which can be attributed to inaccuracies in the balance measurements and setting tunnel conditions was determined for a confidence level of 95 percent and is presented in Table I of Appendix II. The precision in setting the Mach number was ±0.002. The Mach number variation in the portion of the test section occupied by the model was no greater than ±0.005 for Mach numbers up to 0.95 and ±0.01 for Mach numbers greater than 1.0. The precision of the model angle of attack was ±0.1 deg, and the precision of the stabilator angle setting was ±0.1 deg.

SECTION IV
TEST RESULTS, ANALYSIS, AND DISCUSSION

4.1 GENERAL

In addition to accomplishing the objectives set forth in Section I, it is the intent of the author to provide under one cover a concise documentation of the pertinent effects produced by a number of different external stores on the untrimmed and trimmed aerodynamic characteristics of the F-4C airplane and to present data over a range of trim conditions that will allow for interpolation of the results to particular flight conditions of interest. Aerodynamic characteristics at trim conditions are presented for each configuration to be discussed. Trim characteristics were determined for altitudes of sea level, 10,000, 20,000, and 30,000 ft at aircraft cg locations of 25, 33, and 36 percent of the mean aerodynamic chord (MAC). Aircraft and aircraft-plus-store gross weights of

38,000, 46,000, and 58,000 lb were used as representative weights to categorize the various configurations and are indicated on each plot. The configurations tested are shown in Fig. 16 and are referred to in the text by number in most cases.

The aerodynamic characteristics at trim conditions were determined from the wind tunnel data utilizing a computer program which curve-fit the data and determined values of slopes and coefficients at specified trim-lift coefficients. The curve-fit procedure is explained in detail in Ref. 2 and is based on a mathematical method developed for interpolation from a given set of data points in a plane and for fitting a smooth curve to the points. The method is devised in such a way that the resultant curve will pass through the given data points and will appear smooth and natural. The method is based on a piecewise function composed of a set of polynomials, each of degree three, at most, and applicable to successive intervals of the given points. In this method, the slope of the curve is determined locally at each given point, and each polynomial representing a portion of the curve between a pair of given points is determined by the coordinates of the points and the slopes at the points. Determination of the slopes and the coordinates of points that fall between the two given points reduces to evaluating second-degree and third-degree polynomials, respectively, at the point of interest. Since the resultant curve passes through all the given data points, one must be careful to eliminate data points which are obviously bad.

A discussion of the tuck-under problem and the effect of external stores on the static longitudinal stability, lift and drag, and longitudinal control effectiveness characteristics are presented in the following sections.

4.2 TUCK-UNDER PROBLEM

4.2.1 Wind Tunnel Verification

"Tuck-under," as explained in Section I, is a compressibility effect that is characterized by an abrupt and reverse sense change in elevator angle to counteract nose-down moments encountered as an aircraft accelerates through the transonic Mach number range. Coupled with this "control stick reversal" is an increase in longitudinal stability which gives the pilot the impression that the control stick has become frozen. Classically (Ref. 3), these effects have been associated with changes in the lift characteristics and the angle of zero lift. Tuck-under was experienced with early wing designs of relatively thick cambered sections whose characteristics showed a positive shift in the angle of zero lift and a reduction in the lift-curve slope. The analysis of the wind tunnel data for the Pavestorm 0, I, and II (configurations 5, 6, and 7) shows some of these same classical tuck-under characteristics. The results of that analysis are presented in Figs. 17 through 27. Presented are plots of the stabilator angle required to trim as a function of Mach number, altitude, and cg location for the Pavestorm stores on the F-4C. These data show that as the F-4C accelerates from Mach number 0.9 to 0.975 loaded with Pavestorm 0, I, and II stores the stabilator angle has to be deflected first in the negative direction and then in the positive direction to counteract the nose-down pitching moments and thus maintain the aircraft trim. A rather sharp increase in longitudinal stability can be noted in Fig. 21

for these configurations in the Mach number range from 0.9 to 0.95 at altitudes of sea level and 10,000 ft. The data presented in Fig. 21 can be used to set the aft cg limit of the aircraft with the Pavestorm stores. It should be noted in Fig. 21b that if the cg were at 32 percent MAC the aircraft would have a static margin of 1 or 2 percent MAC at Mach numbers less than 0.9. As the Mach number was increased to 0.95, the static margin would increase to about 6 percent MAC. However, as the Mach number was further increased to 0.975, the static margin would decrease to about the subsonic values. The data in Fig. 21c show that at 20,000 ft, the Pavestorm I and II configurations exhibit the same static margin changes (within 1 to 2 percent MAC) over the same Mach number range. The increase in longitudinal stability characteristic of tuck-under is classically associated with a reduction in the slope of the lift curve; however, this was not the case for the F-4C at Mach numbers from 0.9 to 0.95 when configured with the Pavestorm series of stores, as indicated by the data in Fig. 22. Presented in this figure is the variation of the lift-curve slope (C_{L_α}) at trim conditions as a function of Mach number for the Pavestorm store configurations. Note that for Mach numbers from 0.9 to 0.95, where the sharp increase in stability was noted (Fig. 21), that an increase in the values of the lift-curve slopes occurs. The increase in stability noted in Fig. 21 occurs because the slope of the pitching-moment coefficient (C_{m_α}) curve (Fig. 23) is increasing negatively more rapidly than the lift-curve slope is increasing positively. However, the classical positive shift of angle of zero lift associated with tuck-under did show up in the data analysis, as shown in Fig. 24. Compressibility effects on the aircraft trim angle of attack can also be noted, referring to the data in Figs. 25, 26, and 27, for Pavestorm 0, I, and II, respectively. It can be shown that in the absence of compressibility and aeroelastic and propulsive system effects, and for a given aircraft weight and cg position, the trim angle-of-attack variation with Mach number is of the form $\alpha_{w\,trim} = f(1/M_\infty^2)$. The trim angle of attack in these figures exhibits deviations from this form of variation with Mach number in the Mach number range from 0.85 to 0.975, where compressibility effects dominate. As the Mach number increases from 0.85 to 0.975, the aircraft trim angle shifts more negatively because of compressibility effects; this is also characteristic of tuck-under (Ref. 3).

A similar analysis of the wind tunnel data was performed for configurations 1, 2, 8, and 12, and the results are presented in Figs. 28 through 43. Comparison plots of the data for configurations 1, 6, and 12 are presented in Figs. 44 and 45. The stabilator angle required to trim is presented as a function of Mach number (Fig. 44) for configurations 6 and 12 and shows very little difference in the required setting except at H = 30,000 ft. When comparing results of these configurations to those for the clean configuration (configuration 1), one notes that the change in trim stabilator angle with Mach number for Mach numbers from 0.85 to 1.1 is significantly greater than that of the clean configuration at altitudes of sea level and 10,000 ft; however, at H = 20,000 and 30,000 ft, the differences between the required angles for all three configurations are small. Based on the preceding discussion of tuck-under, it appears from the data presented in Figs. 44 and 45 that even the clean configuration exhibits this characteristic, but to a lesser degree than do configurations 6 and 12.

It is obvious from the data in Fig. 45b for an altitude of 10,000 ft that the static margin is reduced about 3 percent MAC at the subsonic Mach numbers when the Pavestorm I is installed on the aircraft. However, the significant point is that the clean aircraft does not exhibit a reduction in static margin as the Mach number increases toward 1.0, whereas with the Pavestorm configuration the static margin decreases significantly (about 5.5 percent MAC) at Mach number 0.975. A close examination of the neutral point data (Fig. 45) reveals that the real problem may possibly be subjective: the pilot of the F-4C carrying the Pavestorm stores encounters a handling-qualities problem associated with the aft and forward shifting of the neutral point as the aircraft is accelerated from Mach number 0.9 to 1.025. To the pilot, this change in static margin would be experienced as a change in stick force required to trim the aircraft. As the neutral point shifts aft (larger static margin), a greater stick force is required to keep the aircraft trimmed and, as the neutral point shifts forward, less stick force is required. When the F-4C configured with Pavestorm I is in a dive and accelerating through the Mach number range from 0.9 to 1.025, the changes in stick force occur rather quickly, as implied by the steep changes in the neutral point with Mach number (Figs. 45a and b), so that the pilot first feels the stick become quite heavy as the Mach number increases from 0.9 to 0.95, and then light from Mach number 0.95 to 0.975. Throughout this Mach number range, aft stick movement is required, but, as the aircraft continues to accelerate above Mach number 0.975, the required direction of the stick movement reverses, and the stick feeling becomes heavy again because of the aft shifting of the neutral point.

The SUU-51B/B data presented in Fig. 45 also show some aft and forward shifting of the neutral point at altitudes of 10,000 ft and above. Flight test data (Ref. 4) for the F-4C carrying a similar weight store, in the same configuration as the SUU-51B/B, indicate that the maximum Mach number attainable is 0.95, at 24,000 ft. This fact, combined with the forward shifting of the neutral point (generally about one percent of the MAC) that occurs near this upper limit ($M_\infty > 0.925$), makes this effect on the handling qualities of the aircraft small for the SUU-51B/B stores. If the aft cg limitation is based on the data at the subsonic Mach number, there appears to be ample static margin through the transonic Mach number range.

Figures 46 and 47 show a comparison of the data for configurations 6 and 8. In this case the stores have the same general aerodynamic profile. The M-118 LGB store fins and canards have a larger area and greater span than the Pavestorm I store. Also, the M-118 LGB store is somewhat larger in diameter than the Pavestorm I store. These data indicate that, through the transonic Mach number range, the F-4C will require larger stick movements to trim when configured with the M-118 LGB store (configuration 8) than when configured with Pavestorm I (configuration 6). In addition, these data show that configuration 8 will not have the handling quality problem experienced with the Pavestorm I store at sea level and 10,000 ft because the neutral point does not shift as drastically as for configuration 6. Again, as was the case for the SUU-51B/B configuration, if the aft cg location is selected, based on the subsonic data, ample static margin will be available through the transonic Mach number range. At 30,000 ft, the

data (Fig. 47d) indicate that for configuration 8 the neutral-point location is moving somewhat; however, the static margin would still be large at Mach number 0.975.

In summary, it appears that tuck-under and certain other handling qualities of aircraft configurations can be determined from analysis of wind tunnel data; this determination was the first objective of these tests.

4.2.2 Downwash Analysis

The second test objective was to attempt to determine whether the tuck-under problem could be traced to downwash changes associated with the various external stores or changes in the aerodynamic center of the wing-body combination caused by the external stores. Configuations 1, 2, 5, 6, 7, 8, and 12 were tested with horizontal stabilator on and off to determine the downwash characteristics ϵ_o and $d\epsilon/d\alpha_w$ as a function of Mach number. These characteristics were determined utilizing the pitching-moment coefficient data referenced to 0.33C and are presented in Figs. 48 and 49. Aerodynamic theory provides the following equations, which allow one to determine the influence of the downwash on the aircraft pitching-moment coefficient at zero lift.

$$C_{m_o} = \left(C_{m_o}\right)_{WB} + \left(C_{m_o}\right)_{HT} \tag{1}$$

$$\left(C_{m_o}\right)_{HT} = -\left(C_{m_{\delta_s}}\right)\left(\epsilon_o - \delta_s\right) \tag{2}$$

Comparisons of the variations of C_{m_o} with Mach number are presented in Fig. 50. These data show that when external stores are added to the F-4C, significant variations in C_{m_o} occur with Mach number in the transonic Mach number range.

Total changes in C_{m_o} caused by the stores were determined from the wind tunnel data for each of the above configurations for a stabilator setting of -0.6 deg and a cg location of 0.33C. Figure 51 presents these data along with the incremental change in the wing-body contribution and the incremental change that resulted from the downwash changes at the tail associated with adding the Pavestorm I stores and the 370-gal fuel tanks to the F-4C aircraft. It is easily seen from these data that for Mach numbers up to 0.95 the change in the wing-body contribution was the major factor responsible for the changes noted in C_{m_o}. Above a Mach number of 1.025 the horizontal tail contribution is approximately equal to the wing-body contribution. The effect of downwash changes at the horizontal tail (Fig. 52) becomes more significant for configuration 8 (M-118 LGB), but the wing-body contribution still is dominant. In this case the store loading is the same as for configuration 6, and the store itself is of the same basic shape as that of configuration 6. The major differences in the two stores are that the M-118 LGB is of larger diameter and has somewhat more fin area than the Pavestorm I store.

The analysis of the downwash data for configuration 12 (Fig. 53) shows that the horizontal tail contribution offsets the wing-body contribution, resulting in only small net changes in C_{m_o} for Mach numbers up to 0.95. Note also that the wing-body contribution is positive where for configurations 6 and 8 it was negative. At Mach number 0.975, the horizontal tail contribution is comparable to that of the wing-body, thus resulting in a large total ΔC_{m_o}. At Mach number 1.025 these two contributions again offset each other, and finally, above Mach number 1.1, the wing-body contribution dominates the change in C_{m_o}.

Comparison of the data in Figs. 50 and 54 shows that the variations of C_{m_o} with Mach number for configurations 8 and 10 are remarkably similar even though configuration 10 is a multiple-mounted store installation and configuration 8 is a single-mounted store installation. What is common between these two configurations is that the aircraft centerline is clean and the stores are carried at the same wing stations. Figure 54 shows that when SUU-30H/B stores are added to the aircraft centerline a positive shift in C_{m_o} results. Further comparison of the data in Figs. 50 and 54 shows that the C_{m_o} variations for configurations 11 and 12 have about the same level and variations with Mach number. Based on the downwash analysis of configurations 8 and 12, these comparisons imply that adding stores to the centerline of the aircraft could be beneficial in terms of eliminating large static margin changes and minimizing tuck-under.

The effect on C_{m_o} of adding various external stores and store suspension equipment to the F-4C aircraft is shown in Fig. 54. Data necessary for downwash analysis were not acquired during the wind tunnel tests for most of these configurations. These data, in general, show that adding stores to the inboard armament pylons produces a negative shift in aircraft C_{m_o} (compare configurations 2 and 3 and 3 and 10), whereas adding store racks and stores to the fuselage centerline (compare configurations 3 and 4 and 10 and 11) produces a positive shift in C_{m_o}.

4.3 EFFECT OF EXTERNAL STORES ON LONGITUDINAL STABILITY

The F-4 aircraft was originally designed as an air defense interceptor/air superiority fighter. The primary armament consisted of four AIM-7 Sparrow III missiles carried semisubmerged in four fuselage stations. However, since its first flight, the F-4 has been modified to carry, launch, and/or deliver a wide variety of external stores or weapons, as the Air Force, Navy, and Marines have adapted the aircraft as a multimission fighter.

Although the F-4 aircraft has proven adaptable to its role as a multimission fighter, the certification of the wide variety of weapons on the F-4 has posed problems in many areas of aircraft technology. One area of particular importance is the effect of the external stores on the longitudinal stability of the F-4. The addition of external stores to the F-4 aircraft generally has an adverse effect on the longitudinal stability characteristics. Some success at generalizing these effects for an arbitrary store and store loading on the F-4 longitudinal stability characteristics for wing-mounted stores has been achieved by

McDonnell Aircraft Corporation (Ref. 5). They showed a correlation of the changes in neutral-point location, determined at a lift coefficient of 0.2 and a stabilator angle of 0 deg, with the frontal area of wing-mounted weapons. Based on this correlation, a stability index number system was devised by McDonnell Aircraft and is used as described in Ref. 5. For stores and store configurations where this correlation cannot be used, wind tunnel testing is required. Based on the wind tunnel data, stability numbers can be assigned to provide neutral-point location and corresponding cg limitation for the conditions with the most forward neutral-point position. Data from the current wind tunnel tests have been reduced in terms of neutral-point shifts as a function of Mach number using the clean configuration as the baseline. These data evaluated at $C_L = 0.2$ are presented in Figs. 55 through 60. It is not within the scope of this report to assess whether the loss in stability noted for these external stores precludes acceptable stability limits based upon the cg characteristics of the F-4. However, some general comments on these forward shifts of the neutral-point location are in order.

It must be kept in mind that the neutral-point discussion here differs from that of section 4.2.1 in that here the discussion will center on the change in neutral-point location caused by the addition of external stores to the aircraft. These data (Figs. 55 through 60) show that wing-mounted external stores produce large changes in the neutral-point location in the transonic Mach number range (configurations 5 through 16). Destabilizing movements of about 10 percent C are noted for some configurations. This forward shift generally peaks out at Mach number 0.975 and is followed by a sharp aft shift as the Mach number increases to 1.025. Data were not obtained at Mach numbers between 0.975 and 1.025 for some of the configurations. Another forward movement of the neutral-point location occurred between Mach numbers 1.025 and 1.1 and was generally followed by an aft shift as the Mach number increased from 1.1 to 1.3. It should be emphasized that the maximum difference in the neutral-point location between the clean aircraft and one with stores generally occurs at a Mach number of about 0.975.

A comparison of the change in the neutral-point location (ΔNP_x) determined from the data in Figs. 55 through 60 with the empirically determined prediction curves of Ref. 5 is shown in Fig. 61a. The correlating parameter used in this figure is wing-mounted weapon frontal area. For configurations 4, and 11 through 16, the centerline stores and centerline suspension equipment frontal areas are not included in the reference areas used in this figure. The experimental data and correlation curve in Fig. 61a are presented for Mach number 0.85, which is the Mach number at which Ref. 5 reported that the largest losses in stability were experienced. Note that the finned store correlation curve of Ref. 5 in this figure is very close to an average curve through the wind tunnel data. In general, the experimental data deviate about ±1 percent of the MAC from the curve for the finned bodies. If the correlation could be made at Mach number 0.975, larger values for ΔNP_x would be found since the present data indicate that at Mach number 0.975 the maximum destabilizing effect occurs.

Reference 6 presents another method for predicting the effects of arbitrary external stores on aircraft performance. This method is semiempirical in that it is based on a

parametric correlation of extensive test data obtained from a comprehensive data search of both military and contractor facilities. A computer program has been developed by Ling-Temco-Vought, Inc. under Air Force sponsorship (Flight Dynamics Laboratory, FXM) and is currently available at AEDC. This program is capable of computing incremental neutral-point shifts, incremental lift losses, and incremental drag rise for both single- and multiple-mounted store installations in the subsonic, transonic, and supersonic speed regimes. The increments calculated by this technique are at trim conditions. For example, the incremental change in neutral-point location (ΔNP_{TR}) is the neutral-point location of the aircraft with stores at trim minus the neutral-point location of the clean aircraft at trim. Figure 61b presents a comparison of the neutral-point loss obtained for configuration 6 utilizing the wind tunnel data with the results obtained using the prediction technique of Ref. 6. These data show that this method in general predicts less neutral-point shift than was measured experimentally. Differences of 2 percent C are noted subsonically, and differences as great as 7 percent C are noted transonically. It should be noted that specific experimental data for aerodynamic shapes similar to the Pavestorm series were not in the computer program. Moreover, the data utilized were not obtained at M_∞ = 0.975, which is the most critical area.

Comparing the two techniques on the basis of the results of these tests, it appears that the frontal area correlation of Ref. 5 and the general prediction technique of Ref. 6 predict results of about the same accuracy. Both methods underpredict neutral-point location by about 1 to 2 percent MAC at Mach number 0.85. Both techniques should be used with caution since, according to Ref. 5, the McDonnell Aircraft Company test pilots have established a one-percent stable static margin as the minimum acceptable value for formation flying and/or weapons delivery. This fact obviates the use of either technique for aircraft that will carry or deliver external stores in the high transonic or supersonic Mach number ranges.

4.4 EFFECT OF EXTERNAL STORES ON DRAG CHARACTERISTICS

The carriage of external stores also has a marked effect on the drag characteristics of the F-4C. Trim drag as a function of Mach number, altitude, and cg is presented in Figs. 62, 63, and 64 for configurations 1, 2, 5, 6, 7, 8, and 12. The results presented were obtained through analysis of the wind tunnel data. These data show that at a given altitude the addition of external stores to the F-4C increases the trim drag by approximately a constant increment subsonically. Larger incremental increases in trim drag are generally noted supersonically than are noted subsonically. From these data, incremental drag rise can be derived as a function of Mach number, altitude, and cg location for incorporation into the aircraft flight manual performance to predict range and speeds when the aircraft is to carry these stores. Since it is obviously impractical to test and/or define drag performance characteristics in this manner for all conceivable external store configurations, a generalized technique for accomplishing this is highly desirable. McDonnell Aircraft Company reported in Ref. 5 a technique whereby transonic drag rise and drag-rise Mach number could be favorably predicted. This technique is based on the fact that the drag and the drag-rise Mach number could be correlated with a configuration's subsonic drag

level. Once this correlation was established, a numbering system for each weapon and each piece of mounting hardware was derived based upon subsonic test data. The number (drag number, DN) assigned to each pylon, rack, and/or weapon is obtained by dividing the incremental drag area $[(\Delta C_D)_{M_\infty=0.5} S]$ for all weapons or all mounting hardware by the total number of weapons or the total number of items of mounting hardware and then multiplying the number obtained by 10. The number thus obtained is a measure of the incremental drag rise at Mach number 0.5 attributable to that particular weapon or item of mounting hardware. The sum of all drag numbers thus obtained for a particular configuration is an index of the total drag increment for that configuration. Figures 65 and 66 present the wind tunnel data from which drag numbers for the various stores used during these tests have been derived and tabulated on the figures. Utilizing these numbers and the correlation curve in Ref. 7, the drag rise was determined for configurations 6 and 12 at Mach numbers 0.6, 0.8, 0.9, and 0.95. The drag coefficient increments thus determined were then added to the drag coefficient data of the clean configuration of Fig. 64b to obtain the total drag coefficient of each configuration. A comparison of the predicted drag values thus obtained is made with the drag values measured in the wind tunnel in Fig. 67. Presented also in this figure are the results of the more generalized prediction technique of Ref. 6. The data here show that the drag index technique (Ref. 5) generally underpredicts the drag rise up to Mach number 0.9, showing as much as a 15-percent difference from the measured value at Mach number 0.6. However, the drag rise increments predicted with this method were within the experimental error at Mach numbers 0.9 and 0.95. Predictions made by the method of Ref. 6 agree very well at Mach number 0.6 and then generally overpredict the drag, indicating about a 12-percent difference from the measured value at Mach number 0.95.

Based on the data presented here it would be difficult to say which prediction technique should be used to give best results for predicting drag rise caused by arbitrary external stores. Each technique has its own merits. The drag index technique requires a knowledge of the subsonic drag level of stores and suspension equipment of interest. However, a great deal of this type of information is already available. Also, this technique has proven its usefulness and value in that it provides external store drag information in a form that is easily used by operational units. This technique is limited to a maximum Mach number of 0.95 and is reported not to be useful for prediction of drag rise in the supersonic speed regime.

Contrasting the more general drag rise prediction technique of Ref. 6, one finds that the only aerodynamic data required by this technique is a knowledge of the free-stream drag of the store in question. All other quantities that are required are geometrical quantities peculiar to the store installation in question. This technique, like the drag index technique, is currently limited in its drag-rise prediction capability to Mach number 0.95, but there are wind tunnel tests currently planned which will extend this capability and fill in and refine some of the data correlations in other areas. Based on the results of these tests, this technique shows considerable promise.

4.5 EFFECT OF EXTERNAL STORES ON LONGITUDINAL CONTROL

Longitudinal control derivatives $C_{m_{\delta_s}}$ (elevator power) and $C_{L_{\delta_s}}$ (elevator lift effectiveness) at the selected trim conditions are presented in Figs. 68 through 74 for configurations 1, 2, 5, 6, 7, 8, and 12 as a function of Mach number, altitude, and cg location. A comparison of these data for configurations 1, 6, and 12 at a cg location of 0.33C is presented in Fig. 75. These data show that the effect of the external stores on the elevator power and elevator lift effectiveness was generally small for the configurations tested; however, some large gradients do occur with changes in Mach number from Mach number 0.9 to 1.1.

SECTION V
CONCLUSIONS

Wind tunnel tests were conducted using a 0.05-scale model of the F-4C aircraft configured with various external stores. The data from these tests were analyzed, and the following conclusions were reached:

1. The data presented show the change in stabilator trim angle and increased longitudinal stability associated with "tuck-under" when the F-4C is configured with the Pavestorm missiles and 370-gal fuel tanks. Moreover, the results indicate a substantial reduction in static margin with the Pavestorm stores at an altitude of 10,000 ft at Mach number 0.975, as compared to the clean aircraft. In general, only the configurations with the Pavestorm stores displayed large variations in the neutral-point location at the transonic Mach numbers.

2. Large negative changes in the value of pitching-moment coefficient at zero lift were observed at the transonic Mach numbers when wing-mounted stores were added to the clean configuration. From the downwash analysis of the Pavestorm I and the M-118 LGB it was apparent that the predominant contribution to the increment of change noted in C_{m_o} was the wing-body contribution. For the SUU-51B/B, the horizontal tail and the wing-body contributions were equal and opposite at Mach numbers less than 0.975, resulting in essentially no change in C_{m_o} when the F-4C was configured with these stores. At Mach number 0.975, the tail contribution was equal to the wing-body contribution, producing a large negative shift in C_{m_o}. Comparison of data for configurations with and without stores on the fuselage centerline imply that adding stores to the aircraft centerline could be beneficial in terms of eliminating or reducing adverse handling characteristics such as tuck-under and large static-margin changes in the transonic Mach number range.

3. A comparison of two prediction techniques showed that each technique predicted neutral-point shifts and drag rise caused by adding external stores to the F-4C to about the same degree of accuracy. However, neither technique predicted the gross reduction in static stability that was observed in the wind tunnel tests at Mach number 0.975.

REFERENCES

1. Test Facilities Handbook (Ninth Edition). "Propulsion Wind Tunnel Facility, Vol. 4." Arnold Engineering Development Center, July 1971.

2. Akima, Hiroshi. "A New Method of Interpolation and Smooth Curve Fitting Based on Local Procedures." Journal of the Association for Computing Machinery, Vol. 17, No. 4, October 1970, pp. 589-602.

3. Abbot, Ira H. and von Doenhoff, Albert E. Theory of Wing Sections. Dover Publications, New York, 1959.

4. Twinting, William T. and Williams, George H. "F-4C Category II Stability and Control Test." AFATL-TR-65-30, Eglin AFB, Florida, December 1965.

5. Weber, William B. "Effect of External Stores on the Stability, Control and Drag Characteristics of the McDonnell Douglas F-4 Aircraft." Aircraft/Stores Compatibility Symposium Proceedings, Vol. III, Eglin AFB, 1969, pp. 28-54.

6. Dyer, R. D. and Gallagher, R. D. "Technique for Predicting External Store Aerodynamic Effects on Aircraft Performance." Aircraft/Stores Compatibility Symposium Proceedings, Vol. I, Dayton, Ohio, 1972, pp. 115-141.

7. Model F/RF-4B-C Aerodynamic Derivatives, McDonnell Aircraft Corporation Report 9842, Revised 10 Dec 1971, p. 4.35.

APPENDIXES

I. ILLUSTRATIONS
II. TABLE

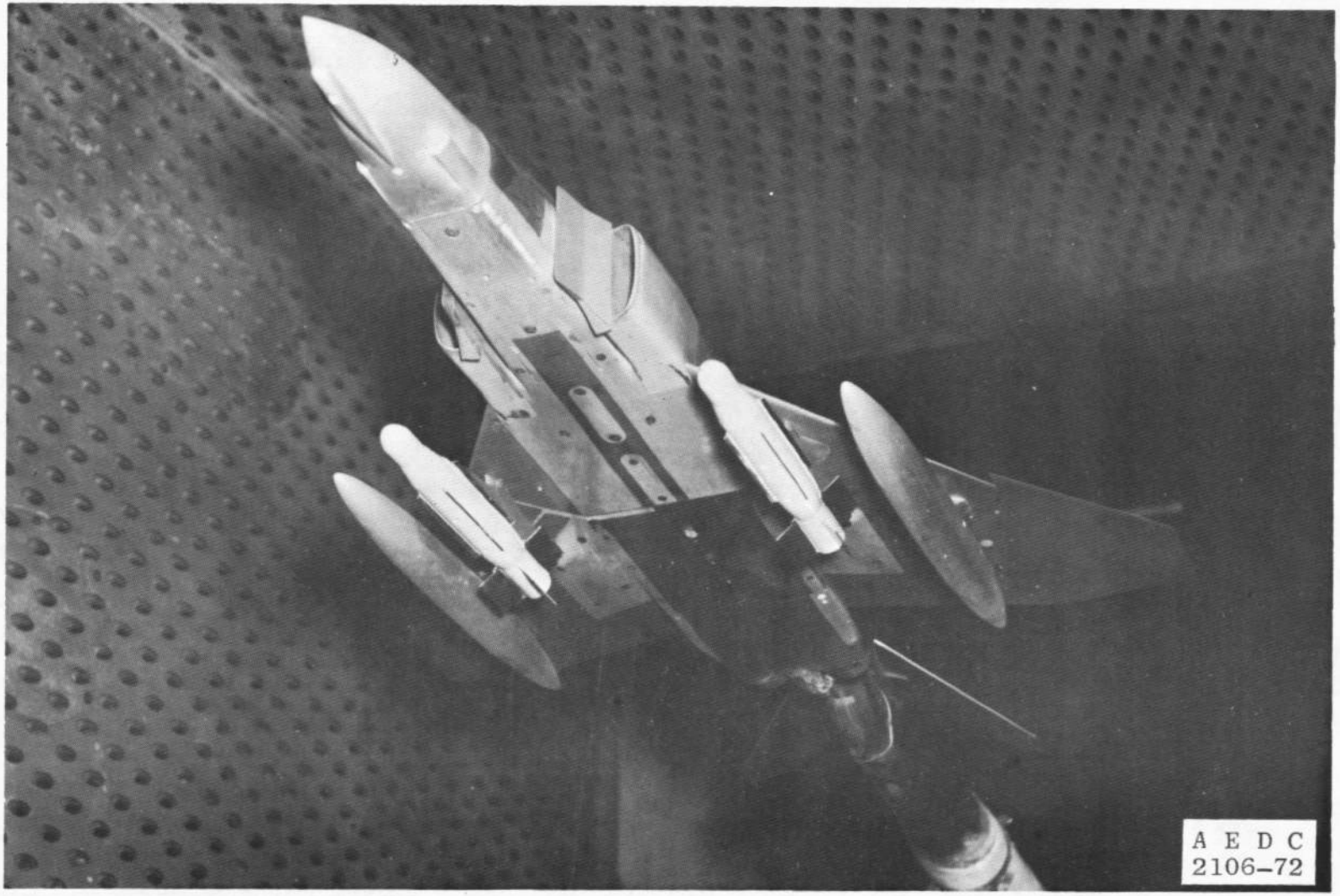

Fig. 1 Wind Tunnel Installation of the F-4C Model Configuration with Pavestorm II Stores and 370-gal Fuel Tanks

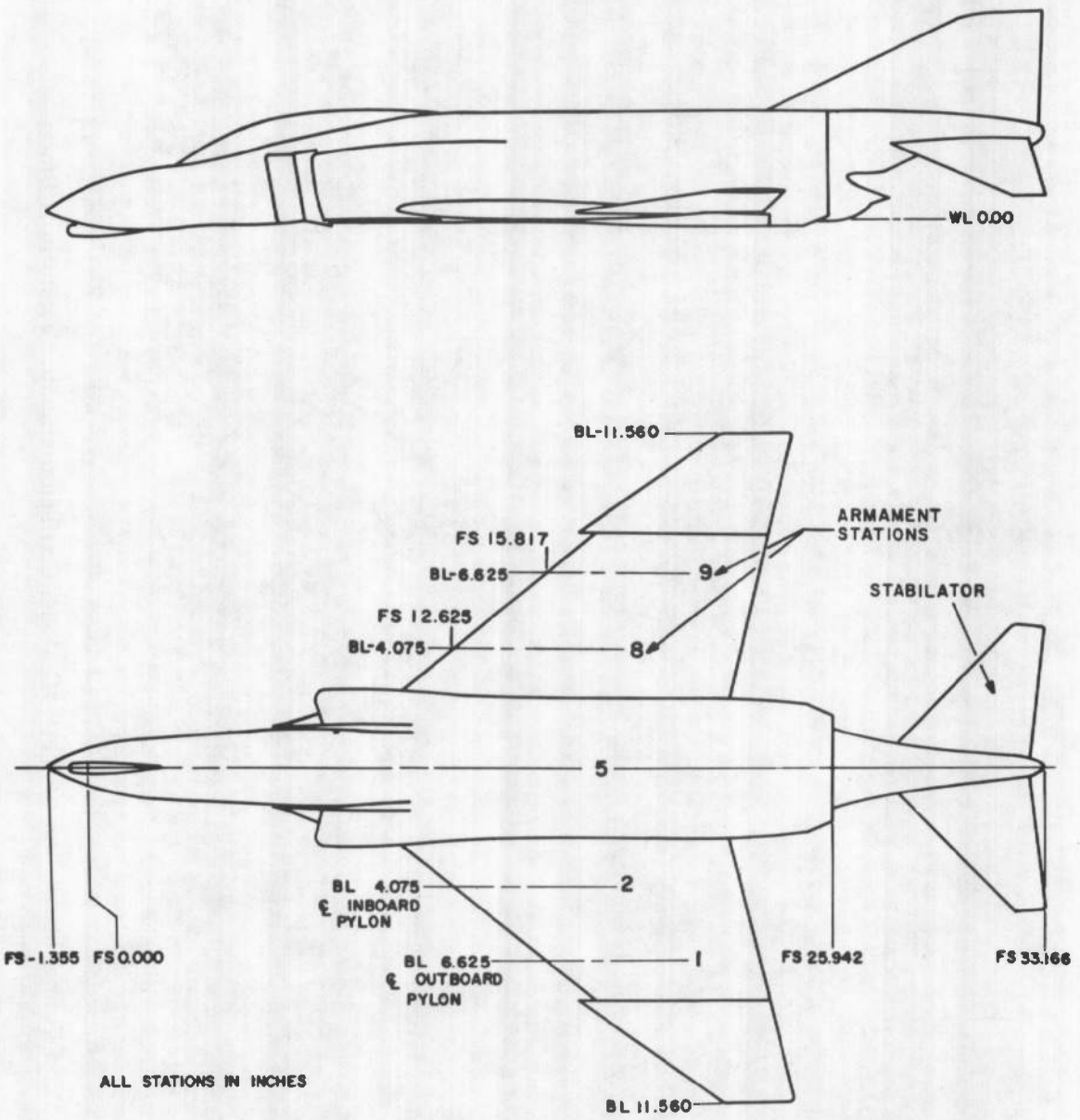

Fig. 2 Sketch of Wind Tunnel Model of F-4C

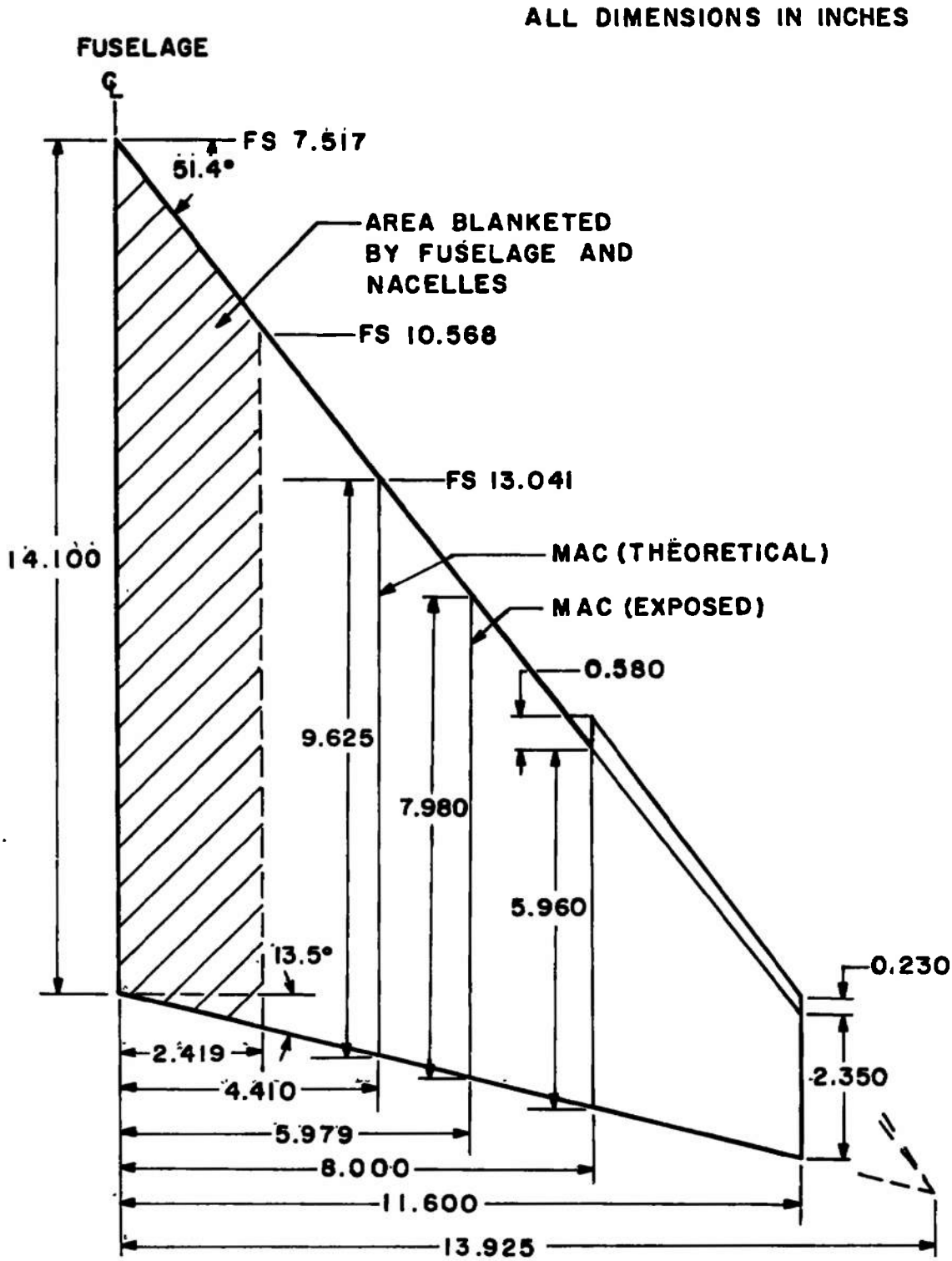

Fig. 3 Sketch of F-4C Wind Tunnel Model Wing Panel

ALL DIMENSIONS IN INCHES

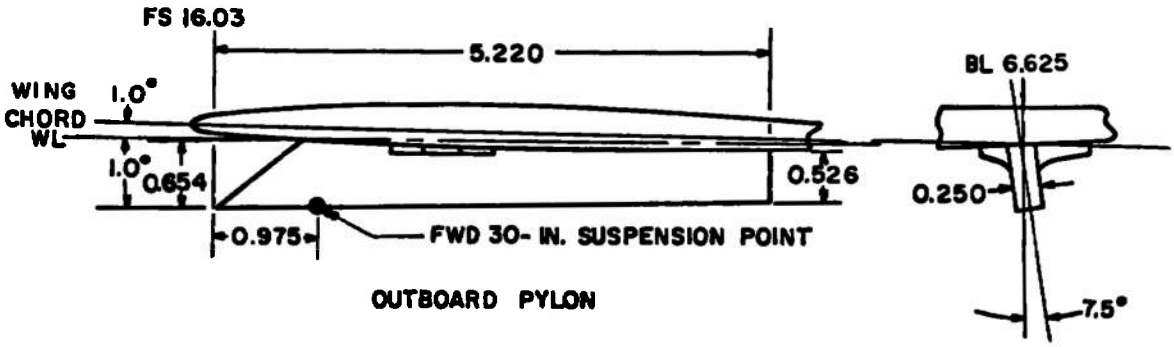

OUTBOARD PYLON

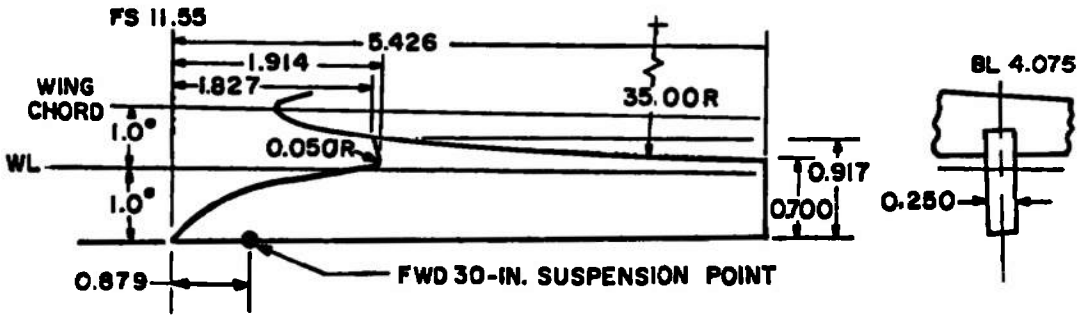

INBOARD PYLON

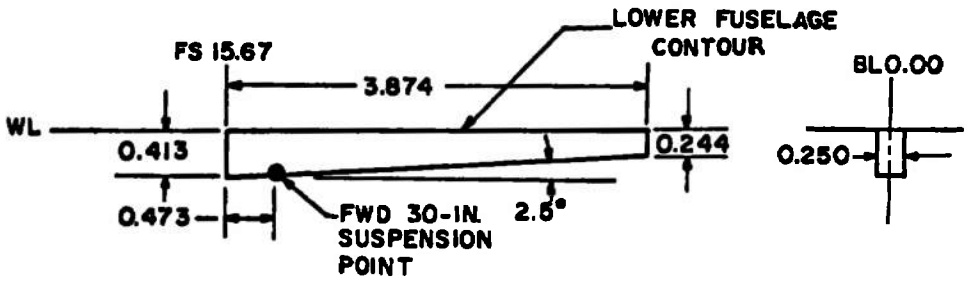

CENTERLINE MER ADAPTOR

Fig. 4 F-4C Armament Suspension Equipment

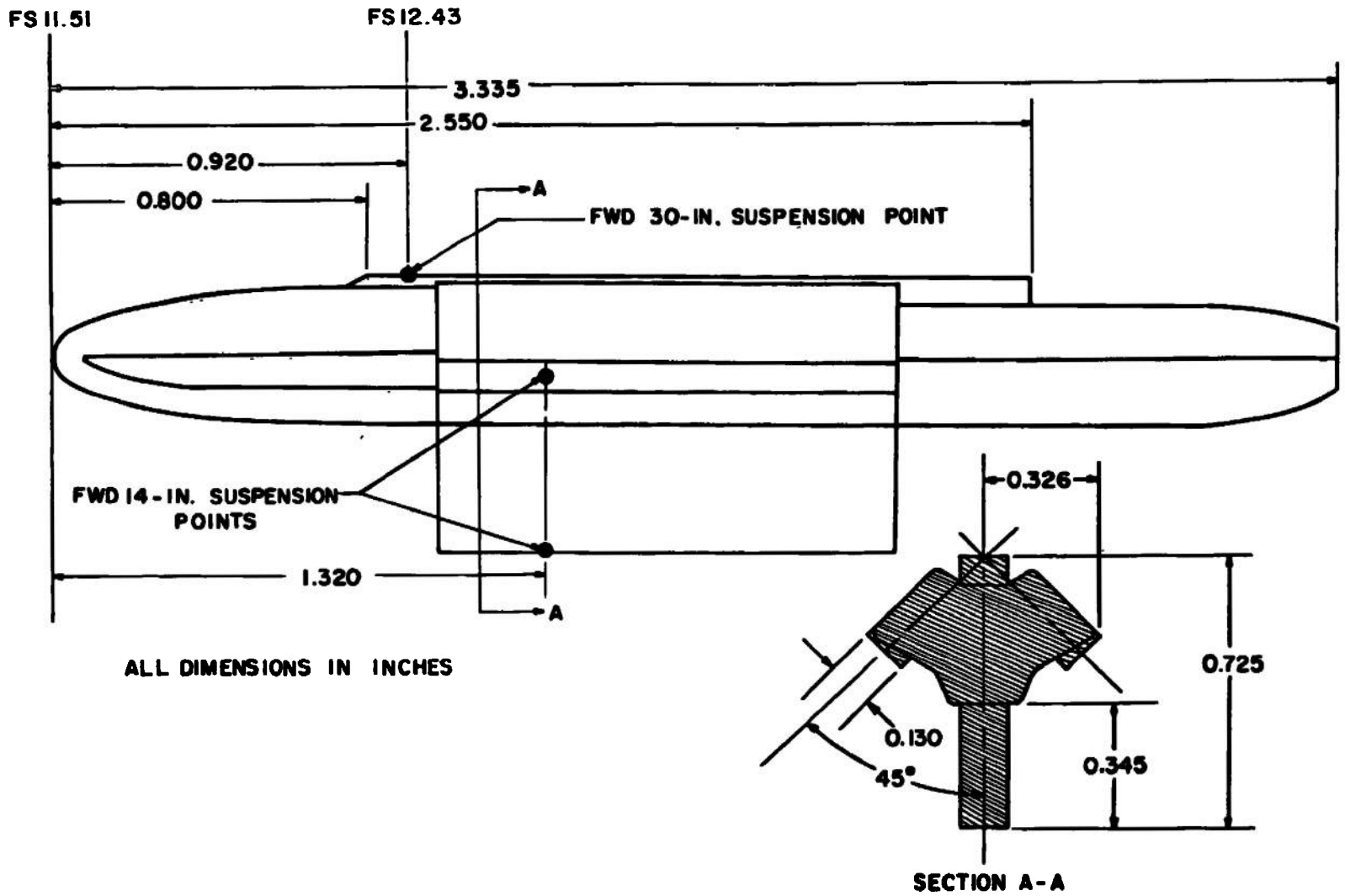

Fig. 5 Triple Ejection Rack

FORWARD SHIFTED
FS 12.307

ALL DIMENSIONS IN INCHES

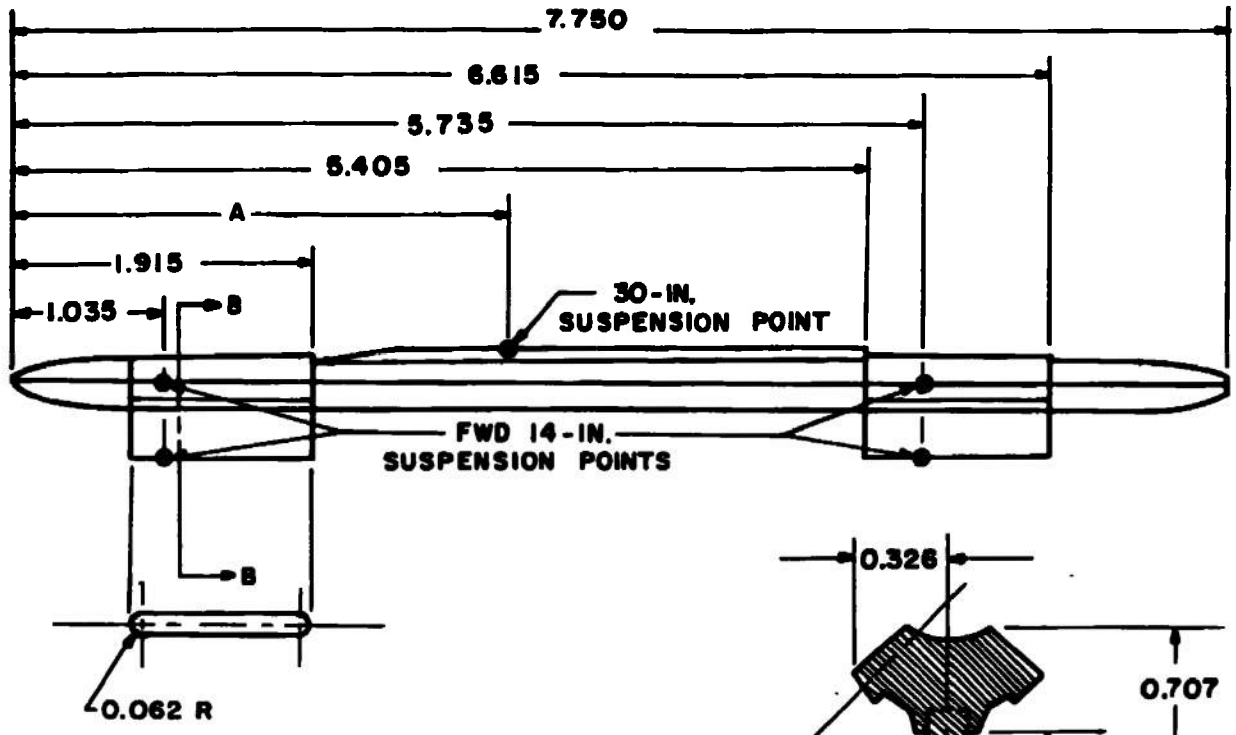

DIMENSION "A"		
WING STATION	FORWARD SHIFTED	AFT SHIFTED
OUTBOARD	3.453	2.336
℄	3.836	2.685

Fig. 6 Multiple Ejection Rack

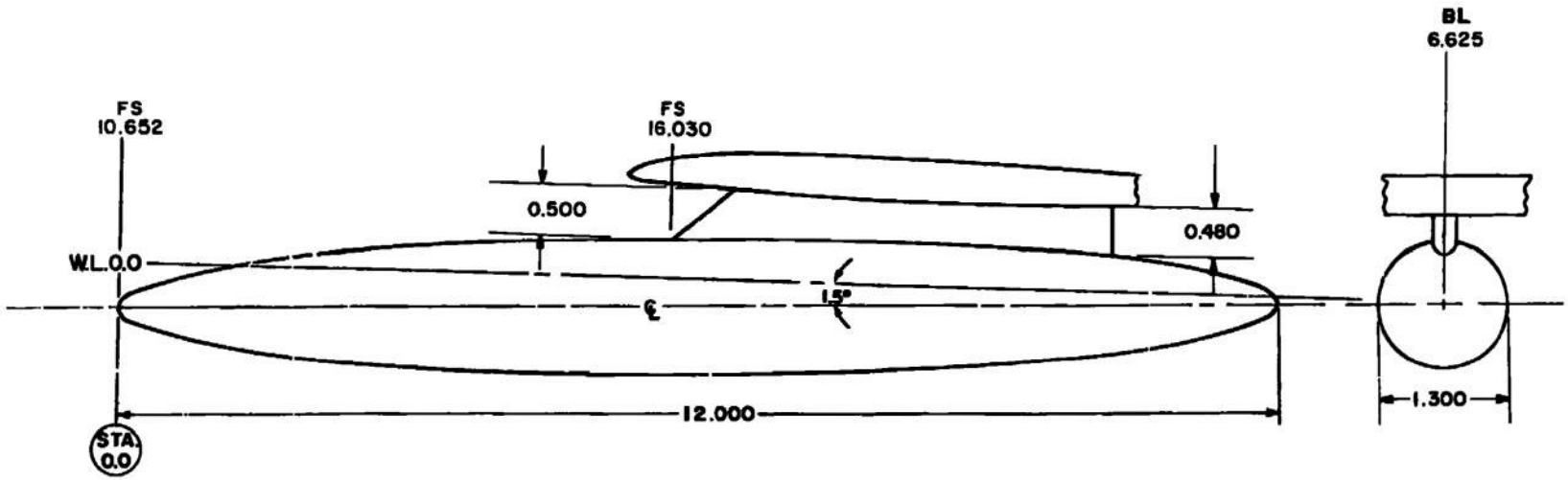

NOTE: MODEL STATIONS AND DIMENSIONS IN INCHES

BODY CONTOUR, TYPICAL BOTH ENDS

STATION	BODY DIAM	STATION	BODY DIAM
0.000	0.000	2.500	1.116
0.025	0.100	2.750	1.156
0.050	0.144	3.000	1.190
0.150	0.258	3.250	1.218
0.250	0.340	3.500	1.242
0.500	0.498	3.750	1.260
0.750	0.622	4.000	1.274
1.000	0.724	4.250	1.286
1.250	0.812	4.500	1.294
1.500	0.890	4.750	1.298
1.750	0.958	5.000	1.300
2.000	1.016	6.000	1.300
2.250	1.070		

Fig. 7 F-4C 370-gal Fuel Tank

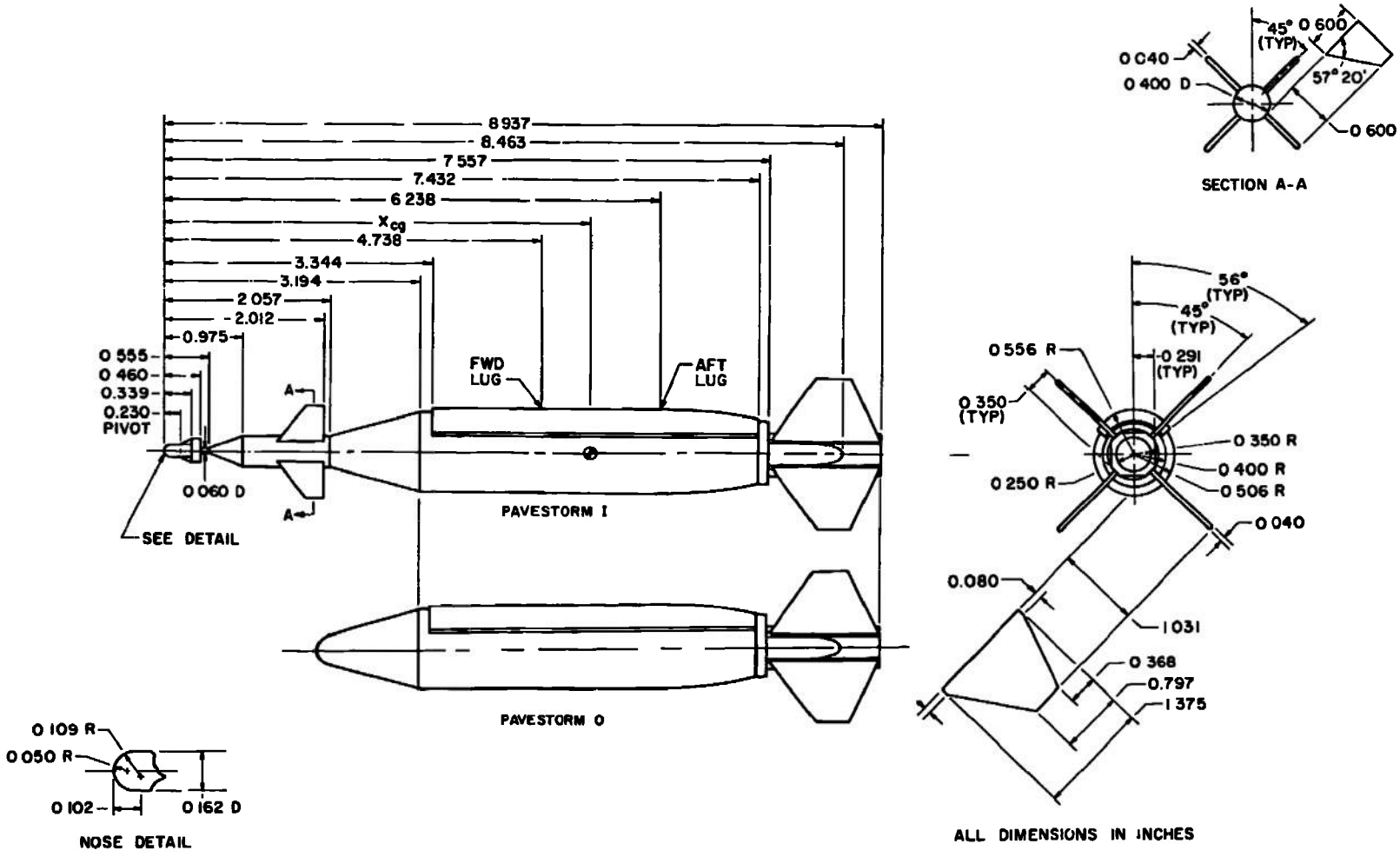

Fig. 8 Pavestorm 0 and Pavestorm I Stores

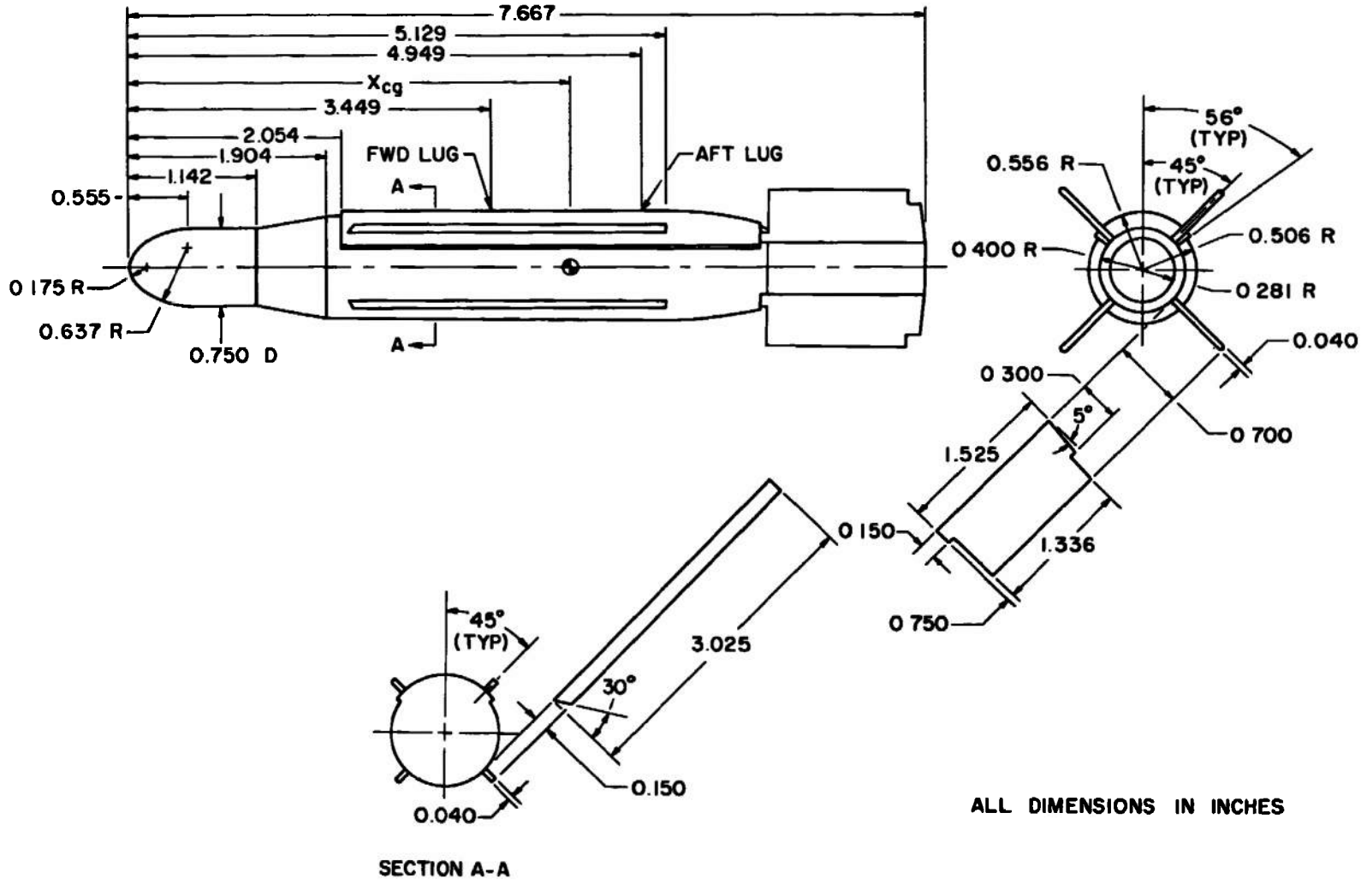

Fig. 9 Pavestorm II Store

ALL DIMENSIONS IN INCHES

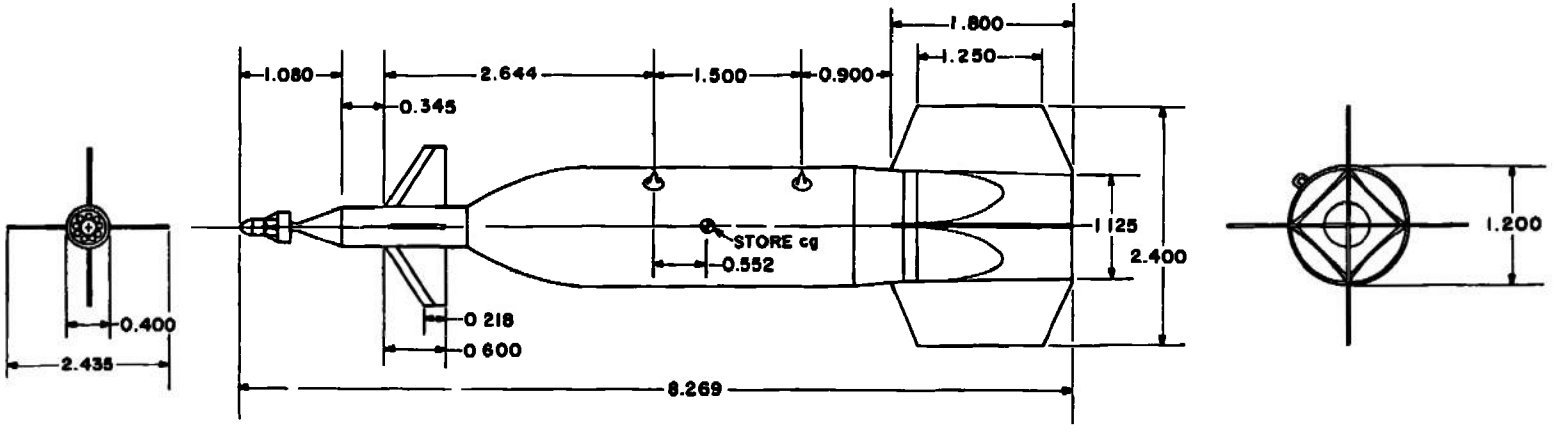

Fig. 10 M-118 Laser Guided Bomb Store

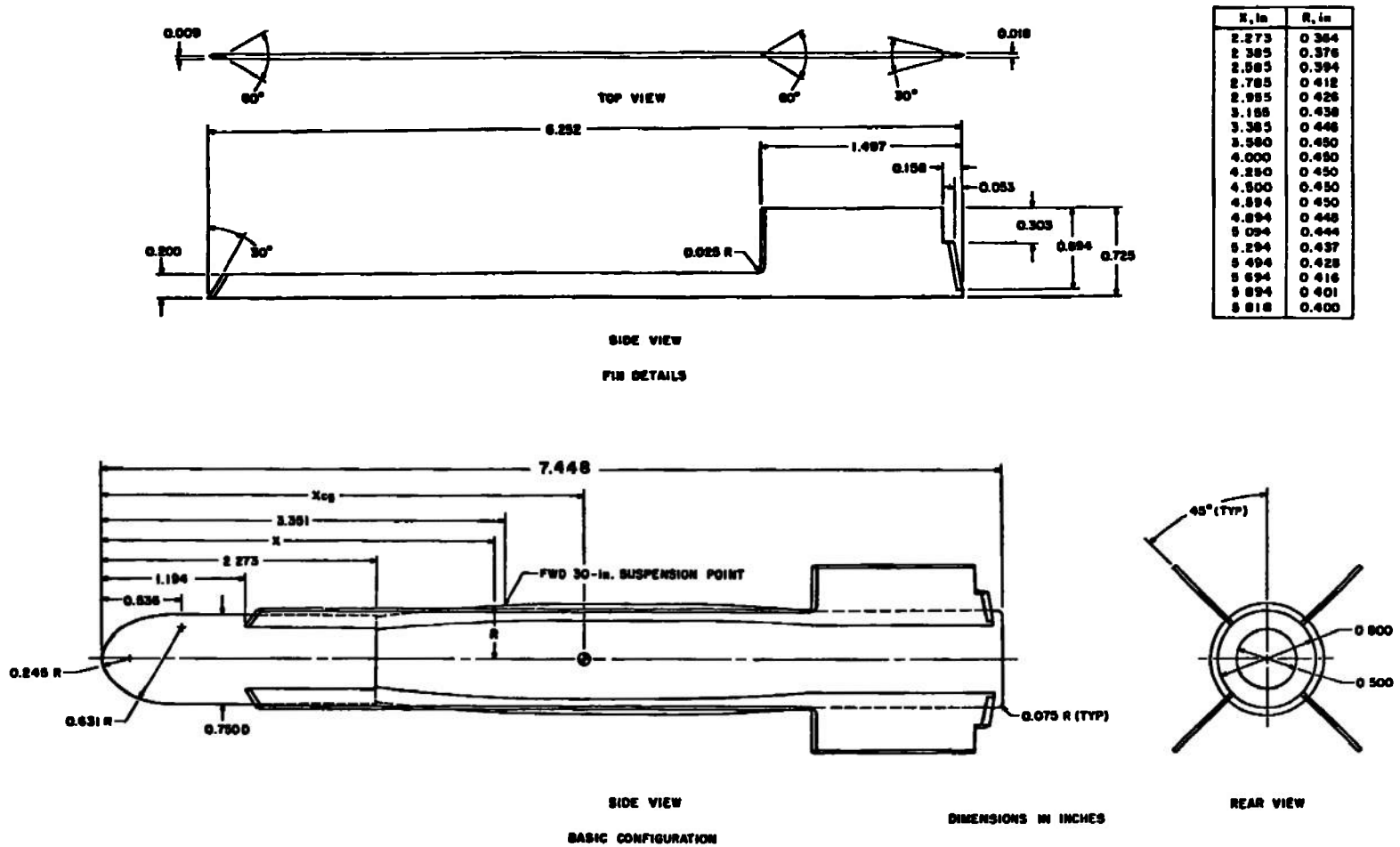

X, in	R, in
2.273	0.364
2.385	0.376
2.585	0.394
2.785	0.412
2.985	0.426
3.185	0.438
3.385	0.446
3.585	0.450
4.000	0.450
4.250	0.450
4.500	0.450
4.894	0.450
4.894	0.448
5.094	0.444
5.294	0.437
5.494	0.428
5.694	0.416
5.894	0.401
5.818	0.400

Fig. 11 MK 84 Electro-Optical Guided Bomb

ALL DIMENSIONS IN INCHES

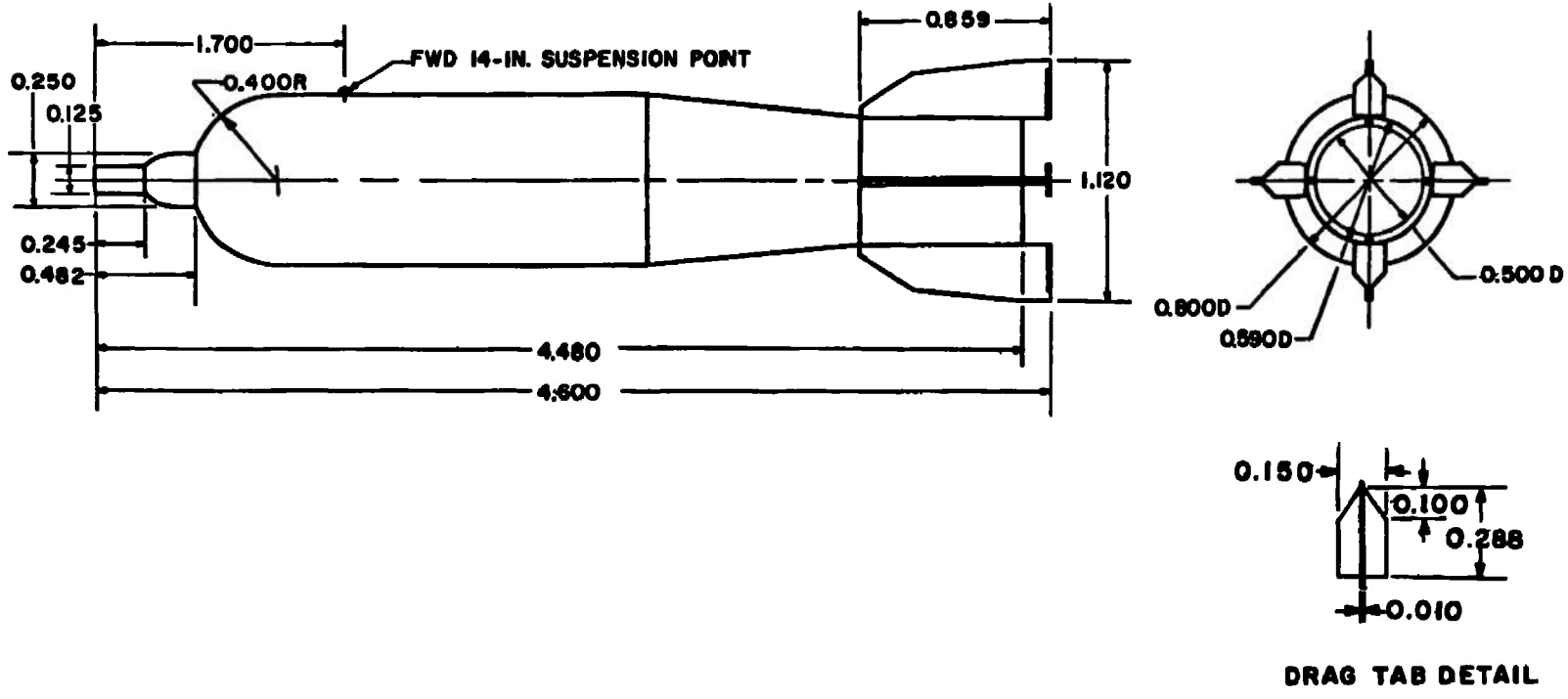

Fig. 12 SUU-30H/B Store

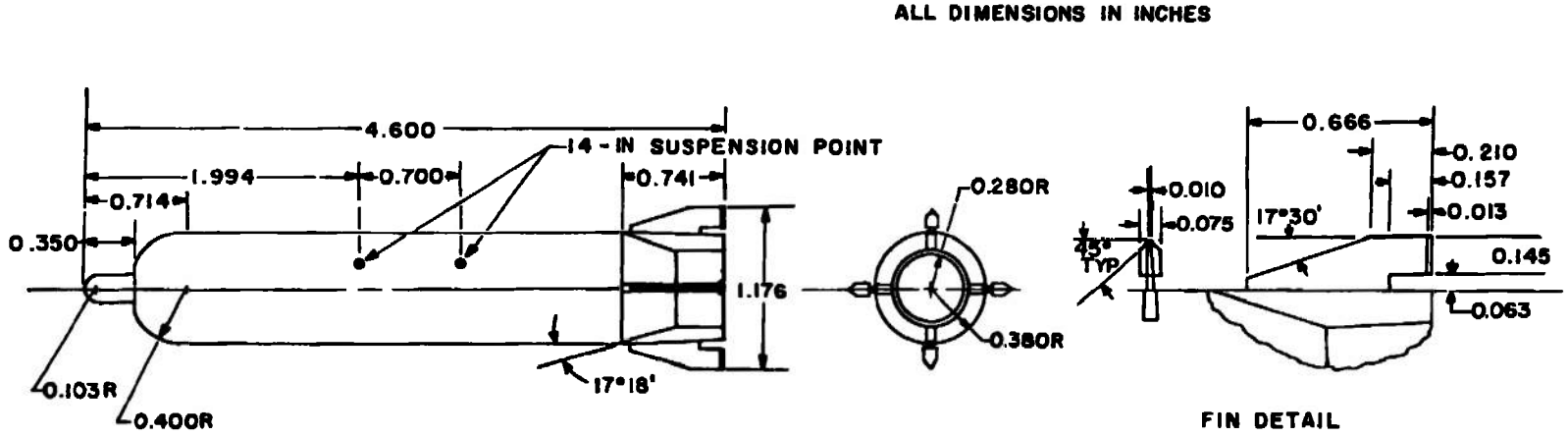

Fig. 13 SUU-51B/B Store

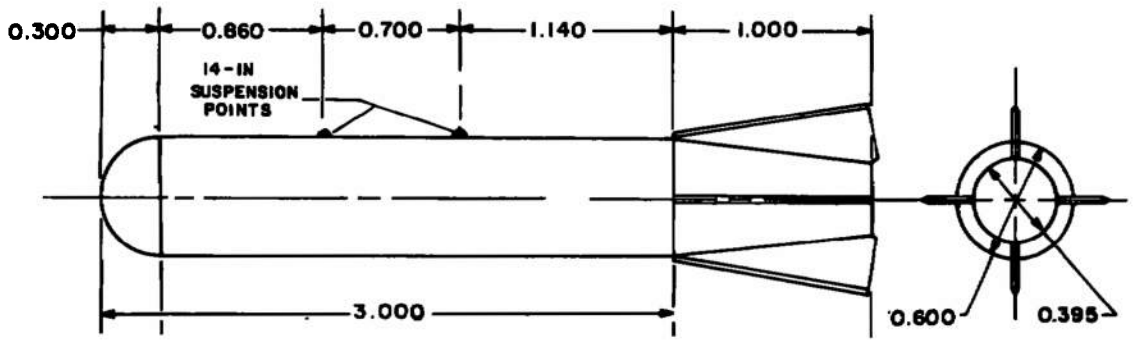

a. N1T2

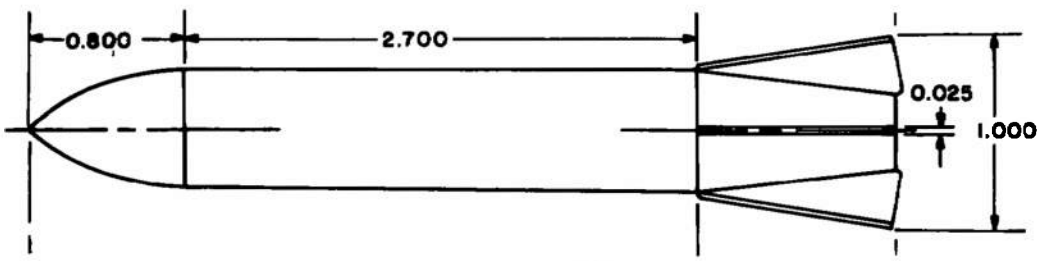

b. N2T2

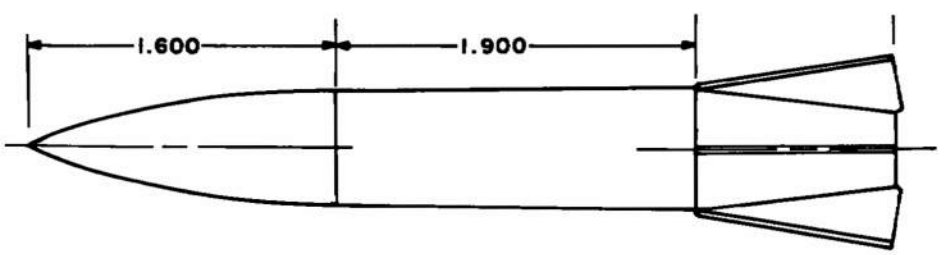

c. N3T2

Fig. 14 Modular Weapons Stores

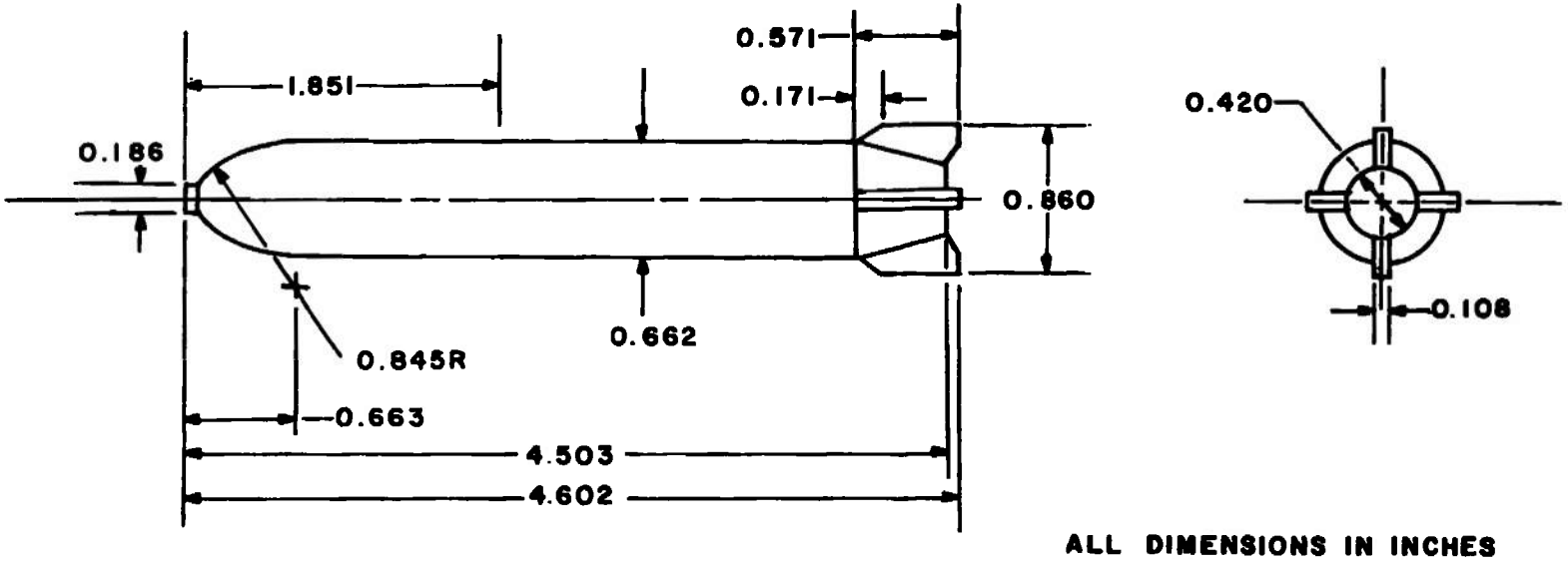

Fig. 15 Rockeye Store

NOTE: PYLONS ARE SHOWN ON AIRCRAFT PROFILE ONLY TO INDICATE ARMAMENT STATIONS

CONFIG NO.	EXTERNAL ARMAMENT	ARMAMENT PROFILE	ARMAMENT STATIONS 1	2	3	4	5
1	NONE	NONE	CLEAN	CLEAN	CLEAN	CLEAN	CLEAN
2	370 GALLON FUEL TANK NONE			PYLON	CLEAN	PYLON	
3	370 GALLON FUEL TANK NONE			▽	CLEAN	▽	
4	370 GALLON FUEL TANK NONE			▽	▽ FWD ▽ AFT	▽	
5	370 GALLON FUEL TANK PAVESTORM O			☼	CLEAN	☼	
6	370 GALLON FUEL TANK PAVESTORM I			☼	CLEAN	☼	
7	370 GALLON FUEL TANK PAVESTORM II			☼	CLEAN	☼	
8	370 GALLON FUEL TANK M 88 LGB			☼	CLEAN	☼	
9	370 GALLON FUEL TANK MK84 EOGB			☼	CLEAN	☼	
10	370 GALLON FUEL TANK SUU 30 H/B			☼	CLEAN	☼	
11	370 GALLON FUEL TANK SUU 30 H/B			☼	☼ FWD ☼ AFT	☼	
12	370 GALLON FUEL TANK SUU 30 B/B			☼	☼ FWD ☼ AFT	☼	
13	370 GALLON FUEL TANK MOD WEAPONS R1T2			☼	☼ FWD ☼ AFT	☼	
14	370 GALLON FUEL TANK MOD WEAPONS R2T2			☼	☼ FWD ☼ AFT	☼	
15	370 GALLON FUEL TANK MOD WEAPONS R3T2			☼	☼ FWD ☼ AFT	☼	
16	370 GALLON FUEL TANK ROCKEYE			☼	☼ FWD ☼ AFT	☼	

Fig. 16 F-4C Configuration Identification Key

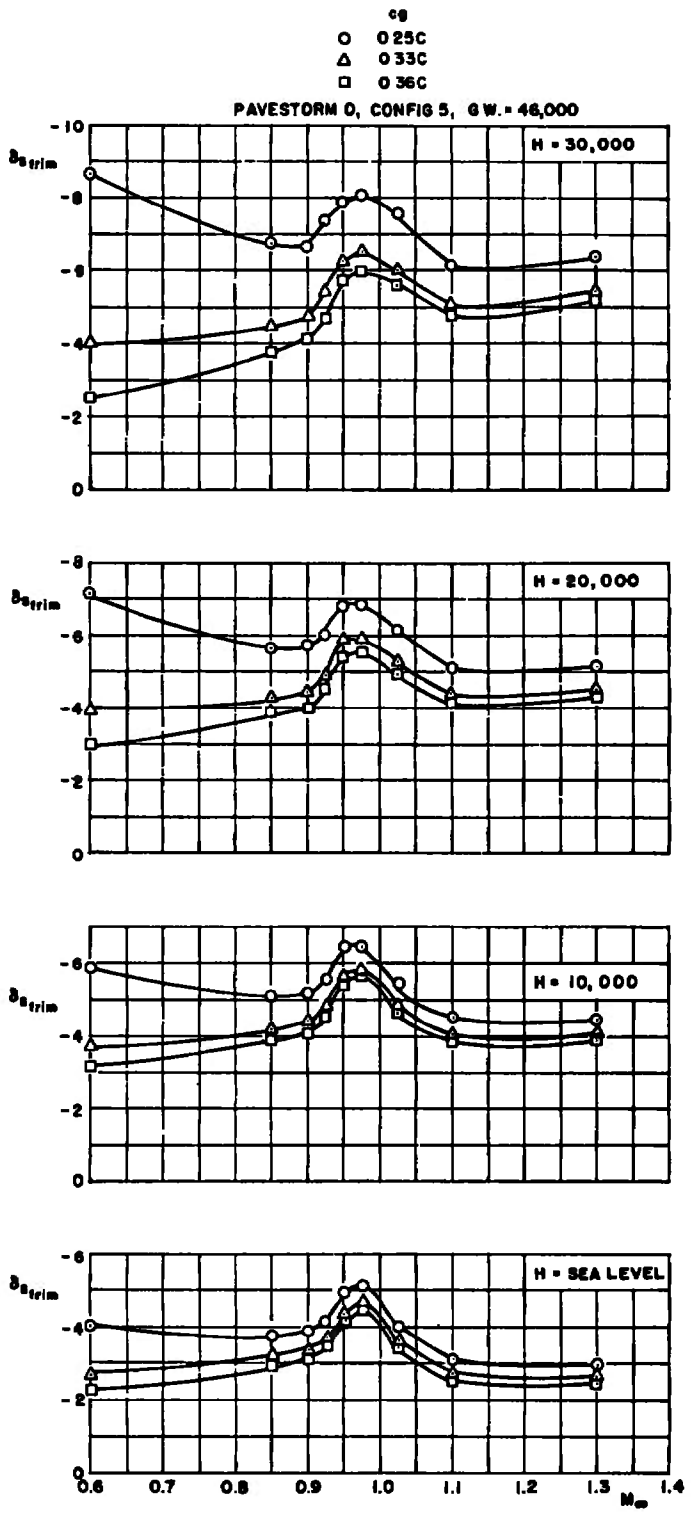

Fig. 17 Trim Stabilator Angle as a Function of Mach Number, Altitude, and cg Location for Configuration 5

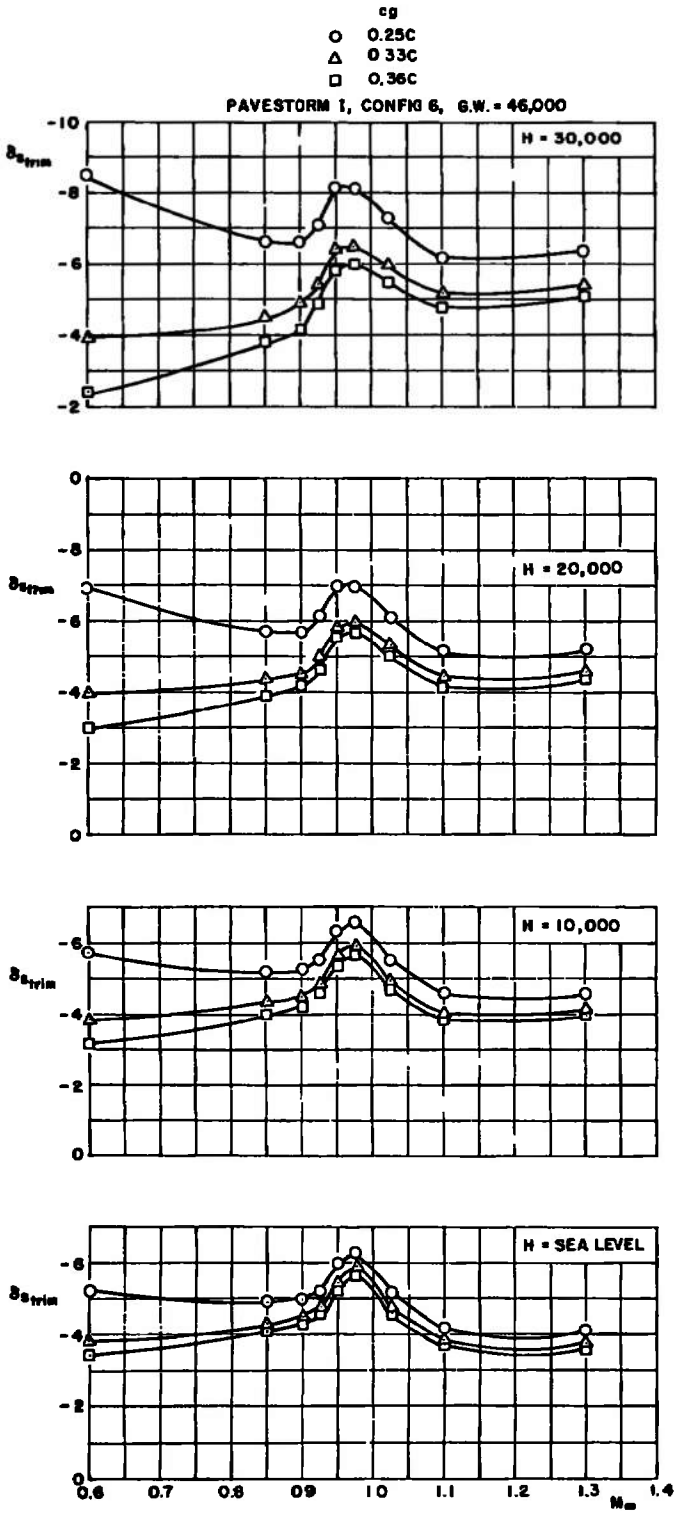

Fig. 18 Trim Stabilator Angle as a Function of Mach Number, Altitude, and cg Location for Configuration 6

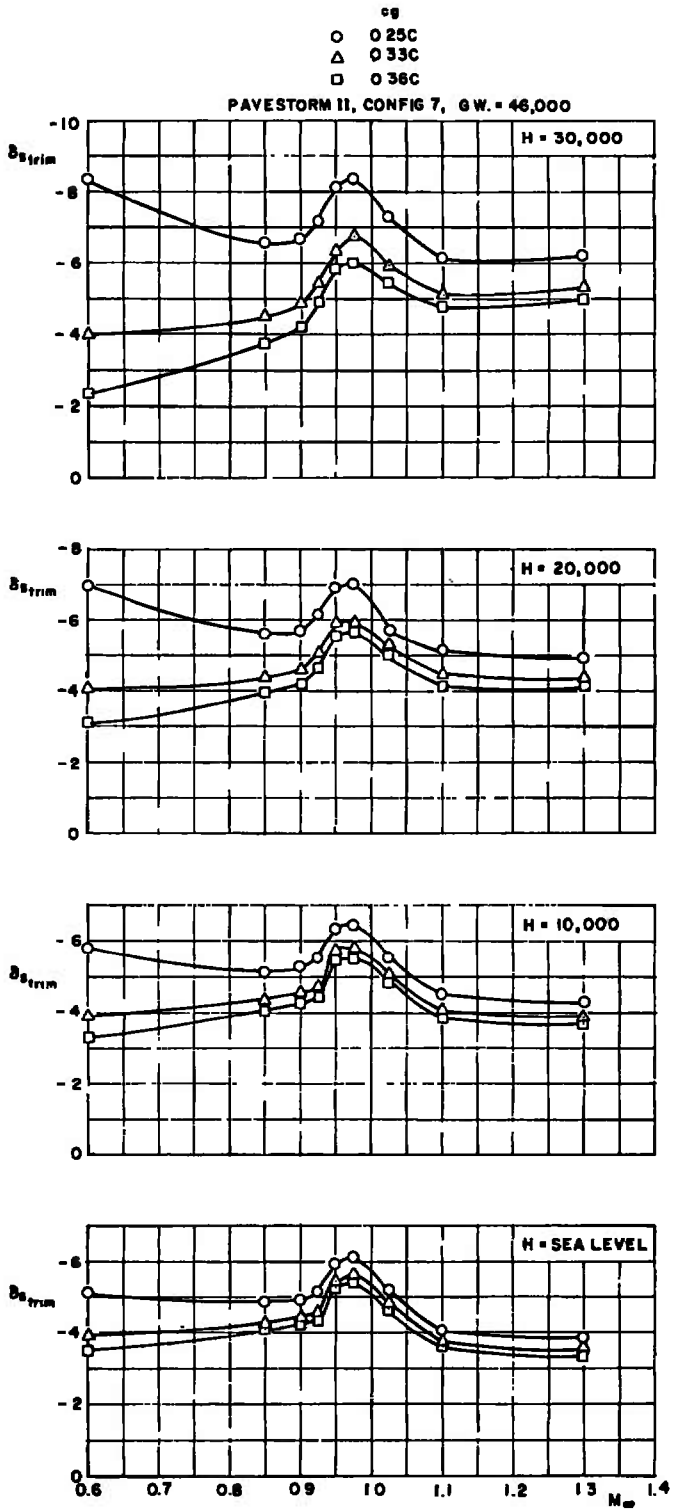

Fig. 19 Trim Stabilator Angle as a Function of Mach Number, Altitude, and cg Location for Configuration 7

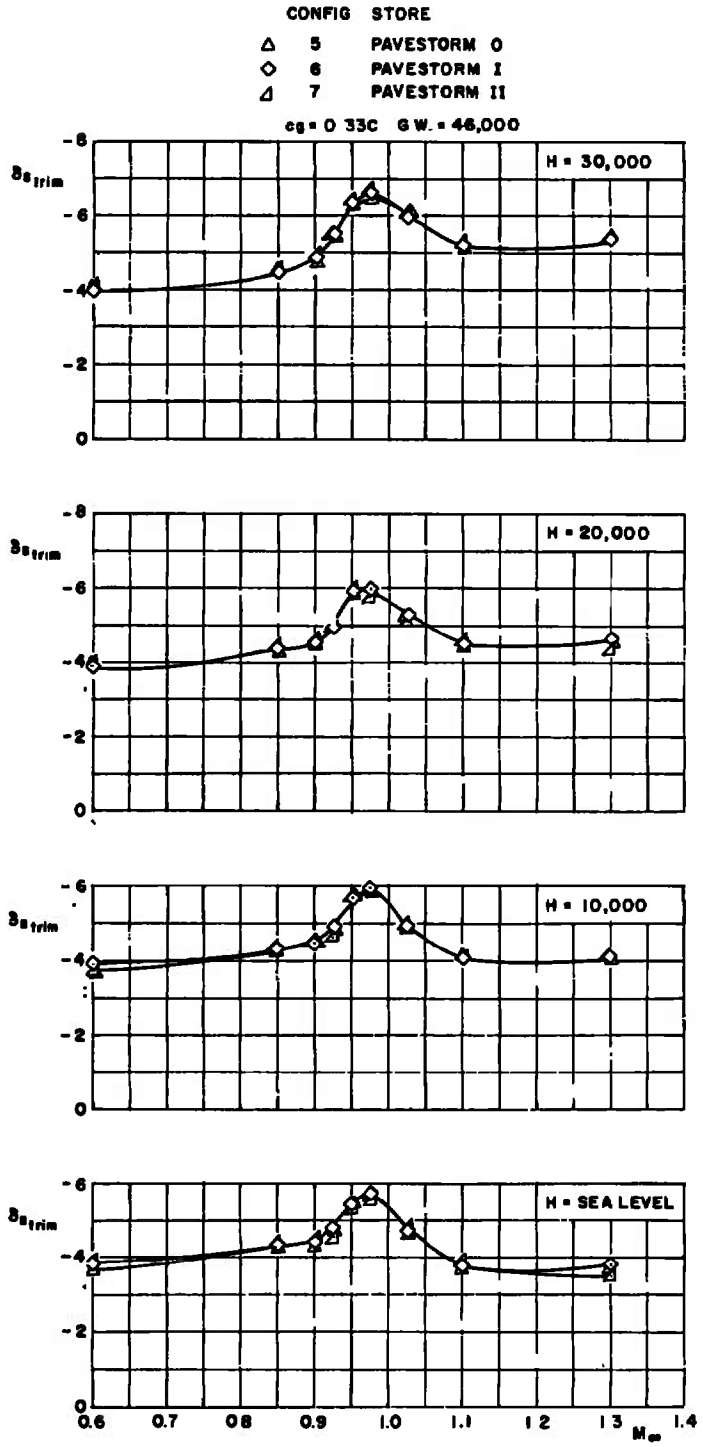

Fig. 20 Comparison of Trim Stabilator Angle as a Function of Mach Number and Altitude for Configurations 5, 6, and 7 at a cg Location of 0.33C

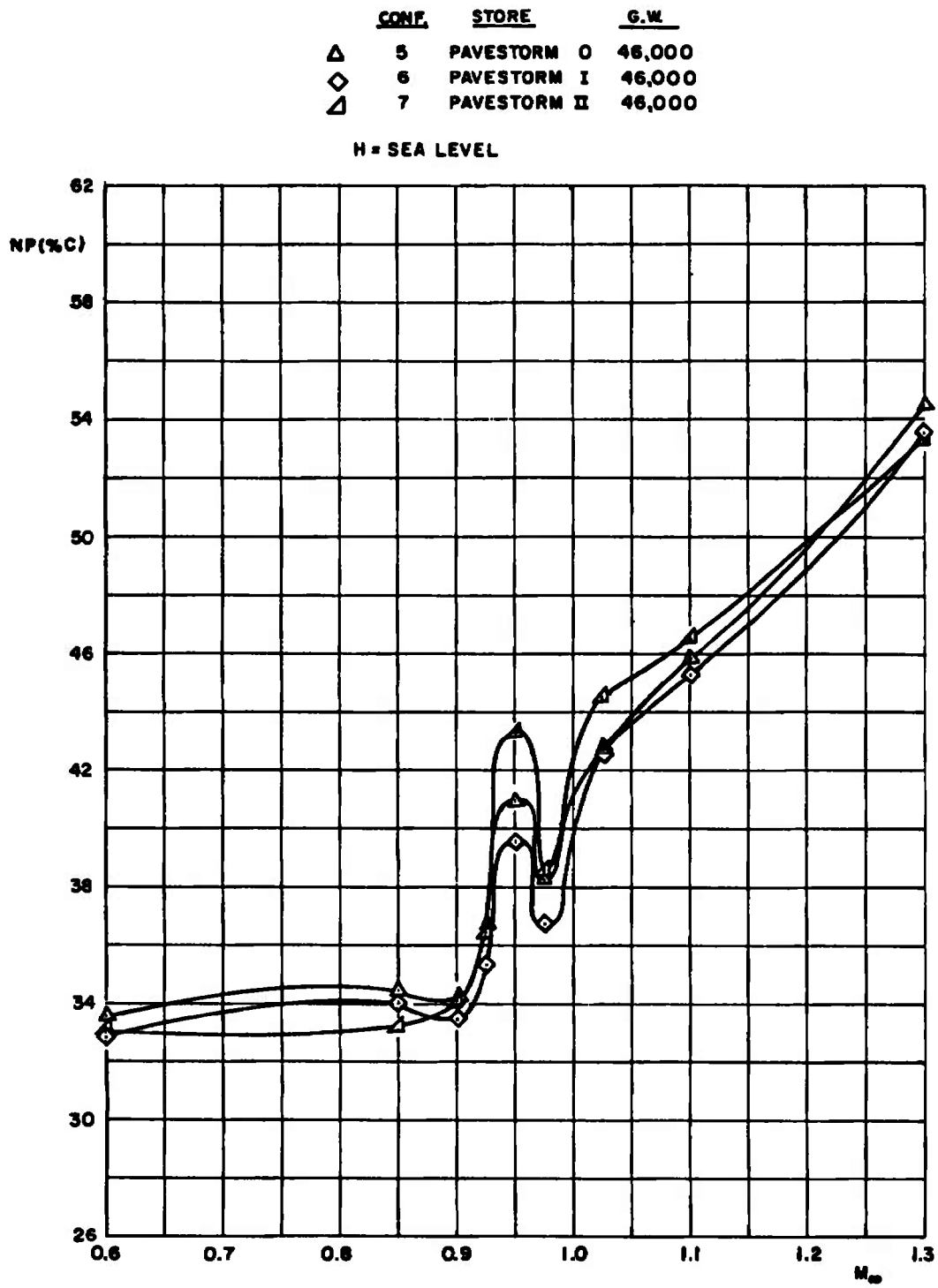

a. H = Sea Level

Fig. 21 Comparison of the Neutral-Point Location as a Function of Mach Number and Altitude for Configurations 5, 6, and 7

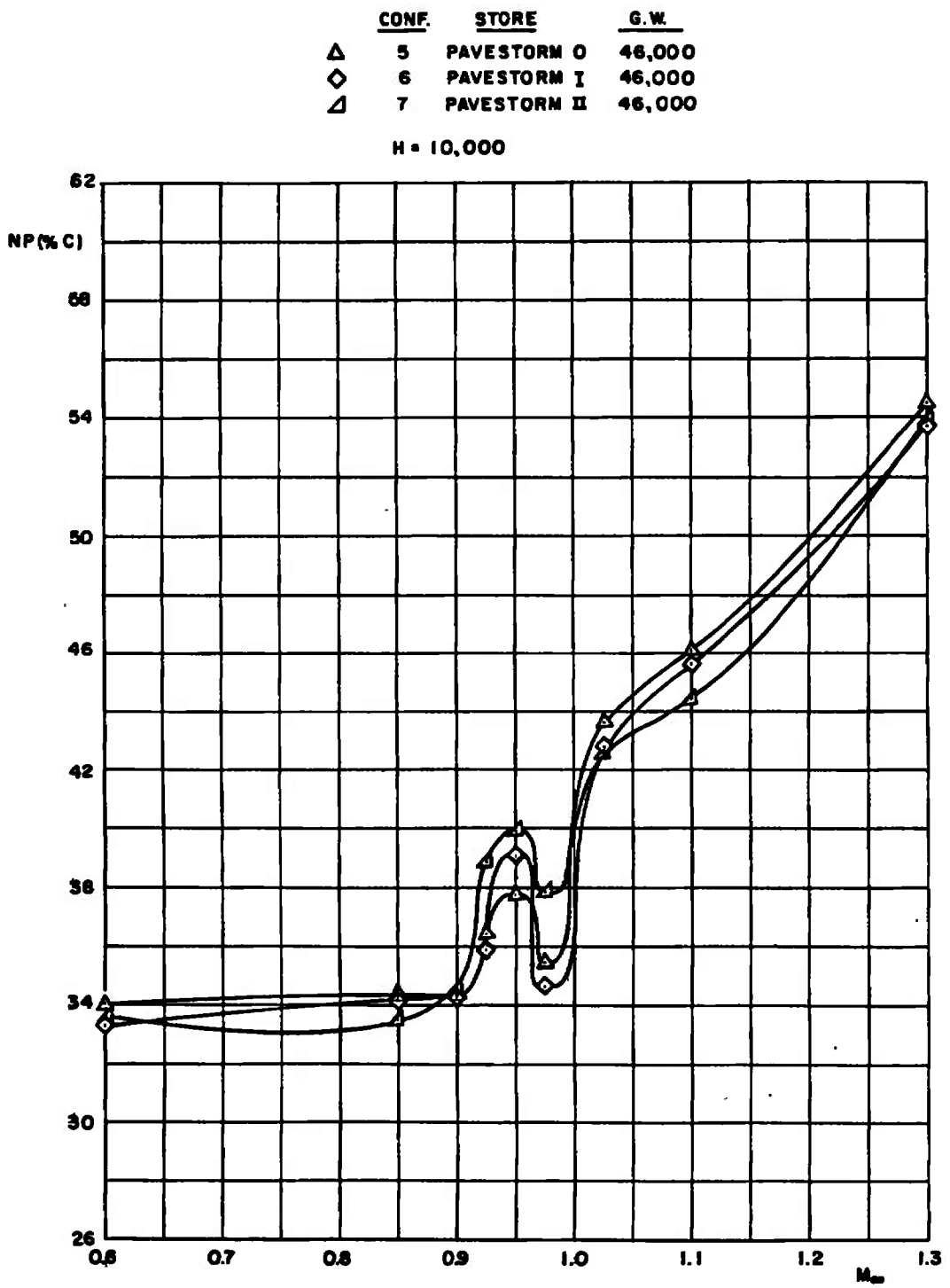

b. H = 10,000 ft
Fig. 21 Continued

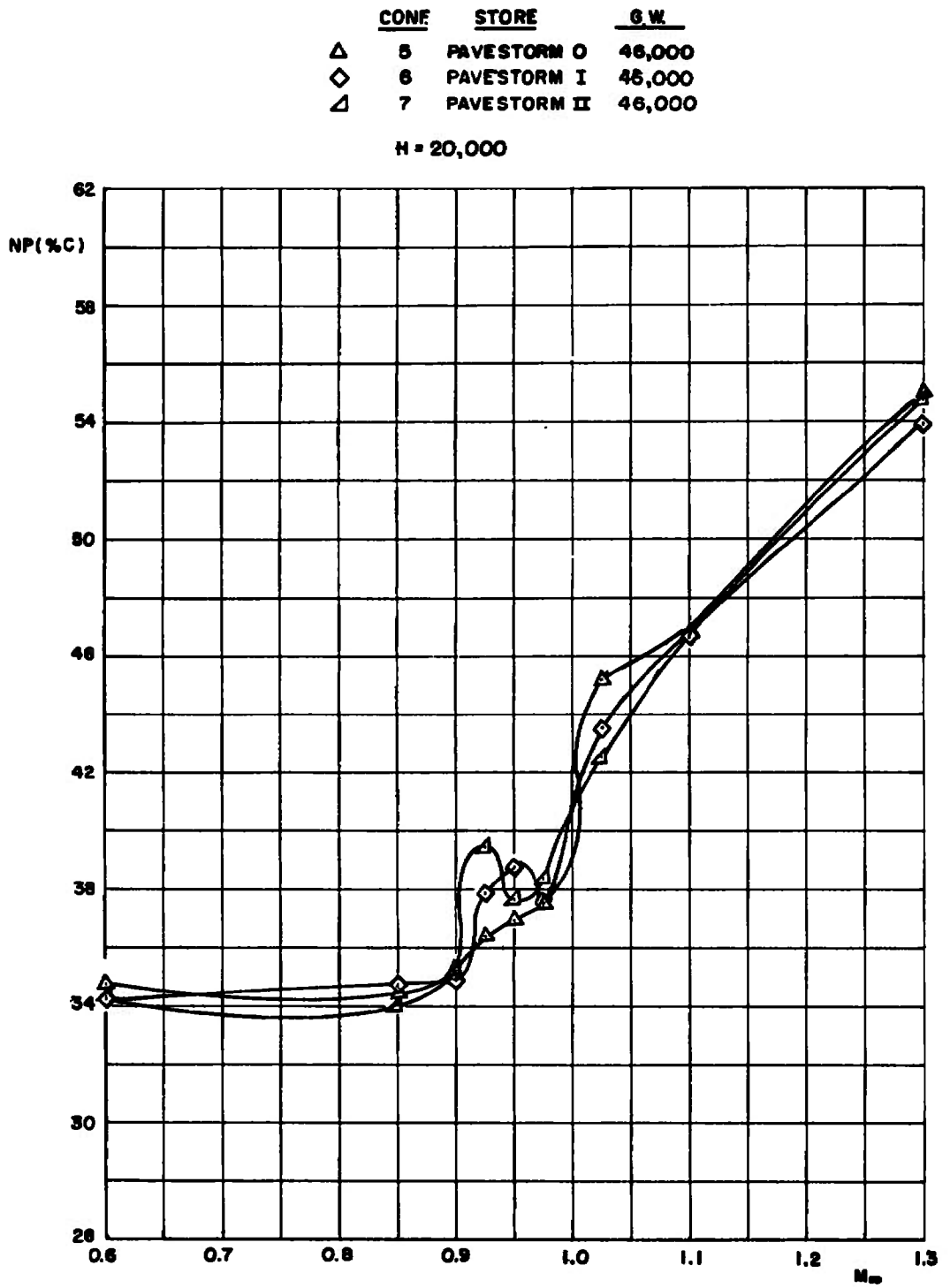

c. H = 20,000 ft
Fig. 21 Continued

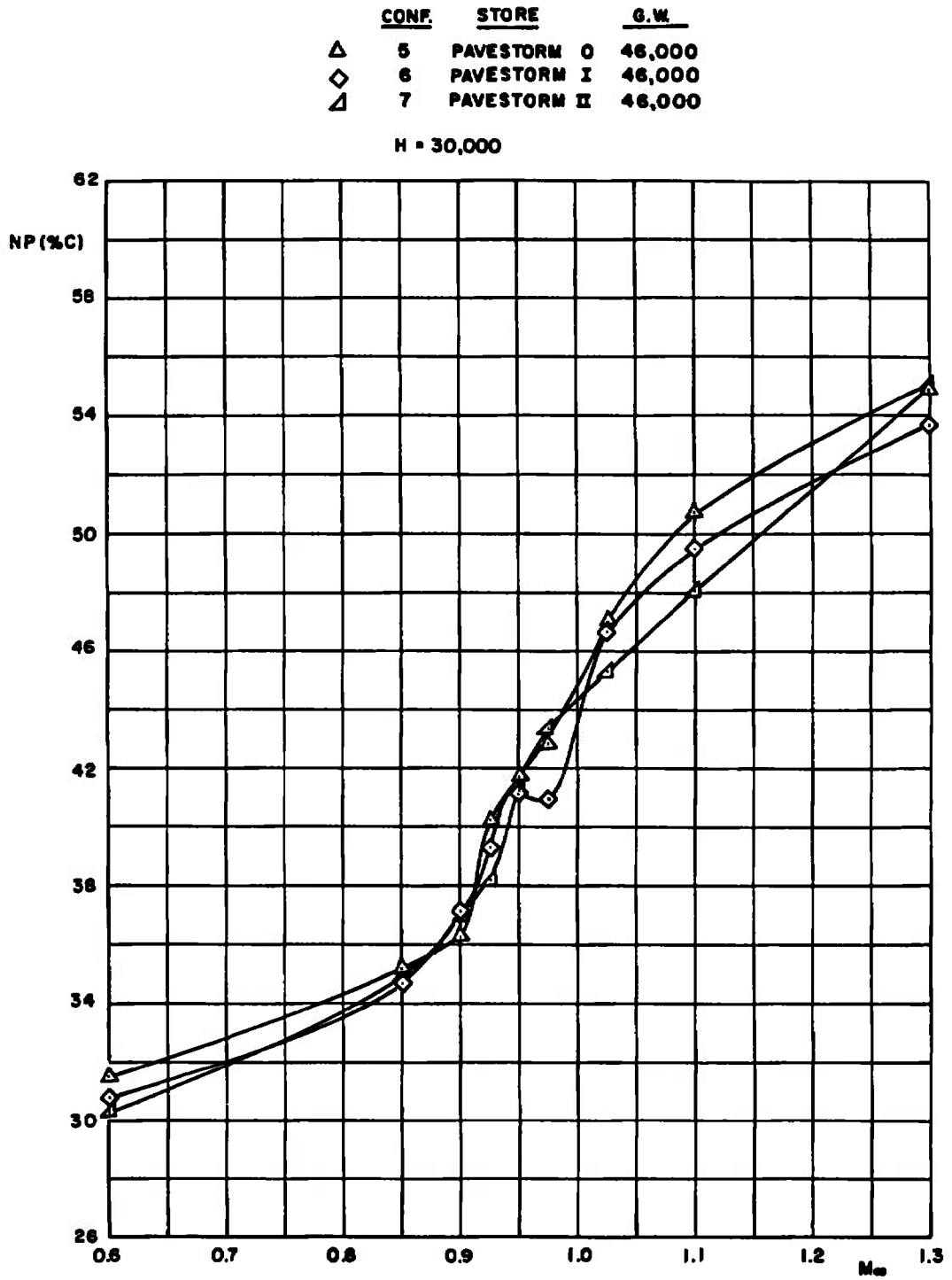

d. H = 30,000 ft
Fig. 21 Concluded

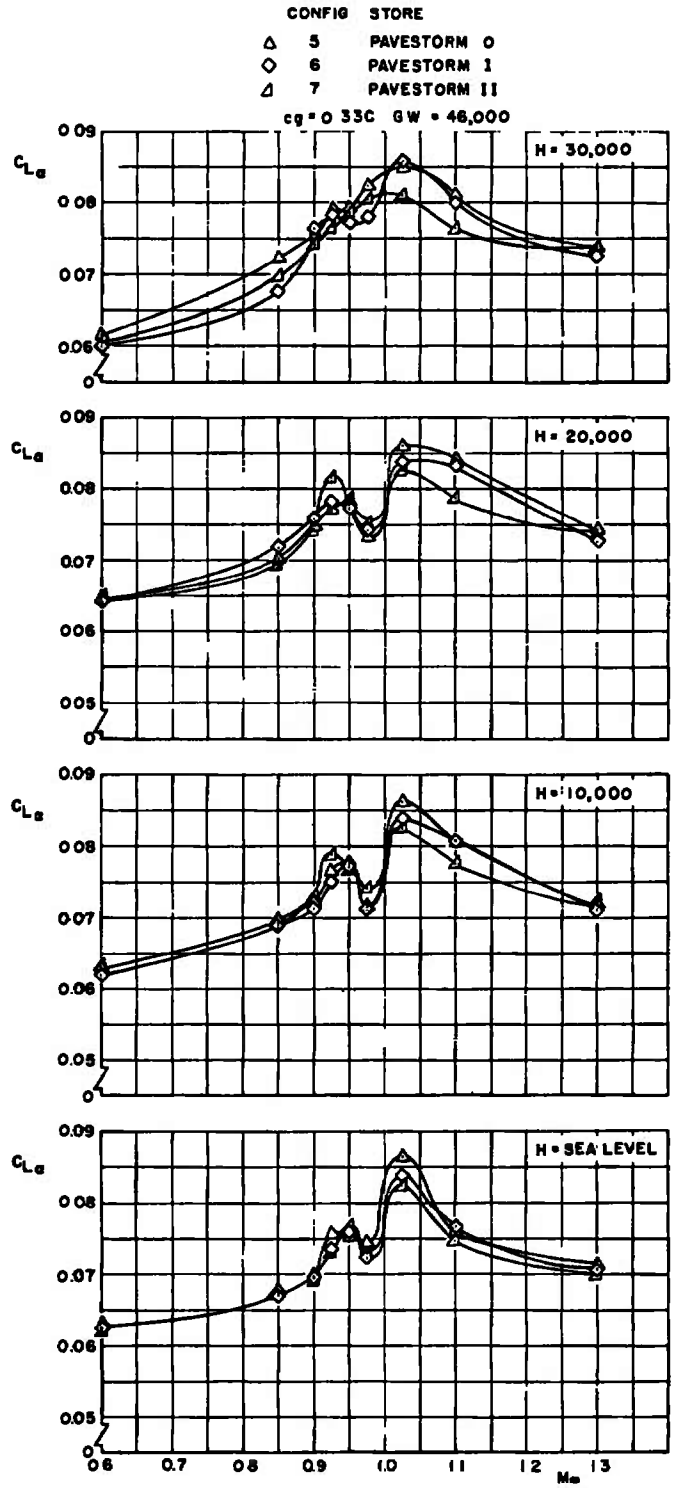

Fig. 22 Lift Curve Slope at Trim as a Function of Mach Number and Altitude for Configurations 5, 6, and 7

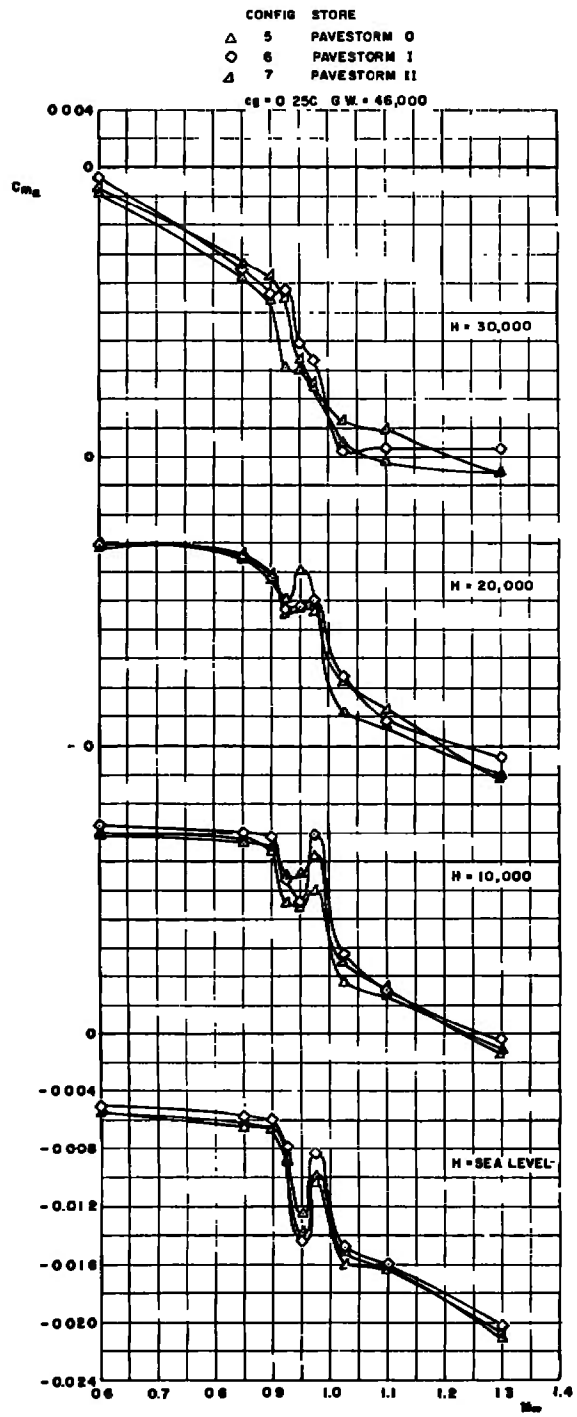

a. cg = 0.25C

Fig. 23 Slope of Pitching-Moment Coefficient versus Angle-of-Attack Curve at Trim as a Function of Mach Number, Altitude, and cg Location for Configurations 5, 6, and 7

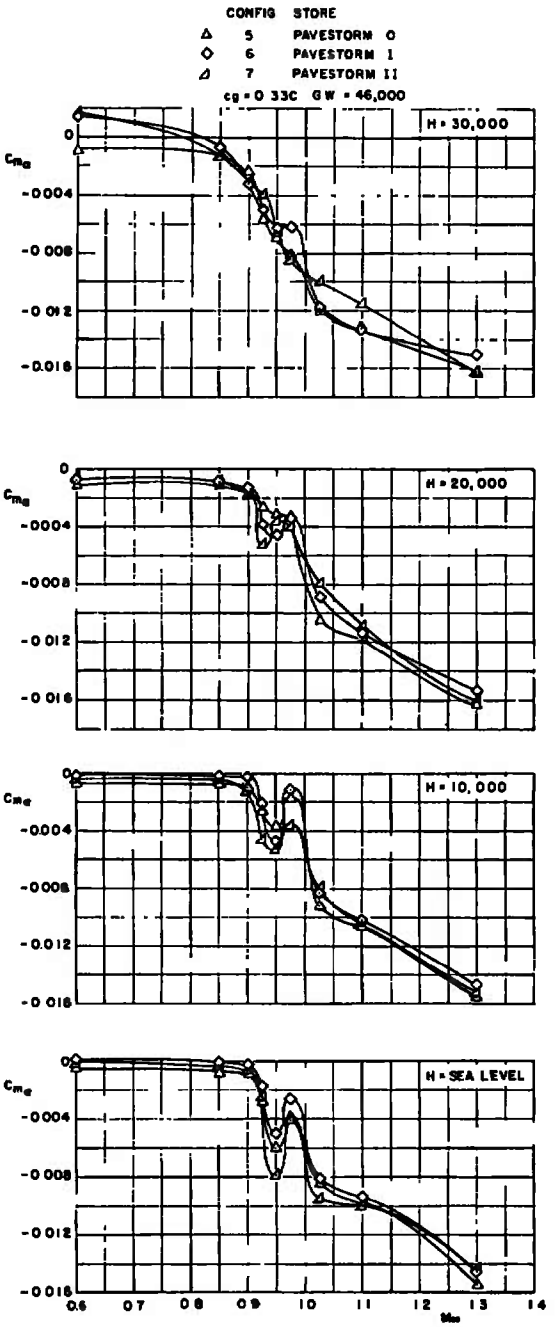

b. cg = 0.33C
Fig. 23 Continued

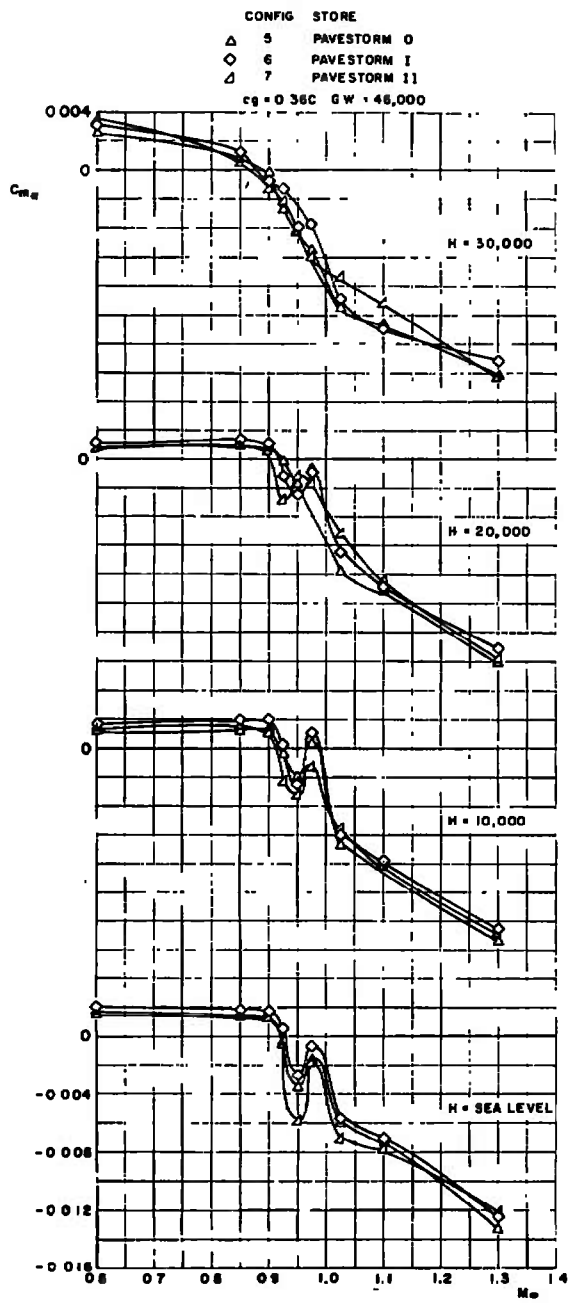

c. cg = 0.36C

Fig. 23 Concluded

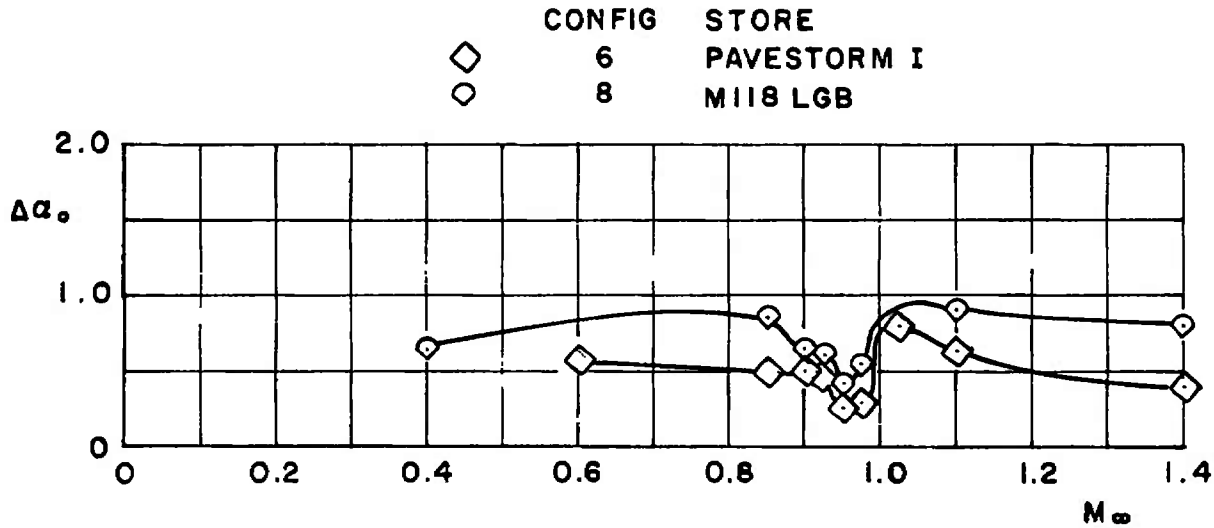

a. Single-Mounted Stores

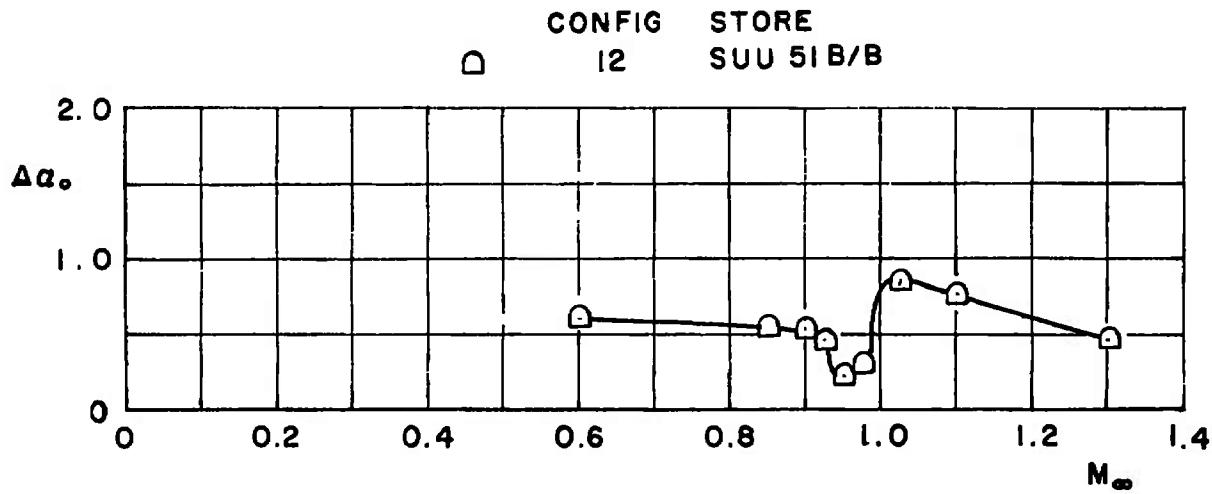

b. Multiple-Mounted Stores

Fig. 24 Change in Angle of Zero Lift for Various Store Configurations

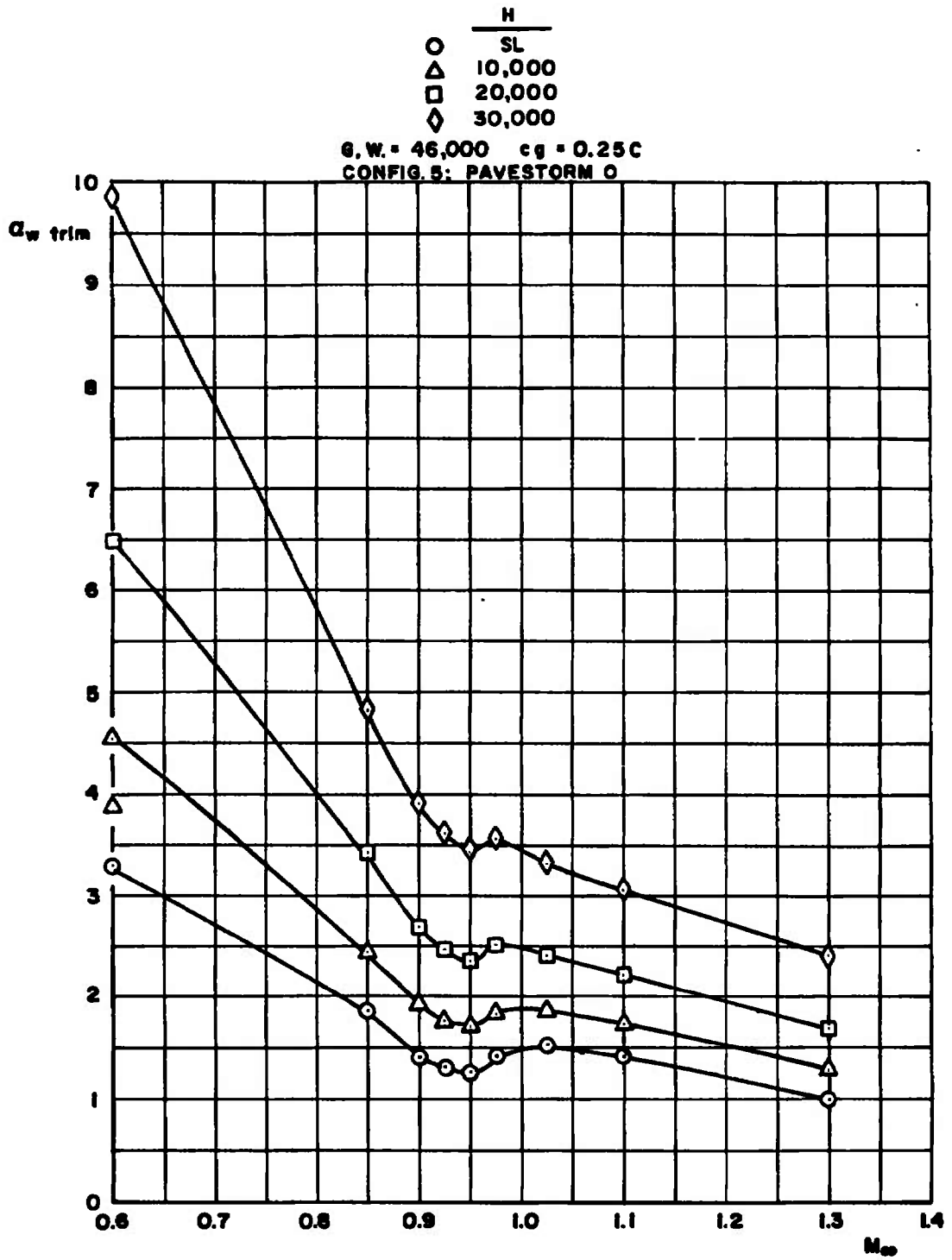

a. cg = 0.25C

Fig. 25 Trim Angle of Attack as a Function of Mach Number, Altitude, and cg Location for Configuration 5

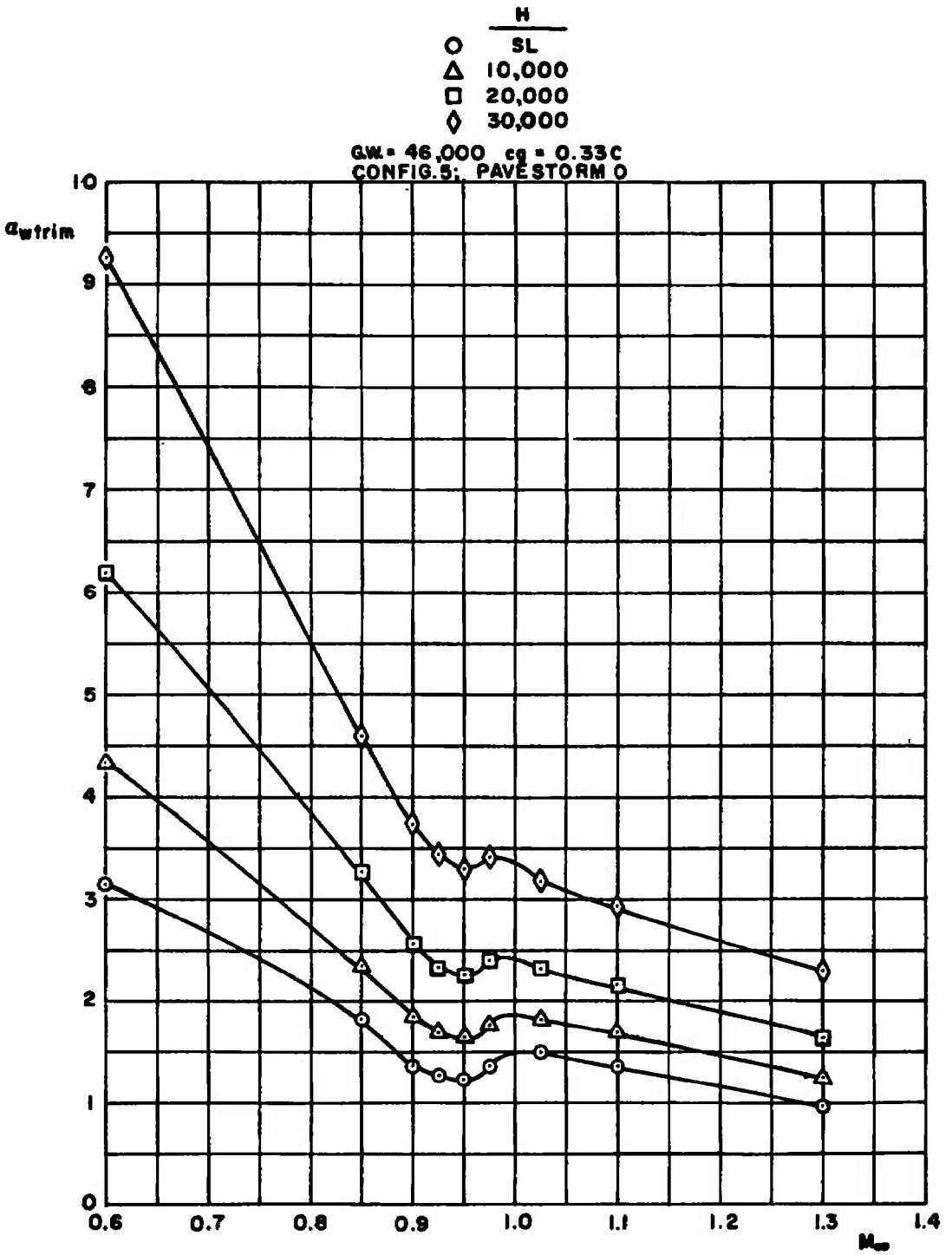

b. cg = 0.33C

Fig. 25 Continued

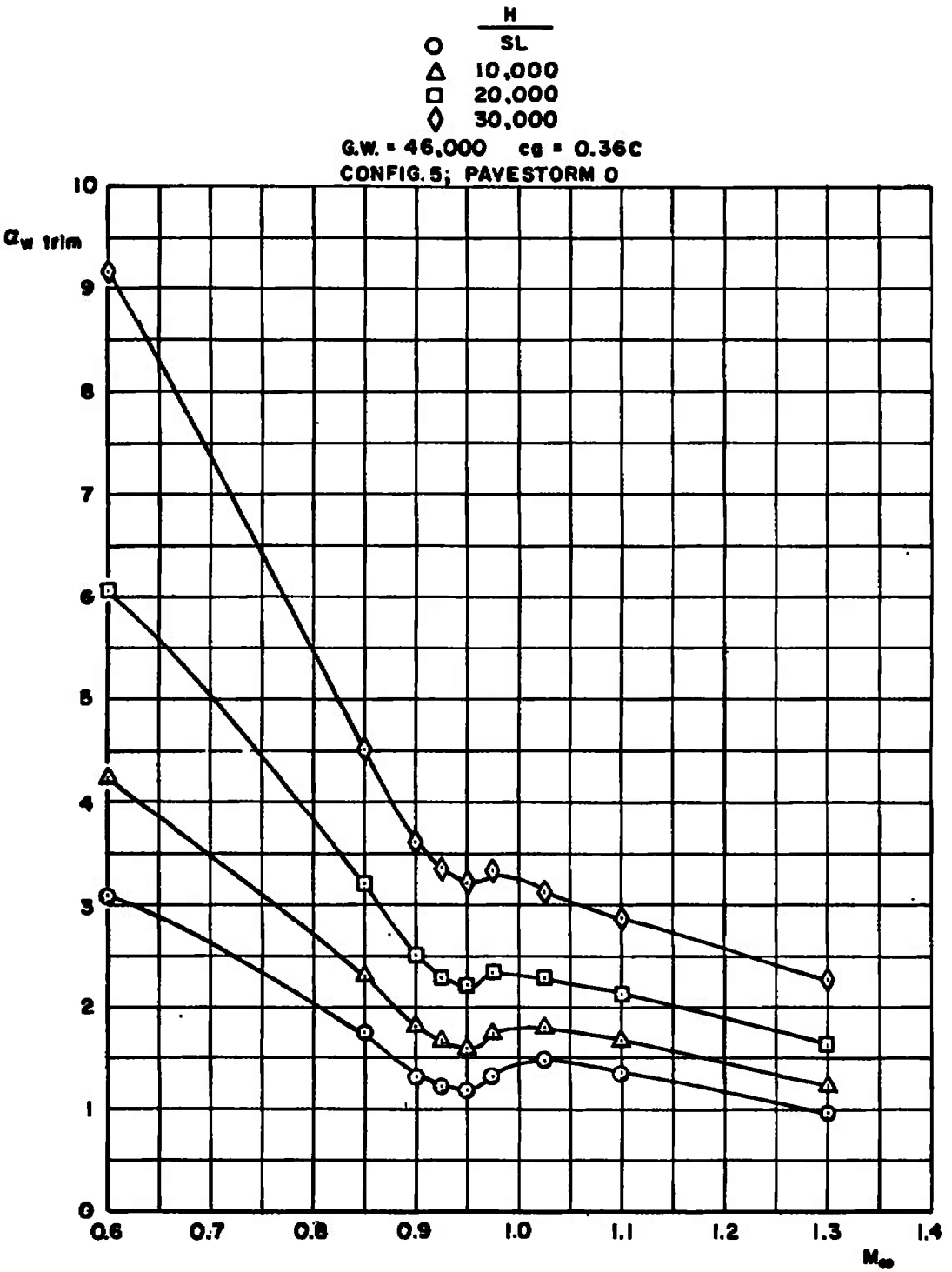

c. cg = 0.36C
Fig. 25 Concluded

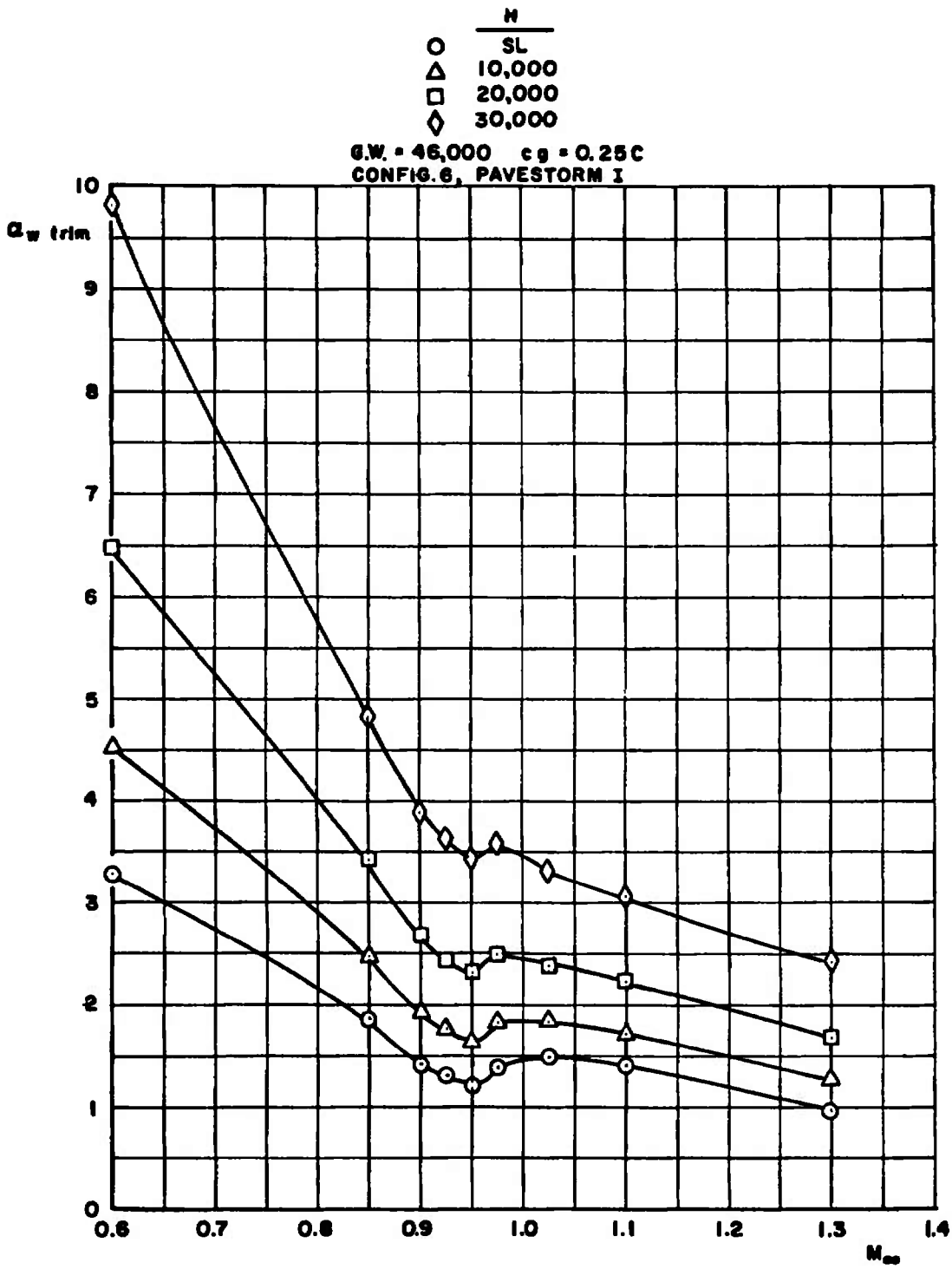

a. cg = 0.25C

Fig. 26 Trim Angle of Attack as a Function of Mach Number, Altitude, and cg Location for Configuration 6

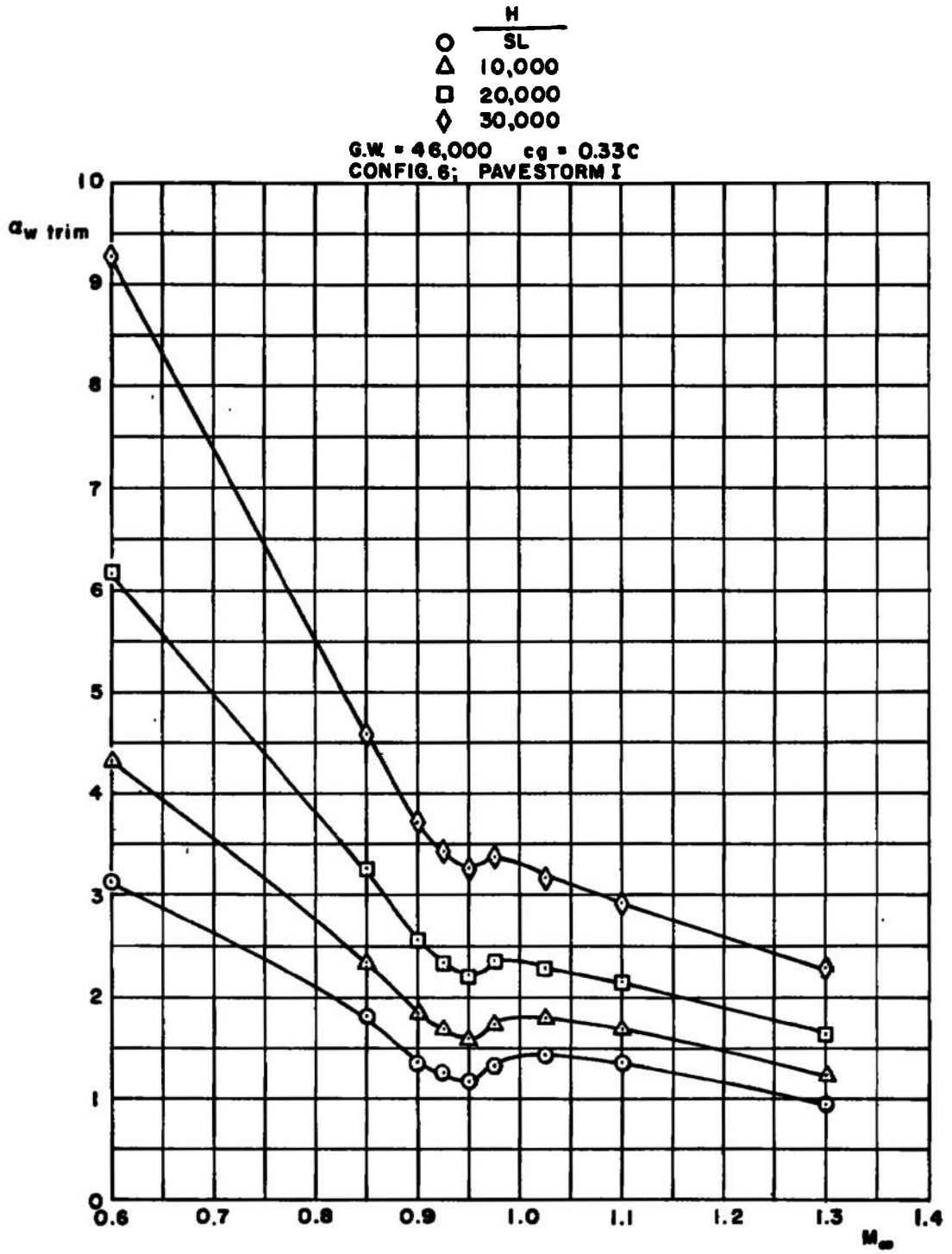

b. cg = 0.33C
Fig. 26 Continued

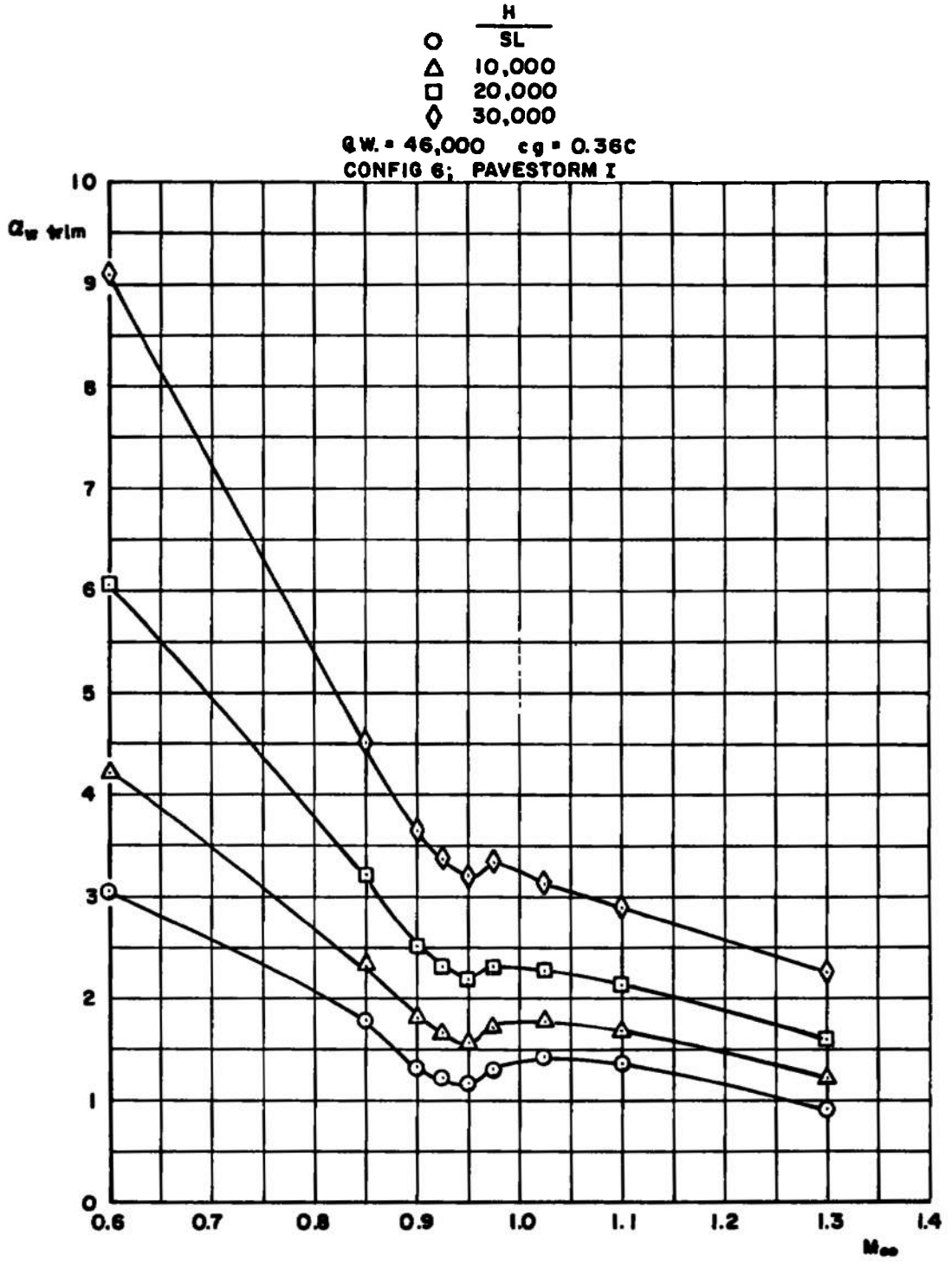

c. cg = 0.36C

Fig. 26 Concluded

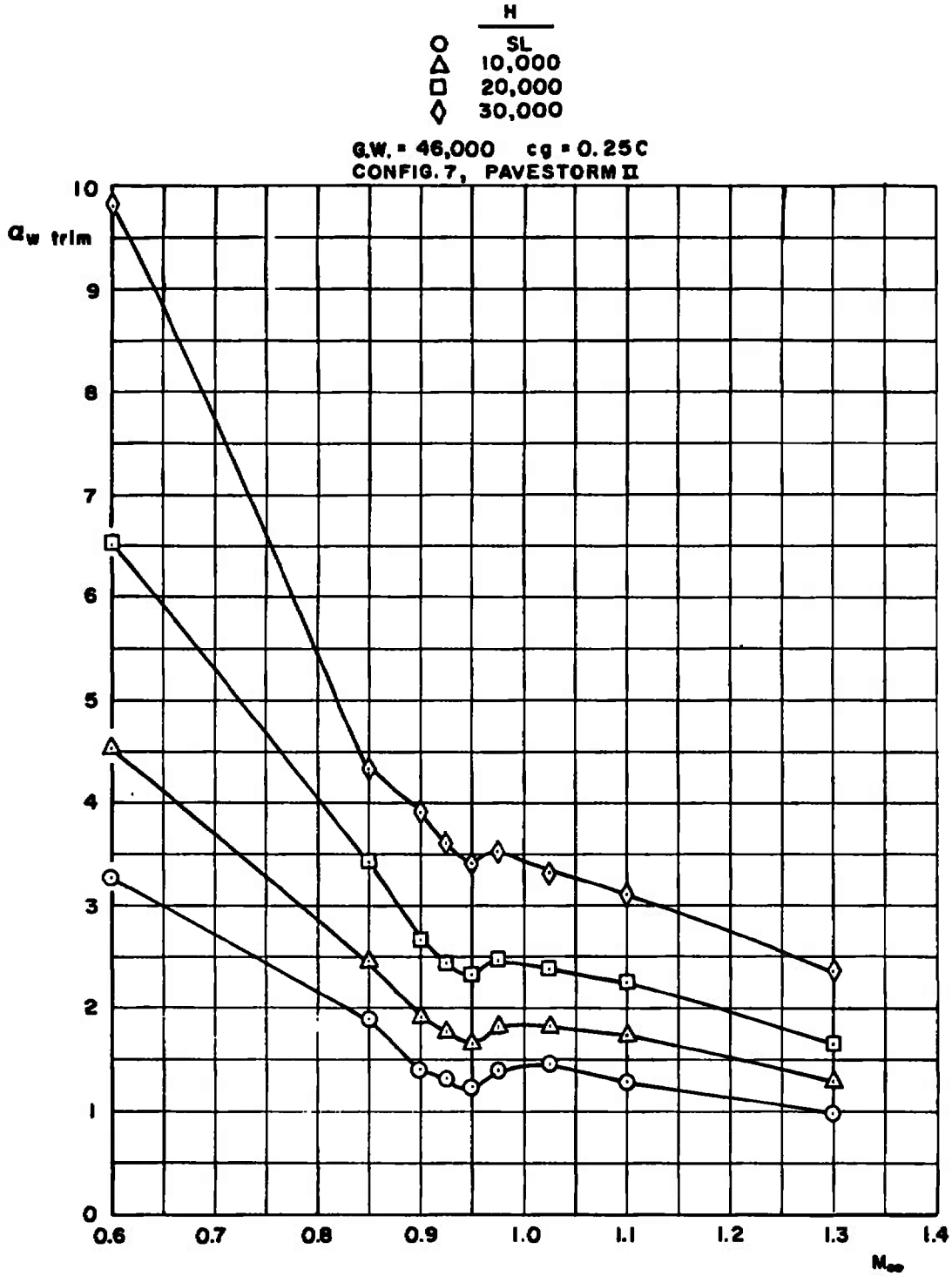

a. cg = 0.25C

Fig. 27 Trim Angle of Attack as a Function of Mach Number, Altitude, and cg Location for Configuration 7

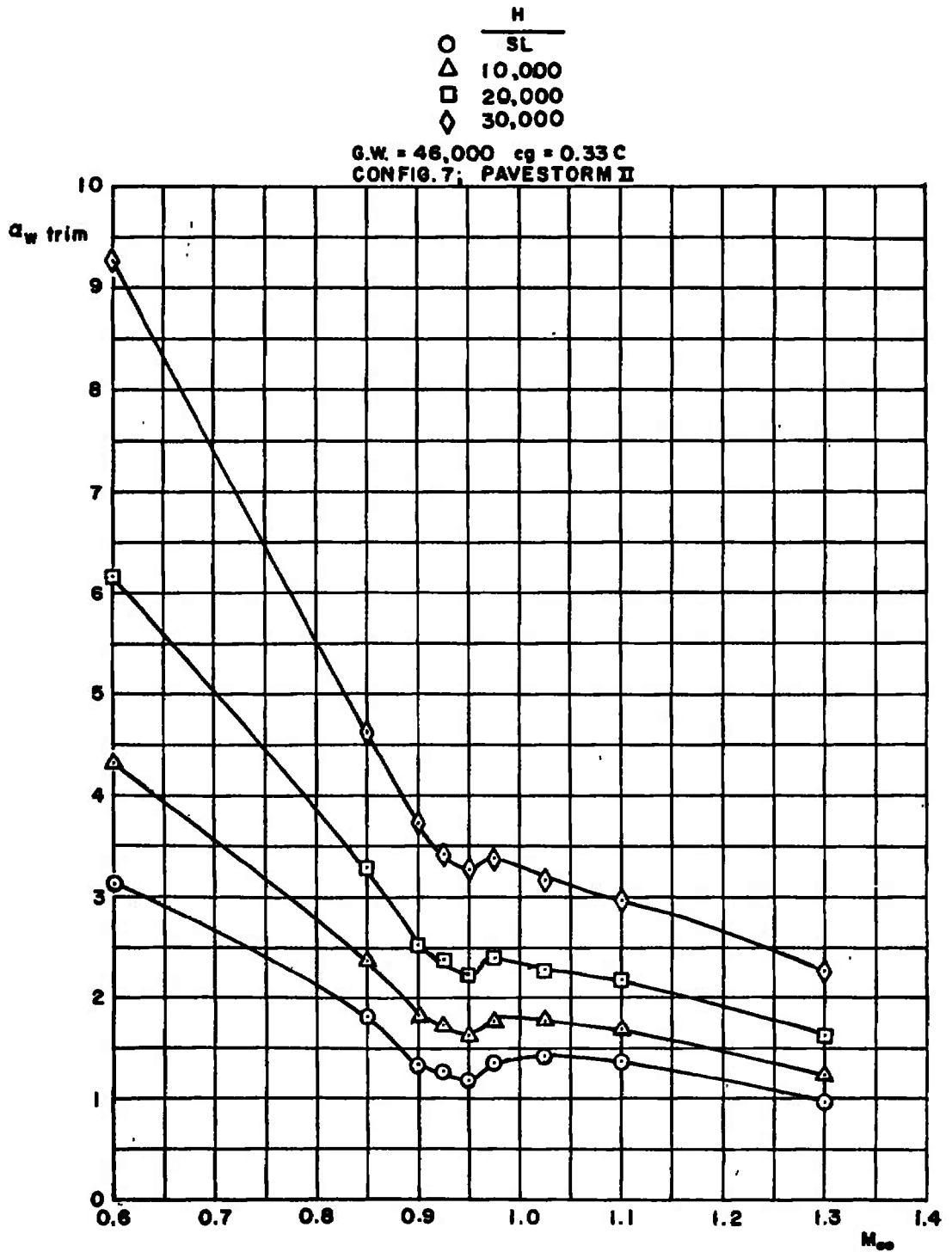

b. cg = 0.33C
Fig. 27 Continued

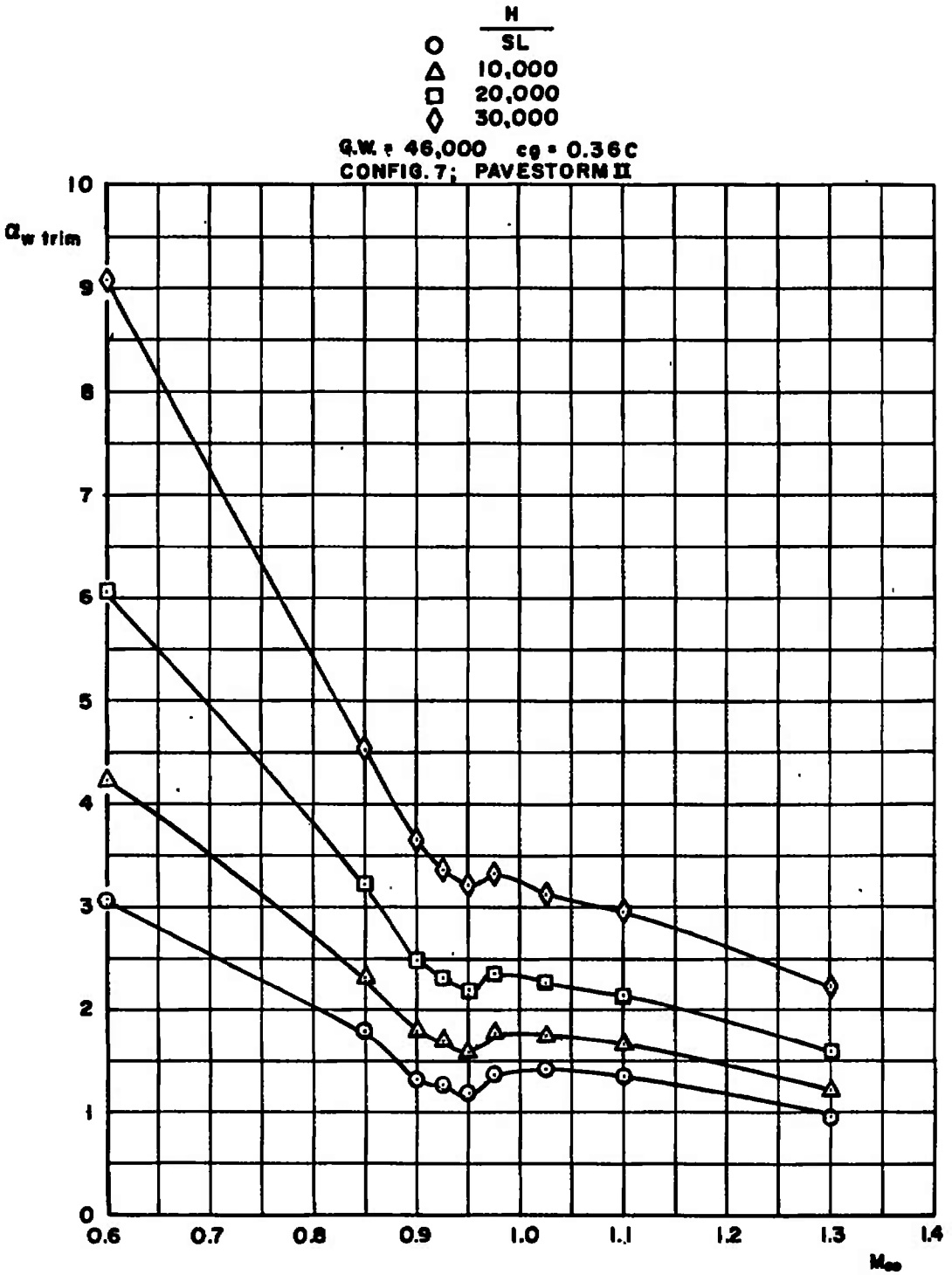

c. cg = 0.36C

Fig. 27 Concluded

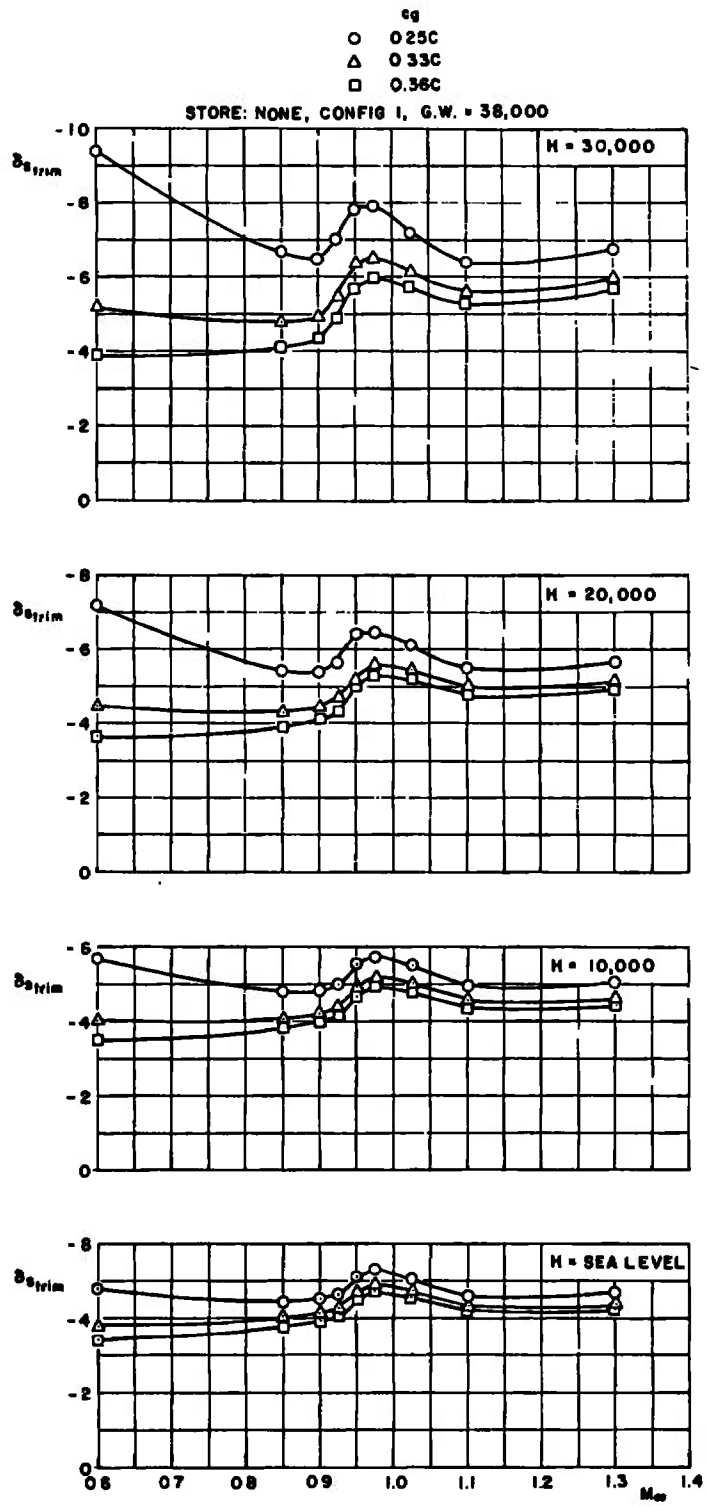

Fig. 28 Trim Stabilator Angle as a Function of Mach Number, Altitude, and cg Location for Configuration 1

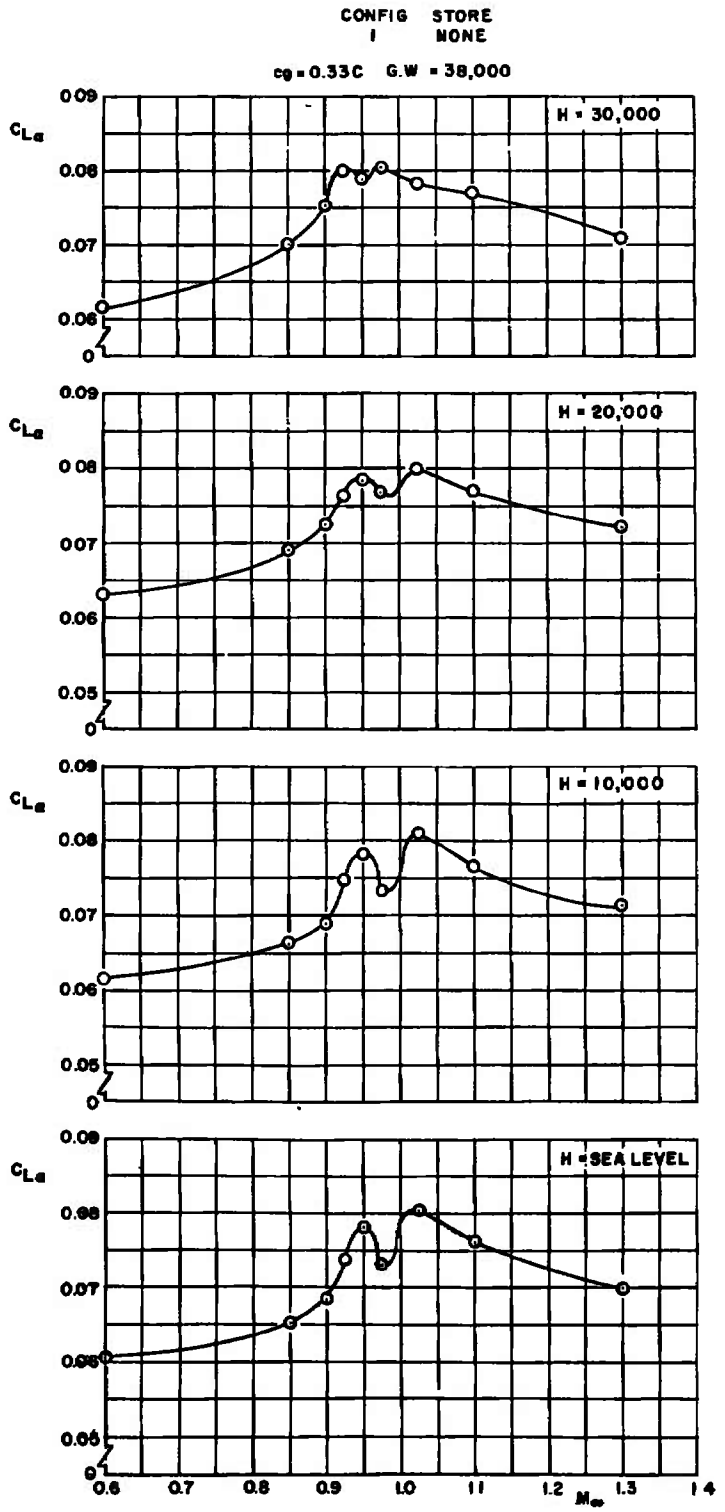

Fig. 29 Lift-Curve Slope at Trim as a Function of Mach Number and Altitude for Configuration 1

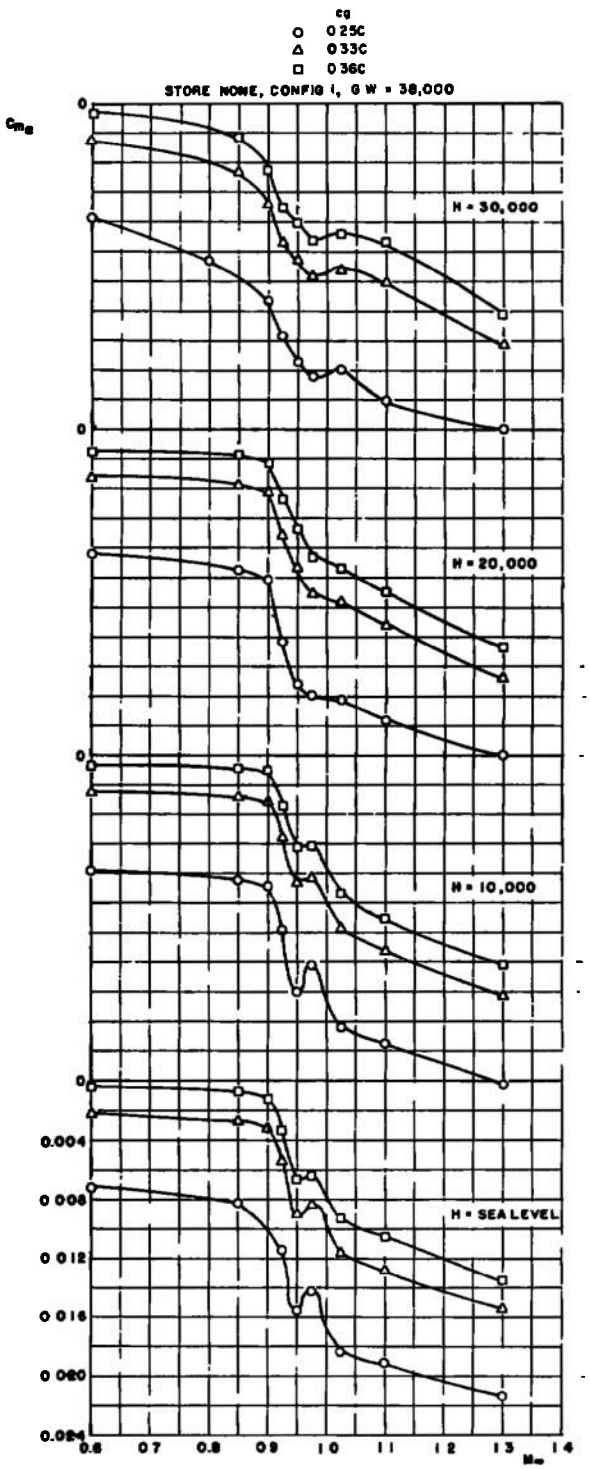

Fig. 30 Slope of Pitching-Moment Coefficient versus Angle-of-Attack Curve as a Function of Mach Number, Altitude, and cg Location for Configuration 1

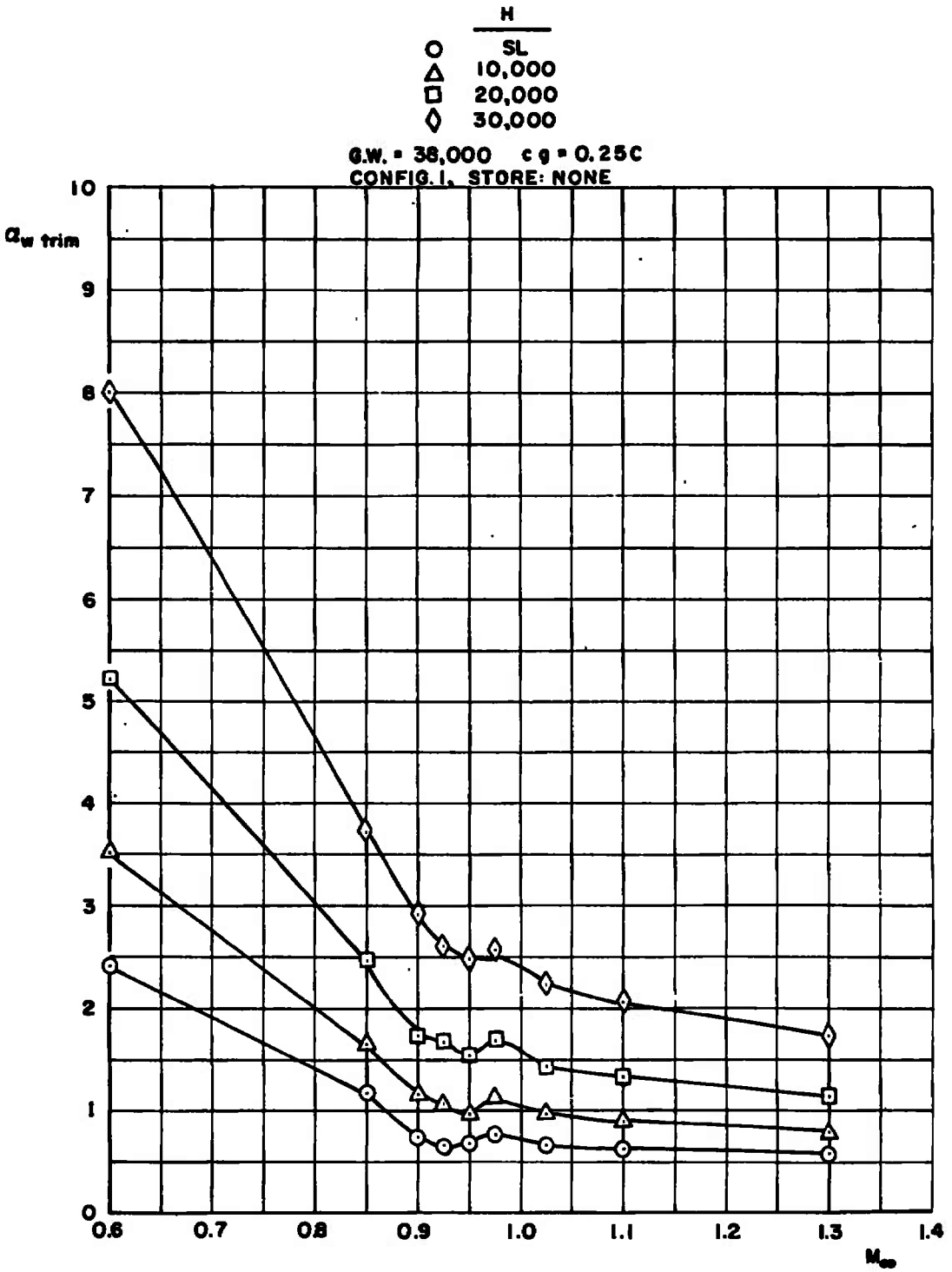

a. cg = 0.25C

Fig. 31 Trim Angle of Attack as a Function of Mach Number, Altitude, and cg Location for Configuration 1

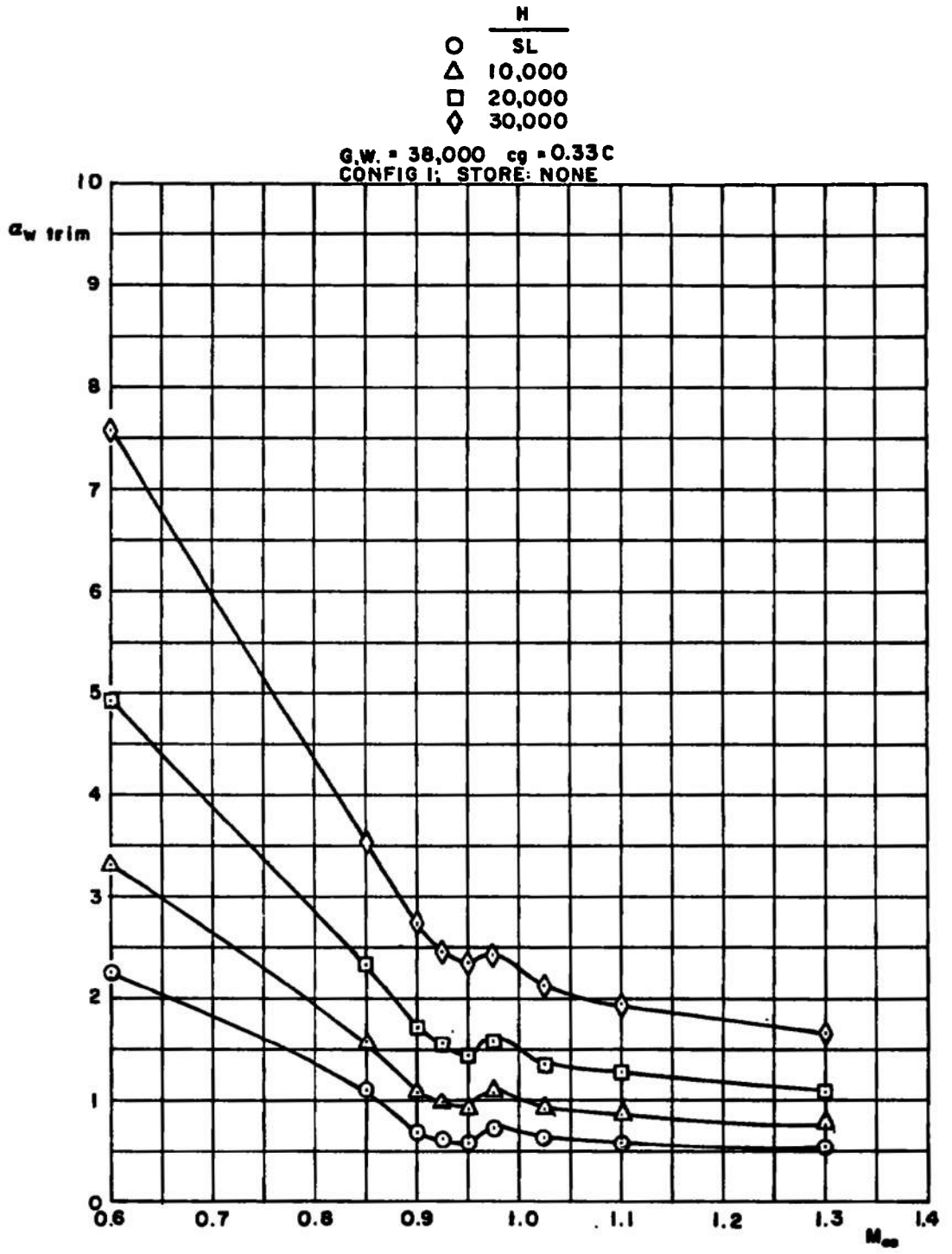

b. cg = 0.33C
Fig. 31 Continued

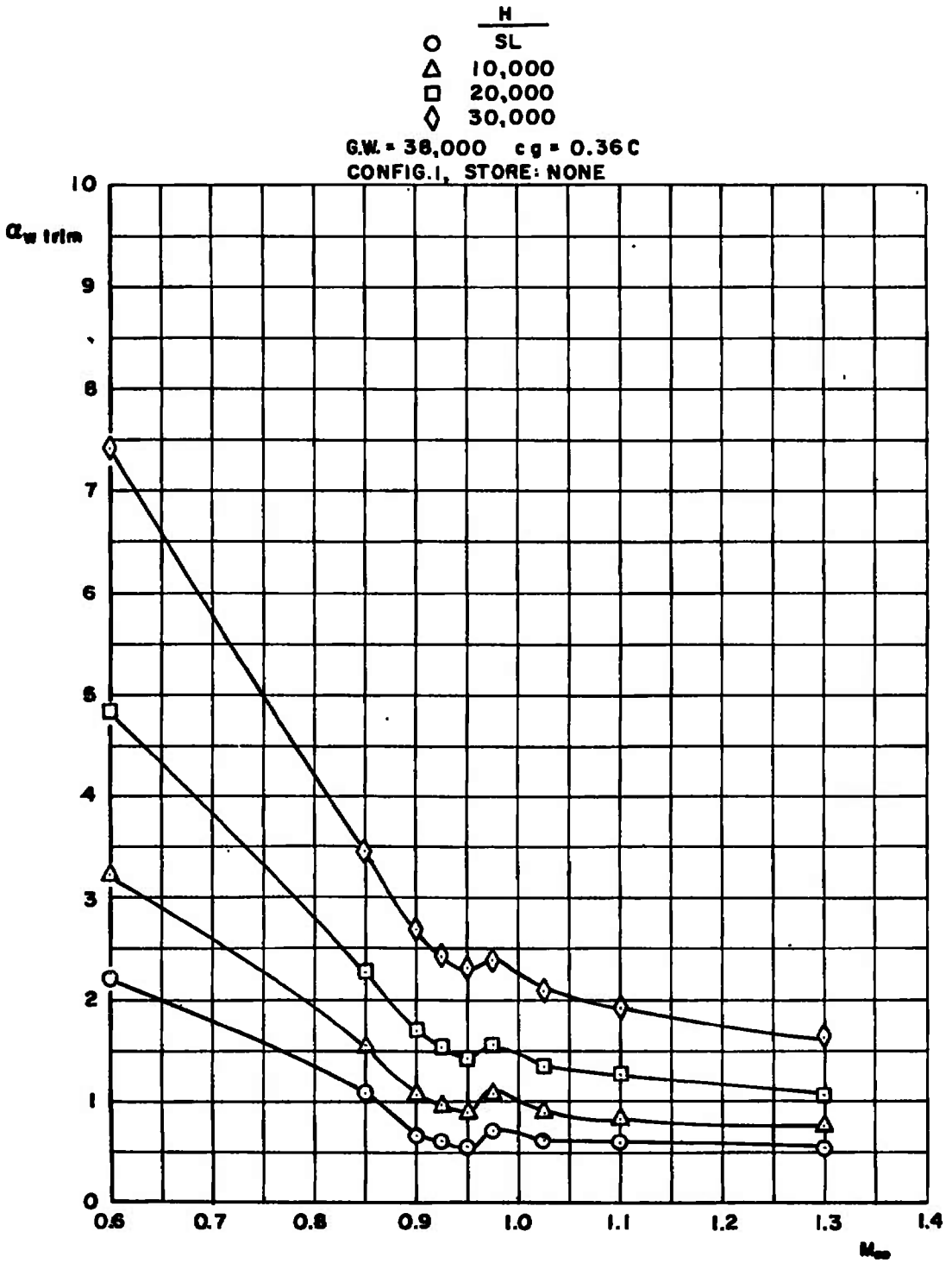

c. cg = 0.36C

Fig. 31 Concluded

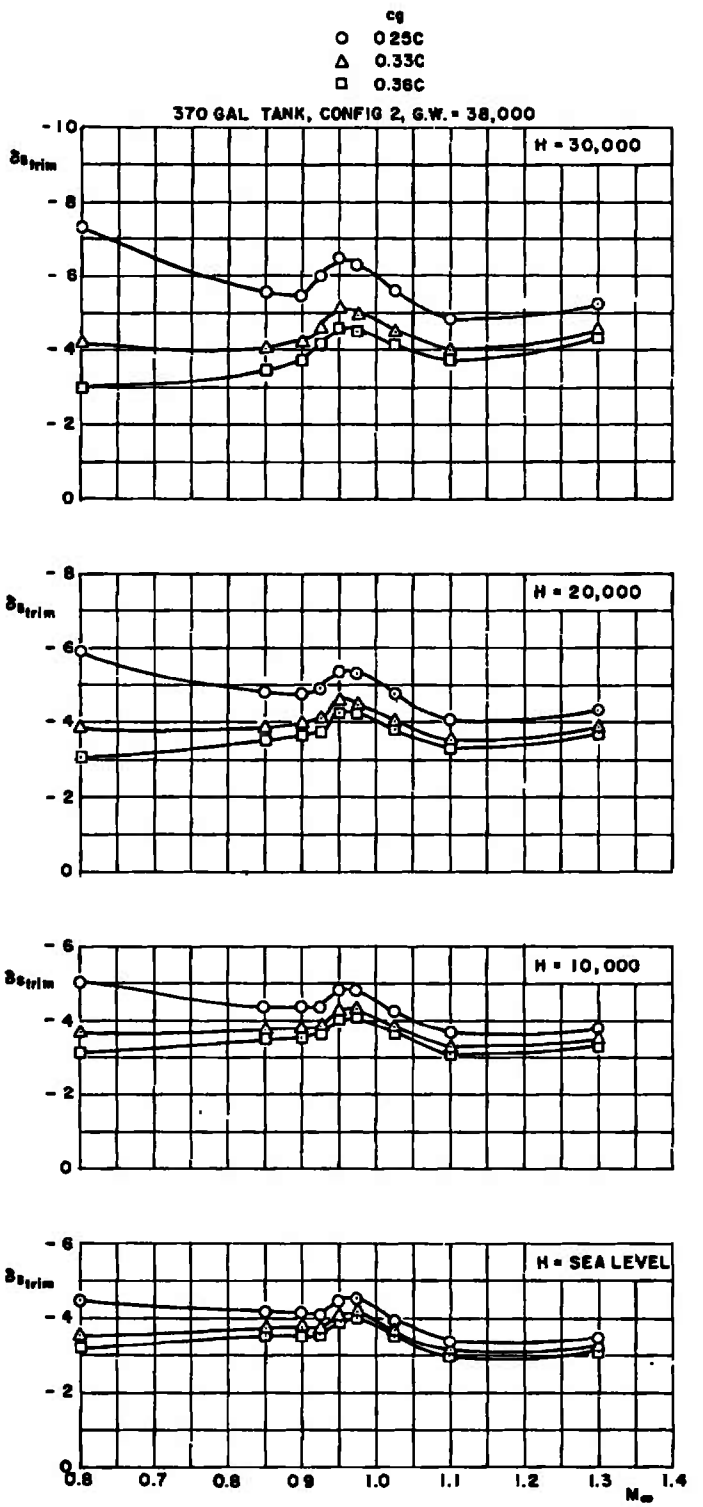

Fig. 32 Trim Stabilator Angle as a Function of Mach Number, Altitude, and cg Location for Configuration 2

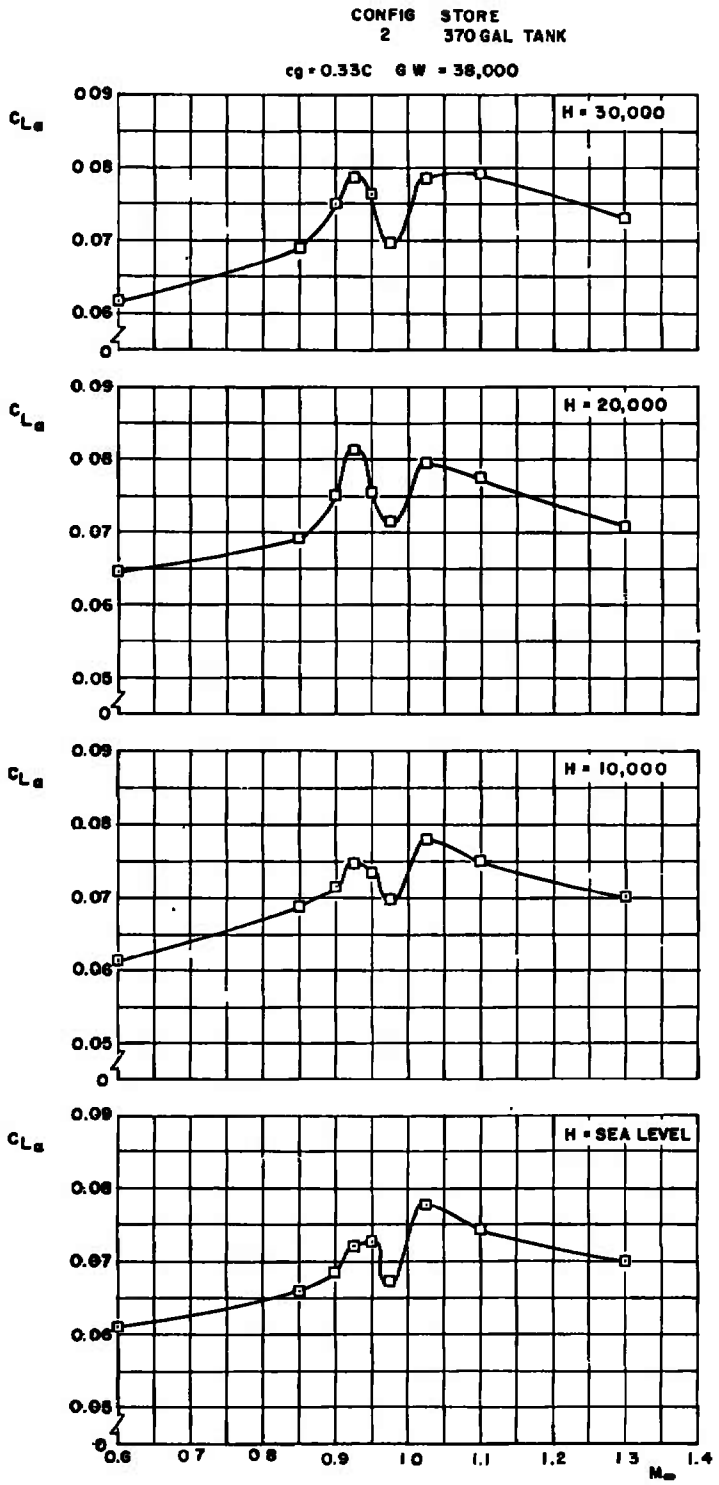

Fig. 33 Lift-Curve Slope at Trim as a Function of Mach Number and Altitude for Configuration 2

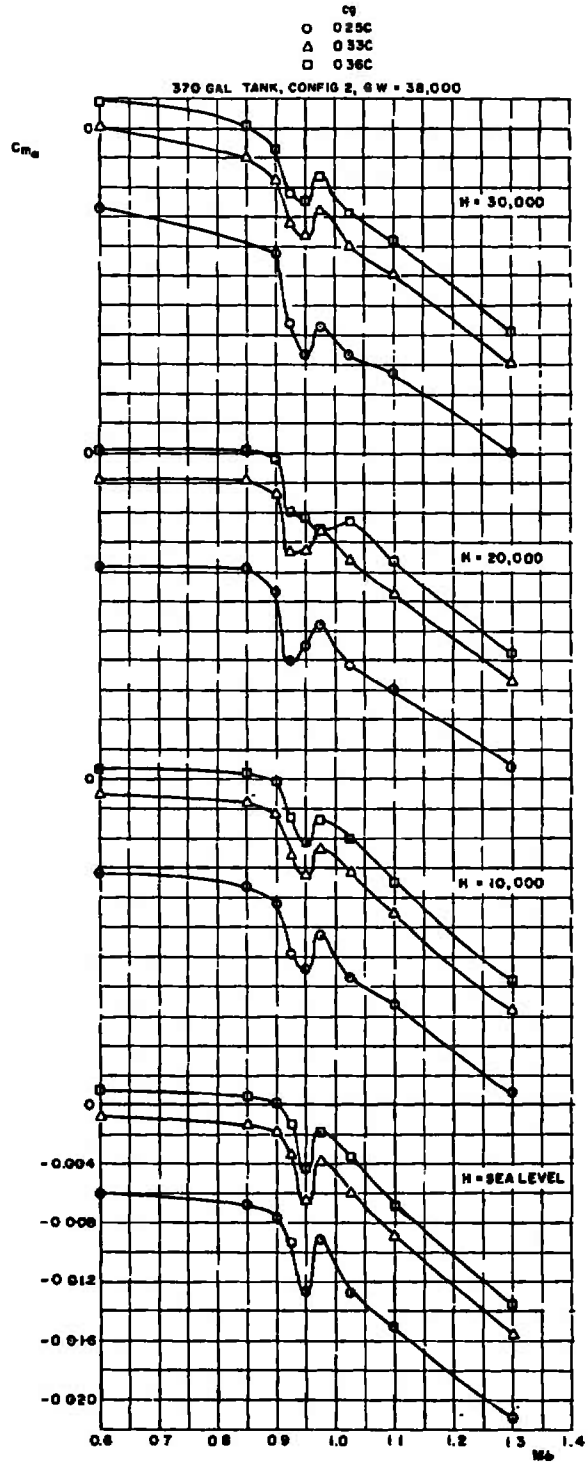

Fig. 34 Slope of Pitching-Moment Coefficient versus Angle-of-Attack Curve at Trim as a Function of Mach Number, Altitude, and cg Location for Configuration 2

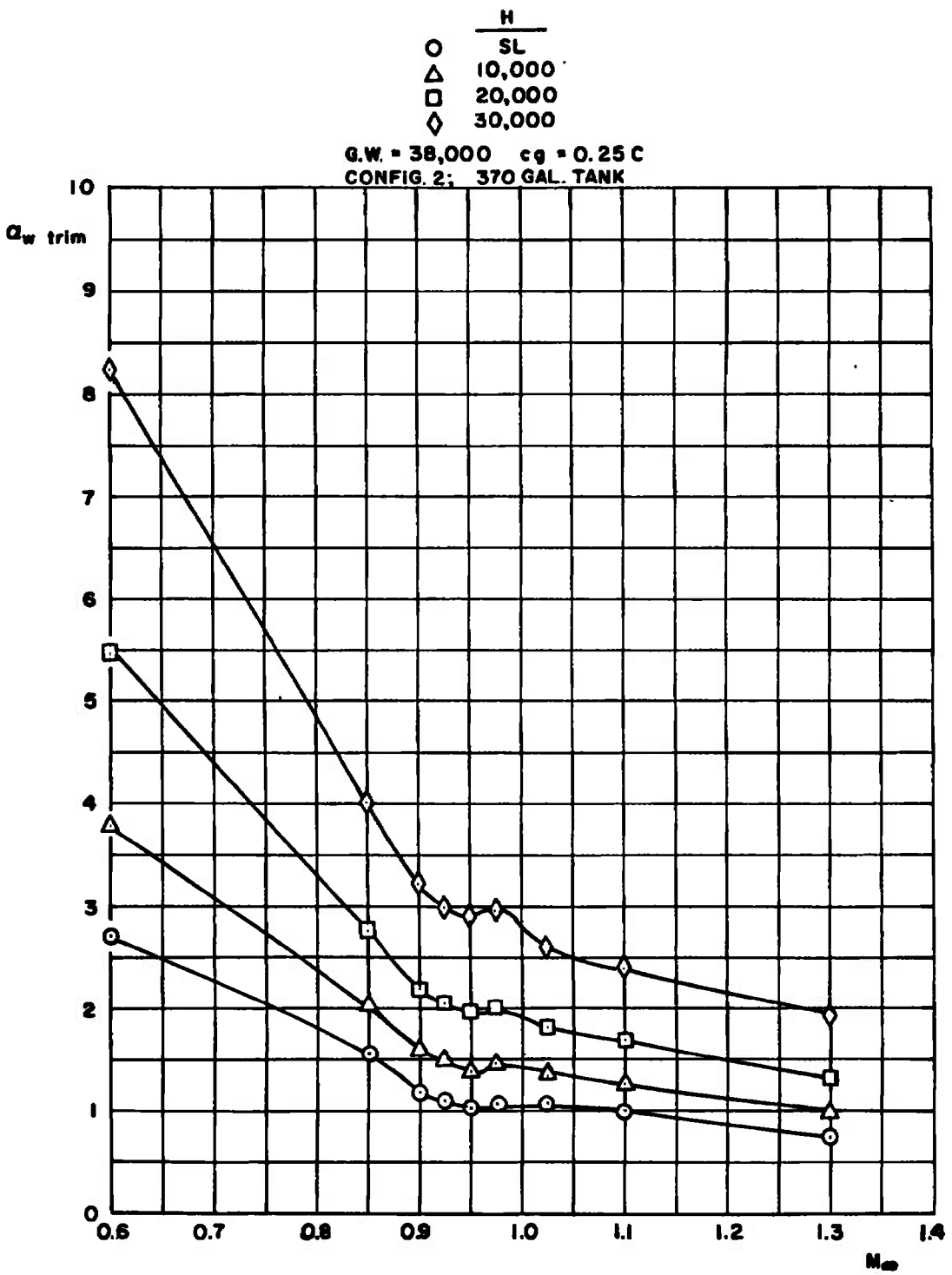

a. cg = 0.25C

Fig. 35 Trim Angle of Attack as a Function of Mach Number, Altitude, and cg Location for Configuration 2

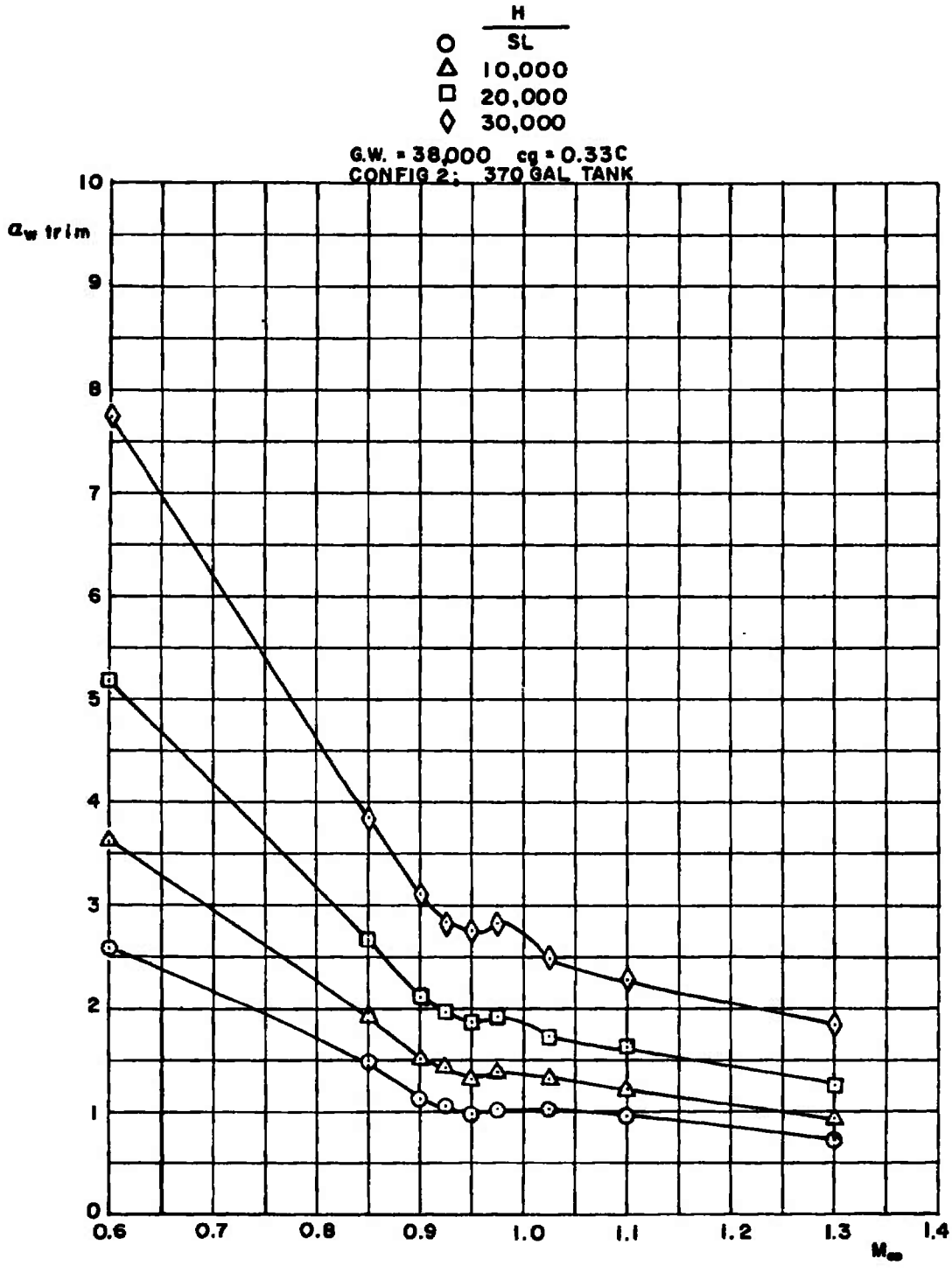

b. cg = 0.33C
Fig. 35 Continued

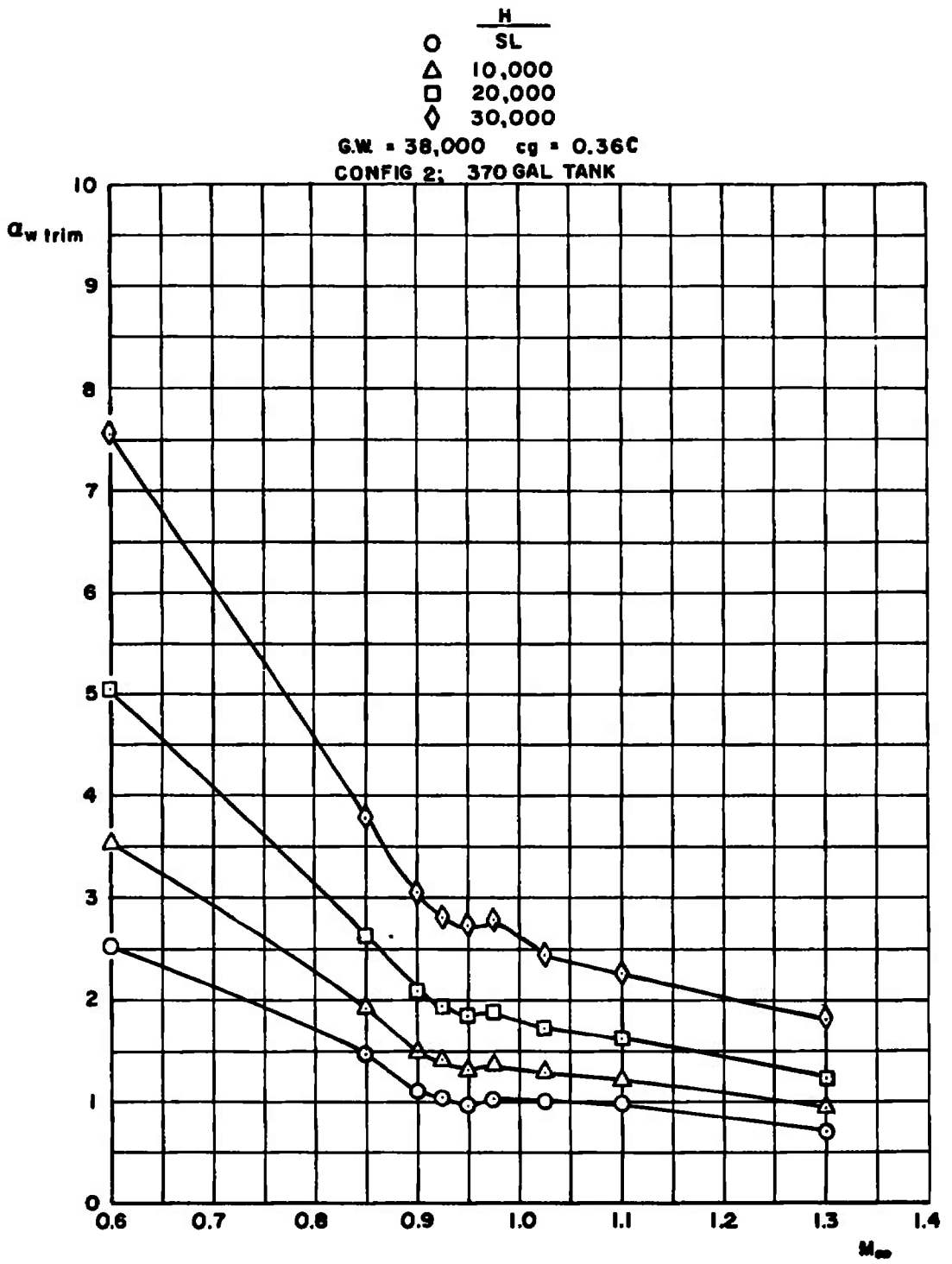

c. cg = 0.36C

Fig. 35 Concluded

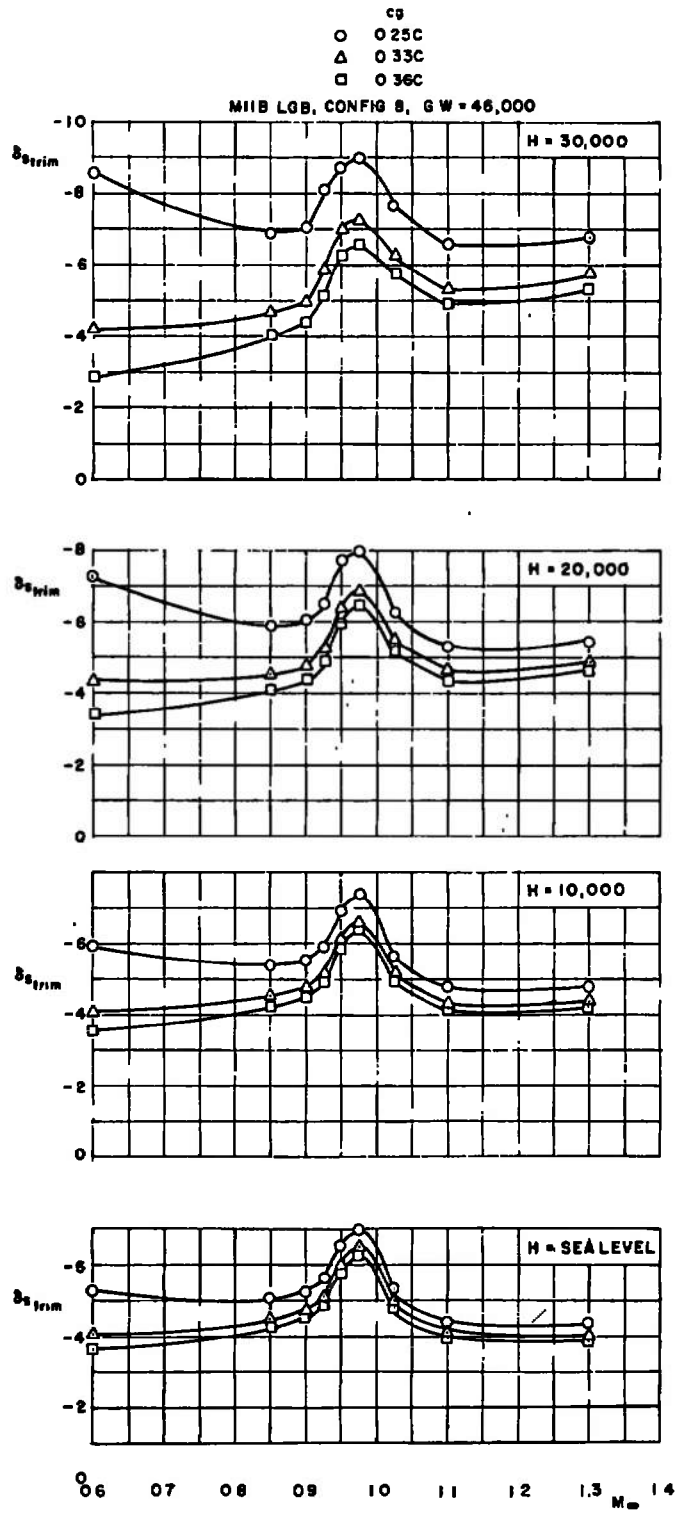

Fig. 36 Trim Stabilator Angle as a Function of Mach Number, Altitude, and cg Location for Configuration 8

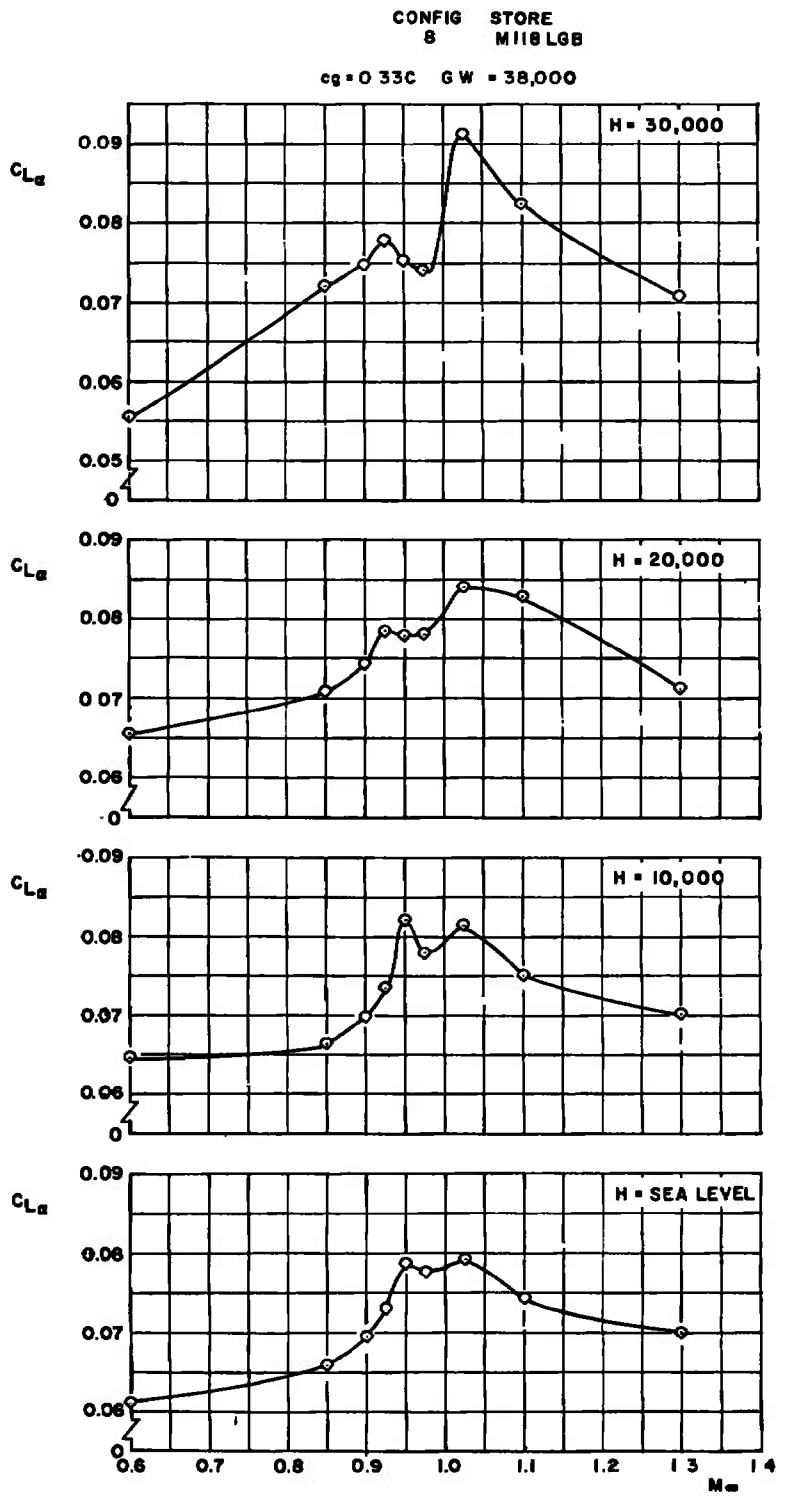

Fig. 37 Lift-Curve Slope at Trim as a Function of Mach Number and Altitude at a cg Location of 0.33C for Configuration 8

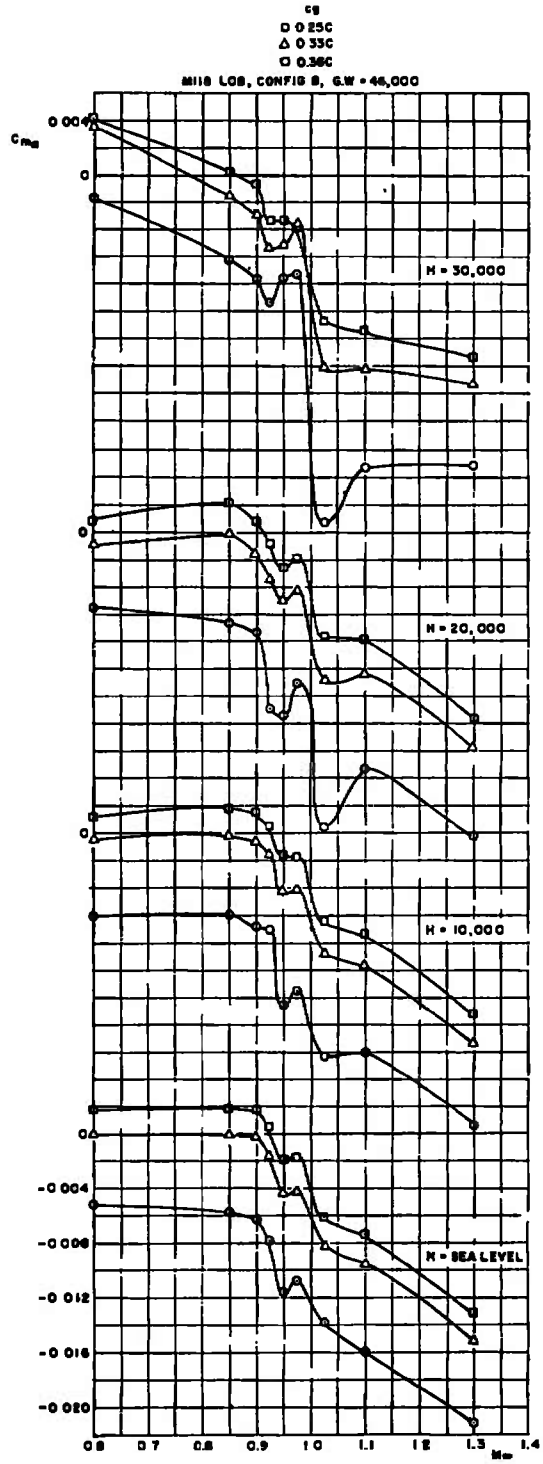

Fig. 38 Slope of Pitching-Moment Coefficient versus Angle-of-Attack Curve at Trim as a Function of Mach Number, Altitude, and cg Location for Configuration 8

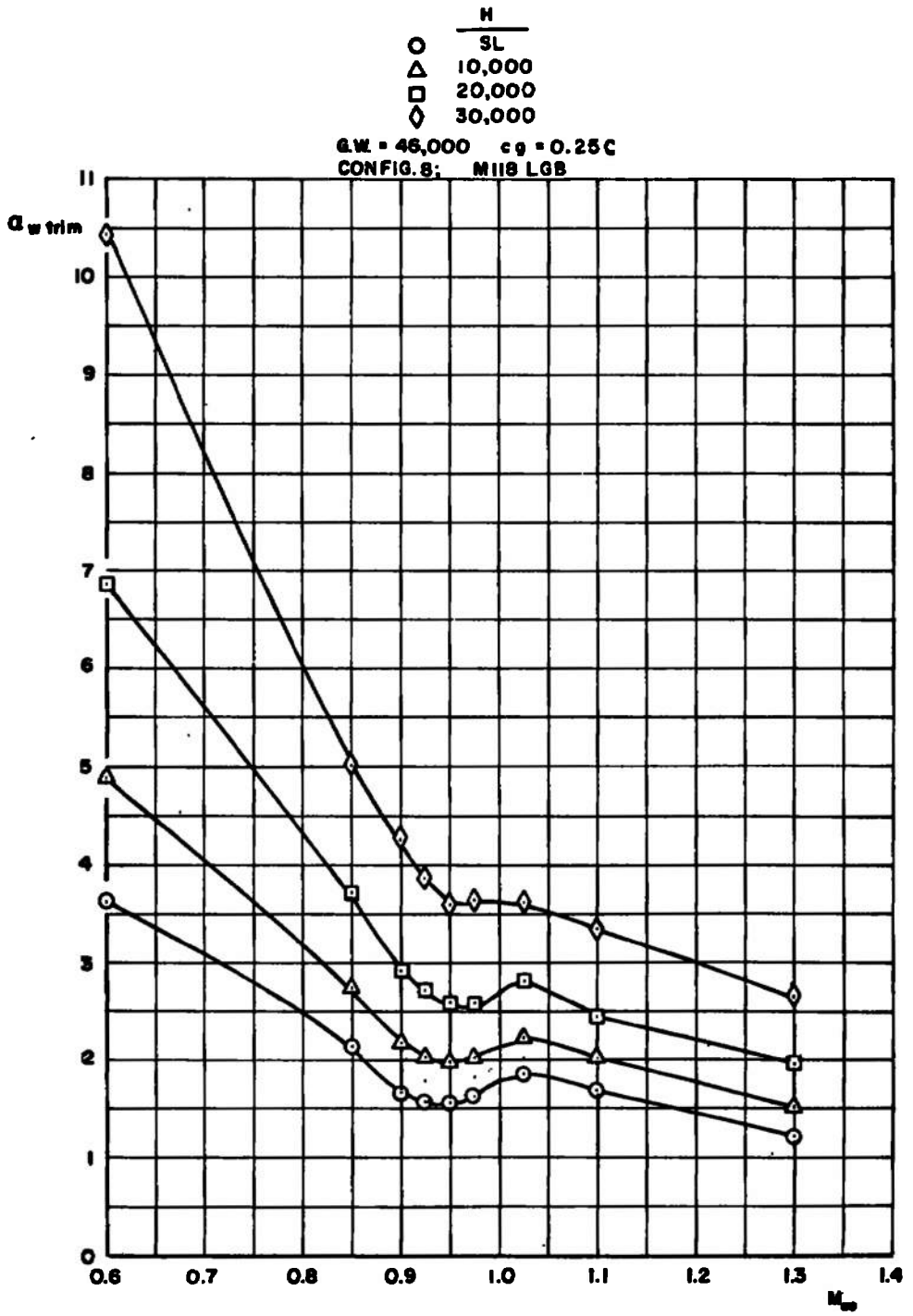

a. cg = 0.25C

Fig. 39 Trim Angle of Attack as a Function of Mach Number, Altitude, and cg Location for Configuration 8

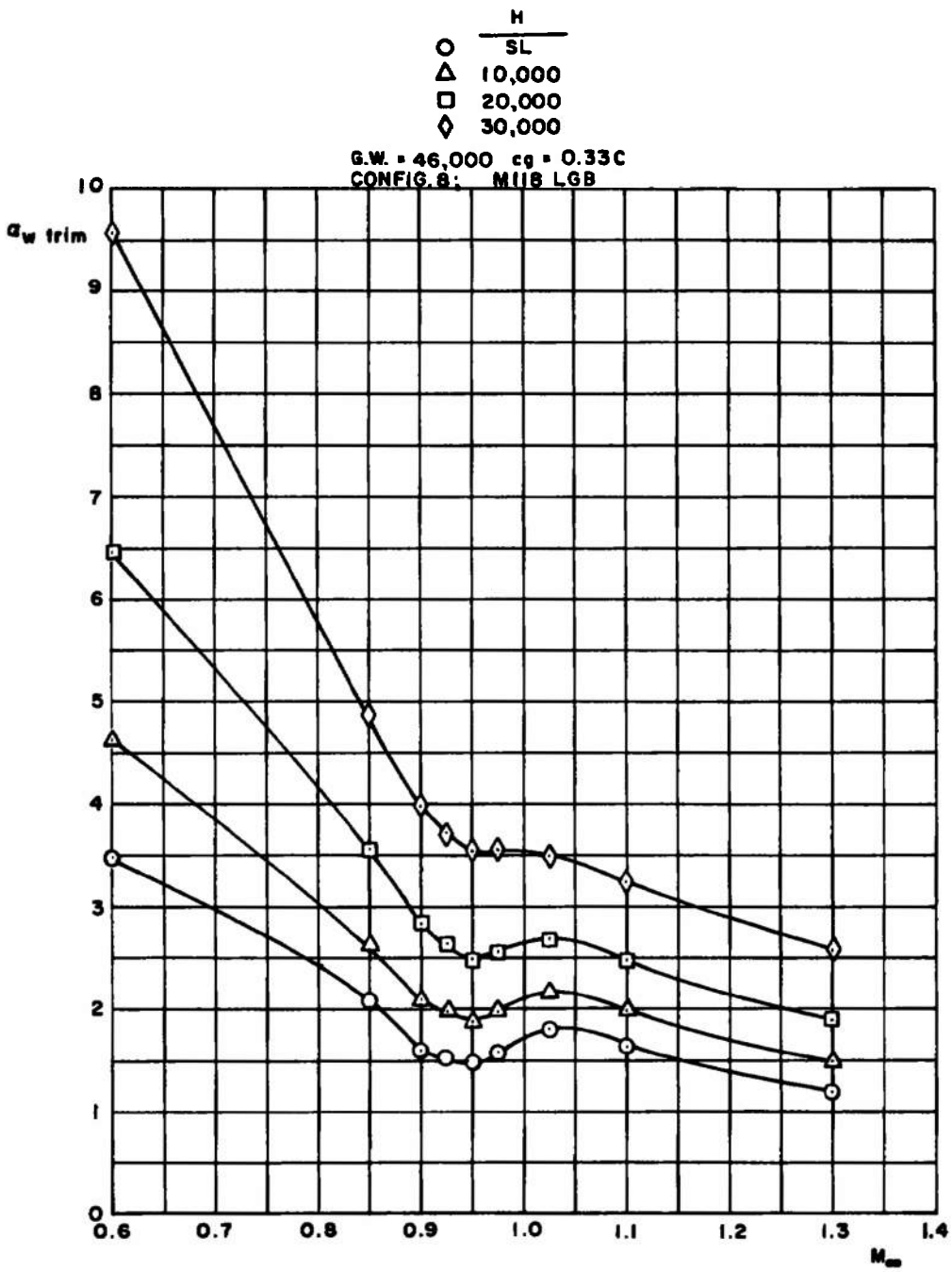

b. cg = 0.33C

Fig. 39 Continued

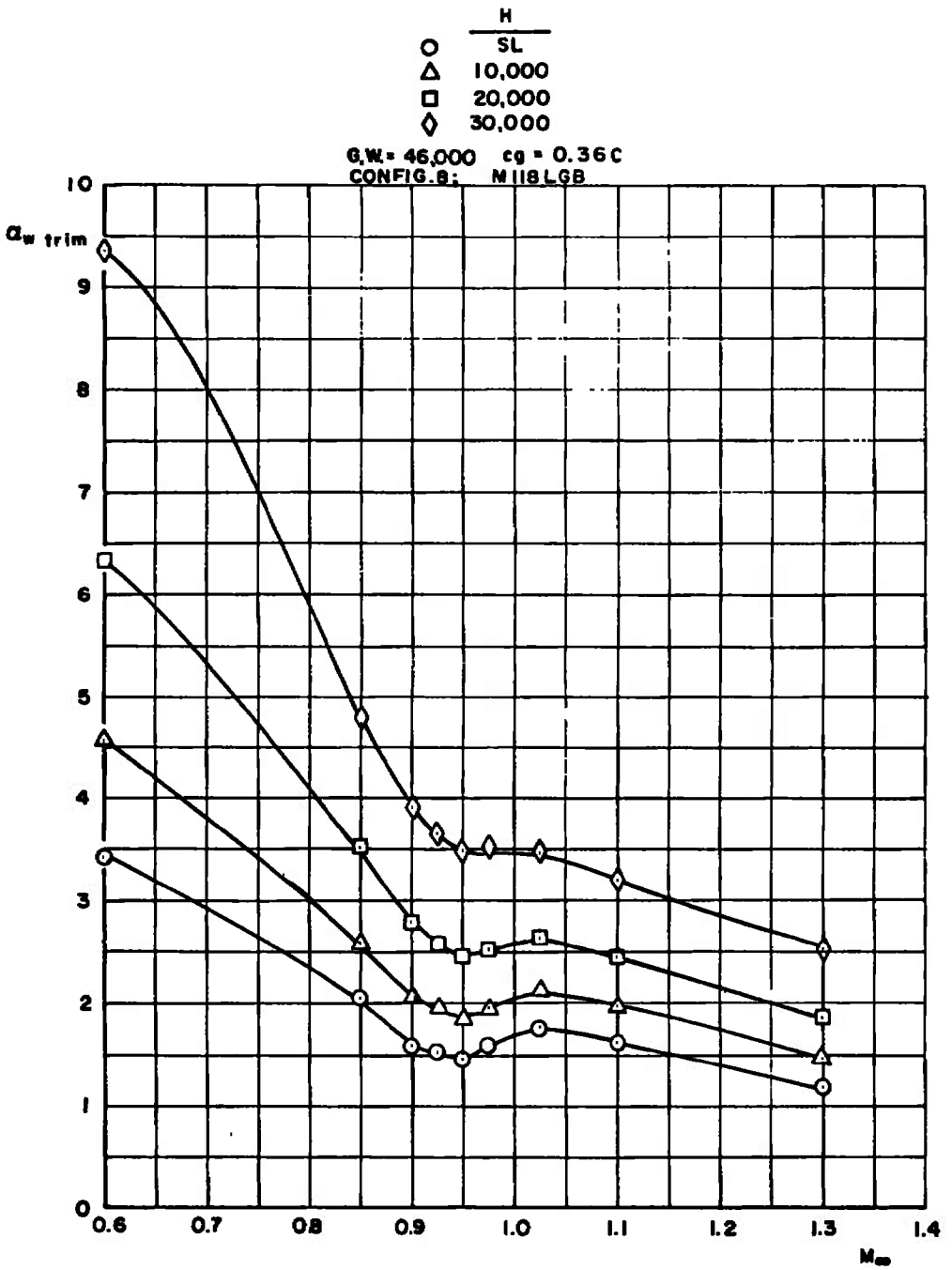

c. cg = 0.36C

Fig. 39 Concluded

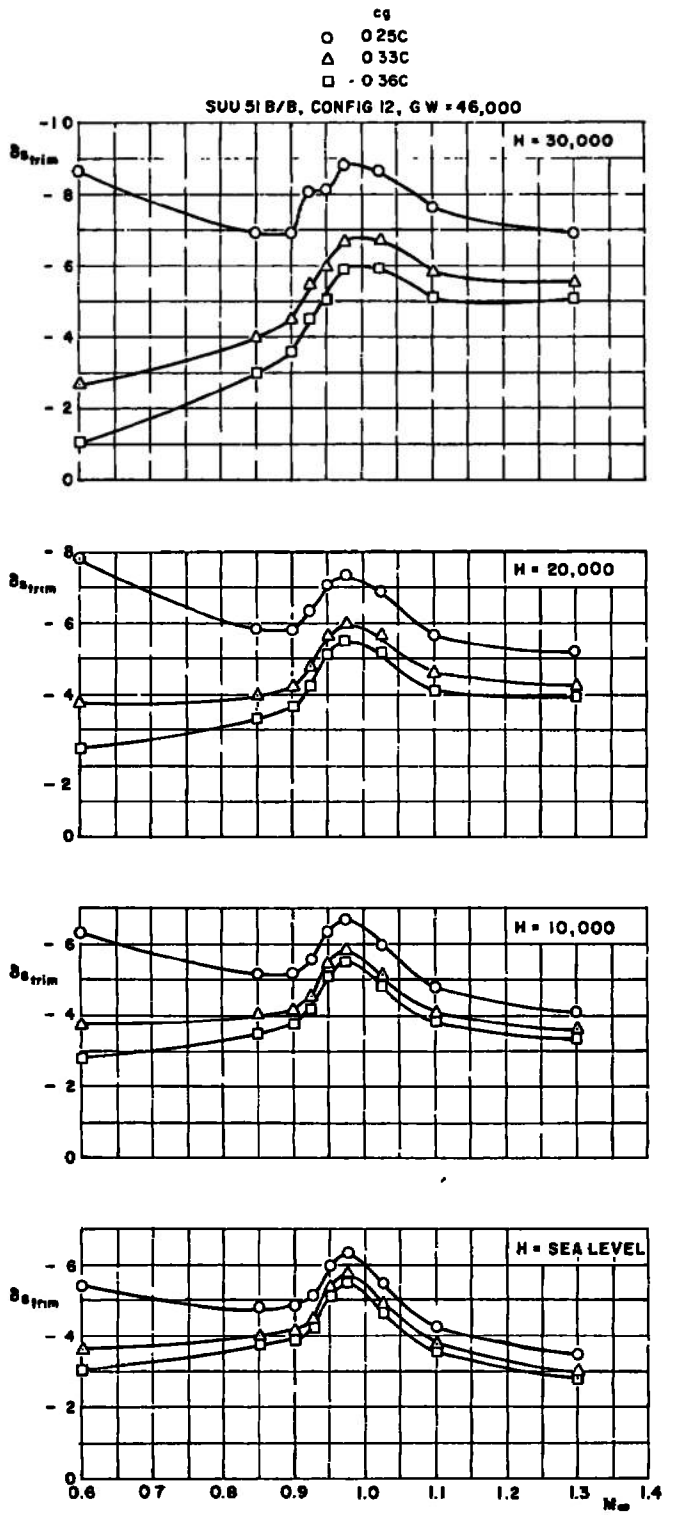

Fig. 40 Trim Stabilator Angle as a Function of Mach Number, Altitude, and cg Location for Configuration 12

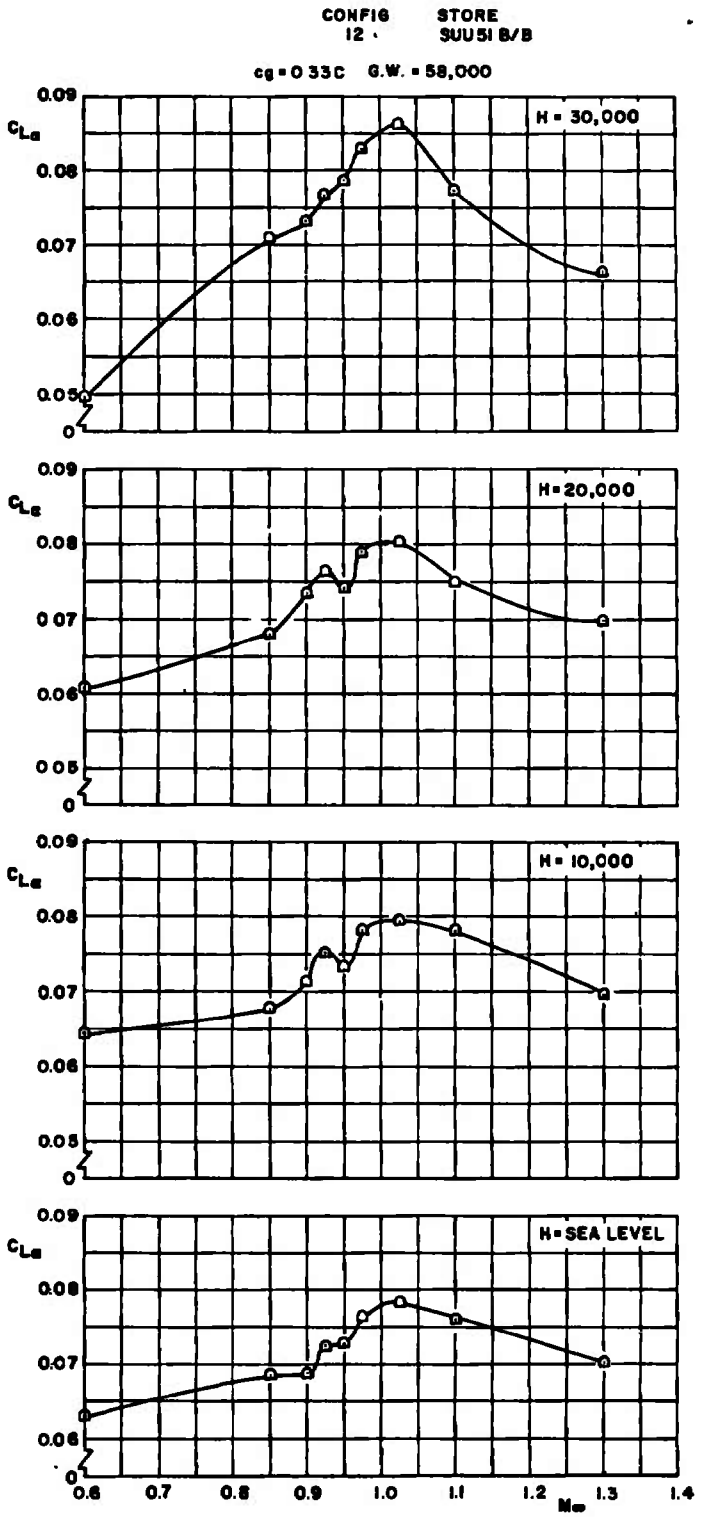

Fig. 41 Lift-Curve Slope at Trim as a Function of Mach Number and Altitude for Configuration 12

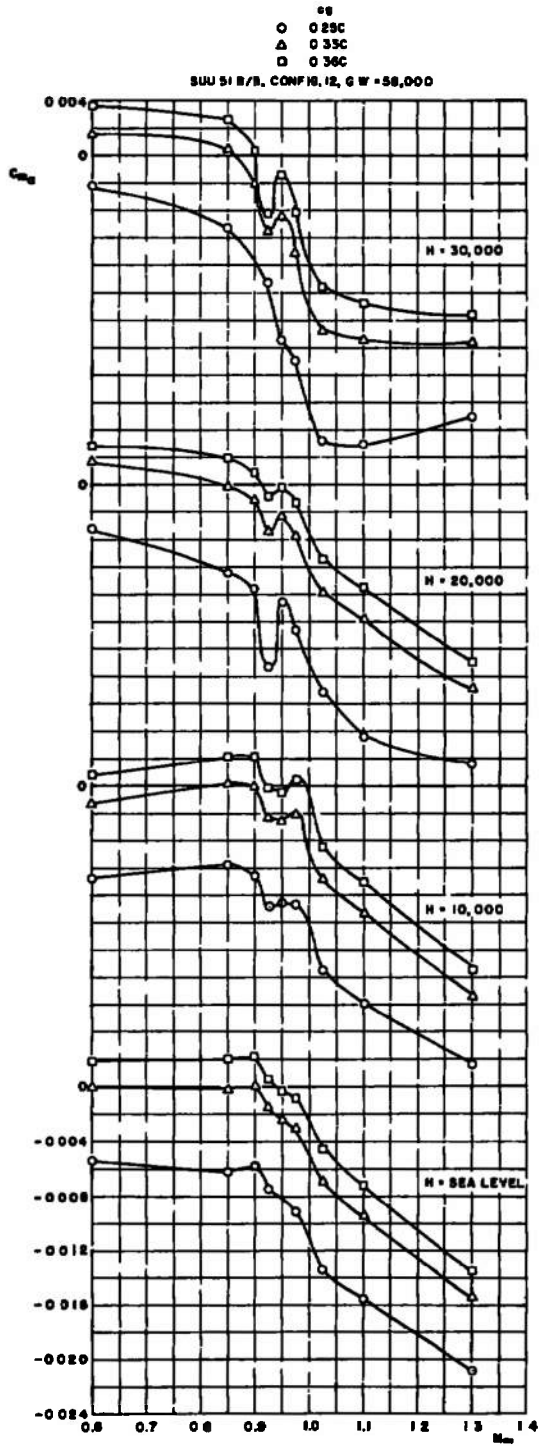

Fig. 42 Slope of Pitching-Moment Coefficient Curve versus Angle-of-Attack Curve at Trim as a Function of Mach Number, Altitude, and cg Location for Configuration 12

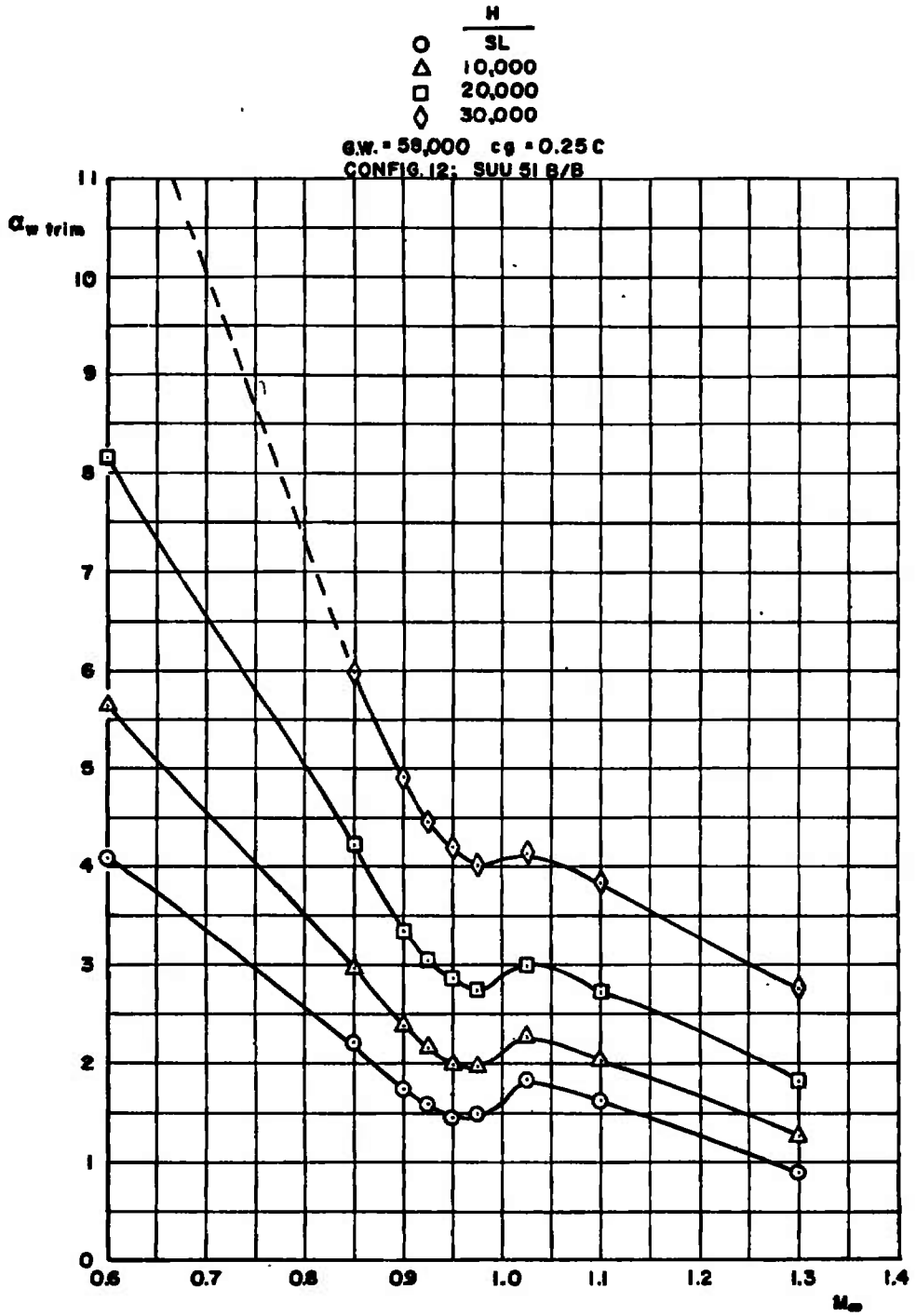

a. cg = 0.25C

Fig. 43 Trim Angle of Attack as a Function of Mach Number, Altitude, and cg Location for Configuration 12

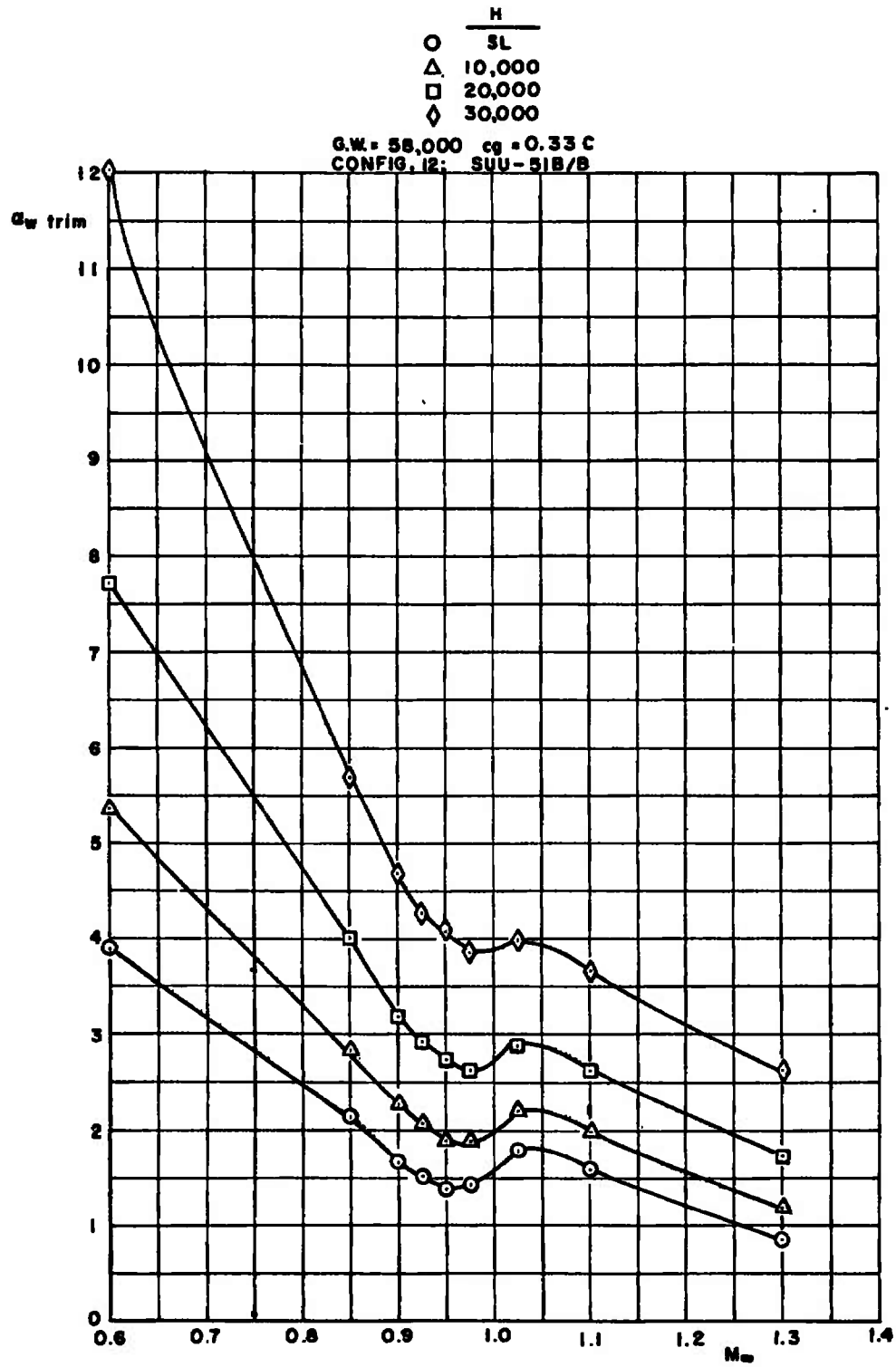

b. cg = 0.33C
Fig. 43 Continued

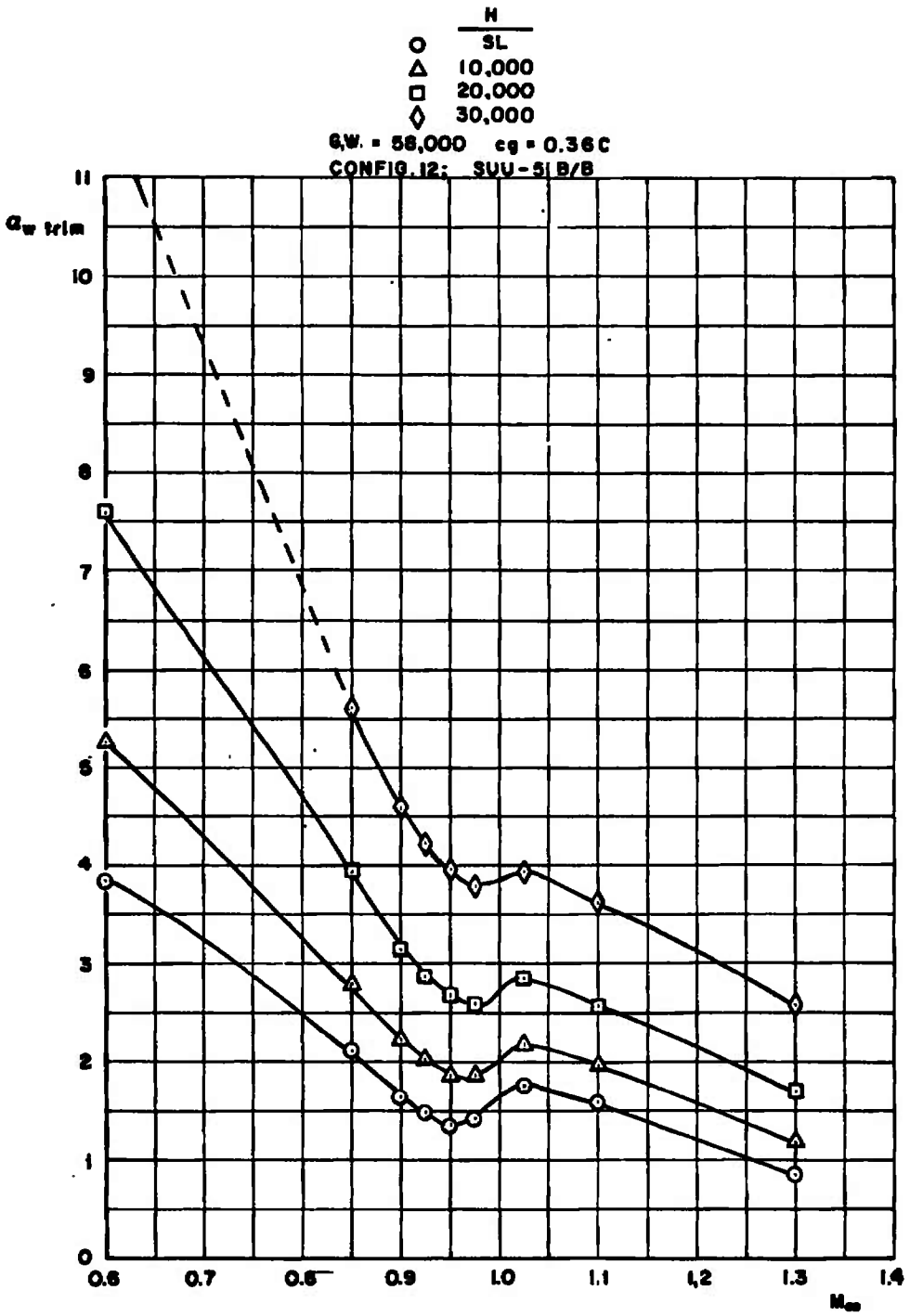

c. cg = 0.36C

Fig. 43 Concluded

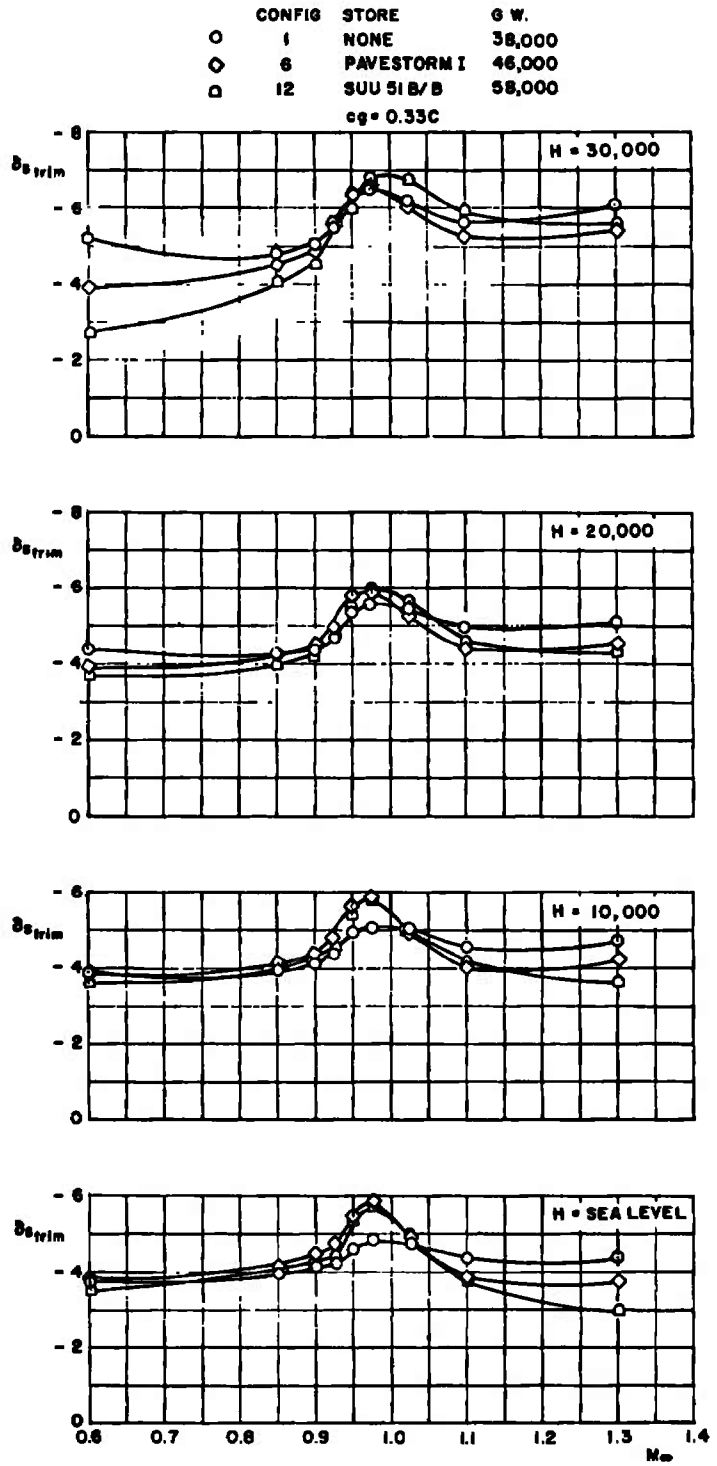

Fig. 44 Comparison of Trim Stabilator Angle as a Function of Mach Number and Altitude at a cg Location of 0.33C for Configurations 1, 6, and 12

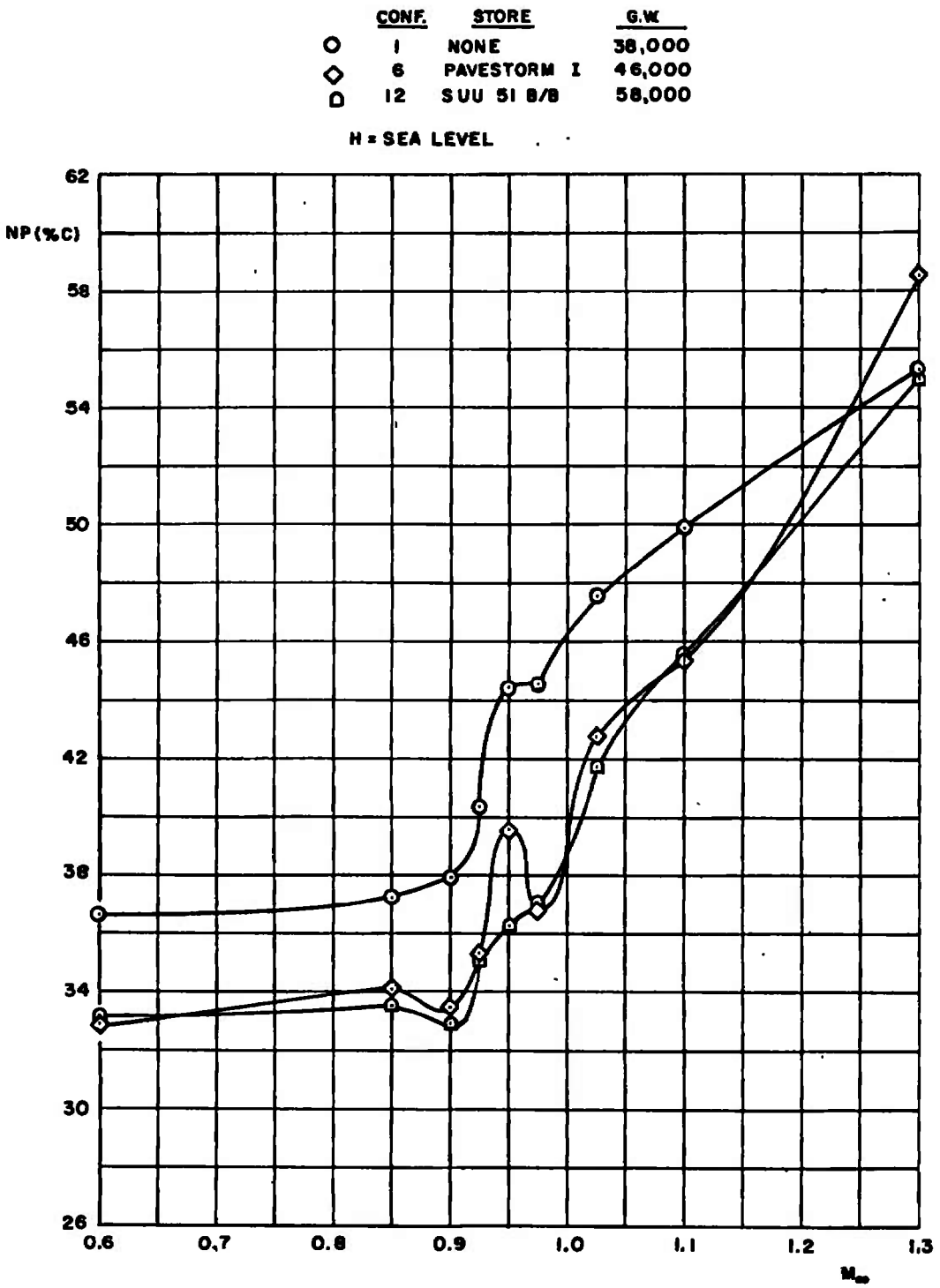

a. H = Sea Level

Fig. 45 Comparison of the Neutral-Point Location as a Function of Mach Number and Altitude for Configurations 1, 6, and 12

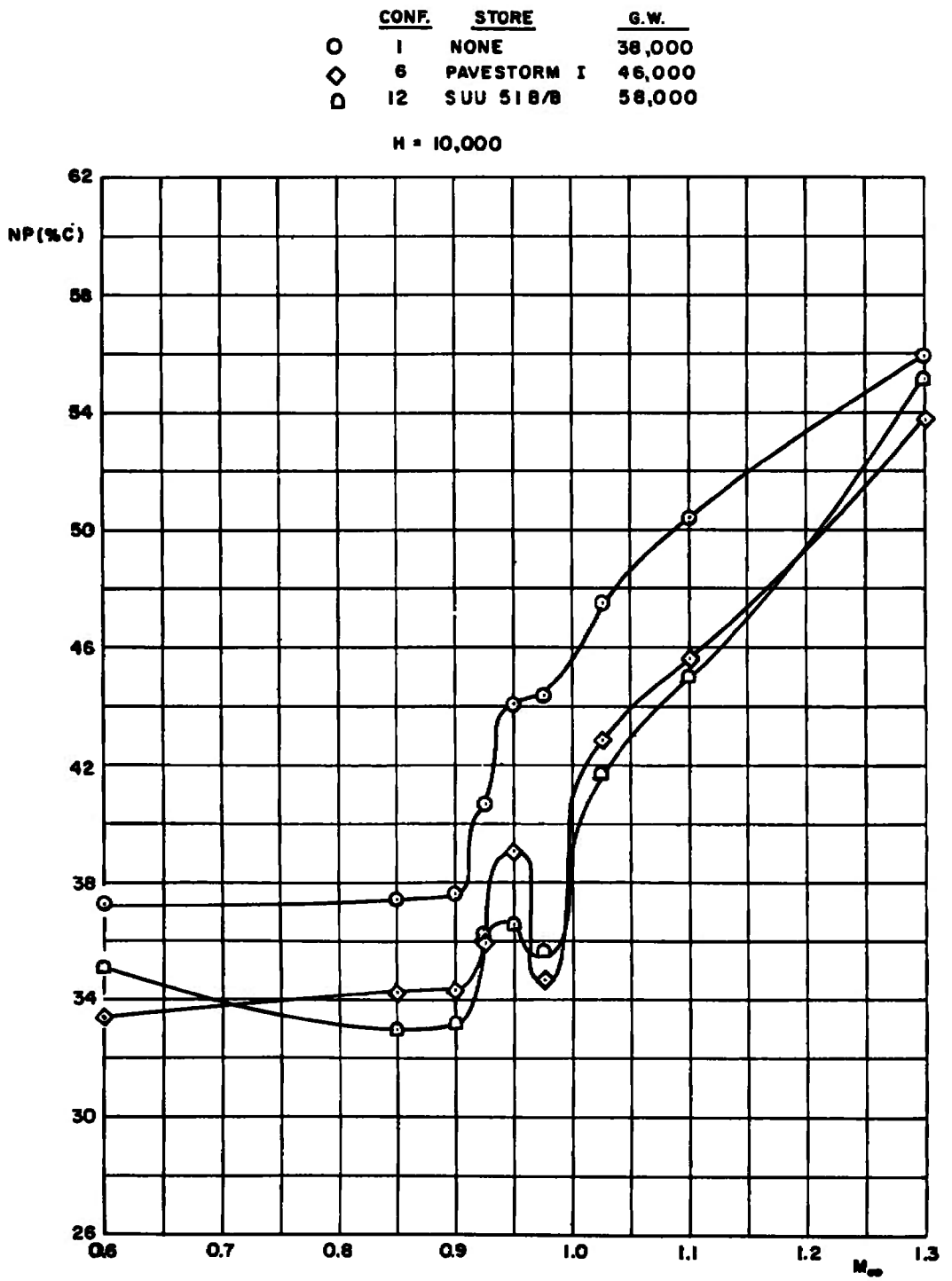

b. H = 10,000 ft
Fig. 45 Continued

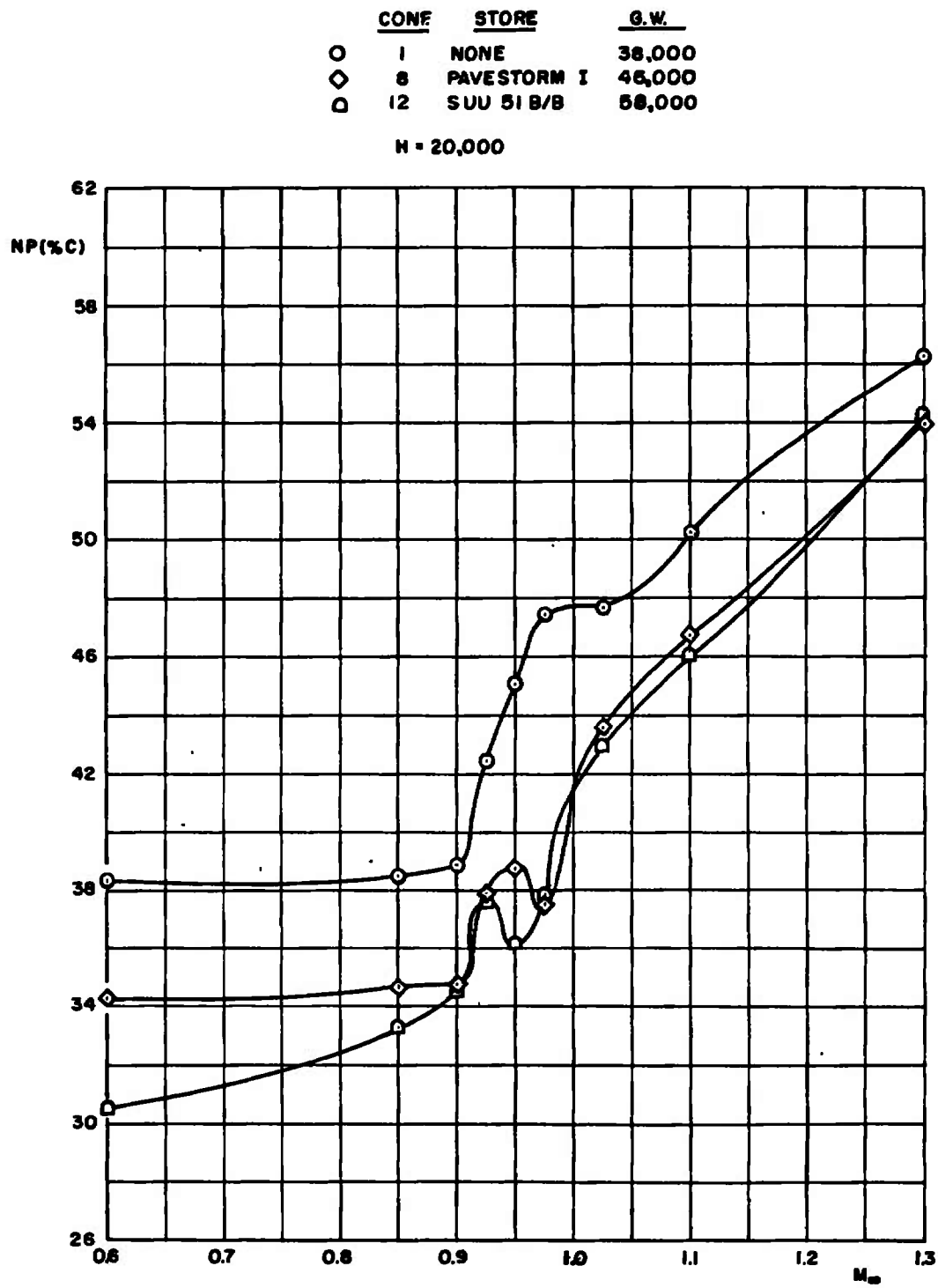

c. H = 20,000 ft
Fig. 45 Continued

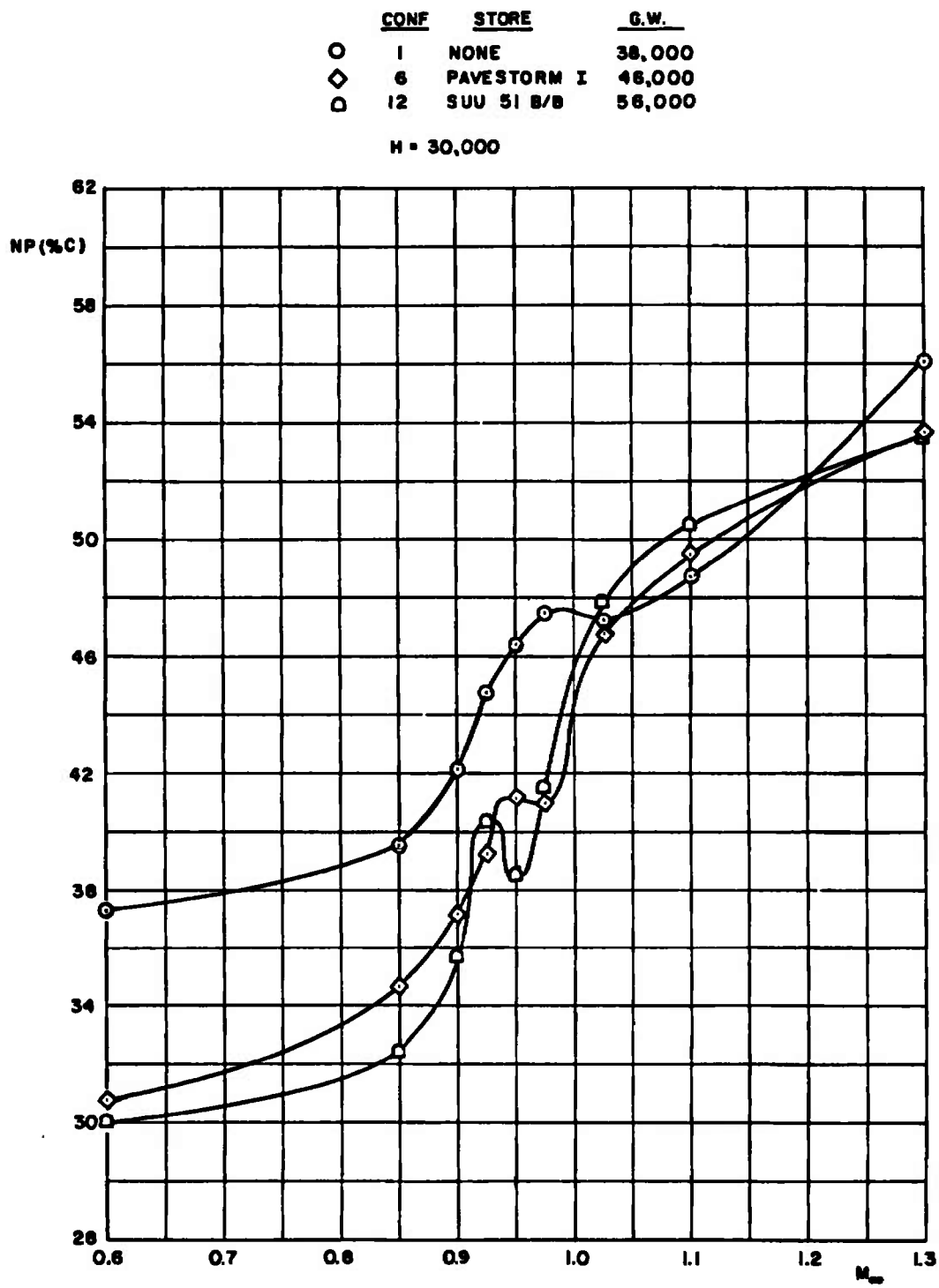

d. H = 30,000 ft
Fig. 45 Concluded

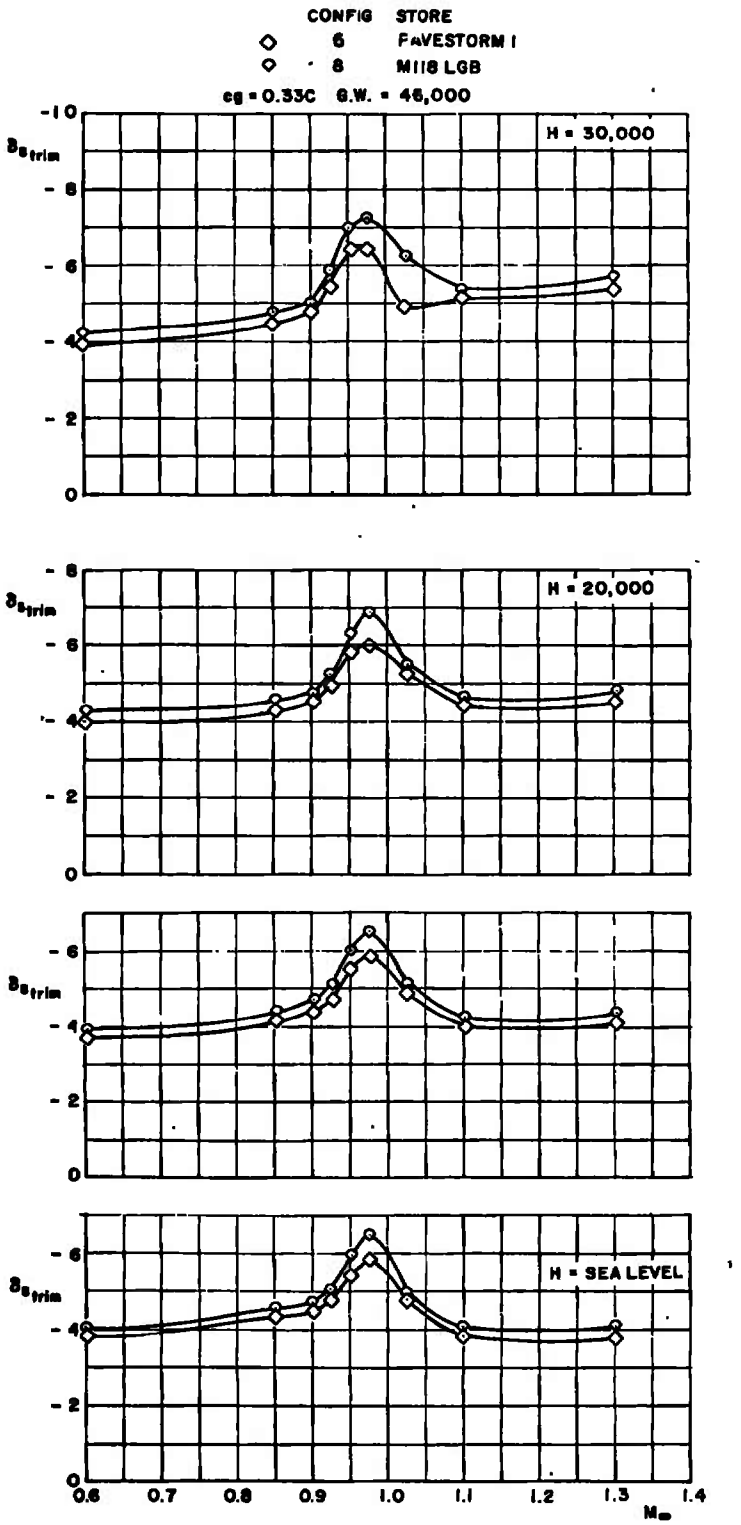

Fig. 46 Comparison of Trim Stabilator Angle as a Function of Mach Number and Altitude at a cg Location of 0.33C for Configurations 6 and 18

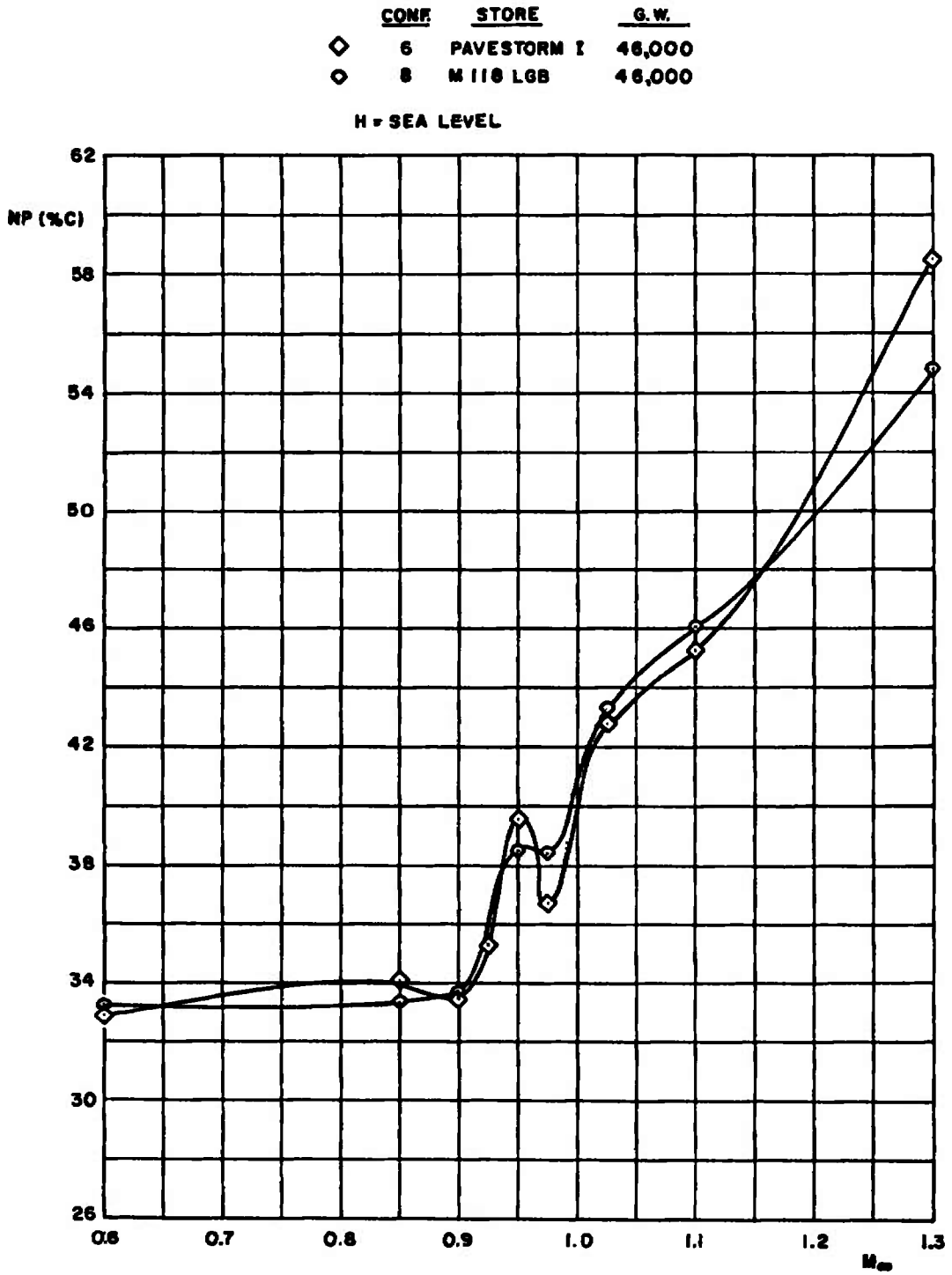

a. H = Sea Level

Fig. 47 Comparison of Neutral-Point Location as a Function of Mach Number and Altitude for Configurations 6 and 8

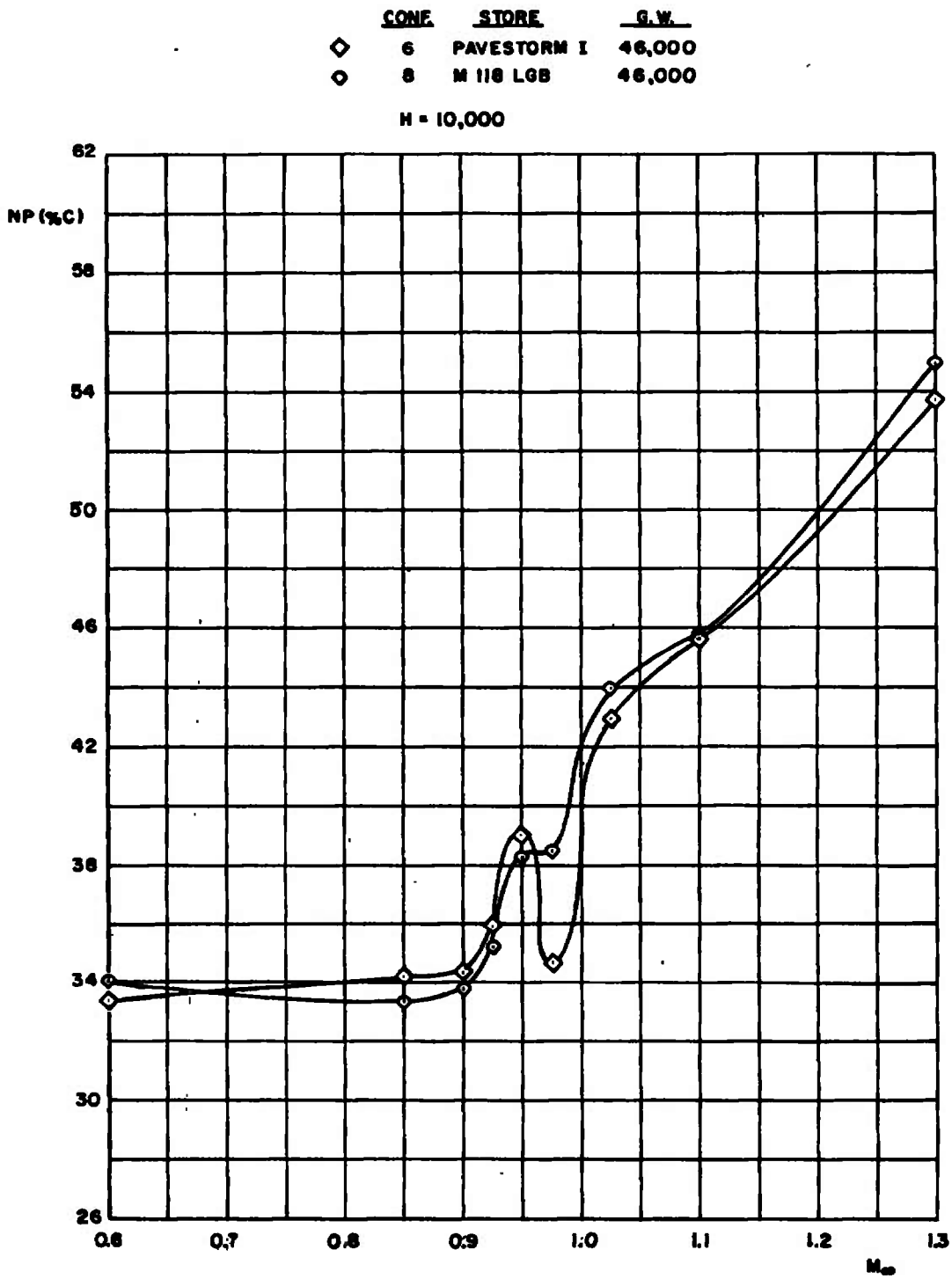

b. H = 10,000 ft
Fig. 47 Continued

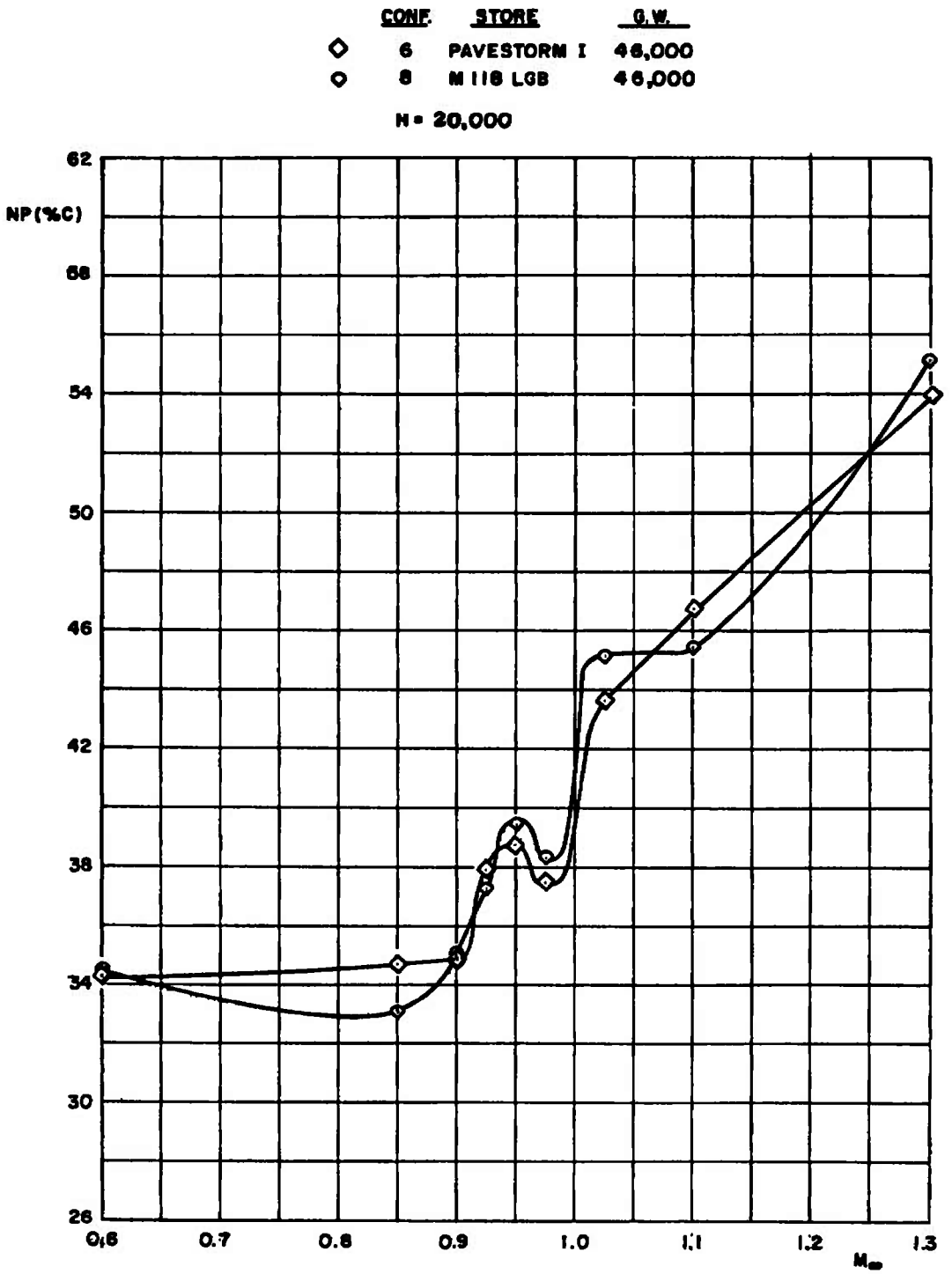

c. H = 20,000 ft
Fig. 47 Continued

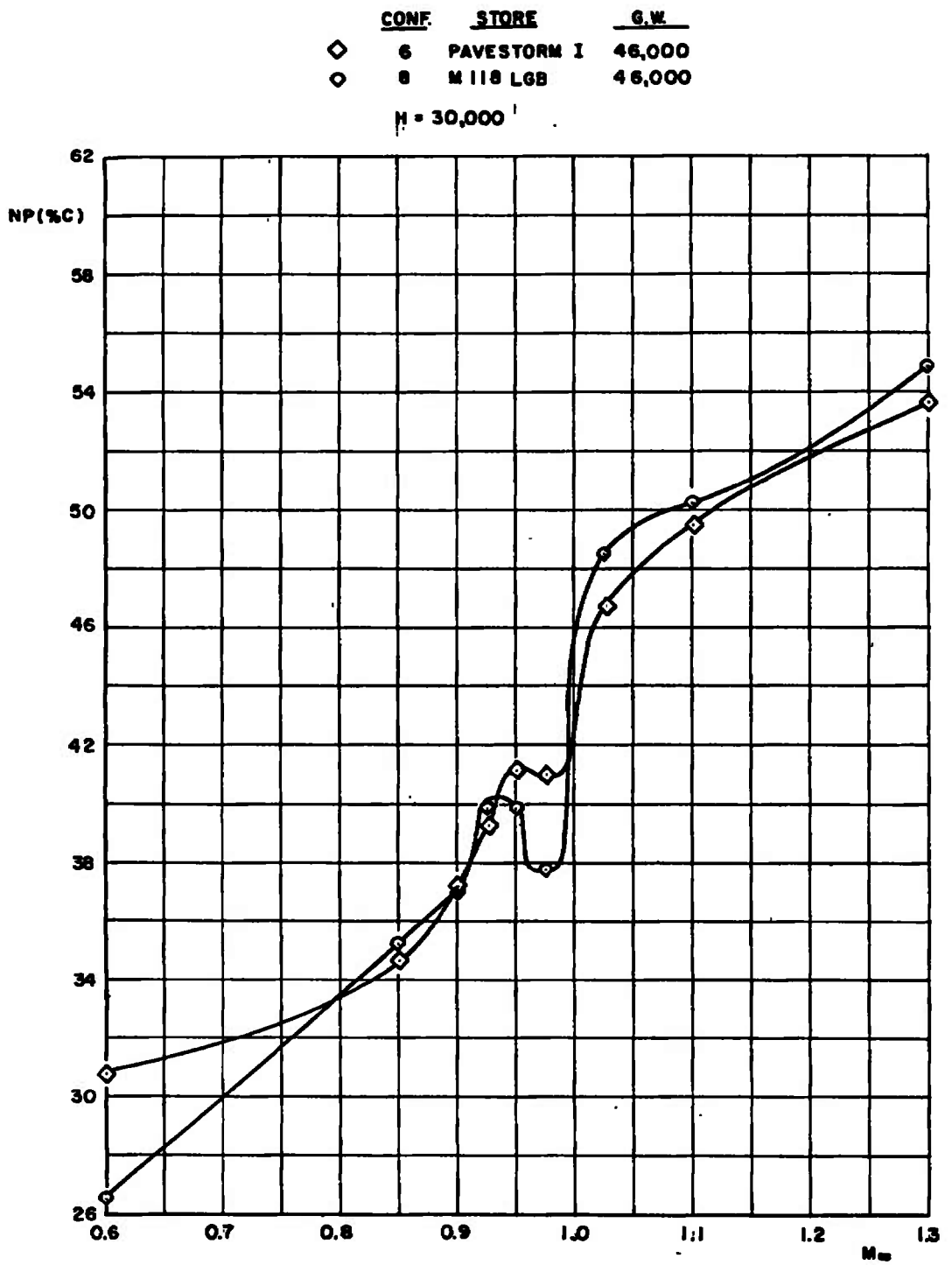

d. H = 30,000 ft
Fig. 47 Concluded

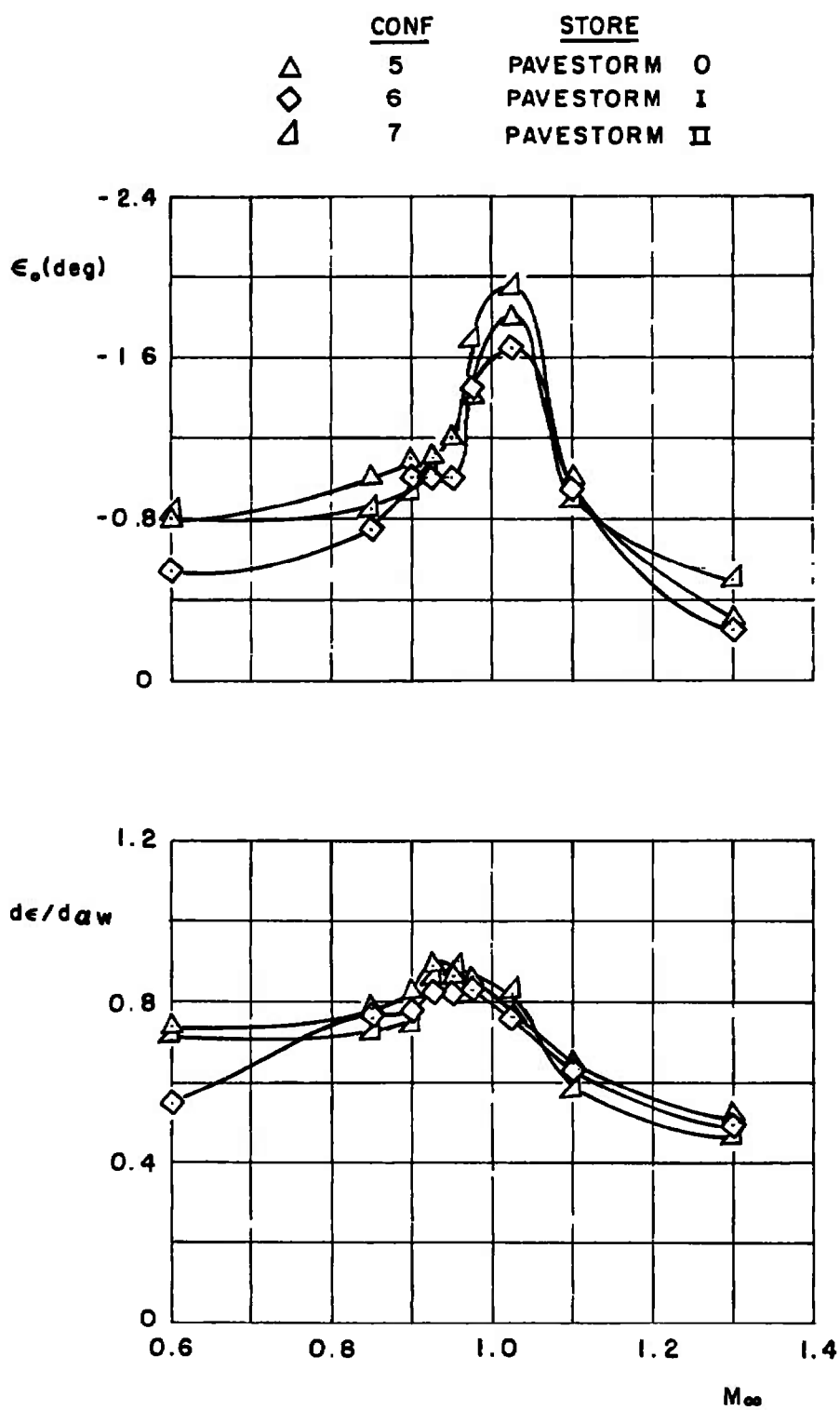

Fig. 48 Downwash Characteristics of Configurations 5, 6, and 7

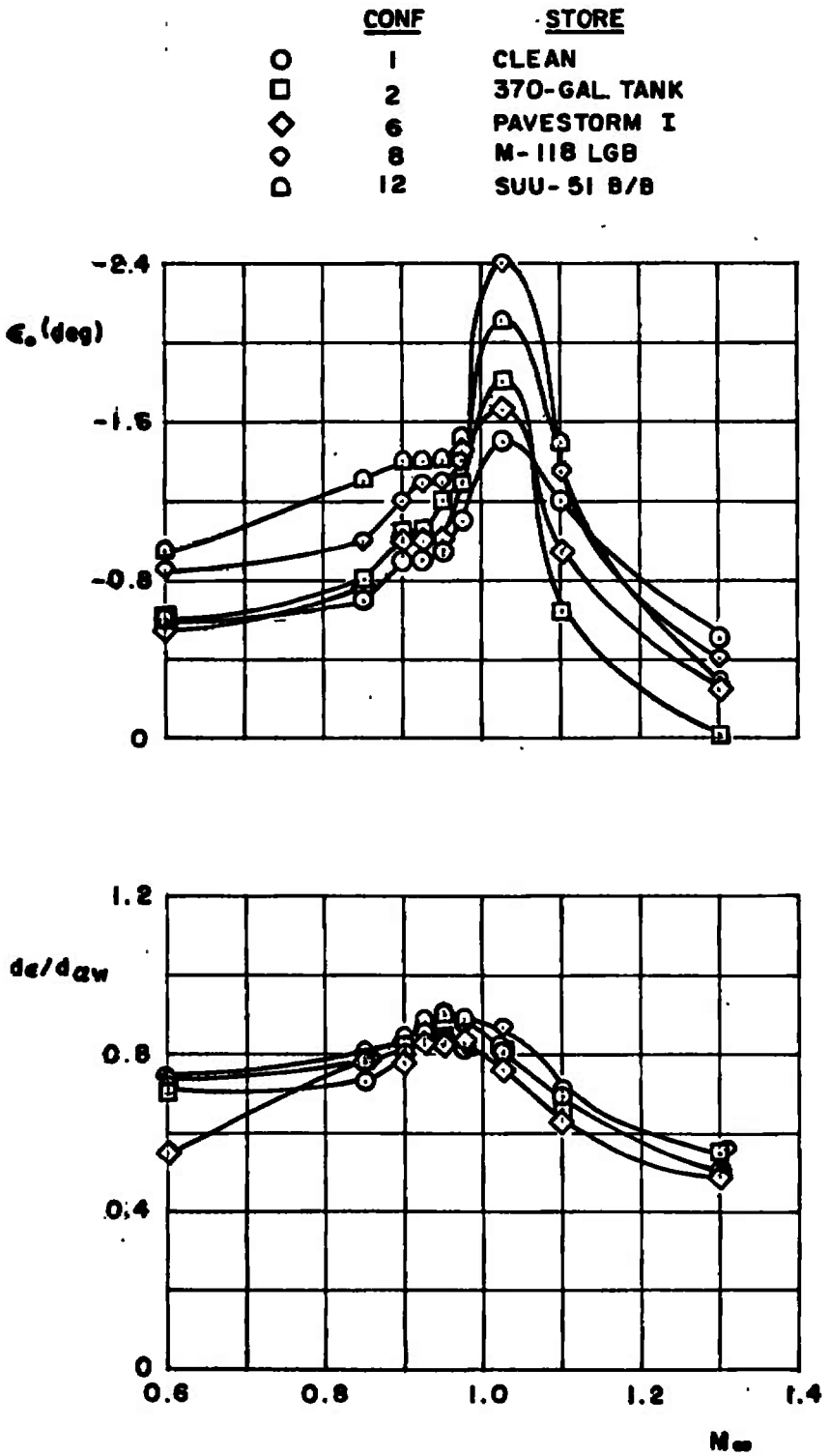

Fig. 49 Downwash Characteristics of Configurations 1, 2, 6, 8, and 12

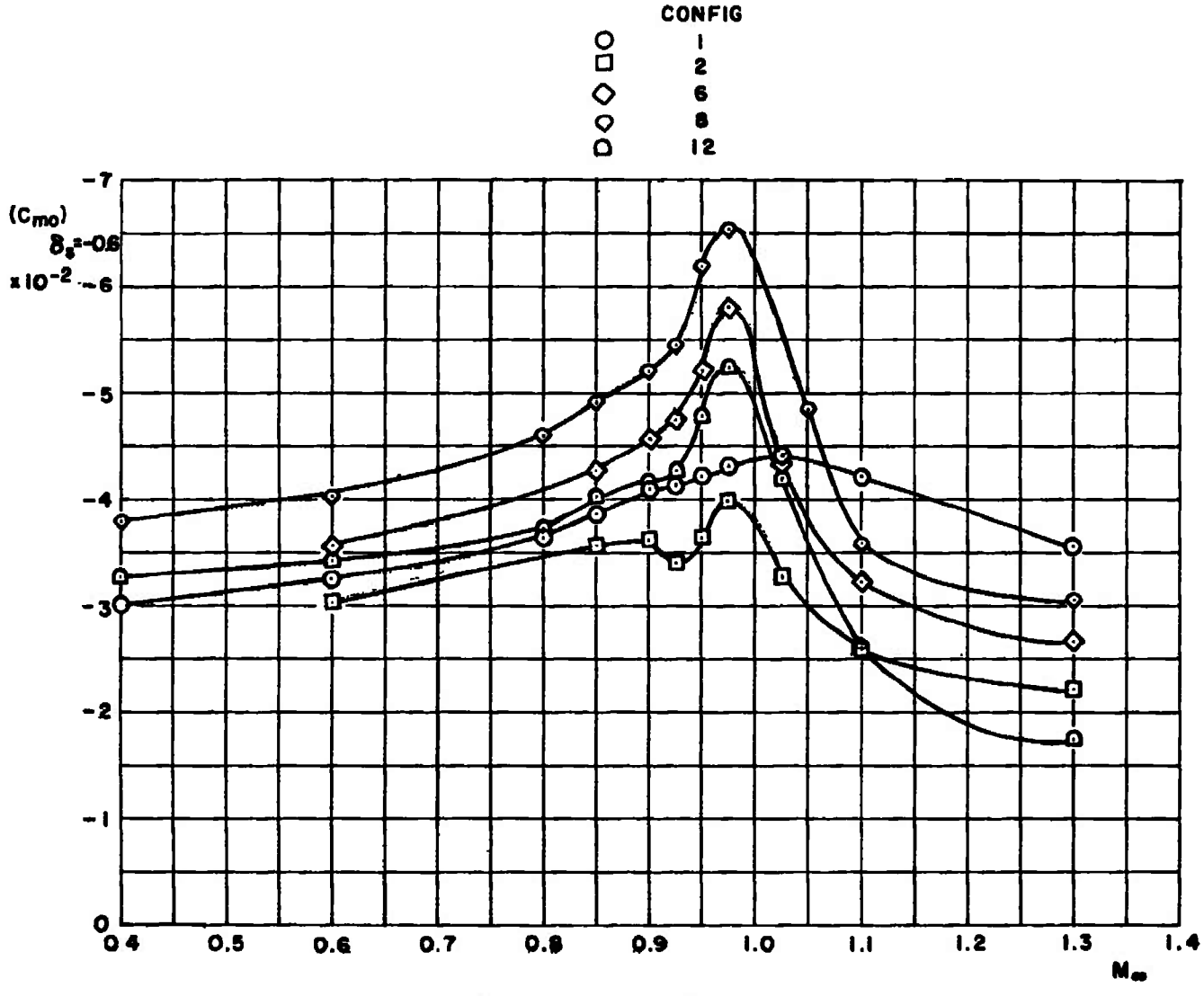

Fig. 50 Effect of External Stores on C_{m_o}

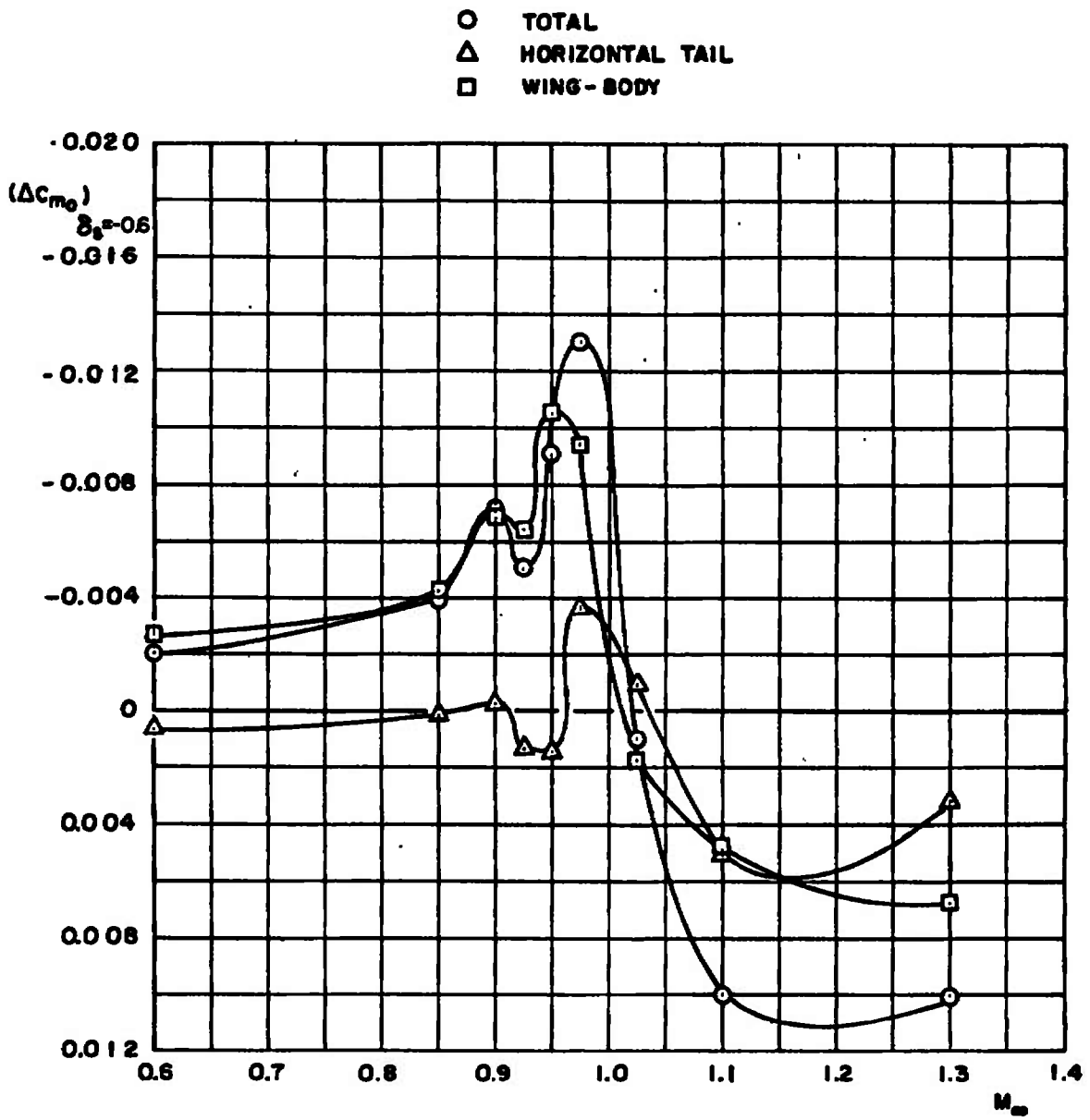

Fig. 51 Results of Downwash Analysis for Configuration 6

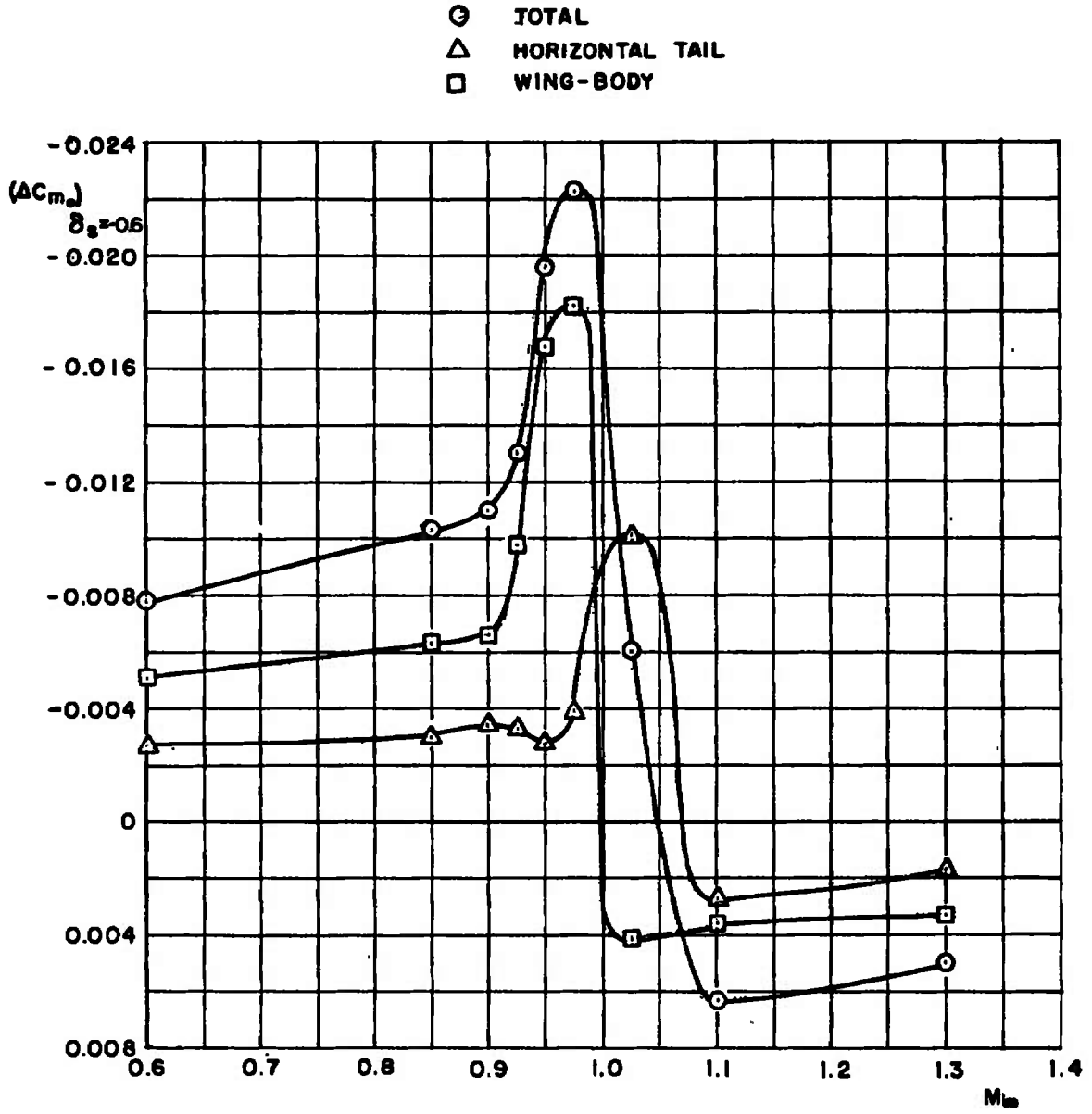

Fig. 52 Results of Downwash Analysis for Configuration 8

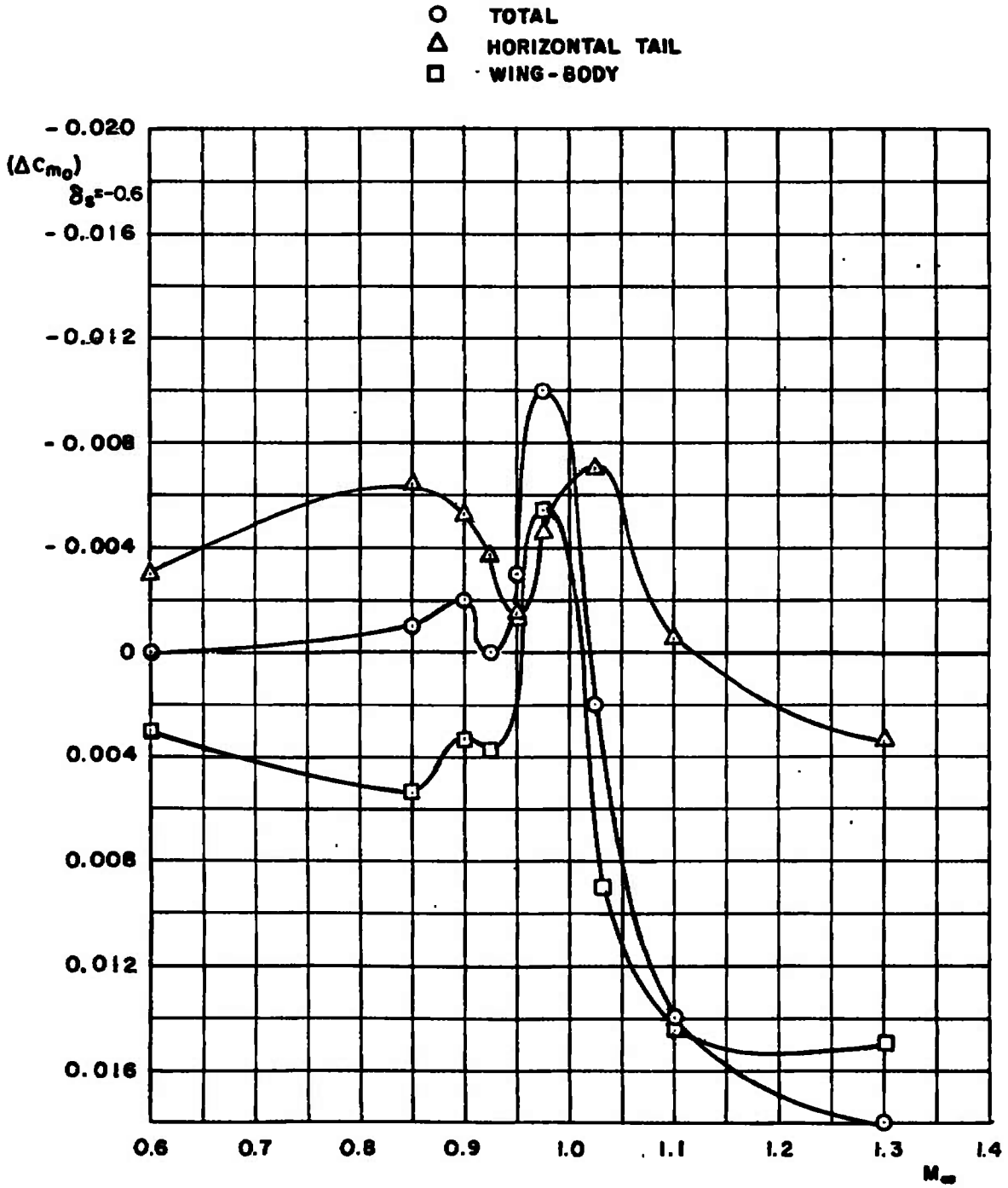

Fig. 53 Results of Downwash Analysis for Configuration 12

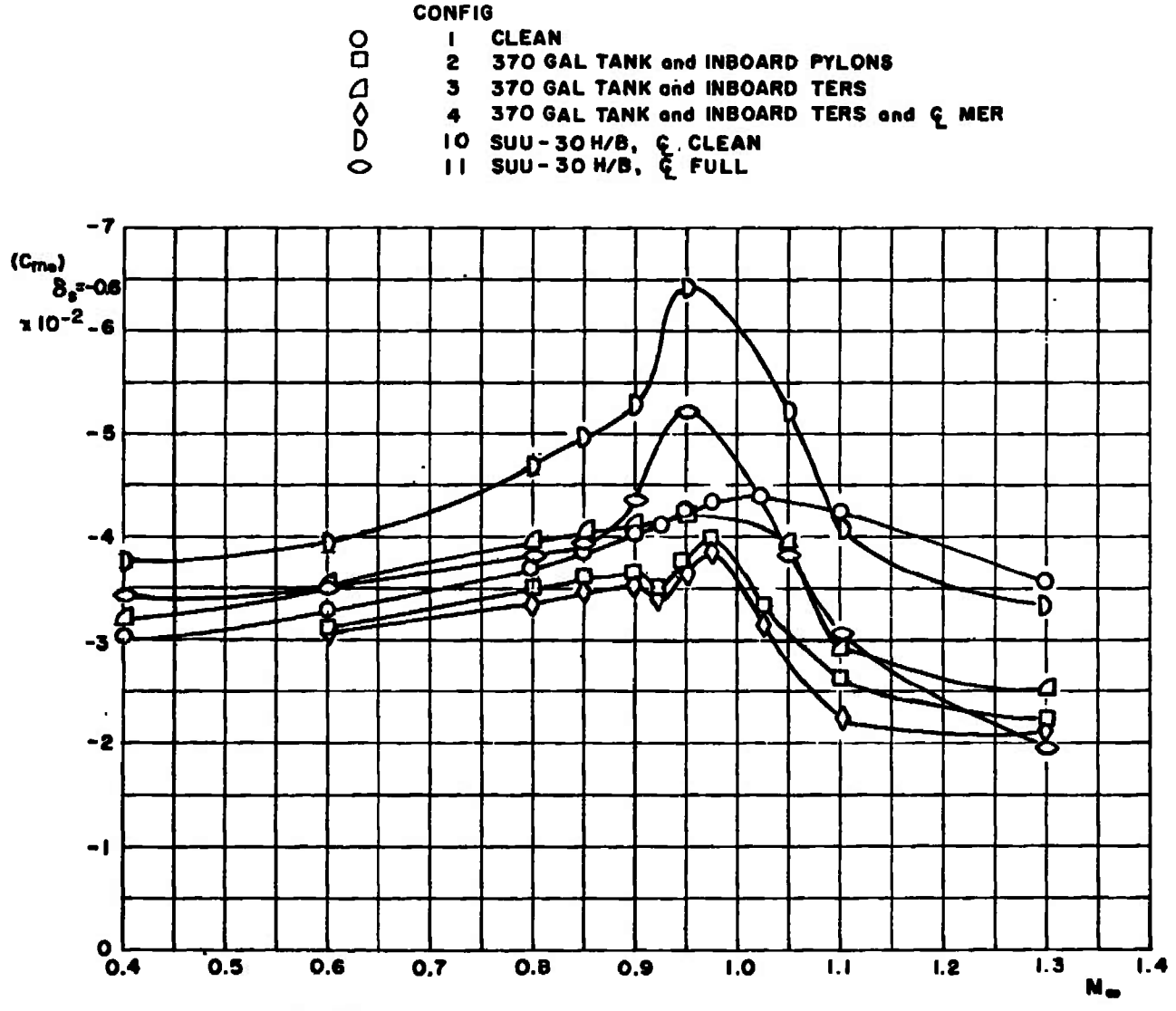

Fig. 54 Effect of Various External Stores on C_{m_o}

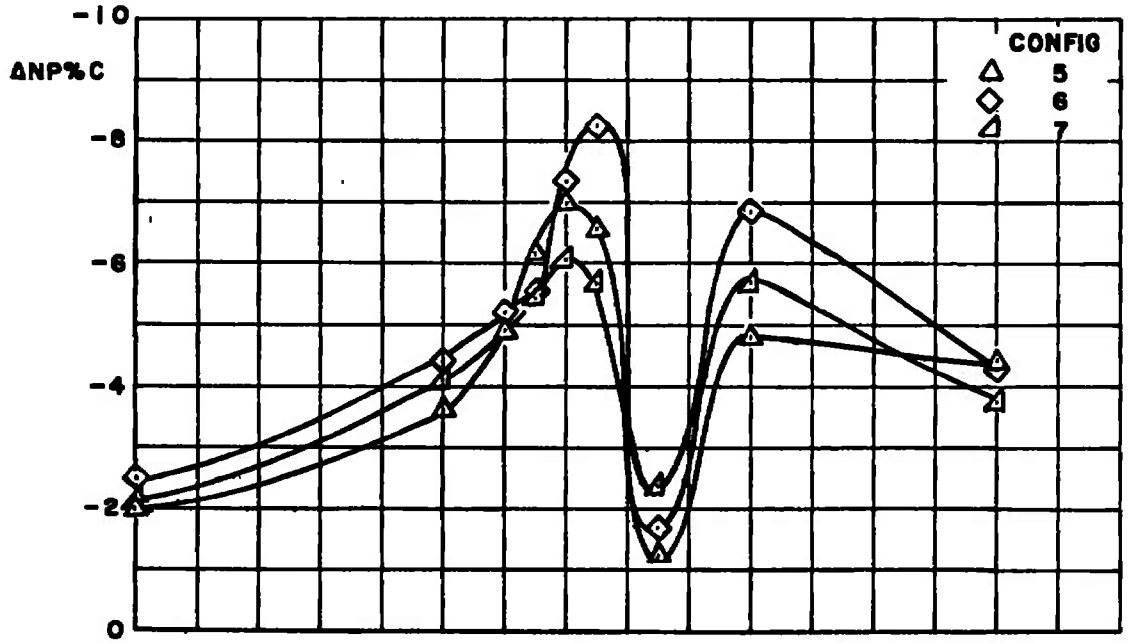

Fig. 55 Comparison of Incremental Change in Neutral-Point Location for Configurations 5, 6, and 7

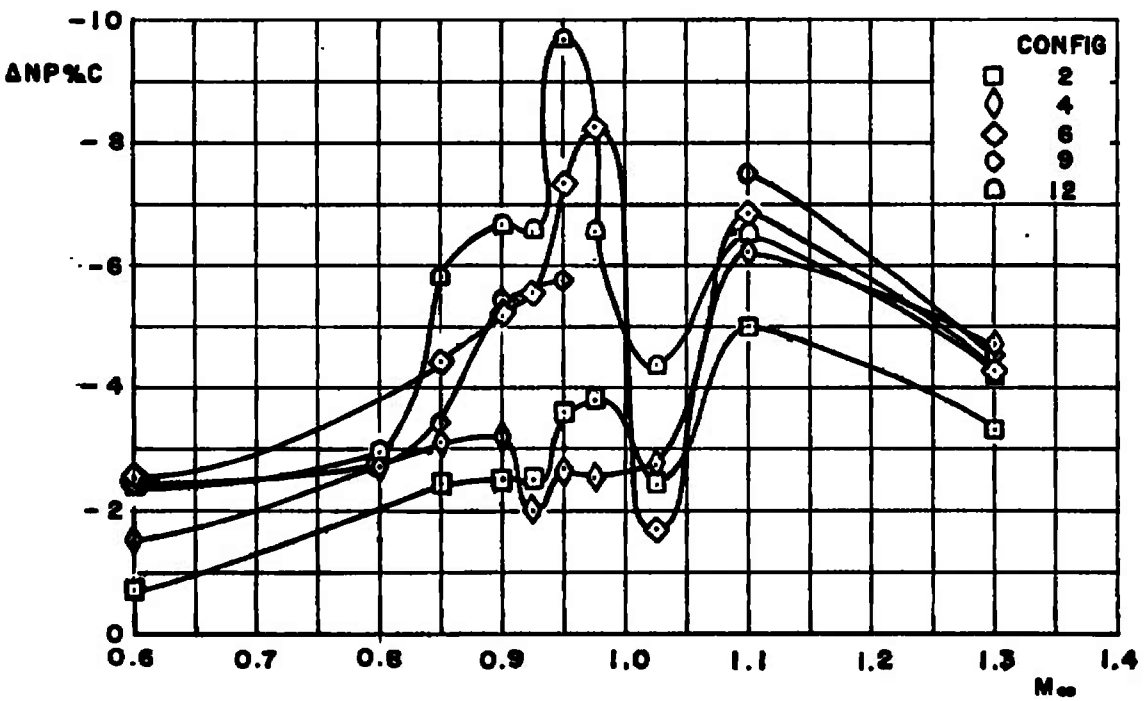

Fig. 56 Comparison of Incremental Change in Neutral-Point Location for Configurations 2, 4, 8, 9, and 12

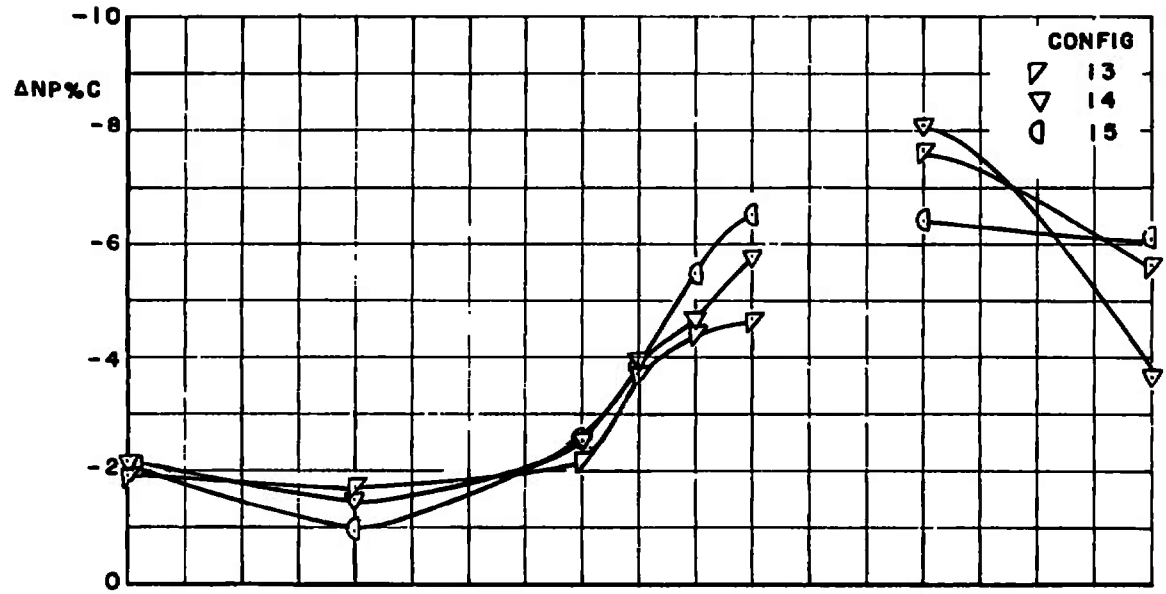

Fig. 57 Comparison of Incremental Change in Neutral-Point Location for Configurations 13, 14, and 15

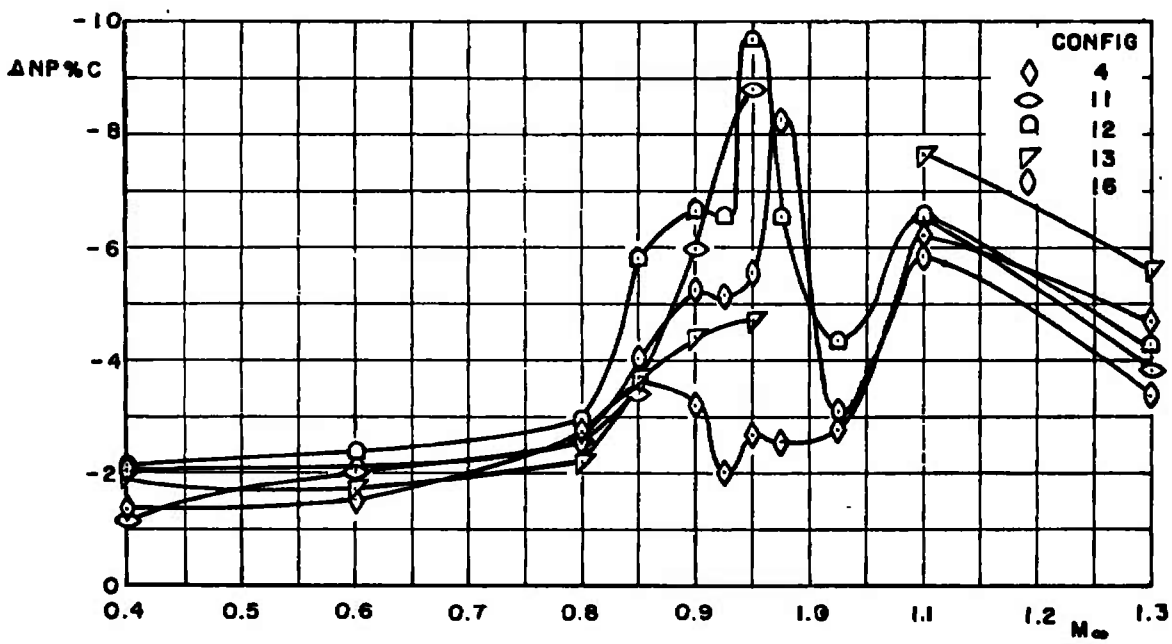

Fig. 58 Comparison of Incremental Change in Neutral-Point Location for Configurations 4, 11, 12, 13, and 16

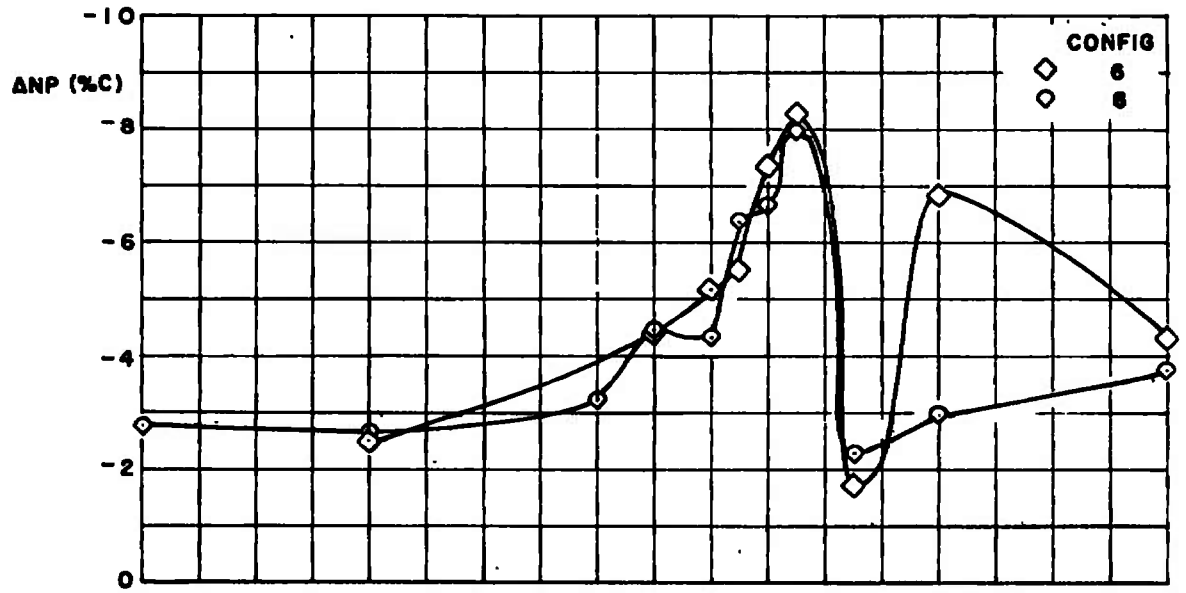

Fig. 59 Comparison of Incremental Change in Neutral-Point Location for Configurations 6 and 8

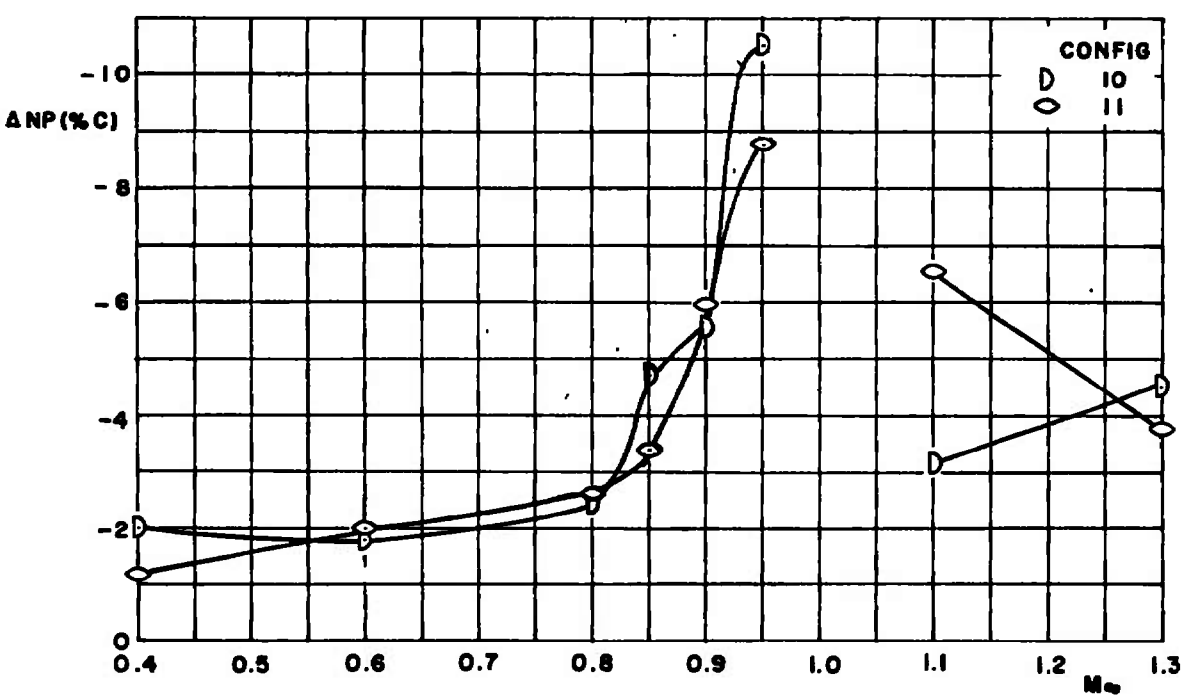

Fig. 60 Comparison of Incremental Change in Neutral-Point Location for Configurations 10 and 11

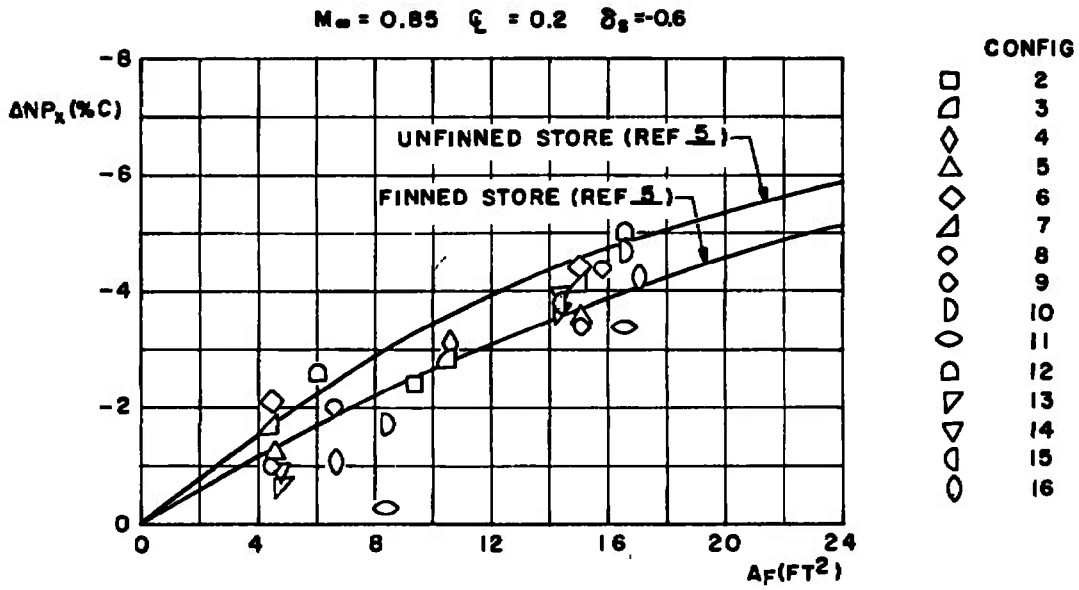

a. Wing-Mounted Store Frontal Area Correlation

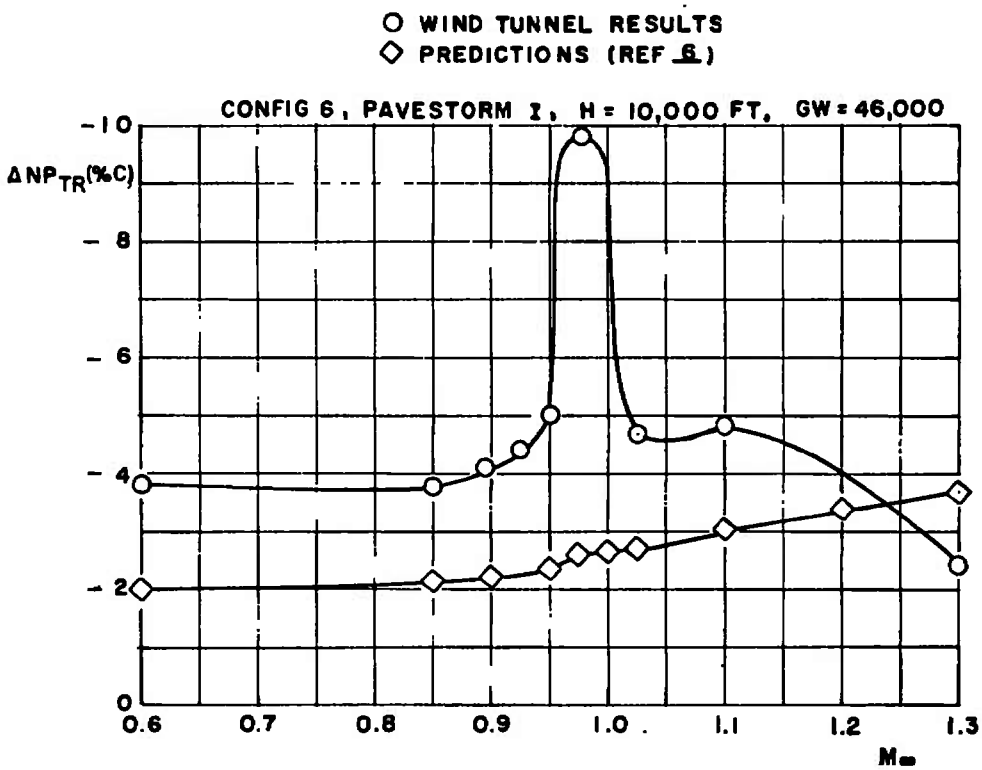

b. Generalized Prediction Technique of Ref. 6

Fig. 61 Comparison of Measured Neutral-Point Shifts with Results from Existing Prediction Techniques

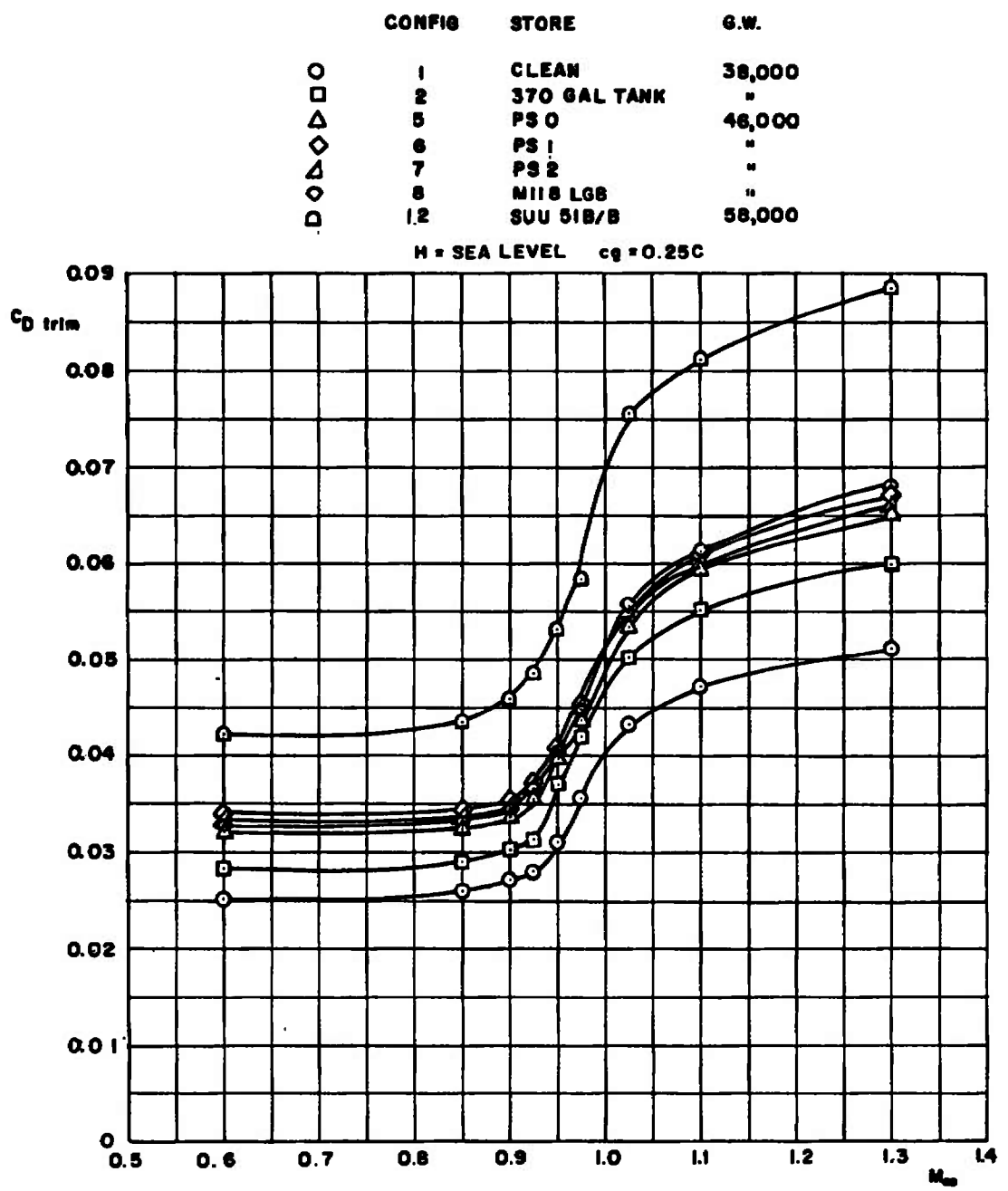

a. H = Sea Level

Fig. 62 Trim Drag Characteristics of the F-4C with Various External Store Configurations for Several Altitudes at a cg Location of 0.25C

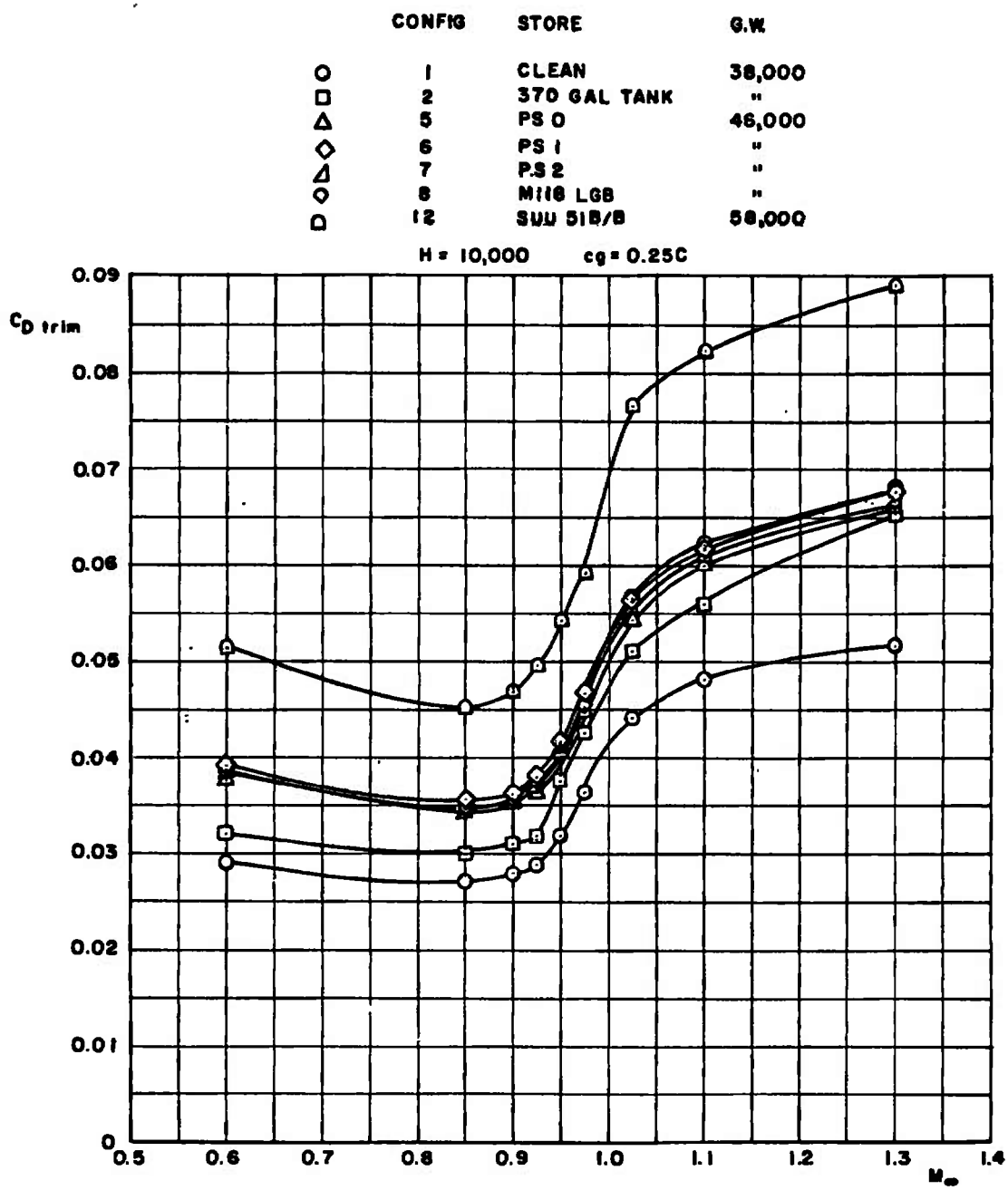

b. H = 10,000 ft
Fig. 62 Continued

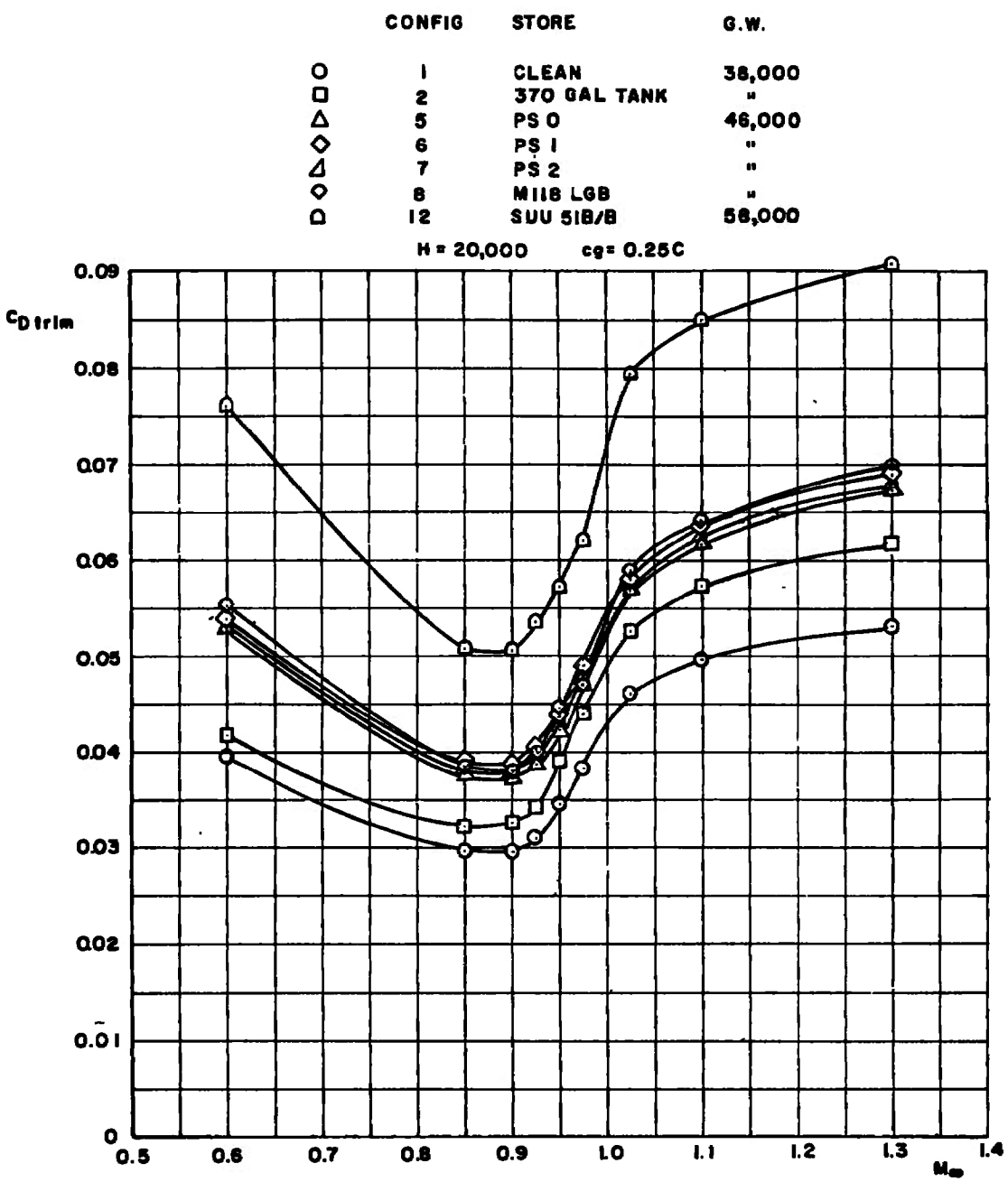

c. H = 20,000 ft
Fig. 62 Continued

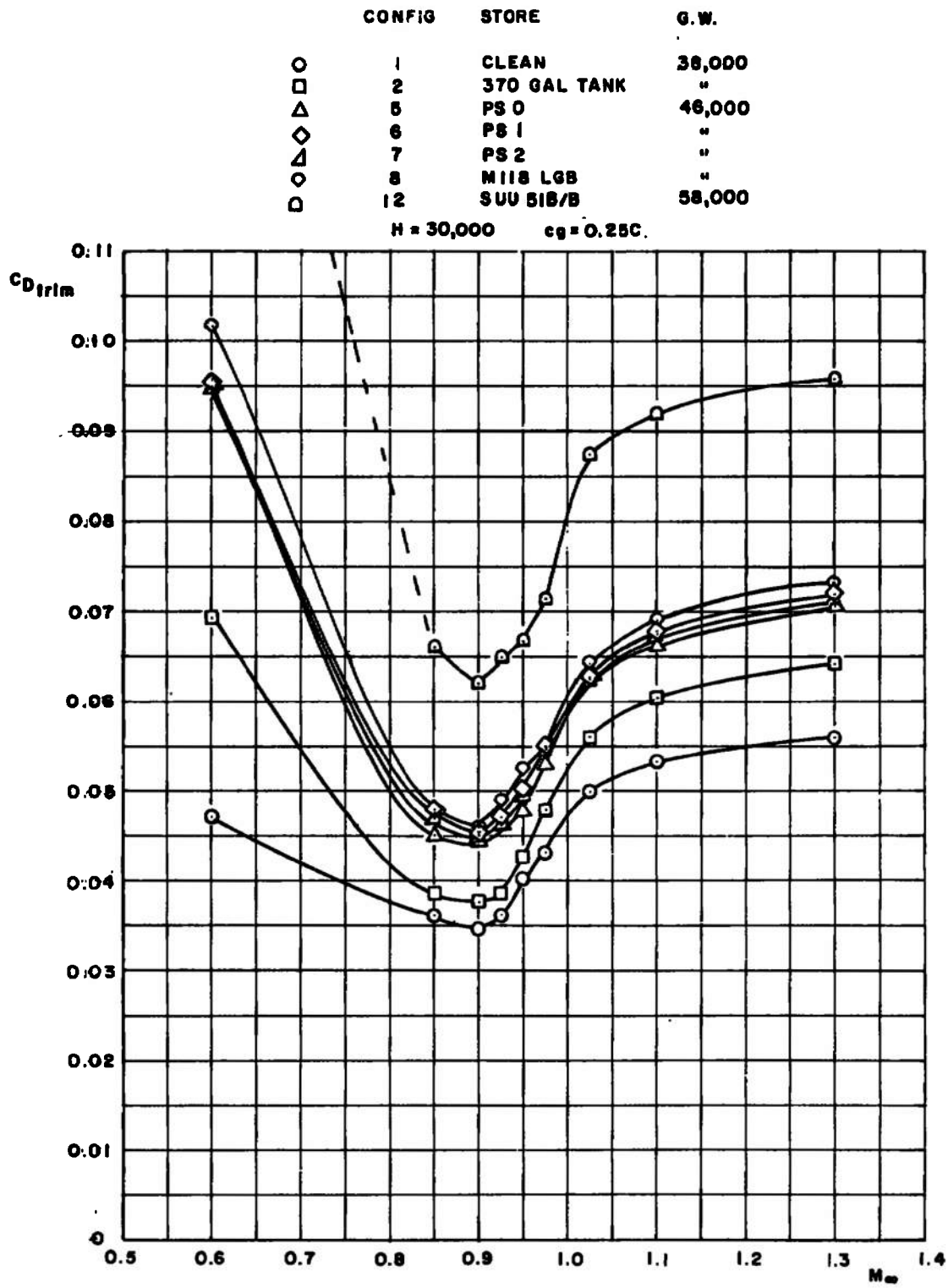

d. H = 30,000 ft

Fig. 62 Concluded

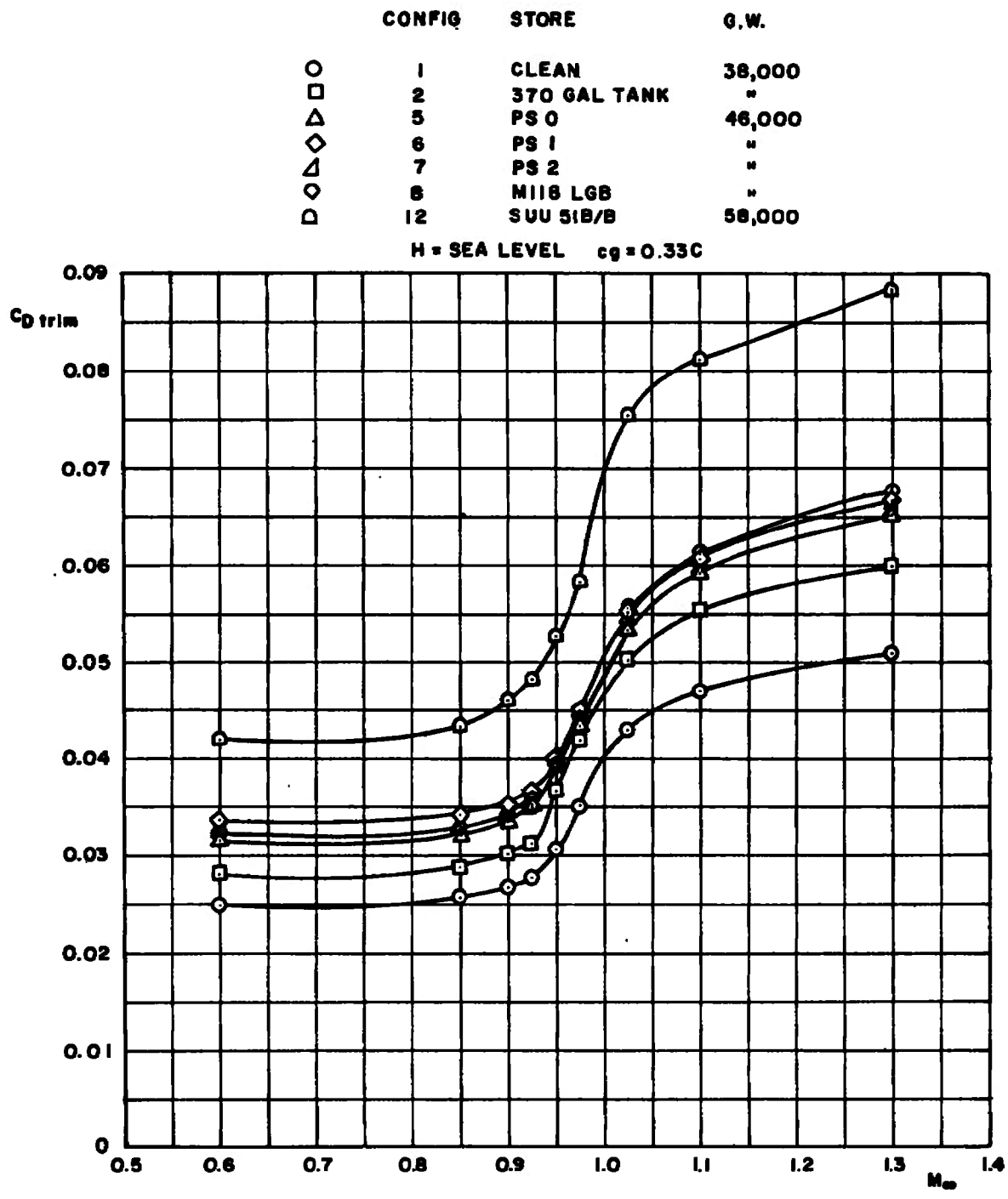

a. H = Sea Level

Fig. 63 Trim Drag Characteristics of the F-4C with Various External Store Configurations for Several Altitudes at a cg Location of 0.33C

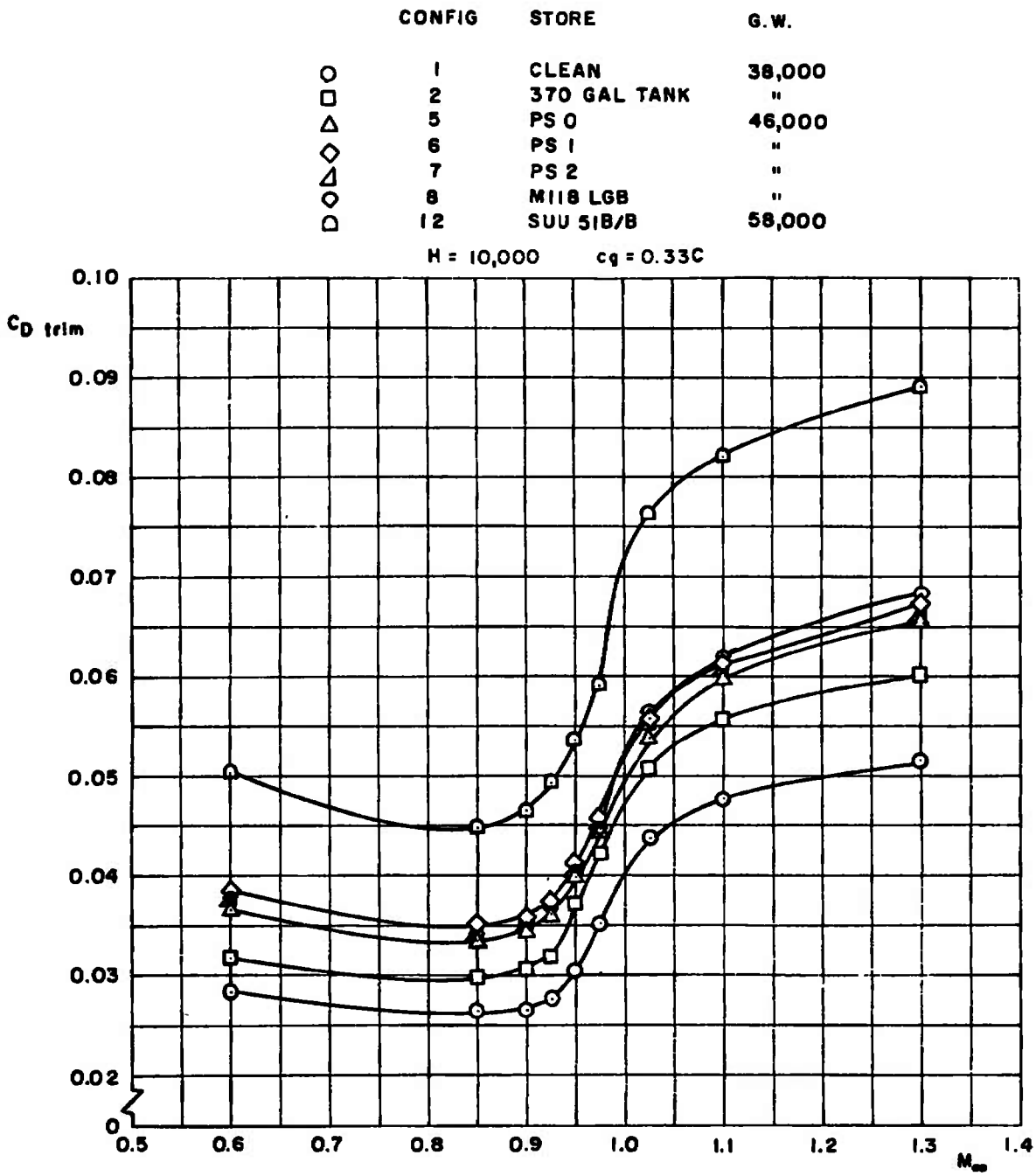

b. H = 10,000 ft
Fig. 63 Continued

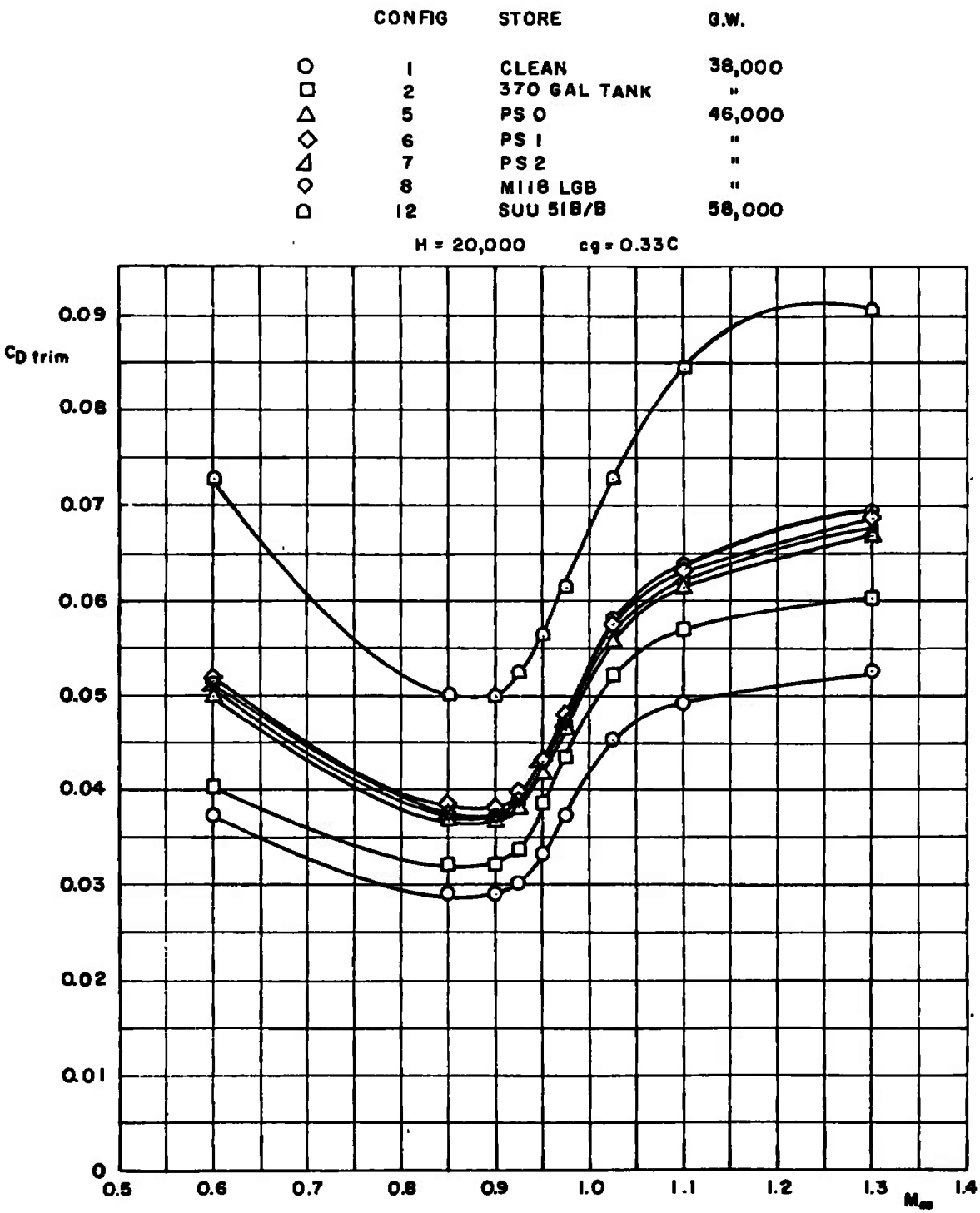

c. H = 20,000 ft
Fig. 63 Continued

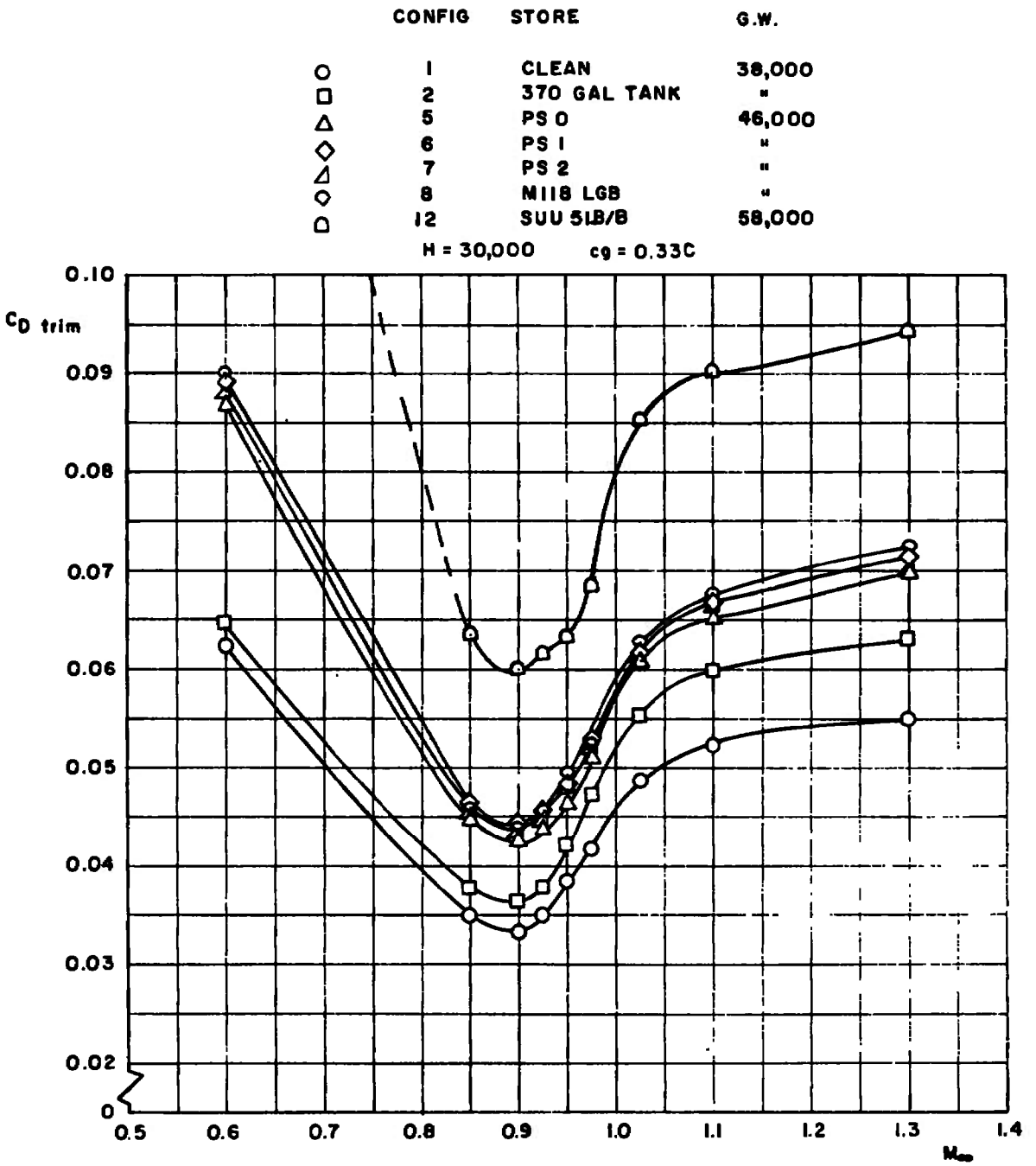

d. H = 30,000 ft
Fig. 63 Concluded

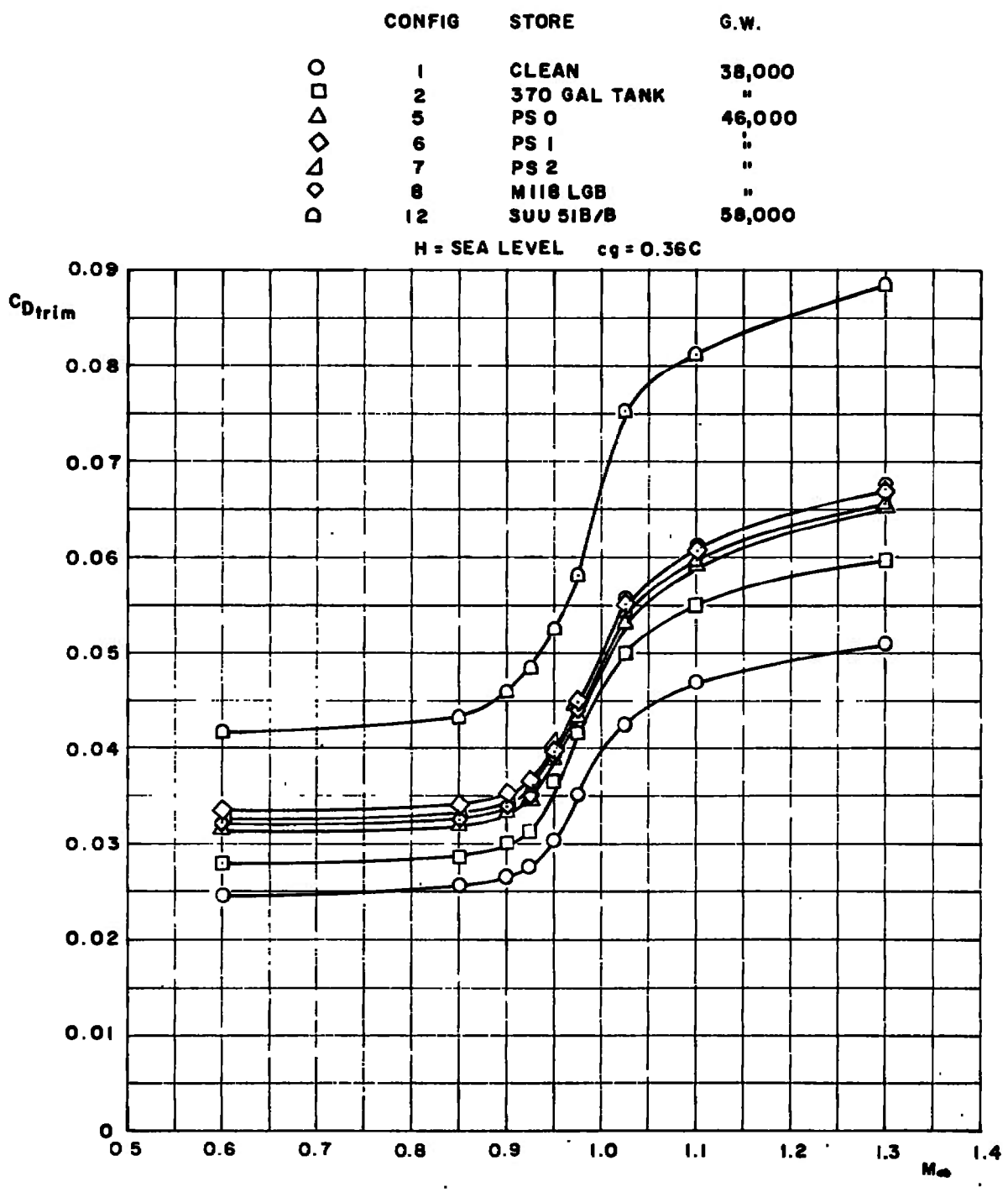

a. H = Sea Level

Fig. 64 Trim Drag Characteristics of the F-4C with Various External Store Configurations for Several Altitudes at a cg Location of 0.36C

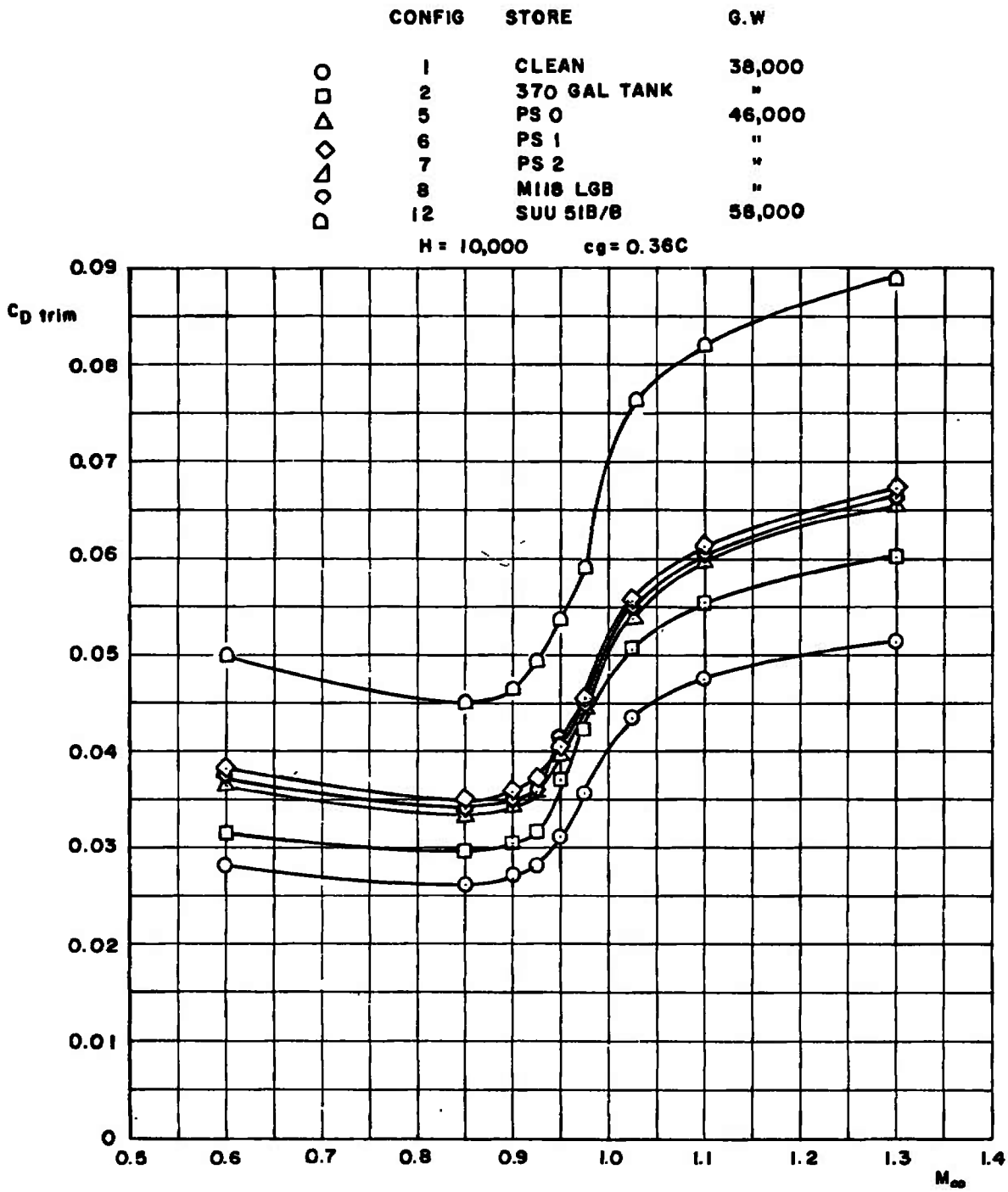

b. H = 10,000 ft
Fig. 64 Continued

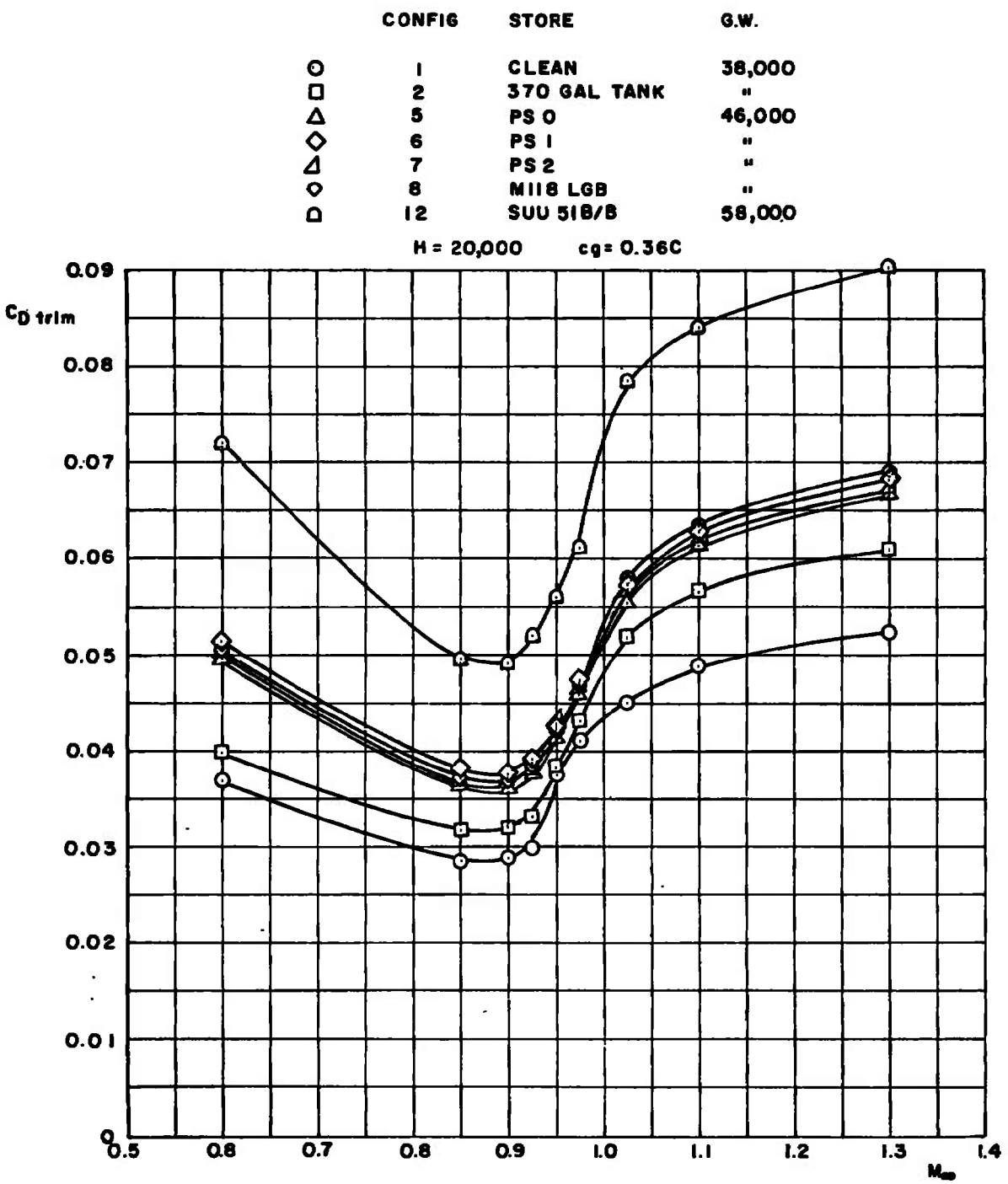

c. H = 20,000 ft

Fig. 64 Continued

	CONFIG	STORE	G.W.
○	1	CLEAN	38,000
□	2	370 GAL TANK	"
△	5	PS 0	46,000
◇	6	PS 1	"
◁	7	PS 2	"
◇	8	MIIB LGB	"
⏢	12	SUU 51B/B	58,000

H = 30,000 cg = 0.36C

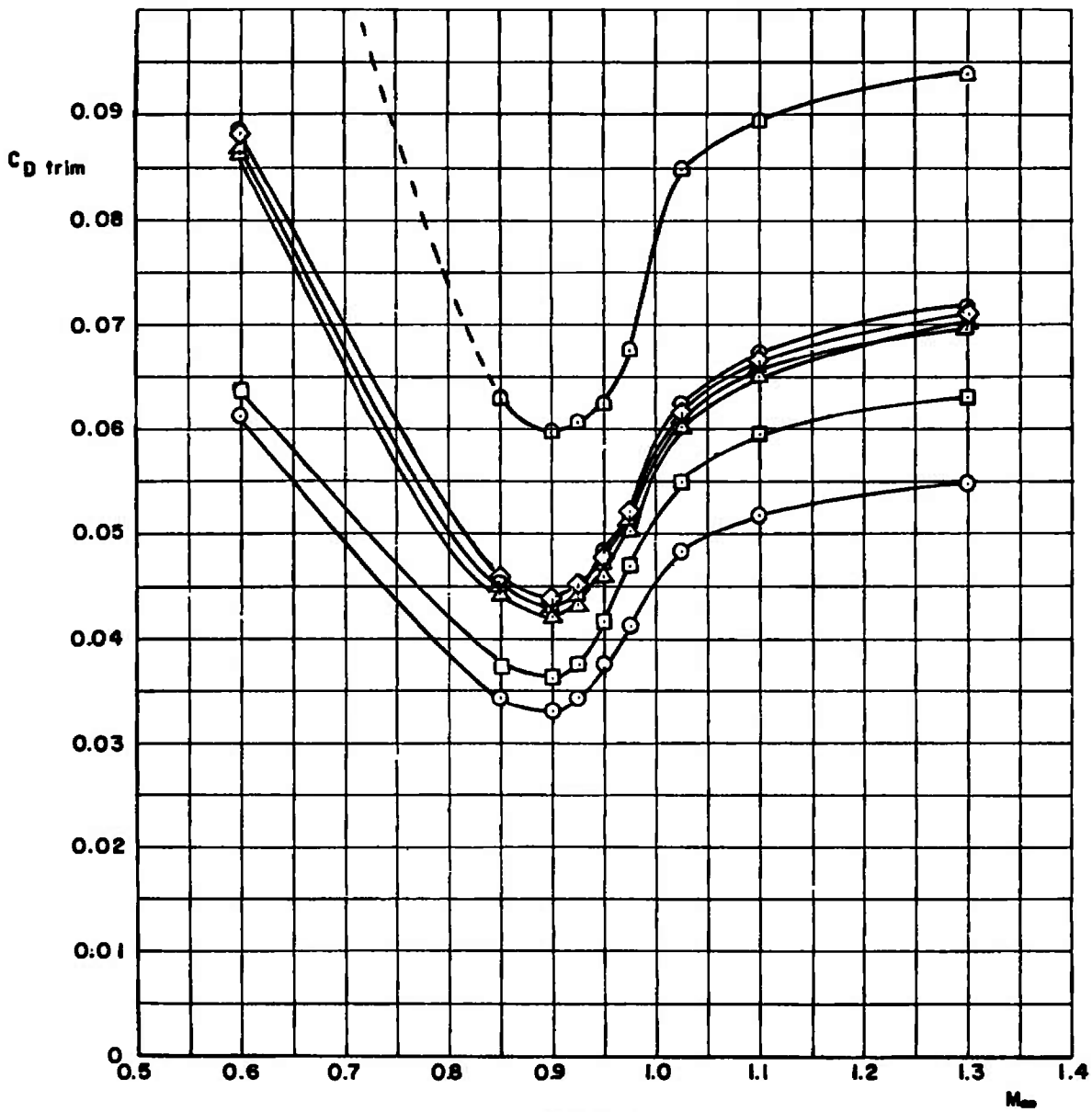

d. H = 30,000 ft

Fig. 64 Concluded

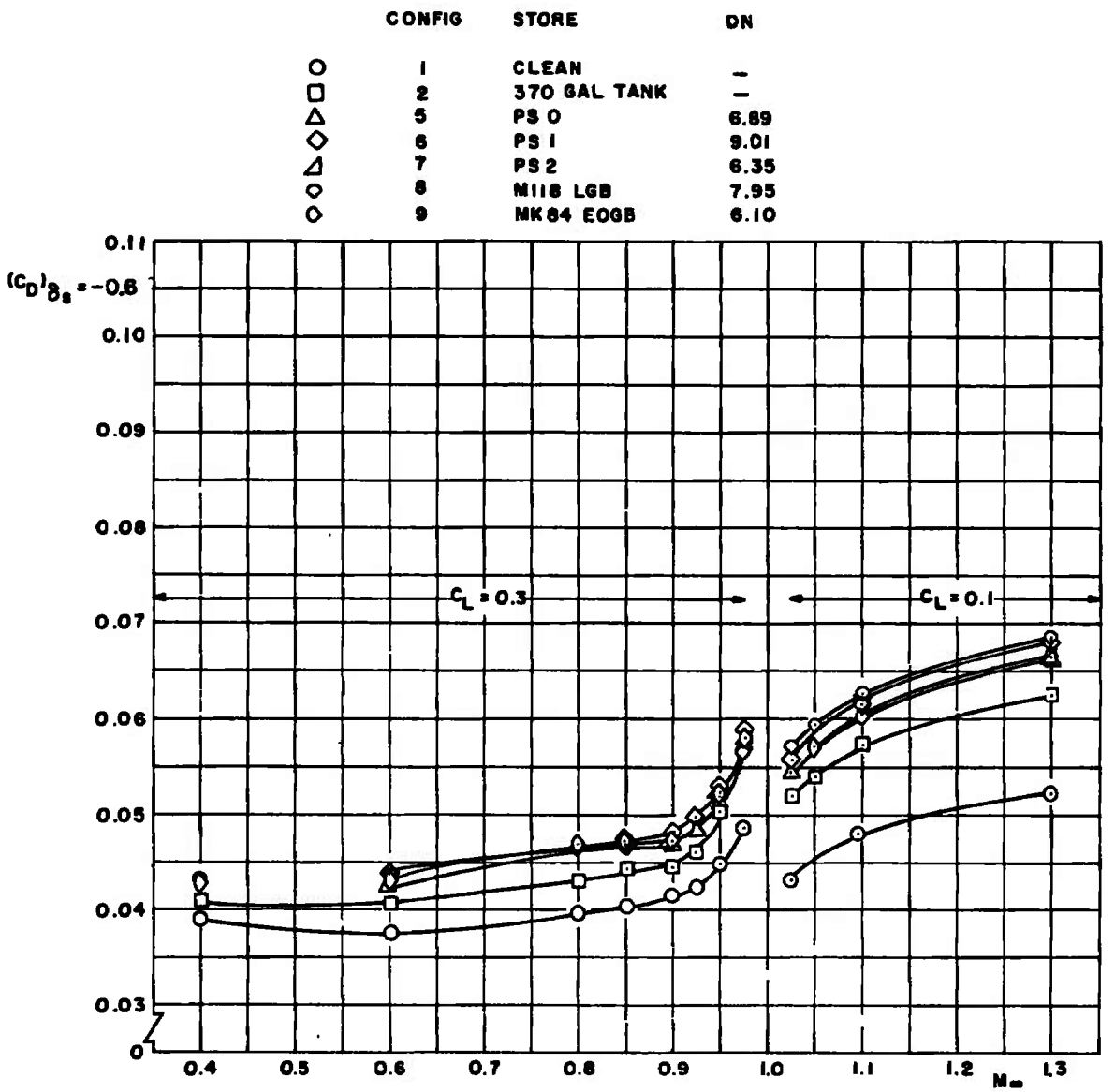

Fig. 65 Drag Variation with Mach Number for Several Single-Mounted External Store Configurations

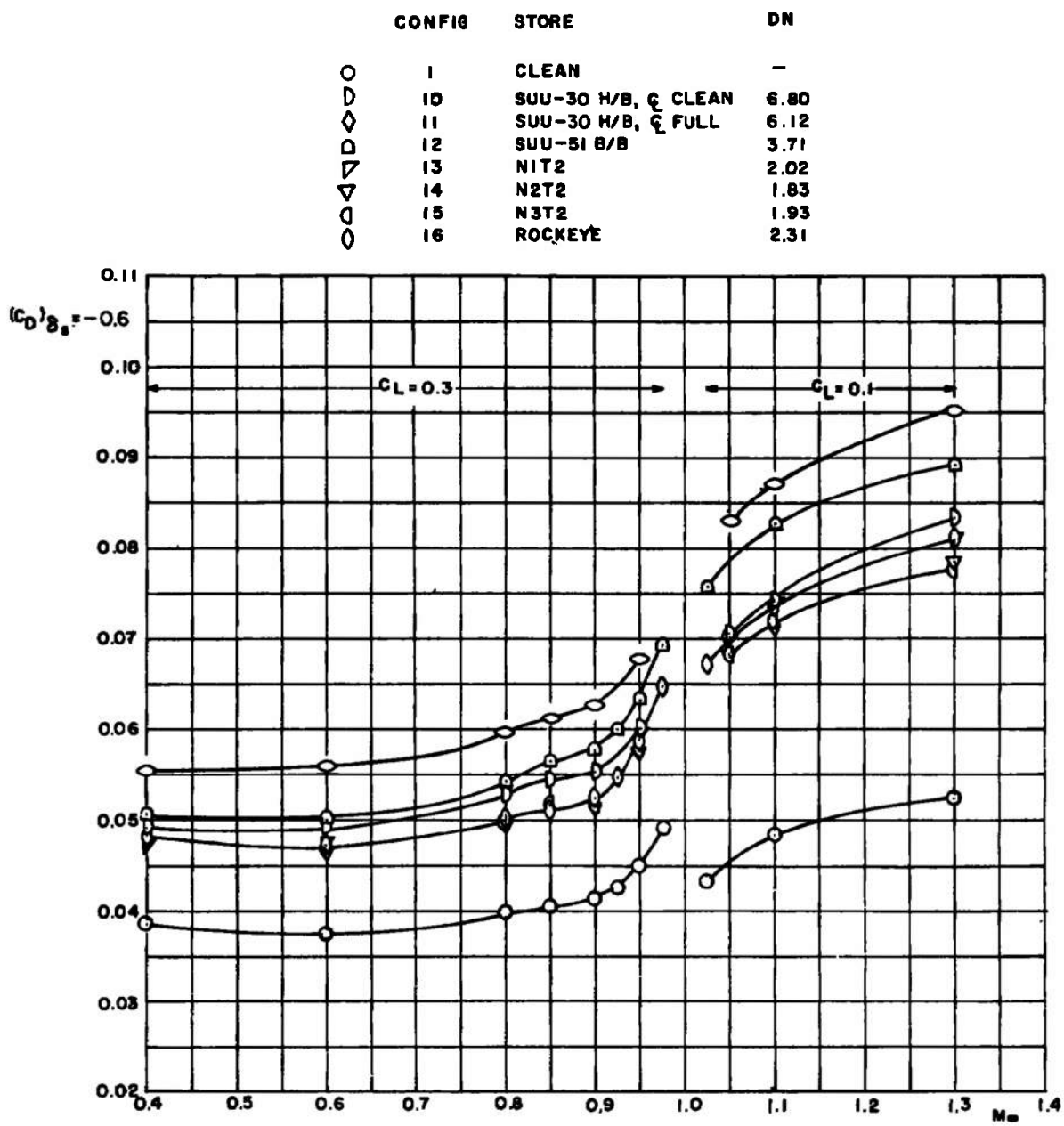

Fig. 66 Drag Variation with Mach Number for Several Multiple-Mounted Store Configurations

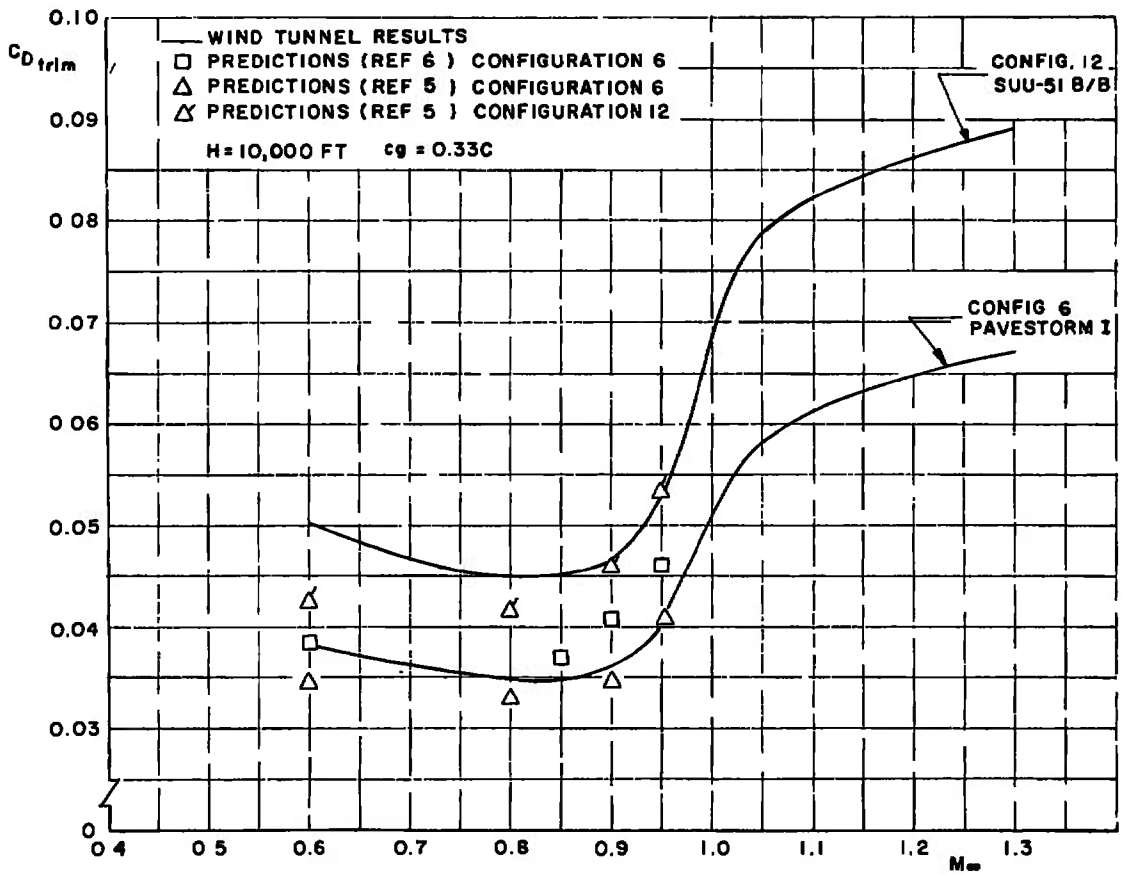

Fig. 67 Comparison of Predicted and Measured Drag for Configurations 6 and 12

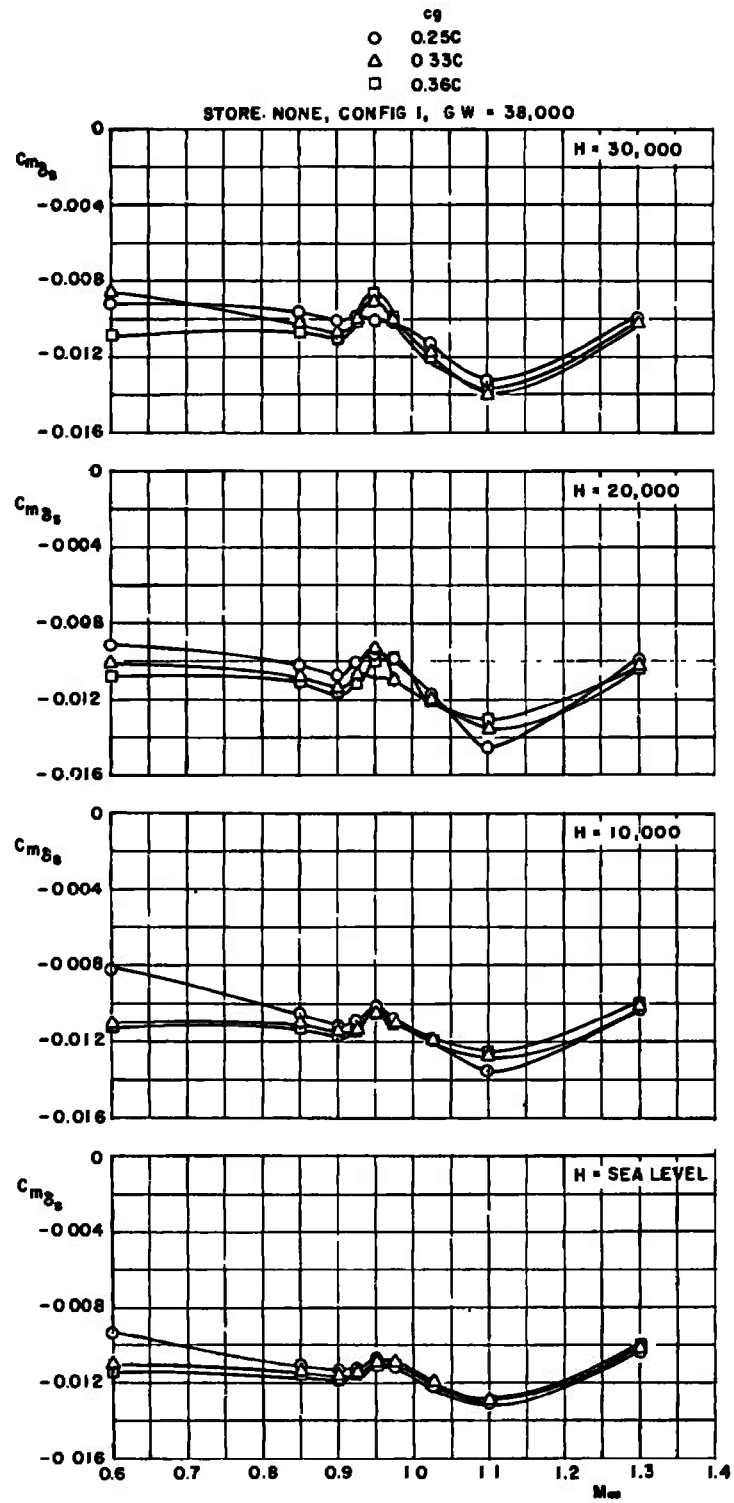

a. $C_{m_{\delta_s}}$ versus Mach Number

Fig. 68 Longitudinal Control Derivatives at Trim for Configuration 1

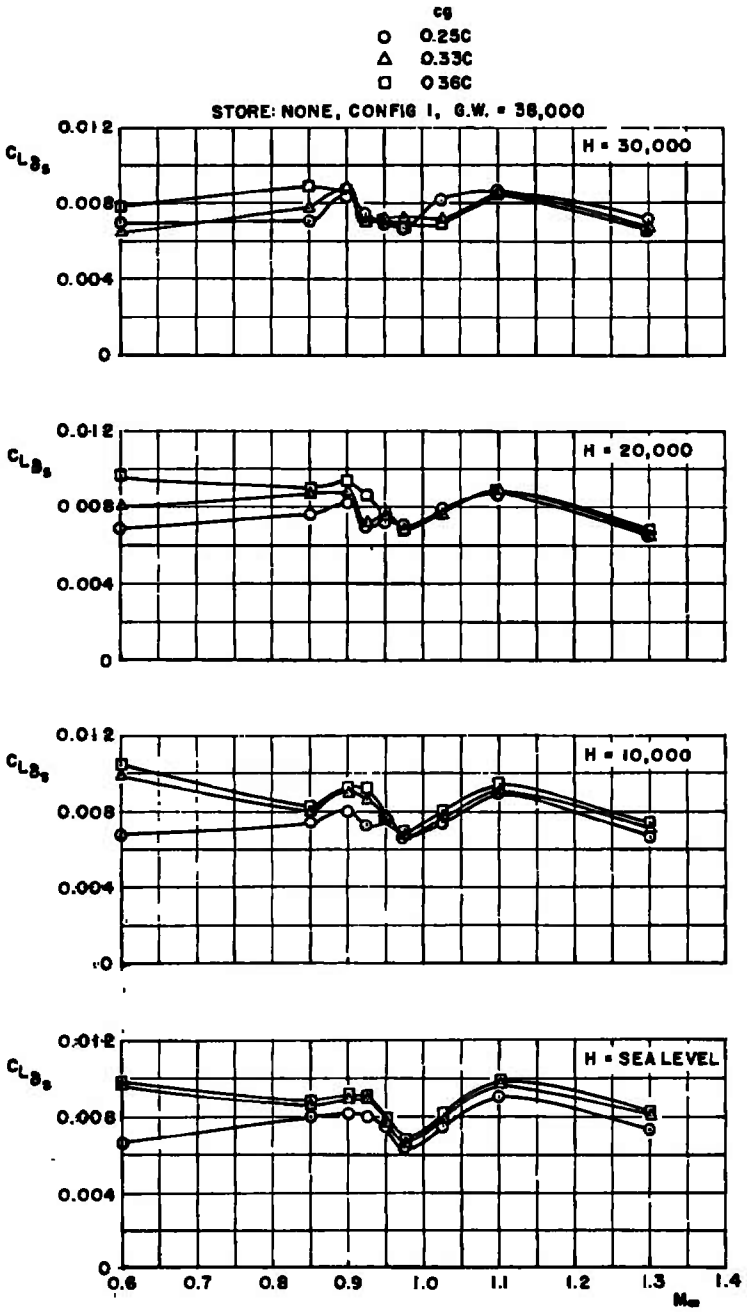

b. $C_{L_{\delta_s}}$ versus Mach Number

Fig. 68 Concluded

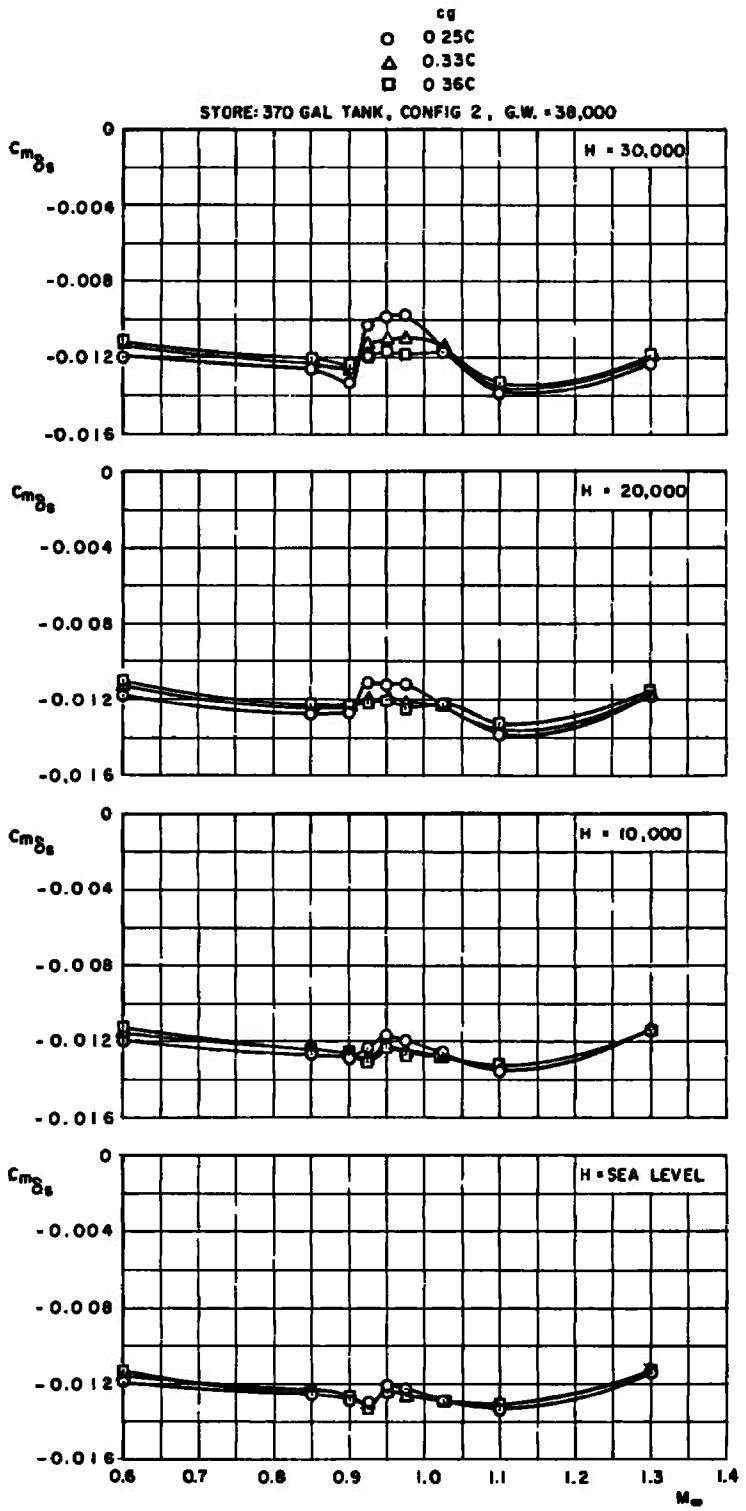

a. $C_{m_{\delta_s}}$ versus Mach Number

Fig. 69 Longitudinal Control Derivatives at Trim for Configuration 2

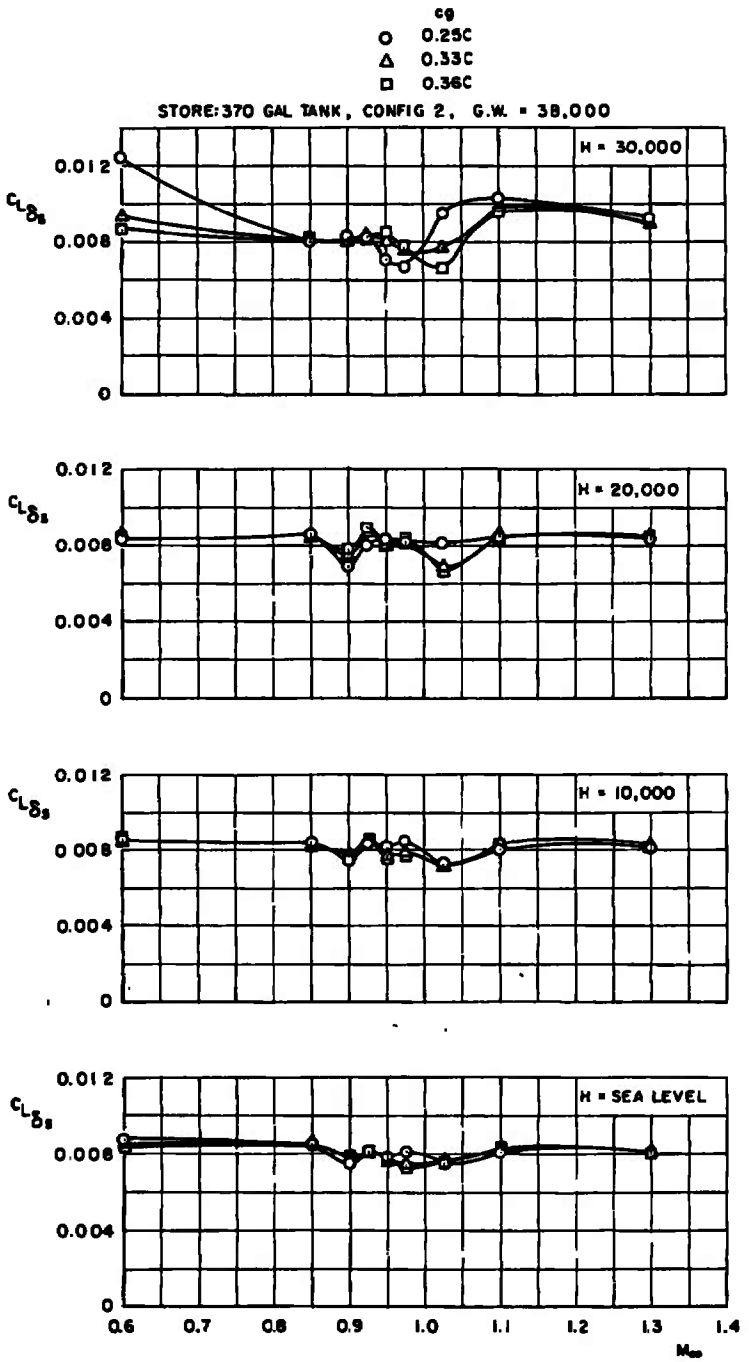

b. $C_{L_{\delta_s}}$ versus Mach Number

Fig. 69 Concluded

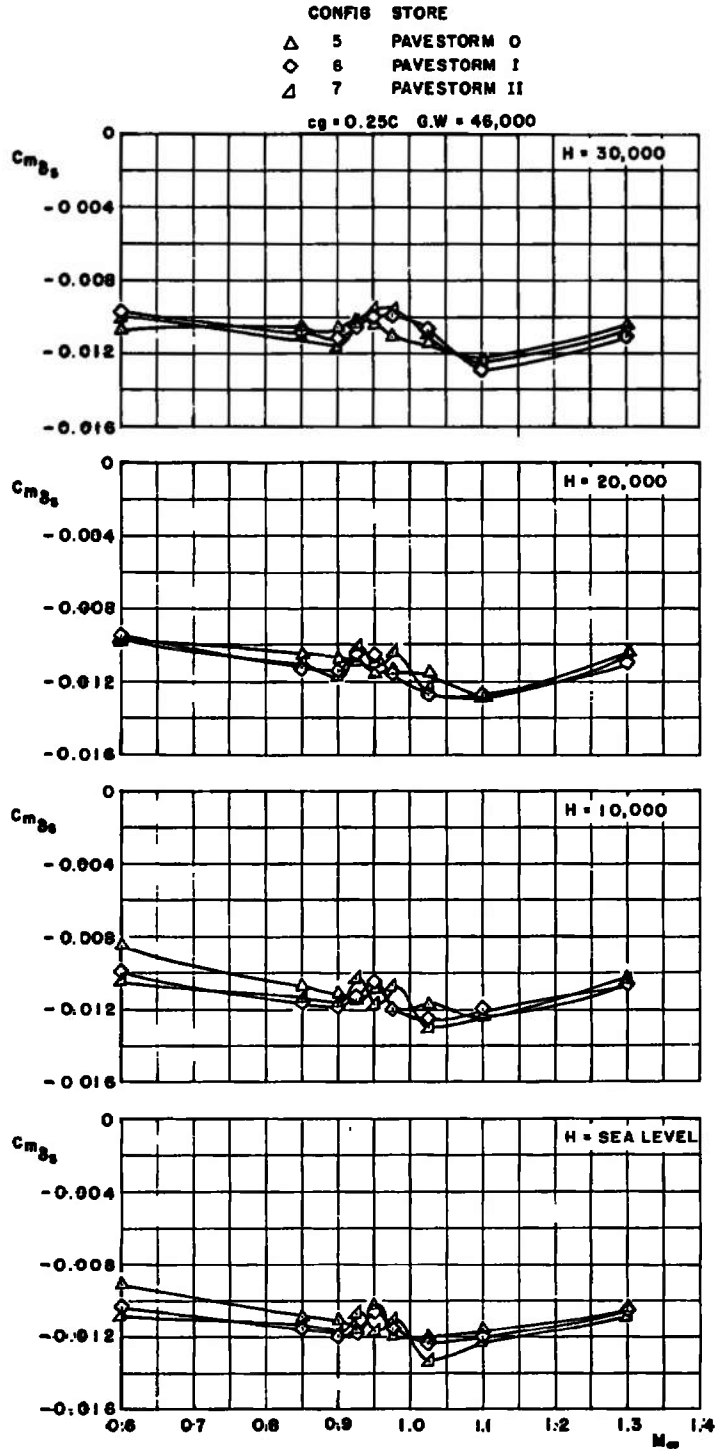

a. $C_{m_{\delta_s}}$ versus Mach Number

Fig. 70 Longitudinal Control Derivatives at Trim for Configurations 5, 6, and 7 at a cg Location of 0.25C

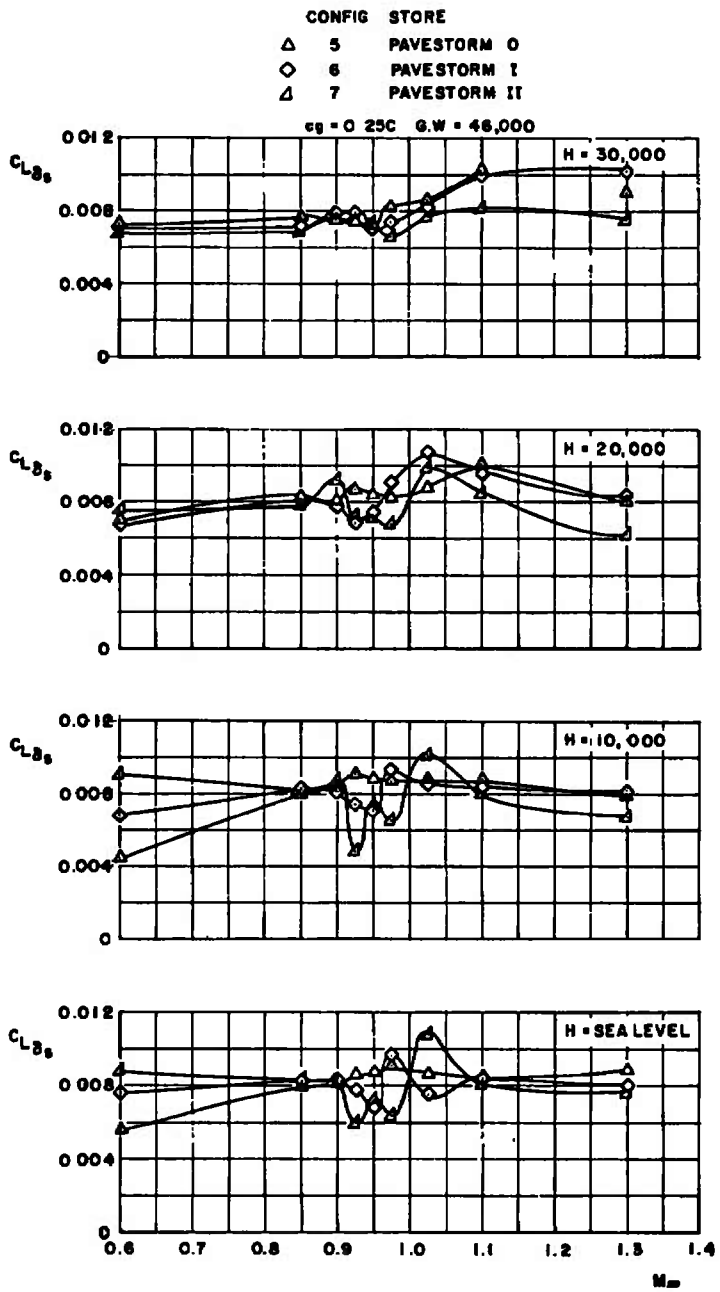

b. $C_{L_{\delta_s}}$ versus Mach Number

Fig. 70 Concluded

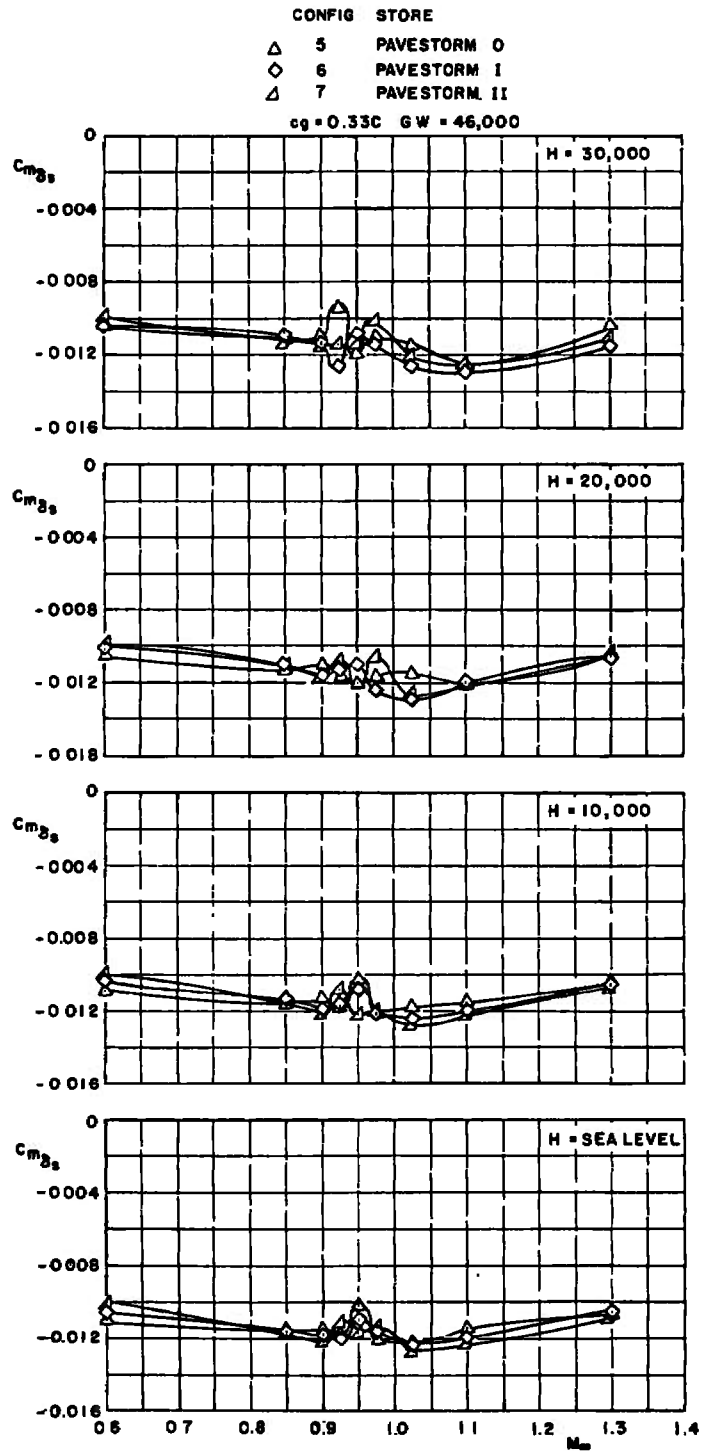

a. $C_{m_{\delta_s}}$ versus Mach Number

Fig. 71 Longitudinal Control Derivatives at Trim for Configurations 5, 6, and 7 at a cg Location of 0.33C

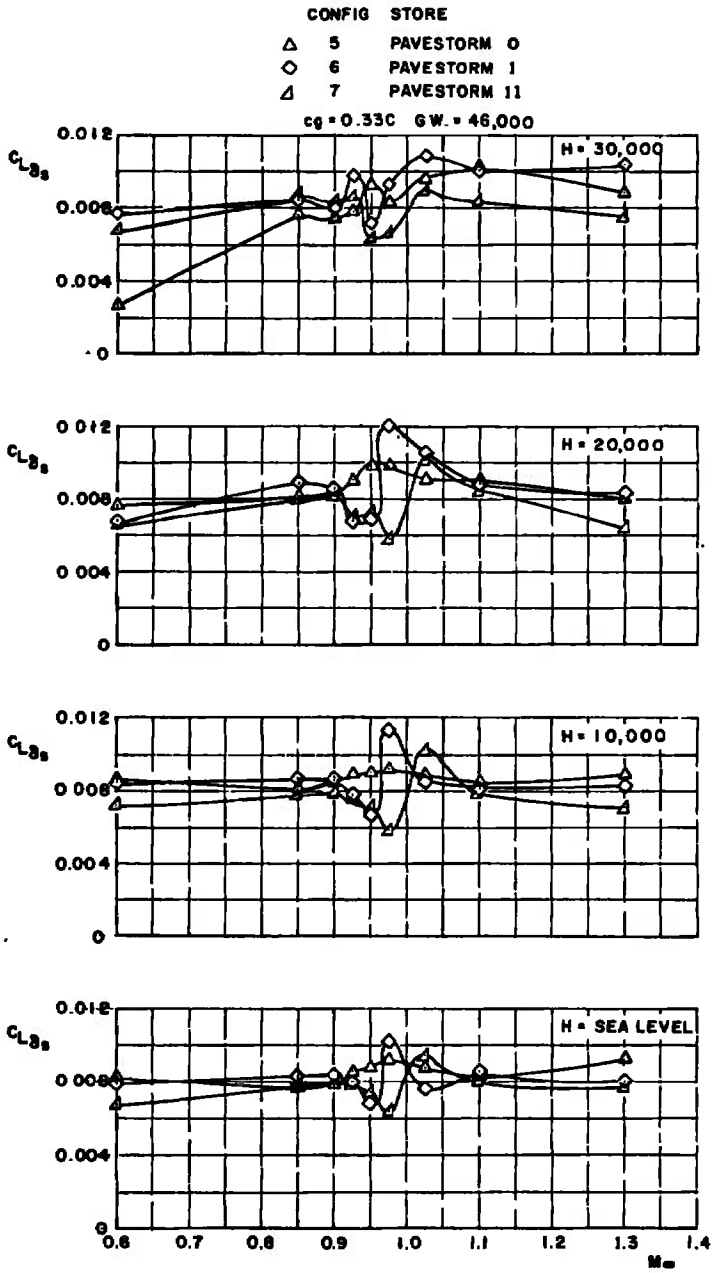

b. $C_{L_{\delta_s}}$ versus Mach Number

Fig. 71 Concluded

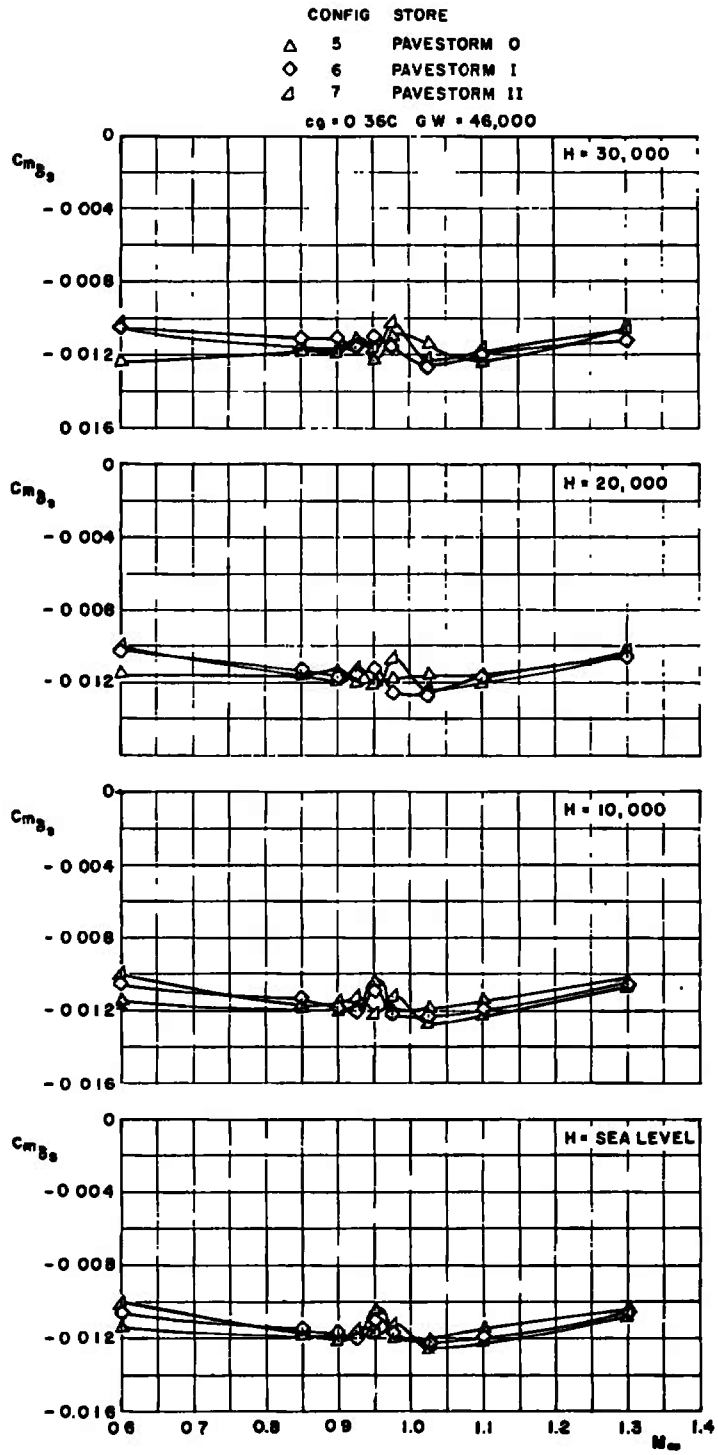

a. $C_{m_{\delta_s}}$ versus Mach Number

Fig. 72 Longitudinal Control Derivatives at Trim for Configurations 5, 6, and 7 at a cg Location of 0.36C

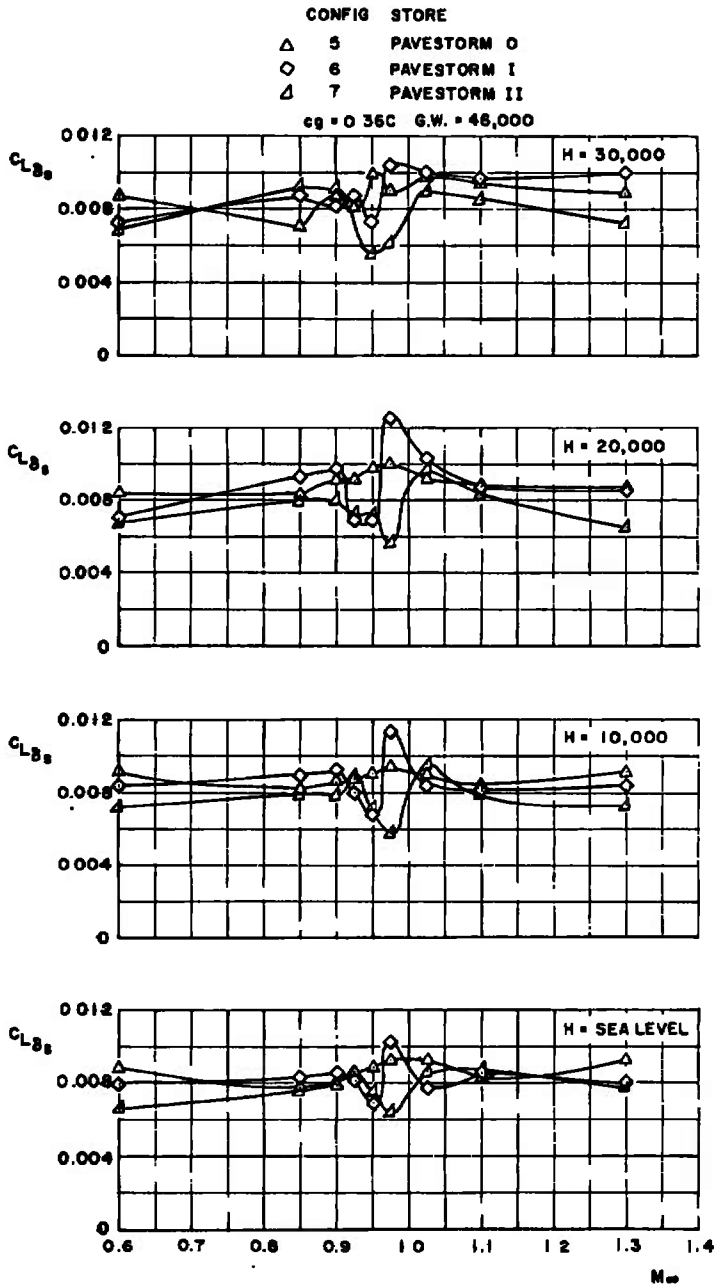

b. $C_{L_{\delta_s}}$ versus Mach Number

Fig. 72 Concluded

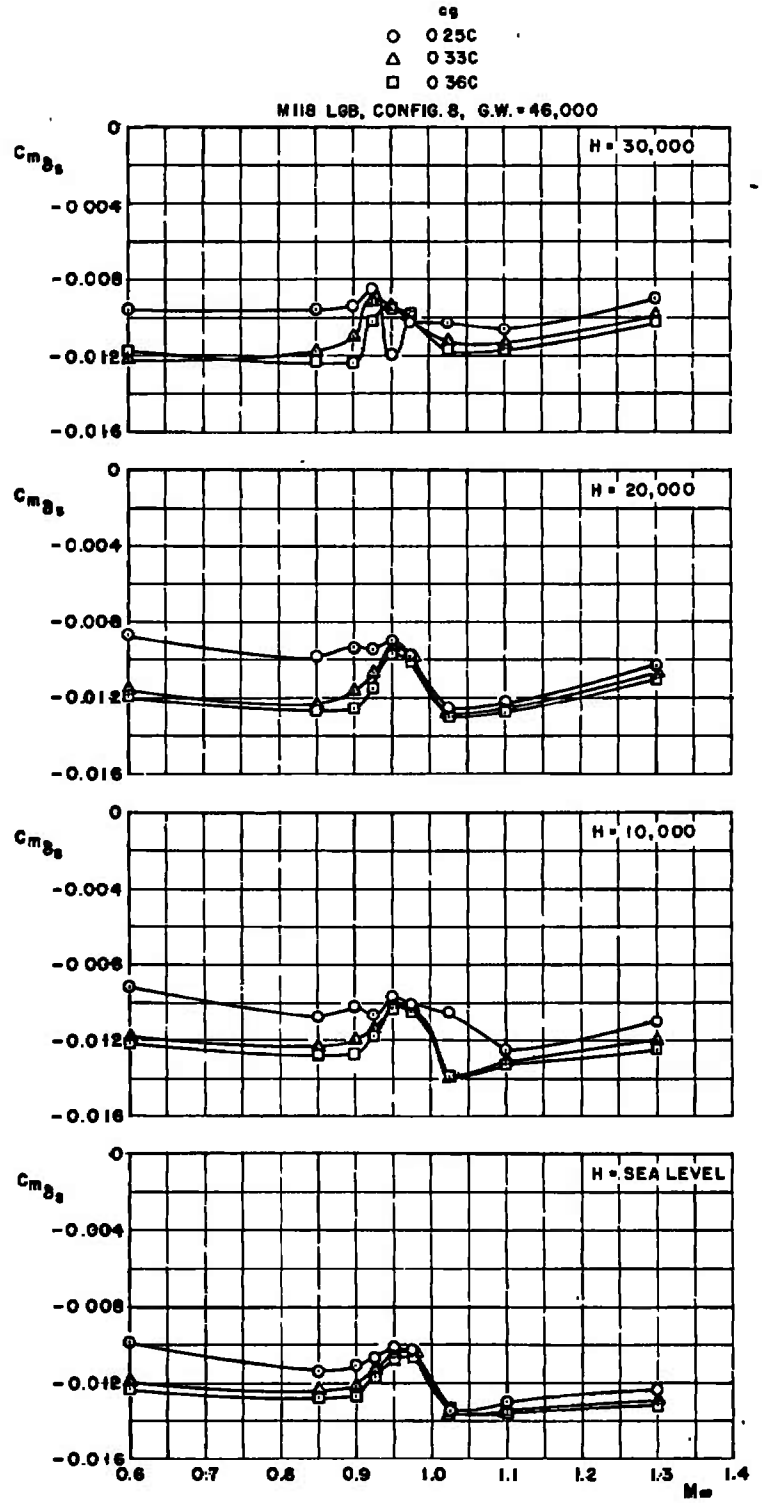

a. $C_{m_{\delta_s}}$ versus Mach Number

Fig. 73 Longitudinal Control Derivatives at Trim for Configuration 8

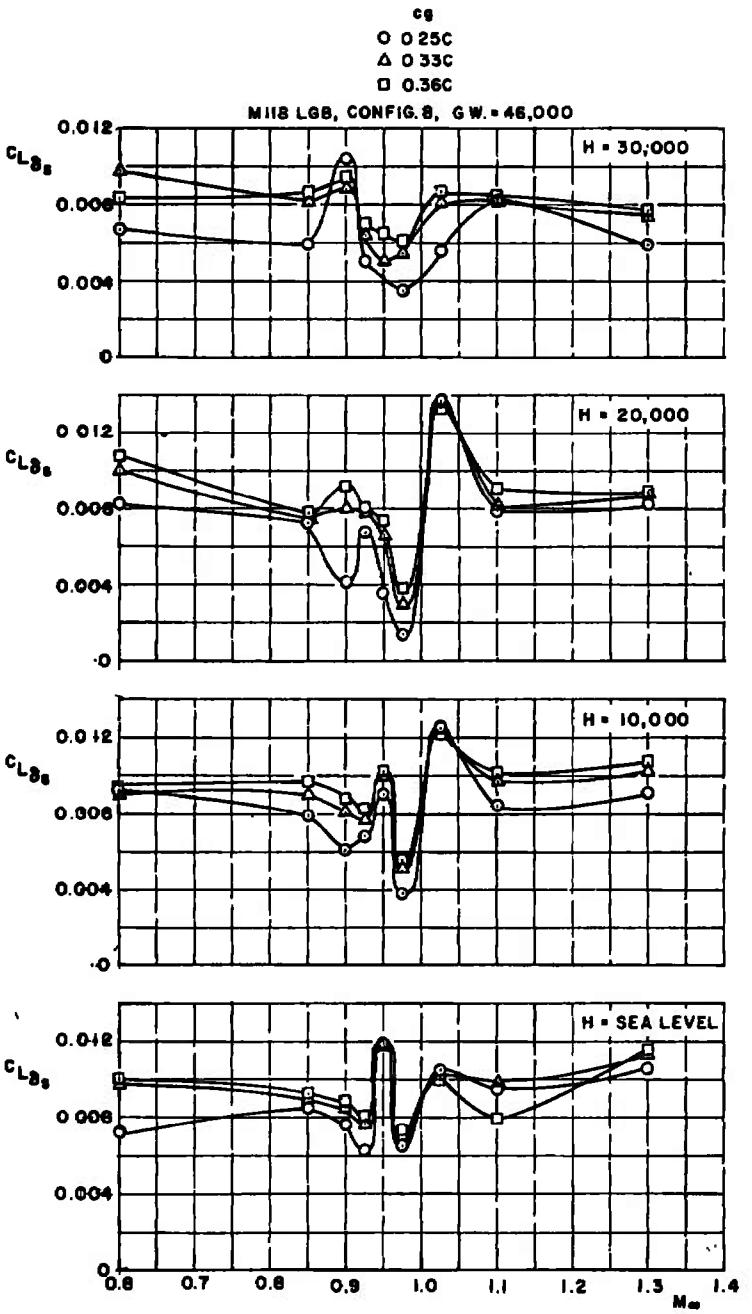

b. $C_{L_{\delta_s}}$ versus Mach Number

Fig. 73 Concluded

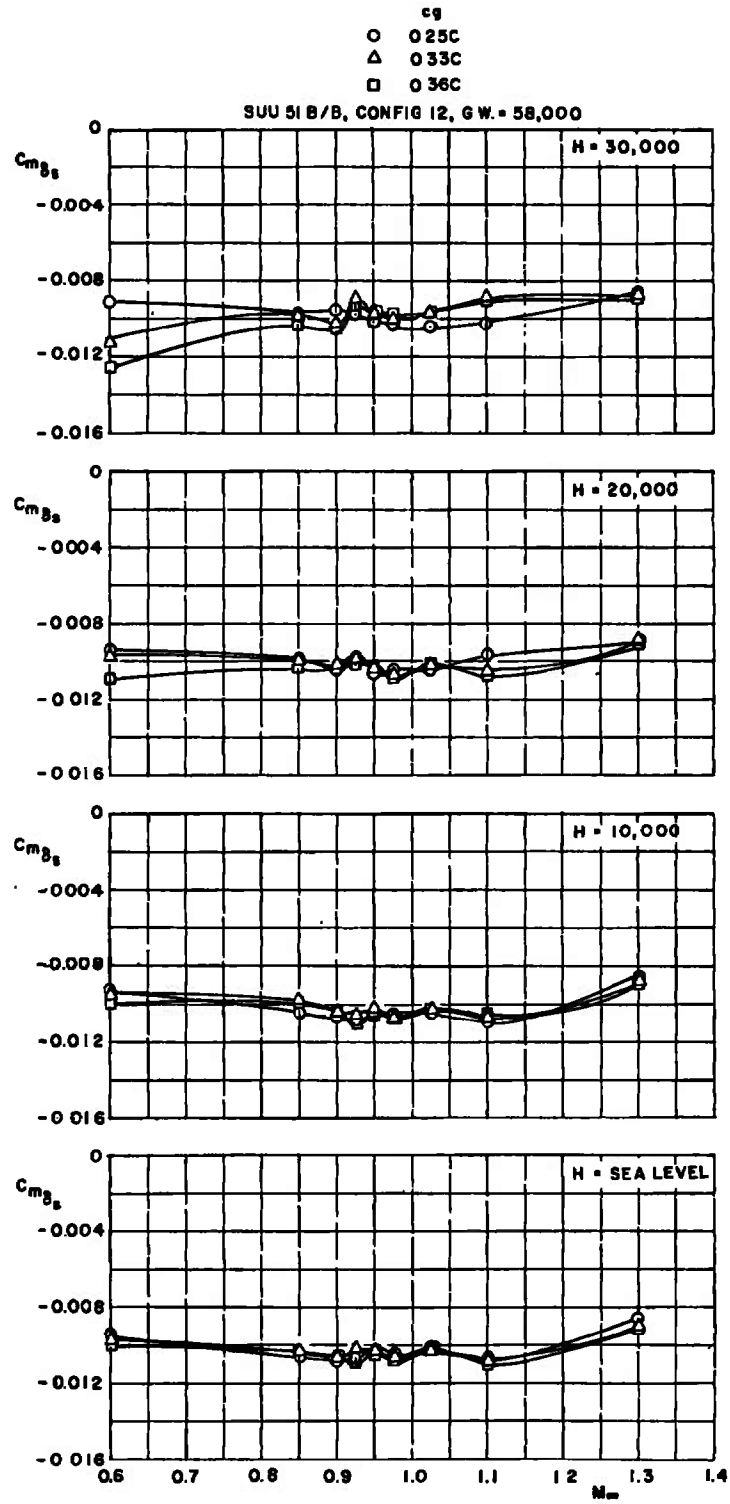

a. $C_{m_{\delta_s}}$ versus Mach Number

Fig. 74 Longitudinal Control Derivatives at Trim for Configuration 12

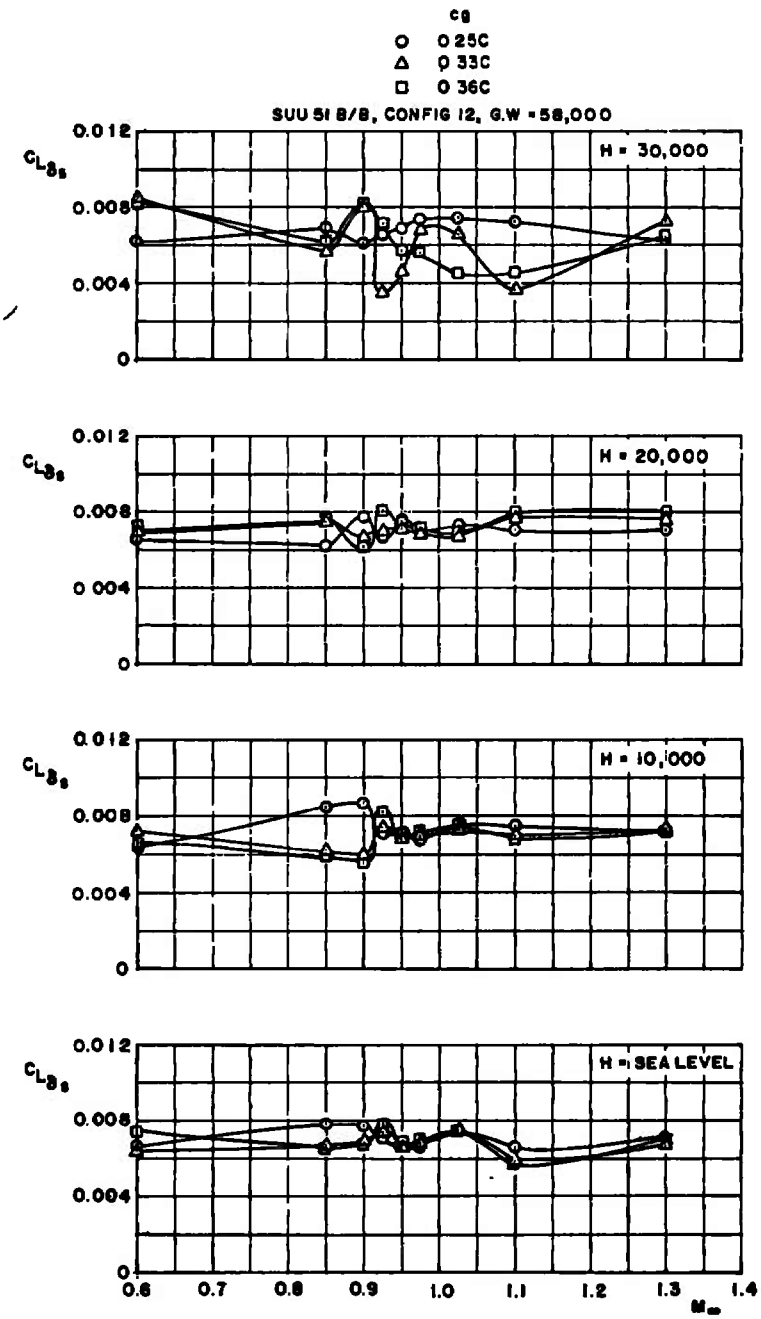

b. $C_{L_{\delta_s}}$ versus Mach Number

Fig. 74 Concluded

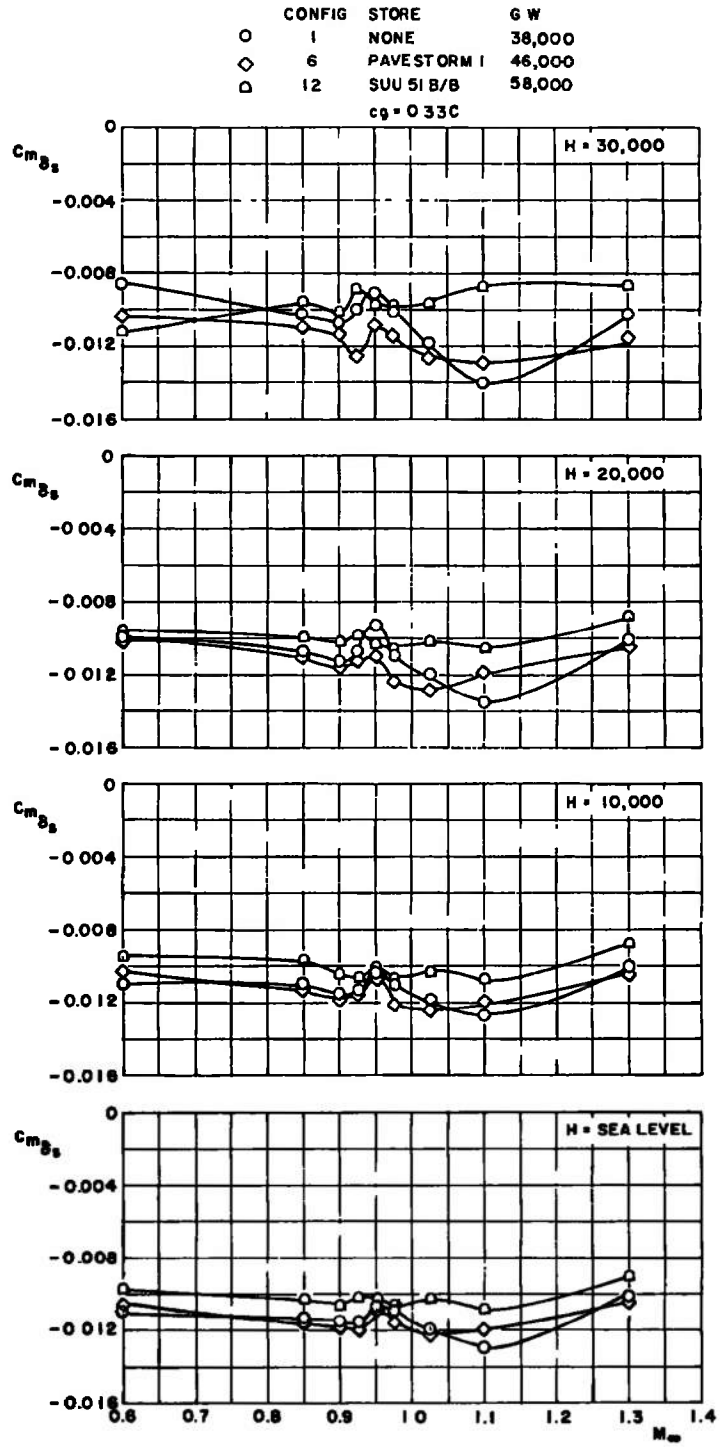

a. $C_{m_{\delta_s}}$ versus Mach Number

Fig. 75 Comparison of Longitudinal Control Derivatives for Configurations 1, 6, and 12 at Trim

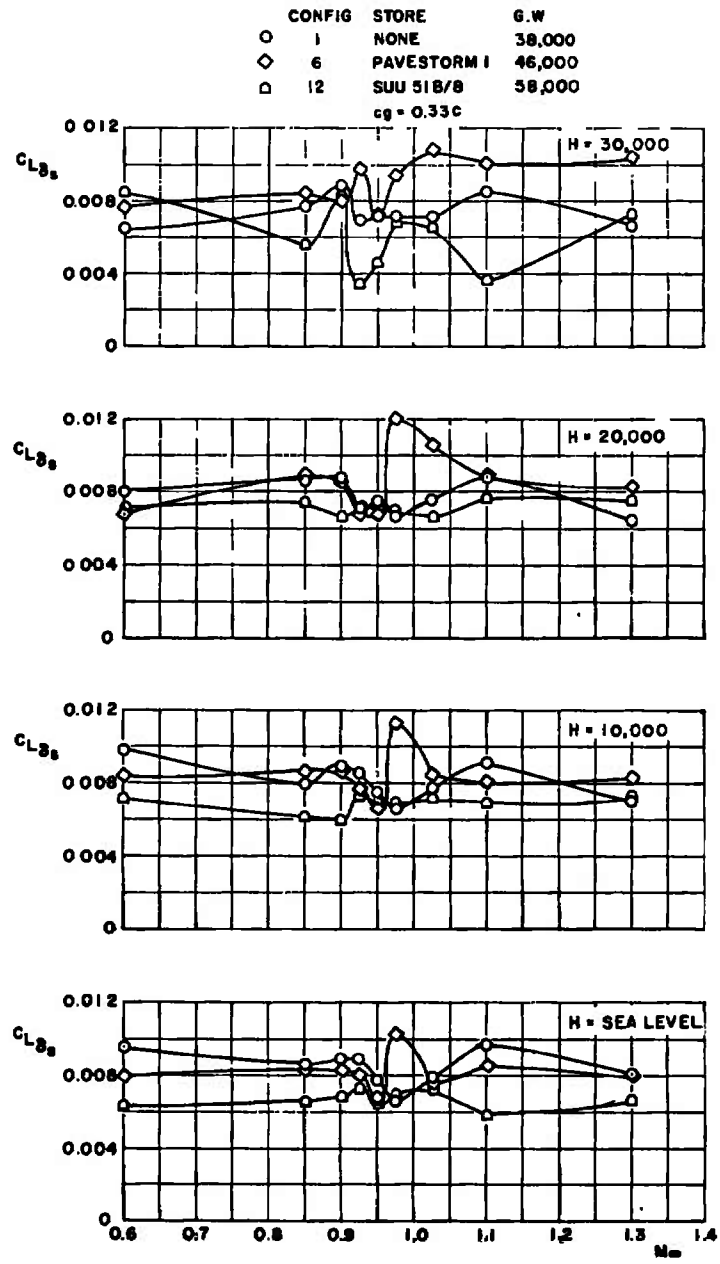

b. $C_{L_{\delta_s}}$ versus Mach Number

Fig. 75 Concluded

TABLE I
AERODYNAMIC COEFFICIENT PRECISION

M_∞	q_∞, psf	$\pm\Delta C_m$	$\pm\Delta C_L$	$\pm\Delta C_D$
0.400	340	0.0060	0.0219	0.0066
0.600	635	0.0027	0.0118	0.0035
0.800	805	0.0022	0.0073	0.0025
0.850	820	0.0017	0.0066	0.0026
0.900	840	0.0016	0.0060	0.0024
0.925	860	0.0015	0.0056	0.0024
0.950	885	0.0015	0.0053	0.0021
0.975	905	0.0014	0.0050	0.0021
1.025	945	0.0013	0.0047	0.0021
1.100	990	0.0012	0.0040	0.0021
1.300	905	0.0011	0.0027	0.0018

UNCLASSIFIED

Security Classification

DOCUMENT CONTROL DATA - R & D

(Security classification of title, body of abstract and indexing annotation must be entered when the overall report is classified)

1 ORIGINATING ACTIVITY (Corporate author)	2a. REPORT SECURITY CLASSIFICATION
Arnold Engineering Development Center Arnold Air Force Station, Tennessee 37389	UNCLASSIFIED
	2b. GROUP N/A

3 REPORT TITLE

EFFECT OF VARIOUS EXTERNAL STORES ON THE STATIC LONGITUDINAL STABILITY, LONGITUDINAL CONTROL, AND DRAG CHARACTERISTICS OF THE MODEL F-4C AIRPLANE

4 DESCRIPTIVE NOTES *(Type of report and inclusive dates)*

Final Report -- March 14, 1972, through January 18, 1973

5 AUTHOR(S) *(First name, middle initial, last name)*

J. M. Whoric, ARO, Inc.

This document has been approved for public release
its distribution is unlimited. per TWB 16-1
26 January 1974

6 REPORT DATE	7a. TOTAL NO OF PAGES	7b. NO OF REFS
November 1973	144	7

8a. CONTRACT OR GRANT NO	9a. ORIGINATOR'S REPORT NUMBER(S)
b. PROJECT NO 2567	AEDC-TR-73-186 AFATL-TR-73-211
c. Program Element 62602F	9b OTHER REPORT NO(S) *(Any other numbers that may be assigned this report)* ARO-PWT-TR-73-125
d.	

10 DISTRIBUTION STATEMENT Distribution limited to U.S. Government agencies only; this report contains information on test and evaluation of military hardware; November 1973; other requests for this document must be referred to Air Force Armament Laboratory (DLJA), Eglin AFB, FL 32542.

11 SUPPLEMENTARY NOTES	12 SPONSORING MILITARY ACTIVITY
Available in DDC.	Air Force Armament Laboratory (DLJA), Eglin AFB, FL 32542

13 ABSTRACT The results from analysis of data obtained from wind tunnel tests, which were conducted to determine the effect of various external stores on the aerodynamic characteristics of the model F-4C airplane, are presented and discussed. The analysis includes evaluation of the static longitudinal stability, drag, and longitudinal control characteristics of the F-4C when loaded with the Pavestorm missile series, Modular Weapons series, Mark 84 EOGB, M-118 LGB, SUU-51B/B, SUU-30H/B, and Rockeye stores. Moreover, analysis of the probable cause as well as the wind tunnel verification of a pilot-reported "tuck-under" problem with the F-4C when carrying the Pavestorm series of stores is presented and discussed. Incremental drag rise and neutral point shift associated with store loading are compared with results obtained from existing prediction methods and techniques. Data are presented for aircraft weights representative of each store loading at altitudes of sea level, 10-, 20-, and 30-thousand feet for aircraft center-of-gravity locations of 25, 33, and 36 percent of the mean aerodynamic chord over the Mach number range from 0.4 to 1.3.

Distribution limited to U. S. Government agencies only; this report contains information on test and evaluation of military hardware; November 1973; other requests for this document must be referred to Air Force Armament Laboratory (DLJA), Eglin AFB, FL 32542.

DD FORM 1 NOV 65 1473

UNCLASSIFIED

Security Classification

14. KEY WORDS	LINK A		LINK B		LINK C	
	ROLE	WT	ROLE	WT	ROLE	WT
F-4C aircraft						
aircraft external stores						
longitudinal stability						
aerodynamic drag						
flight characteristics						
aerodynamic configurations						

1. Airplanes - Stores Effects
2 " Drag
3 Stores Stability
4 " Effects
5 Airplanes - F-4C

AFSC
Arnold AFS Tenn